Greener solvents to replace toluene in the polymerisation and coating industry

Fergal Patrick Byrne

Doctor of Philosophy

University of York
Chemistry

August 2017

Abstract

Toluene is a volatile, non-polar solvent, commonly used throughout the chemical industry, which is facing increasing scrutiny due to its reprotoxicity and production from petroleum. Therefore, replacements which are safe and bio-based are required.

A solvent selection method has been developed which involved solubility tests, solvent modelling computer-aided molecular design and chemical intuition to find new, potentially bio-based solvents. Five candidates were identified: 2,2,5,5-tetramethyltetrahydrofuran (TMTHF), methyl butyrate, ethyl isobutyrate, methyl pivalate and pinacolone.

TMTHF is one of a new class of ethers, called quaternary ethers, which were identified not to possess the same issues of peroxide formation as traditional ethers due to a key structural difference. In addition, TMTHF has been synthesized from potentially renewable feedstocks where it was found to have similarly non-polar solubility properties (able to dissolve synthetic rubber), and a similar boiling point (112 °C), melting point (< 90 °C) and autoignition temperature (417 °C) to toluene. Application testing showed that TMTHF was able to facilitate radically-initiated polymerisations for the production of vinyl polymers suitable for use as pressure-sensitive adhesives (high M_w), and behaved more like toluene than traditional ethers in esterification, amidation and Grignard reactions. As such, it is an ideal candidate to replace toluene in the polymerisation and coating industry, as well as in many other applications.

In addition, four secondary candidates (methyl butyrate, methyl pivalate, ethyl isobutyrate and pinacolone) were also identified to be of low-polarity, like toluene. Methyl pivalate and pinacolone were the best of the four secondary candidates as ethyl isobutyrate could not produce sufficiently high M_w polymers and the odour of methyl butyrate was too unpleasant for large-scale use. Testing in a Menschutkin reaction confirmed that each candidate had similar solubility properties to toluene.

Finally, TMTHF, methyl pivalate, pinacolone and methyl butyrate were found to be non-mutagenic in the Ames test (ethyl isobutyrate not tested), but full toxicity testing is required before registration with REACH.

Contents

Abstract 3

Contents 5

List of figures 11

List of tables 17

Acknowledgements 22

Declaration 25

1 Introduction 27

1.1 The project 27

1.2 Solvent properties and measurements 28

1.2.1 Physical properties 29

1.2.2 Solubility predictions 30

1.2.3 Toxicity measurements 41

1.3 Green chemistry 43

1.3.1 Homogeneous catalysts 45

1.3.2 Heterogeneous catalysts 45

1.3.3 Green metrics 48

1.3.4 Bio-based platform molecules 48

1.4 Bio-based solvents 52

1.4.1 Current state-of-the-art in bio-based solvents 53

1.4.2 Challenges facing bio-based solvents 57

1.5 New solvent selection 57
1.5.1 Solvent selection guides 58
1.5.2 ICAS ProPred/ProCAMD 59
1.5.3 GRASS and the "top-down" approach 61
1.5.4 Mixed method 62
1.6 Introduction to the solvent selection process carried out in this thesis 63
2 Solvent selection process 66
2.1 Introduction 66
2.2 The pressure-sensitive adhesive (PSA) manufacturing process and solvent property requirements 67
2.3 Determination of the polymer HSPs and solvent polarity requirements 68
2.3.1 Testing method 68
2.3.2 Scoring of polymers and rubbers 69
2.4 The search for new solvents 75
2.4.1 Solvent guide search 75
2.4.2 Solvent modelling 76
2.4.3 Manual search for new solvents 91
2.4.4 Final results of solvent search 95
2.5 Synthetic routes to the top five candidates from biomass 96
2.5.1 Methyl pivalate and pinacolone 96
2.5.2 Ethyl Isobutyrate and methyl butyrate 97
2.5.3 TMTHF 98
2.6 Summary of top candidates 100
3 Synthesis, characterisation and testing of esters and ketones 102
3.1 Introduction 102
3.2 Application testing of esters and ketones 102
3.2.1 Radical-initiated vinyl polymerisation 102
3.2.2 Peroxide tests 104

3.2.3 Menschutkin reaction 106
3.3 Analysis of esters and ketones 111
3.3.1 Physical properties of esters and ketones 111
3.3.2 Solubility properties of esters and ketones 113
3.3.3 Toxicity properties 115
3.4 Synthesis of esters and ketones 117
3.4.1 Catalyst screen in the esterification of BA with methanol 117
3.4.2 Reactive distillation in the production of methyl butyrate and methyl pivalate 119
3.5 Conclusion 121
4 Synthesis, characterisation and testing of 2,2,5,5-Tetramethyltetrahydrofuran (TMTHF) 122
4.1 Introduction 122
4.2 Synthesis of TMTHF 122
4.2.1 Synthesis of TMTHF from DHL 123
4.2.2 Synthesis of TMTHF from DHN 129
4.3 Solvent properties of TMTHF 132
4.3.1 Peroxide formation 132
4.3.2 Physical properties of TMTHF 134
4.3.3 Solubility properties of TMTHF 135
4.3.4 Toxicity properties 145
4.3.5 Acid stability 146
4.4 Application testing of TMTHF 148
4.4.1 Uncatalysed esterification reaction kinetic study rationalised by KT parameters 148
4.4.2 Amidation reaction kinetic study rationalised by KT parameters 151
4.4.3 Grignard reaction testing 154
4.4.4 Radical-initiated vinyl polymerisation 157
4.5 Conclusion 159

5 Assessment of greenness and process suitability of the top candidate replacement solvents 160

5.1 Introduction 160

5.2 CHEM21 solvent guide: CLP assessment of solvents 161

5.2.1 Safety 163

5.2.2 Health 164

5.2.3 Environmental 165

5.2.4 Overall rating 165

5.3 TEST predictions: Toxicity and ecotoxicity 166

5.3.1 Rat (oral) LD_{50} 166

5.3.2 Mutagenicity 166

5.3.3 Tetrahymena pyriformis IGC_{50} (48 hr) / mg L^{-1} 166

5.3.4 Developmental toxicity 168

5.3.5 Fathead minnow LC_{50} (96 hr) 168

5.3.6 Daphnia magna LC_{50} (48 hr) 168

5.3.7 Bioconcentration factor (BCF) 169

5.4 CHEM21 metrics toolkit: Synthesis of solvents 169

5.4.1 Assessment of TMTHF synthesis 171

5.4.2 Assessment of methyl butyrate and ethyl isobutyrate synthesis 180

5.4.3 Assessment of methyl pivalate and pinacolone synthesis 184

5.5 Process suitability: Application in polymerisation and coating 190

5.5.1 Energy requirements and ease of recovery 191

5.5.2 Flammability 192

5.5.3 Incineration 193

5.5.4 Solvent odour 193

5.6 Conclusions 193

6 Concluding remarks and future prospects 195

6.1 Concluding remarks 195

6.2 Future work 198

7 Experimental 200

7.1 Materials and equipment 200

7.1.1 Materials 200

7.1.2 GC-MS analysis 200

7.1.3 1H NMR and 13C NMR analysis 201

7.1.4 UV vis. Analysis 201

7.1.5 GC-FID analysis 201

7.2 Experimental procedures 201

7.2.1 General experimental procedures 201

7.2.2 Solubility tests 204

7.2.3 Catalyst screening for the synthesis of 2,2,5,5-tetramethyltetrahydrofuran (TMTHF) from 2,5-dimethyl-2,5-hexanediol 204

7.2.4 Reactive distillation process for the 1 L scale production and purification of TMTHF 205

7.2.5 Synthesis of 2,2,5,5-tetramethyltetrahydrofuran (TMTHF) via the hydration of 2,5-dimethyl-2,4-hexadiene 205

7.2.6 Synthesis of 2,5-dimethyl-2,4-hexadiene (DHN) polyperoxide by the oxidation 2,5-dimethyl-2,4-hexadiene 206

7.2.7 Amidation kinetic reaction procedure 206

7.2.8 Esterification kinetic reaction procedure 206

7.2.9 Grignard reaction procedure 207

7.2.10 Synthesis of Poly (butyl acrylate-co-acrylic acid) 207

7.2.11 PSA preparation 207

7.2.12 Acid stability tests 208

7.2.13 Differential scanning calorimetry (DSC) analysis 208

7.2.14 Catalyst screen for the synthesis of methyl butyrate 208

7.2.15 Methyl butyrate and methyl pivalate synthesis using Dean-Stark apparatus 210

7.2.16 Radical-initiated vinyl polymerisation 210

7.2.17 Menshutkin reaction procedure 211

7.2.18 Menschutkin reaction order experiment 211

Appendices 212

LEL by volume example calculation 212

CO_2 emissions calculation data. 213

Solute descriptors for Abraham's solvation parameter model. 214

NMR spectra 217

DSC traces 239

GPC chromatograms 240

2,2,5,5-Tetramethyltetrahydrofuran (TMTHF) datasheet 241

List of abbreviations 243

References 253

List of figures

Figure 1.1	Screenshot from the ECHA website showing the hazards associated with toluene.	27
Figure 1.2	The ground and excited states of *N,N*-diethyl-4-nitroaniline.	31
Figure 1.3	Hydrogen-bonding in 4-nitroaniline shown in comparison to N,N-diethyl-4-nitroaniline.	33
Figure 1.4	Ground and excited states of Reichardt's dye	34
Figure 1.5	KT polarity map showing aprotic solvents.	35
Figure 1.6	A simplified image showing the cavity theory of solution.	36
Figure 1.7	HSP map showing the location of a selection of solvents in the HSP space.	38
Figure 1.8	A selection of bio-based platform molecules relevant to this work.	49
Figure 1.9	HSP solvent map showing bio-based solvents and petroleum-based solvents.	54
Figure 1.10	Neoteric and drop-in replacement bio-based solvents.	55
Figure 1.11	Flow chart showing the proposed steps for developing new solvents and the chapters in which they are described.	63
Figure 2.1	A sample HSP map showing blue spheres, red cubes, and the green region in which potential solvents are located.	69

Figure 2.2	Scoring system for polymers mixed with solvents. Scores of 1-6 were given to mixtures depending on the level of dissolution observed.	70
Figure 2.3	HSP spheres for each of Nitto's polymers and rubbers.	73
Figure 2.4	HSP maps showing TSS1 and TSS2.	74
Figure 2.5	The two candidates from the CHEM21 solvent selection guide.	76
Figure 2.6	Results of Run A using ProCAMD.	78-80
Figure 2.7	Results of Run B using ProCAMD.	82
Figure 2.8	Results of Run C using ProCAMD.	83-85
Figure 2.9	HSP map showing the trends of molar mass, branching, boiling point and polarity in esters.	88
Figure 2.10	The nine ester candidate molecules.	89
Figure 2.11	The four ketone candidates.	89
Figure 2.12	HSP map showing the trends of molar mass, branching, boiling point and polarity in ketones.	90
Figure 2.13	The final four candidates generated by ProCAMD.	90
Figure 2.14	Peroxide formation mechanism in 2-MeTHF.	91
Figure 2.15	ArgusLab mapped surface showing areas of high and low electrostatic potential energy on furan, 2-methylfuran and 2,5-dimethylfuran.	94
Figure 2.16	The top five candidates after the search for new solvents.	95
Figure 2.17	Proposed synthetic routes to methyl pivalate and pinacolone.	97
Figure 2.18	Synthetic routes to methyl butyrate and ethyl Isobutyrate.	98
Figure 2.19	Synthetic routes to TMTHF.	99
Figure 3.1	Mechanism of radical formation and chain termination in ethyl isobutyrate.	104
Figure 3.2	Stabilisation by resonance with adjacent pi-orbitals in ethyl isobutyrate.	104

Figure 3.3	Relative stabilities of methyl pivalate, methyl butyrate and ethyl isobutyrate.	105
Figure 3.4	Plot of 1/[A] versus time for the Menschutkin reaction between 1-bromooctadecane and 1-methylimidazole.	107
Figure 3.5	The Menschutkin reaction scheme and an LSER showing the relationship between the reaction rate and π*.	108
Figure 3.6	Graph showing the predictability of the LSER when only π^* is considered in the regression analysis of solvents with $\pi^* > 0.4$.	110
Figure 3.7	HSP map showing the five candidate solvents, toluene and ethyl acetate among a selection of other green solvents.	114
Figure 3.8	Ames test results for methyl butyrate, methyl pivalate and pinacolone.	116
Figure 3.9	Conversion of BA in a reactive distillation-type system using four different catalysts.	119
Figure 3.10	Conversion of PA in a reactive distillation-type system using four different catalysts.	120
Figure 4.1	The synthetic route to TMTHF carried out in this project.	123
Figure 4.2	Conversions and yields from the catalyst screen for the synthesis of TMTHF from DHL.	124
Figure 4.3	(A) ^{1}H NMR spectrum of TMTHF. (B) Mass spectrum showing the fragmentation pattern of TMTHF. (C) IR spectrum of TMTHF.	125
Figure 4.4	Side-products formed during TMTHF synthesis.	126
Figure 4.5	GC-FID chromatogram showing the presence of significant amounts of diol after the reaction mixture was allowed to cool to room temperature while stirring.	127
Figure 4.6	Suggested mechanism for the synthesis of TMTHF from DHL *via* HNL.	128
Figure 4.7	Reactive distillation apparatus employed for the 1 L scale production of TMTHF from DHL.	129
Figure 4.8	Synthesis of TMTHF from DHN.	130
Figure 4.9	GC-FID chromatogram showing the product peaks after reaction between DHN and water.	130

Figure 4.10	Synthetic route to DHL by the peroxidation of DHN.	131
Figure 4.11	TMTHF with mapped surface ESP.	136
Figure 4.12	Graphs showing the distribution of solutes. S versus B, E and V are shown in three graphs.	139
Figure 4.13	Graph comparing the partitioning of solutes in the TMTHF/water system and toluene/water system.	142
Figure 4.14	Predictability of the solvation parameter models.	144
Figure 4.15	Results of Ames test using TA98 and TA100.	146
Figure 4.16	Potential breakdown products of TMTHF in acidic conditions.	147
Figure 4.17	Uncatalysed esterification reaction mechanism.	148
Figure 4.18	Uncatalysed esterification reaction scheme and an LSER showing the deviation of TMTHF from the trend observed in a selection of traditional solvents in the model esterification reaction.	149
Figure 4.19	Comparison between predicted and experimental $\ln(k_2)$ values for the esterification of butanoic anhydride with butanol when both β and δ_H^2 are used to generate the LSER.	150
Figure 4.20	(A) Ideal pathway of the amidation reaction between a carboxylic acid and an amine and (B) Formation of a carboxylate salt.	151
Figure 4.21	The amidation reaction scheme and an LSER showing the deviation of TMTHF from the trend observed in a selection of traditional solvents in the model amidation reaction.	152
Figure 4.22	Graph showing the predictability of the LSER in which both β and π^* are considered.	153
Figure 4.23	General Grignard reaction scheme.	154
Figure 4.24	Typical solubilisation of Grignard reagents by ethers.	155
Figure 4.25	Reaction schemes for the two Grignard reactions carried out in this work and a table showing the results of the Grignard reaction.	156
Figure 4.26	The components of the test radical polymerisation carried out in TMTHF.	157

Figure 4.27	Chain transfer by solvent molecules resulting in chain termination.	158
Figure 5.1	Structural analogues for each of the candidate molecules.	162
Figure 5.2	Synthesis of TMTHF from acetone and acetylene (Route 1).	171
Figure 5.3	Synthesis of TMTHF from isobutanol *via* DHN (Route 2).	174
Figure 5.4	Production of TMTHF *via* the oxidation of DHN (Route 3).	178
Figure 5.5	Synthesis of methyl butyrate and ethyl isobutyrate from glycerol.	181
Figure 5.6	Potential flow diagram for the production of butyric acid and isobutyric acid from glycerol.	182
Figure 5.7	Synthetic routes to methyl pivalate and pinacolone from pivalic acid.	185
Figure 5.8	Koch reaction mechanism.	186
Figure 5.9	Recycling of one equivalent of acetone in the production of pinacolone.	187
Figure 5.10	Synthetic route to methyl pivalate by hydroesterification.	190
Figure 7.1	Calibration curve and equation for the determination of the yield of methyl butyrate.	209
Figure A1	^{1}H NMR spectrum showing the structures of possible impurities in TMTHF.	217
Figure A2	^{1}H NMR spectrum of TMTHF.	218
Figure A3	^{13}C NMR spectrum of TMTHF.	219
Figure A4	^{1}H NMR spectrum of DHL.	220
Figure A5	^{13}C NMR spectrum of DHL.	221
Figure A6	^{1}H NMR spectrum of the HNL.	222
Figure A7	^{13}C NMR spectrum of the HNL.	223
Figure A8	^{1}H NMR spectrum of DHN.	224

Figure A9	^{1}H NMR showing the DHN peroxidation after 3 days (no solvent).	225
Figure A10	^{1}H NMR showing the amount of DHN peroxidation after 5 days (5 mL DHN in 10 mL TMTHF).	226
Figure A11	Zoomed in overlayed ^{1}H NMR spectrum showing TMTHF before and after acid tests at room temperature after 24 hours.	227
Figure A12	Zoomed in overlayed ^{1}H NMR spectrum showing TMTHF before and after acid tests under reflux (~112 °C) after 24 hours.	228
Figure A13	^{1}H NMR spectrum of the esterification product, butyl benzoate.	229
Figure A14	^{13}C NMR spectrum of the esterification product, butyl benzoate.	230
Figure A15	^{1}H NMR spectrum of the amidation product, *N*-benzyl-4-phenylbutanamide.	231
Figure A16	^{13}C NMR spectrum of the amidation product, *N*-benzyl-4-phenylbutanamide.	232
Figure A17	^{1}H NMR spectrum of the Grignard product, 2-methyl-1-phenyl-2-butanol.	233
Figure A18	^{13}C NMR spectrum of the Grignard product, 2-methyl-1-phenyl-2-butanol.	234
Figure A19	^{1}H NMR spectrum of the Wurtz product, bibenzyl.	235
Figure A20	^{13}C NMR spectrum of the Wurtz product, bibenzyl.	236
Figure A21	^{1}H NMR spectrum of the Menschutkin product, 1-octyl-3-methylimidazolium bromide.	237
Figure A22	^{13}C NMR spectrum of the Menschutkin product, 1-octyl-3-methylimidazolium bromide.	238
Figure A23	DSC trace of TMTHF.	239
Figure A24	GPC chromatogram of Poly (butyl acrylate-co-acrylic acid) when TMTHF is used as the polymerisation solvent.	240
Figure A25	GPC chromatogram of Poly (butyl acrylate-co-acrylic acid) when toluene is used as the polymerisation solvent.	240

List of tables

Table 1.1	Advantages and disadvantages of HSP, KT parameters and Abraham's solvation parameter model.	40
Table 1.2	Pore sizes of several zeolites with different frameworks.	46
Table 1.3	Properties of the K-series of montmorillonite clays produced by Süd Chemie.	46
Table 2.1	Physical property criteria for a new solvent as described by Nitto.	68
Table 2.2	Scores for each solvent for their ability to dissolve each polymer.	70-72
Table 2.3	The HSPs and sphere radius of Nitto's polymers and rubbers.	74
Table 2.4	Solvents in the CHEM21 solvent guide with suitable boiling points and which are classed as "Recommended" or "Problematic".	75
Table 2.5	The criteria entered into ProCAMD for each run.	77
Table 2.6	Molecule families which were included and omitted.	77
Table 2.7	PBT and vPvB criteria according to Annex XIII to REACH.	87
Table 2.8	The four most basic quaternary ether structures, the cyclic TMTHF and the acyclic DTBE.	93
Table 2.9	The four most basic furan structures, furan, 2-methylfuran and 2,5-dimethylfuran.	94

Table 2.10	Scores for each of top five candidates for their ability to dissolve each polymer.	95
Table 3.1	Results of an acrylate polymerisation using the fours candidate esters and ketones in comparison to toluene.	103
Table 3.2	Peroxide test results of the esters and pinacolone.	105
Table 3.3	Coefficients for regression analysis of the Menschutkin reaction using the solvatochromic equation.	109
Table 3.4	The physical and solubility properties of the esters and ketone in comparison with TMTHF, toluene and ethyl acetate.	112
Table 3.5	Results of the catalyst screen for the esterification of BA with methanol.	118
Table 4.1	Peroxide test results for TMTHF in comparison with THF, 2-MeTHF and CPME.	132
Table 4.2	Properties of TMTHF in comparison with toluene and ethyl acetate.	134
Table 4.3	The solubility properties of TMTHF in comparison to those of toluene, an aromatic hydrocarbon, and THF, a traditional ether.	135
Table 4.4	Regression data showing the system constants, *s*, *a*, *b*, *e* and *v*, as well as the R^2, *SE*, *p*-value and number of tested solutes, n_s, in each model.	140
Table 4.5	Comparison of the toluene/water system constants from this work and the work of Abraham *et al.*	141
Table 4.6	System constants of the training set models for the toluene/water and TMTHF/water biphasic systems.	143
Table 4.7	Results of the radical polymerisation of butyl acrylate and acrylic acid.	158
Table 5.1	CHEM21 solvent guide showing the five candidate solvents along with 1,8-cineol and toluene.	162
Table 5.2	Safety criteria scoring.	163
Table 5.3	Health criteria scoring.	164
Table 5.4	Environmental criteria score.	165
Table 5.5	Predicted toxicity data using the Consensus method in TEST.	167

Table 5.6	Comparison of predicted Log_{10} BCF with Log $P_{o/w}$.	169
Table 5.7	Metrics toolkit criteria and scoring boundaries.	170
Table 5.8	CHEM21 metrics for the production of TMTHF from DHL.	172
Table 5.9	Additional assessment by the CHEM21 metric toolkit.	173
Table 5.10	CHEM21 metrics for the production of TMTHF from the hydration of DHN.	175
Table 5.11	Additional assessment by the CHEM21 metric toolkit.	176
Table 5.12	CHEM21 metrics for the production of TMTHF from the oxidation of DHN.	179
Table 5.13	Additional assessment by the CHEM21 metric toolkit.	179
Table 5.14	CHEM21 metrics for the production of methyl butyrate and ethyl isobutyrate from glycerol.	181
Table 5.15	Additional assessment by the CHEM21 metric toolkit.	183
Table 5.16	CHEM21 metrics for the production of methyl butyrate and ethyl isobutyrate from glycerol.	186
Table 5.17	Additional assessment by the CHEM21 metric toolkit.	189
Table 5.18	Process suitability assessment.	191
Table 7.1	Solid bases of each polymer/rubber-solvent mixture in the solubility tests.	204
Table 7.2	Calibration sample volume calculation data.	208-209
Table 7.3	Table showing the relative response factors for each point of the calibration curve.	210
Table A1	CO_2 emissions data table.	213
Table A2	Descriptor values and log KP's for 66 solutes tested for partitioning in a biphasic water/organic solvent system.	214-216

Acknowledgements

I would like to thank my supervisors Andy Hunt, Tom Farmer and James Clark, firstly for giving me the opportunity to carry out this project, and then for also providing me with their time, patience, advice and friendship throughout. I have learned so much about so many topics in the past four years from our many meetings and discussions, and I have no doubt that the project would not have been the success it was without your input and presence. The train journeys to Belgium *via* a stop in London for Scotch eggs and beer were a particular highlight!

Thanks also to Nitto for funding this research and particularly Bart Forier, Greet Bossaert and Charly Hoebers for their contribution at our many teleconferences and meetings. I was lucky to have worked with an industrial partner with as much of a passion for the project as I had and who gave such a valuable input.

Special mention to James Sherwood and Rob McElroy for sharing their expertise in the field of green solvents with me at various points of the project, in particular the meeting/lunch in the Deramore Arms that ran on a bit longer than was planned! Also thanks to Paul Elliott for his experience and knowledge in several analytical techniques, Heather Fish for help with NMR, Karl Heaton for carrying out mass spectrometry, the technical team of Hannah Briers, Maria Garcia, Katie Lamb and Charlotte Brannigan for assistance throughout, the administration staff in the GCCE, Alison, Katy, Sophie and Christine, for help organising meetings and travel during the project, and the BDC, especially Fiona Taylor, for the use of their labs and assistance during the Ames testing.

To the many friends I have made during my time in York, in particular Tom, Stefan, Cressie, Paul, Konstantina, Tabitha, Jimmy, Duncan, Katie, Rob, Lucie and Eddie thank you for making the time so enjoyable.

Of course, I have to give huge thanks to my family, especially my mam and dad, for their incredible support and love through the years. I'm sure you will be delighted that I have finally finished school! Also to my friends from home who are all over the world thank you for the constant company and craic on the Whatsapp groups!

Finally, and most importantly, a special thanks to Andrea, who has been with me from the time I started in York five years ago. Despite the challenges and stress that we were both under, your love and company have made the journey so much easier. If we managed to put up with each other while sitting beside each other for four years, then we can put up with each other through anything! ☺

Declaration

I declare that this thesis is a presentation of original work and I am the sole author. This work has not previously been presented for an award at this, or any other, University. All sources are acknowledged as References. Some of the work in this thesis was carried out by, or in collaboration with, other workers who are fully acknowledged in the text and all other results were obtained by the author. Part of the work disclosed herein has been published in the following article and patents. The article was written and by the author of this work and the patents were prepared and submitted by Nitto Belgium.

1. 2,2,5,5-Tetramethyltetrahydrofuran (TMTHF): a non-polar, non-peroxide forming ether replacement for hazardous hydrocarbon solvents

F. Byrne, B. Forier, G. Bossaert, C. Hoebers, T. J. Farmer, J. H. Clark, A. J. Hunt, *Green Chem.* **2017**, *19*, 3671-3678.

2. P32827NL00/WZO - Preparation of TMTHF

F. Byrne, A. J. Hunt, T. J. Farmer, J. H. Clark, B. Forier, G. Bossaert, **2017**.

3. P32826NL00/MKO - A process for the polymerization of vinyl monomers, a process for preparing an adhesive composition, an adhesive composition and a pressure-sensitive adhesive sheet

F. Byrne, A. J. Hunt, T. J. Farmer, J. H. Clark, B. Forier, G. Bossaert, **2017**.

1 Introduction

1.1 The project

This work was carried out in collaboration with Nitto Belgium, a manufacturer of adhesive tapes, surface protective films, sealing materials and membrane products. Toluene is currently used as the polymerisation and coating solvent in their production plant, however, there are several issues with its use. It is suspected of damaging the unborn child (CLP classification H361d)[1] and may cause damage to organs through prolonged or repeated exposure (CLP classification H373), as shown in Figure 1.1.[1,2] REACH, the European body in charge of regulating the use of dangerous chemicals,[3] has placed restrictions on its use as a solvent in adhesives, which state that it cannot be present in concentration of more than 0.01%.[1] Additionally, toluene is produced from crude oil *via* the BTX process.[4–6] The diminishing supply of easily available crude oil means renewable resources must be exploited to maintain our current solvent consumption.[7,8]

Figure 1.1. Screenshot from the ECHA website showing the hazards associated with toluene.[1]

In an effort to reduce the reliance on toluene, ethyl acetate has been used as a greener alternative for the polymerisation and coating of some products. However, the solvation power of ethyl acetate is not suitable for all product lines, so its use is limited.

Therefore, the aim of this project is to find a safer bio-based replacement for toluene for all relevant product lines at Nitto. The replacement should maintain all the benefits of using toluene – suitable physical and solubility properties - but should be sourced from renewable resources to reduce carbon emissions. It should also be less toxic and environmentally benign at the end of its lifetime. Finally, it must be cheap and abundant on a large scale in the future.

1.2 Solvent properties and measurements

The definition of a solution is, "a liquid or solid phase containing more than one substance, when for convenience one (or more) substance, which is called the solvent, is treated differently from the other substances, which are called solutes."[9] However, this definition has become outdated with the emergence of supercritical fluids and solvents which are not liquids at room temperature. An updated definition of a solvent should account for all liquids, low melting solids and supercritical fluids which are capable of homogenising solutes of different phases. A solvent must not be converted in the chemical process for which it is required and, in many cases, should be easy to remove at the end of the process.

The term "traditional solvents" is regularly used throughout this thesis and refers to the petroleum-based solvents which have been most commonly used over the last century, many of which are hazardous. Examples of hazardous traditional solvents are the hydrocarbon solvents hexane, toluene[1] (both suspected of damaging fertility[1,10]) and benzene (known to cause cancer[11]), the halogenated solvents dichloromethane (DCM) and chloroform (both suspected of causing cancer[12,13] and ozone layer depletion[14]), the ethers tetrahydrofuran (THF) (suspected of causing cancer[15] and forms dangerous peroxides[16]) and diethyl ether (highly flammable[17] and forms dangerous peroxides[16]), the dipolar aprotic solvents *N*-methyl-2-pyrrolidinone (NMP) and dimethyl acetamide (DMAc) (both may damage the unborn child).[18,19]

Until recently, legislation restricting the use of certain solvents has been lenient and thus, many of the most commonly used solvents are chosen simply because they are cheap and stable throughout the process, with little thought spared for environmental effects or the potential to enhance the process. The toxicity of a solvent is crucial, as applications can be limited in the case of high toxicity. While physical properties are key factors to be considered when choosing a solvent for a chemical process, it is important to know that a solvent is not simply a medium which

is characterised by its physical properties. The individual molecular interactions within a solvent - hydrogen bonding, dispersion forces, dipolarity - also play a major role in deciding the appropriate solvent for a given process[20,21] and it is these molecular interactions which determine whether a solute will dissolve in a solvent.

1.2.1 Physical properties

Some physical solvent properties which are commonly referred to include melting point (Mp), boiling point (Bp), dynamic viscosity, density, flash point, lower explosion limit (LEL) and autoignition temperature (AIT).

The melting point of a substance is the temperature at which its solid and liquid phases can co-exist in equilibrium at a given pressure.[22] Solvents must be liquids at workable temperatures, and therefore a suitable melting point is required with specific requirements depending upon the process for which it used. Dimethyl sulfoxide (DMSO) (19 °C)[23] and *tert*-butanol (25 °C)[24] are examples of solvents with melting points at the higher end of the scale. If the melting point is too high, energy input is required to keep the solvent in the liquid phase, adding cost to the process.

The boiling point of a substance is the temperature at which the vapour pressure equals the pressure surrounding the liquid.[22] Traditionally, solvents have low boiling points to facilitate easy removal by evaporation and for many applications this remains a requirement.[25] However, this leads to increased atmospheric losses and human exposure.[26] Some non-volatile solvent classes which minimise losses and exposure have been developed more recently, such as ionic liquids.[27]

Dynamic viscosity of a liquid is the ratio of shear stress to the perpendicular velocity gradient.[28] Viscosity of solvents is important, as viscous liquids require more energy to pump and are more difficult to handle, especially at lab scale. The density of a substance is its mass per unit volume[29] and determines how immiscible solvents separate; the denser solvent will form the bottom layer.

The AIT is defined as the lowest temperature at which a substance can combust without a source of ignition.[30] The LEL is the lower end of the concentration range over which a mixture of a flammable gas or vapour in air can combust.[31] Above or below this range, combustion will not occur. The units of LEL are given as a volume percentage and its value varies with temperature and pressure.[32] The flash point is the lowest temperature required for a substance to vapourise enough to flash or burn momentarily.[33] Knowledge of the flammability properties of solvents is vital due to both the large volumes in which they are used and because evaporation is commonly used to remove the solvent from a product, meaning fuel/air mixtures are inevitable.

1.2.2 Solubility predictions

Several methods of predicting solubility exist, each with their advantages and disadvantages. The existence of multiple theories of solubility shows the imperfect state of our understanding of solubility. Four common methods of predicting solubility will be described in the following sections. They are the Hansen solubility parameters, Kamlet-Taft parameters, Abraham's solvation parameter model and kinetic studies using model reactions.

Hansen solubility parameters

To explain the Hansen solubility parameters (HPSs), the Hildebrand solubility parameter must first be understood. The Hildebrand parameter is related to the internal energy of vapourisation of a substance by Equation 1.1 and is therefore expressed in units of $MPa^{0.5}$.[34] The internal energy of vapourisation per unit liquid volume is also known as the cohesive energy density (CED).

Equation 1.1. $$\delta = \sqrt{\frac{\Delta U_{vap}}{V_{mol}}}$$

As there are no interactions between molecules in an ideal gas, the change in internal energy of a substance in going from the liquid to gas phase (ΔU_{vap}) can be used to determine the energy of the molecular interactions in the liquid phase.[34] This is useful when applied to solvation because the same molecular interactions must be overcome to rearrange the solvent molecules to form the cavity into which solvated molecules can reside, and to release the individual solute molecules/ions from a lattice into solution.[37] The energy of the newly formed solvent/solute interaction must also be greater than that required to form the cavity and release the individual molecules.[34] As such, substances with similar Hildebrand parameter values are more likely to dissolve each other.

However, the word "polarity" is often wrongly used as a catch-all phrase which includes both hydrogen-bonding and the permanent dipole as a measurement of solvation. Limitations in the Hildebrand scale exist as it neglects to describe hydrogen-bonding separately from the permanent dipole.[35] The most well-known example where this is exposed is the apparent similarity between ethanol and nitromethane, both of whom have the same Hildebrand parameter value. Based on this, both would be expected to have identical solvation ability. However, ethanol is miscible with water while nitromethane is not (among other major differences). The reason for this is that ethanol can both hydrogen-bond donate and accept with surrounding water molecules while nitromethane can only accept hydrogen-bonds.[35] As hydrogen-bonding is not considered in the Hildebrand scale, no differentiation between the two can be made.

HSPs are an improvement on the Hildebrand solubility parameter as they are composed of three constituent interactions, δ_D (dispersion forces), δ_P (dipolarity) and δ_H (hydrogen-bonding).[20,35] Like in Hildebrand's scale, substances with similar HSPs are likely to dissolve each other and this is very easily visualised on a three-dimensional map, such as that shown in Figure 1.2. As HSPs and the Hildebrand parameter are related to each other by Equation 1.2, the units of the HSPs are also $MPa^{0.5}$.[35]

Equation 1.2. $$\delta^2 = \delta_D^2 + \delta_P^2 + \delta_H^2$$

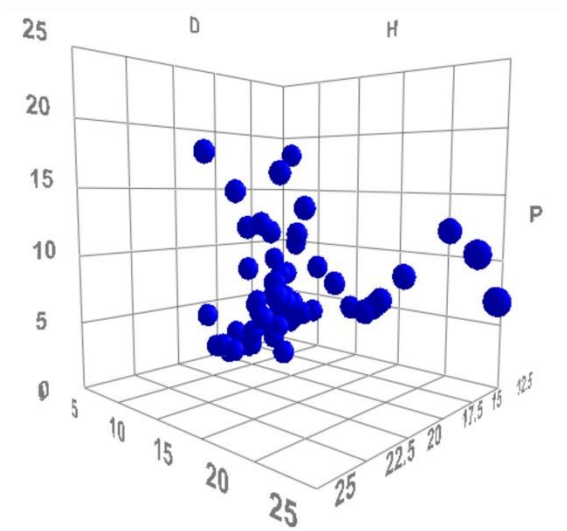

Figure 1.2. HSP map showing the location of a selection of solvents in the HSP space.

The δ_D scale measures the dispersion forces of a molecule. The dispersion forces derive from electrons rotating around a nucleus of an atom and are therefore an atomic force.[36] When the atoms are combined in a molecule, an instantaneous dipole is stimulated in an otherwise non-polar molecule.[36] This weak force provides the only cohesion between the molecules of aliphatic hydrocarbons, in which case it is almost equal to the Hildebrand parameter.[35] It is the cause of the polarisability of a solvent – the ability of a non-polar solvent to increase its polarity by shifting its electrons within itself in response to solutes of higher polarity. Aromatic and chlorinated solvents tend to have high δ_D values. The conjugation in aromatic systems allows its electrons a high degree of internal movement while the large size of the electron-rich chlorinated atoms also allows a high degree of internal movement.

The δ_P scale measures the permanent dipole of a molecule.[35] The dipole is a molecular interaction which is caused by electronegative atoms in a molecule and produces much stronger molecular

interactions than the dispersion force.[35] Highly dipolar molecules tend to be more ordered and tightly bound together.

The δ_H scale measures the hydrogen-bonding ability of a molecule.[35] Hydrogen-bonding is the interaction between electron lone-pairs with hydrogen atoms that are bound to electronegative atoms, such as oxygen or nitrogen, and is therefore an important molecular interaction based on the prevalence of its occurrence and its magnitude relative to other molecular interactions, such as Van der Waals forces.[35] The substance with the strongest hydrogen-bonding interactions is water, as it has two electron lone-pairs and two protons on the oxygen atom, allowing complete interaction with neighbouring molecules.[37] It is this which is responsible for water's unusually high boiling point for such a small molecule.[37]

There are various methods of calculating HSPs of a substance. Initially, Hansen used a base set of 90 liquids and 32 polymers which were determined by experiments and observations.[38] More recently HSPs are determined using the computer program HSPiP which utilises several group contribution methods to predict HSPs.[39,40] Other groups have also developed their own group contribution methods to predict HSPs as well as other properties, such as ProPred, developed by Technical University of Denmark (DTU) which will be described in Section 1.5.2.[41,42]

In group contribution theory, a molecule is broken up into its constituent groups (*e.g.* CH_3, C=O, OH, NH, etc.) and it is assumed that the value of a molecular property is equal to the sum of the contributions for each individual group.[39] For example, it would be assumed that the boiling point of hexane is equal to the sum of two CH_3 groups and four CH_2 groups, and decane would be equal to the sum of two CH_3 groups and eight CH_2 groups. If the contributions of CH_2 and CH_3 groups are known, then the boiling point of any linear alkane can be estimated using quantitative structure activity/property relationships (QSAR/QSPRs). QSAR/QSPRs are statistical models which use a database of chemicals of a known activity, such as boiling point, melting point, HSPs (δ_D, δ_P, δ_H), median lethal dose (LD_{50}) or bioconcentration factor (BCF), to predict the unknown activities of other molecules.[43] The same reasoning applies to other properties and other groups. However, limitations exist with group contribution theory, such as difficulty in differentiating isomers, inability to account for intramolecular interactions and oversimplification of molecules.[44]

HSP has been widely used in a variety of areas of the chemical industry for 50 years. As it only considers three types of molecular interactions, HSP will always contain a margin of error from exact values, but this is more than compensated for by its ease of use.

Kamlet-Taft parameters

The Kamlet-Taft (KT) parameters are a solvatochromic method of quantify the molecular interactions of solvents.[21,45–47] Solvatochromism is the use of dyes to quantify solvent polarity (dipolarity, polarisability, and hydrogen-bonding).[48] The electronic state of a suitable probe dye must change according to the polarity of the solvent in which it is dissolved.[49] Thus, the absorbance of the dissolved probe dyes, when measured by UV-vis. spectroscopy, can be used to create measurable scales of polarity.[50] The KT parameters use three scales to define solvent polarity. The π^* scale measures both dipolarity and polarisability together while the hydrogen-bonding interaction is split into separate hydrogen-bond donating (α) and hydrogen-bond accepting (β) scales.

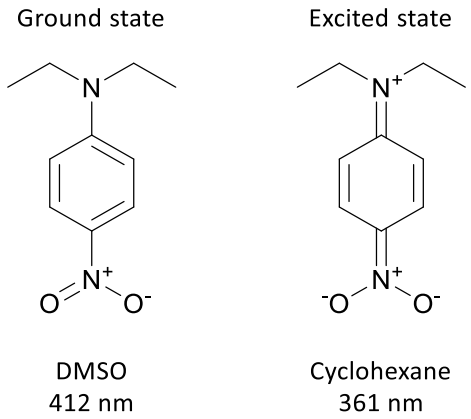

Figure 1.3. The ground and excited states of *N,N*-diethyl-4-nitroaniline.

Many dyes can be used to determine π^*.[47] An ideal dye will selectively respond to the dipolarity and polarisability of the solvent while disregarding hydrogen-bonding interactions.[47] λ_{max} for all test solvents must be highly correlated in linear regression, must not be influenced by peak overlap and must appear in measurable regions of the spectrum.[47] Commonly used dyes are *N,N*-diethyl-4-nitraniline and 4-nitroanisole which are bathochromic, or positively solvatochromic, meaning that their excited state is more polar than their ground state (Figure 1.3). The π^* scale is normalised using cyclohexane and DMSO as the non-polar and polar extremes respectively and can be calculated using Equation 1.3.[47]

Equation 1.3. $$\pi^* = \frac{\lambda_{max},(Test\ solvent) - \lambda_{max}\ (Cyclohexane)}{\lambda_{max}(DMSO) - \lambda_{max}(Cyclohexane)}$$

The β scale quantifies the hydrogen-bond accepting ability of a solvent.[46] Unlike for the π^* scale, the β scale cannot be normalised using only two solvents. This is because with lone-pair

containing heteroatoms, such as oxygen or nitrogen, which are required in a molecule for it to accept hydrogen-bonds, comes a degree of dipolarity due to the electronegativity of the heteroatom.[51] It is difficult to find a dye which selectively responds to hydrogen-bond accepting ability but not dipolarity, so two dyes are used to calculate β. Marcus proposed two methods (Equation 1.4 and 1.5) of calculating β using the wavelengths of two dyes, 4-nitroaniline (NA in Equation 1.4) and 4-nitrophenol (NP in Equation 1.5) respectively.[52] Both equations require known values of π^*. In Equation 1.5, δ^* is a polarisability correction term which is equal to 1.0 for aromatics, 0.5 for polychlorinated aliphatic, and 0.0 for all other aliphatic solvents.

Equation 1.4. $$\beta = 11.134 - \frac{3580}{\lambda_{max}(NA)} - 1.125\pi^*$$

Equation 1.5. $$\beta = 12.126 - \frac{3460}{\lambda_{max}(NP)} - 0.57\pi^* - 0.12\delta^*$$

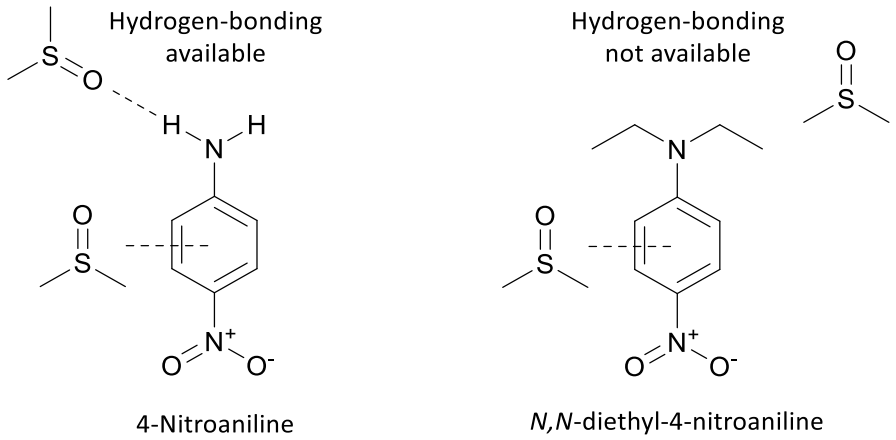

Figure 1.4. Hydrogen-bonding in 4-nitroaniline shown in comparison to N,N-diethyl-4-nitroaniline.[53]

More generally, two dyes are used along with DMSO as a reference solvent (Figure 1.4).[46] First, several non-hydrogen-bond accepting baseline solvents are measured using both the non-hydrogen-bonding *N,N*-diethyl-4-nitroaniline dye (used to measure π^*) and the hydrogen-bond accepting 4-nitroaniline dye.[46] The λ_{max} of 4-nitraniline in each non-hydrogen-bond accepting solvent is plotted on the *x*-axis and the λ_{max} of *N,N*-diethyl-4-nitraniline in each non-hydrogen-bond accepting solvent is plotted on the *y*-axis.

As no hydrogen-bonding occurs between the non-hydrogen-bond accepting baseline solvents and either dye, a linear relationship is observed - the baseline. Hydrogen-bond accepting test solvents will deviate from the baseline at a distance which is proportional to their hydrogen-bond accepting ability.[54] Equation 1.6 is used to calculate β.

Equation 1.6 $$\beta = 0.74\frac{\lambda_{Baseline\ eq.}(Test\ solvent)-\lambda_{Observed}(Test\ solvent)}{\lambda_{Baseline\ eq.}(DMSO)-\lambda_{Observed}(DMSO)}$$

For practical convenience, the β scale is normalised with DMSO. However, earlier versions of the β scale used hexamethylphosphoramide (HMPA) as the upper extreme, in which case DMSO had β = 0.74.[46] When using DMSO the original values can be obtained by multiplying by 0.74.

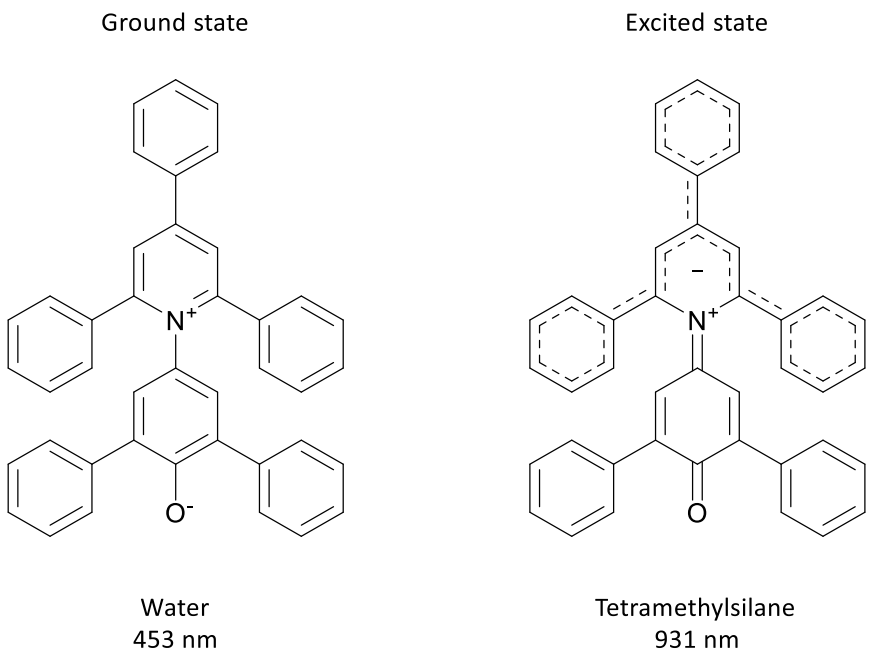

Figure 1.5. Ground and excited states of Reichardt's dye.[53]

The α scale quantifies the hydrogen-bond donating ability of a solvent.[45] Protic solvents such as alcohols and carboxylic acids rate highly in the α scale while aprotic solvents such as many ethers and dipolar aprotics have α = 0. Values of α are found in a similar way to β, except $E_T(30)$, calculated using Reichardt's dye, is used in combination with π^* values (Equation 1.7).[55]

Reichardt's dye is a hydrogen-bond acceptor but also responds to changes in dipolarity (Figure 1.5).[48,56] The excited state of Reichardt's dye is less polar than its ground state making it hypsochromic. The charge of the zwitterion is stabilised in polar media, particularly so in hydrogen-bond donating solvents, while the zwitterion is delocalised over the conjugated system in non-polar media.

Equation 1.7. $$\alpha = \frac{E^T(30)-30.2-(12.35\times\pi^*)}{15.9}$$

Plotting β against π^* on a two-dimensional graph generates solvent polarity maps which can be used as a visual aid (Figure 1.6).[57] α can be represented either by plotting two maps, one for protic solvents ($\alpha > 0.5$) and one for aprotic solvents ($\alpha > 0.5$), or by assigning different colours or symbols to protic and aprotic solvents.[57] Members of the same family of solvents tend to be grouped together in the solvent space.

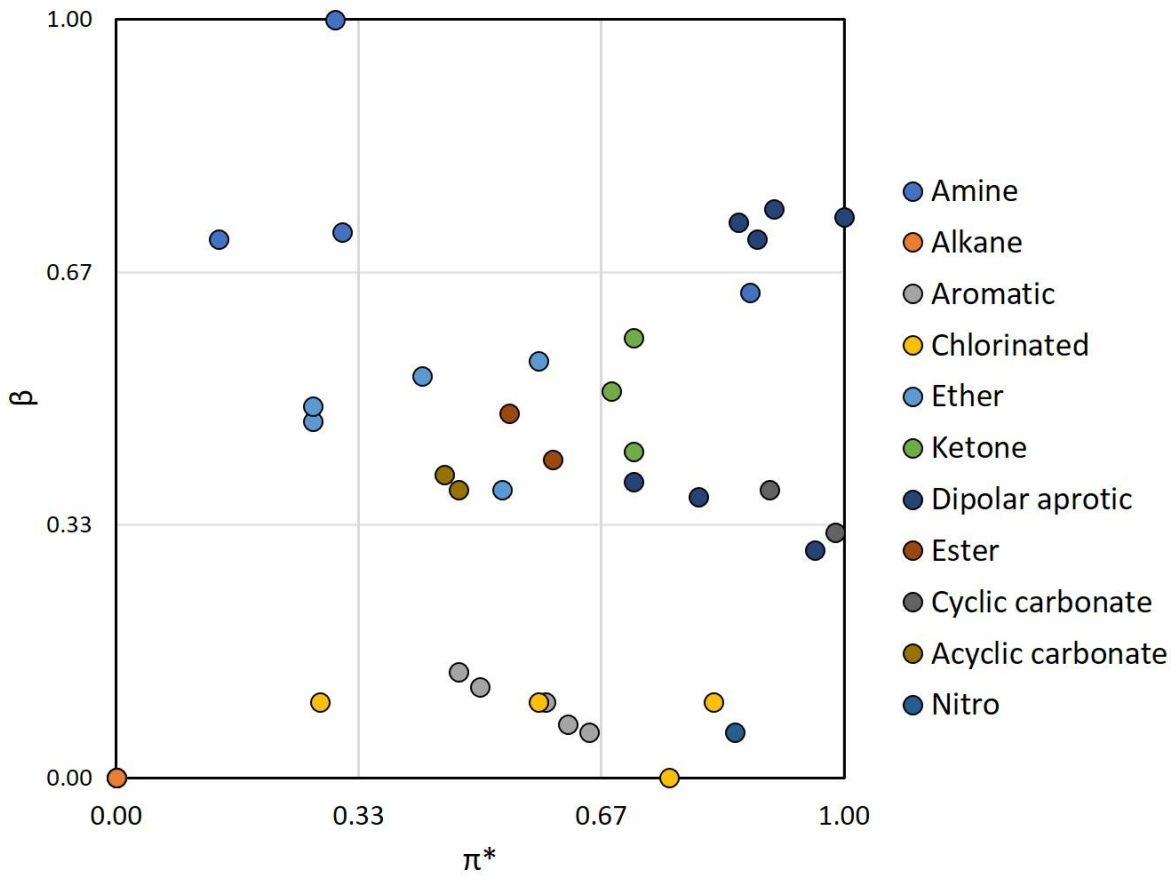

Figure 1.6. KT polarity map showing aprotic solvents. Data collected by Dr. James Sherwood from various published sources.[53]

Kinetic studies

The correlation between an energy term, such as the natural log of a rate constant, and a solvent property (or summation of properties) is known as a linear solvation energy relationship (LSER).[58] If the solvent property is a polarity scale such as a KT parameter, an LSER can be exploited to help in mechanistic studies, to characterise new solvents and also to predict applications in which a new solvent may thrive. An example of an LSER which uses the KT parameters is shown in Equation 1.8 and is known as the solvatochromic equation.[50,59]

Equation 1.8. $$Y = Y_0 + d\delta^* + s\pi^* + a\alpha + b\beta + h(\delta)^2$$

Y is an energy term such as an equilibrium or rate constant of a solute dissolved in a series of solvents, while the independent variables δ^*, π^*, α, β and $(\delta)^2$ are solvent descriptors.[59] A descriptor is a molecular property which can be either calculated or measured.[59] δ^* is a polarisability correction term which helps to differentiate between non-chlorinated aliphatic, polychlorinated and aromatic solvents; π^*, α and β are the KT parameters for polarisability/polarity, hydrogen bond donating ability and hydrogen bond accepting ability respectively;[45–47] and $(\delta)^2$ is the cohesive energy density (the square of the Hildebrand solubility parameter).[34]

Clark *et al*. have used Equation 1.8 to explain the kinetic performance of the bio-based solvents D-limonene and *para*-cymene in model amidation and Fischer esterification reactions in comparison with traditional solvents.[60] An inverse relationship was found between β and the natural log of the second-order rate constant, although acetonitrile deviated from this trend in the Fischer esterification reaction. To account for acetonitrile, $(\delta_H)^2$ was also required, and this two-descriptor model (Equation 1.9) demonstrated excellent predictability when assessed using the test solvents. None of the other descriptors were found to be significant.

Equation 1.9. $$\ln(k_2) = Y_0 + b\beta + h(\delta_H)^2$$

Use of the LSER provided mechanistic information for both model reactions. It indicated that solvents with stronger self-interactions inhibited the reaction, as the activated complex required a larger cavity than the reactants, which is consistent with S_N2 reactions.

Abrahams solvation parameter model

The migration of solutes from one phase to another in biphasic liquid systems is known as partitioning. Solutes partition between different solvents at varying rates, depending on the molecular properties of the solute and solvent pair. Significant efforts have been made to predict this partitioning using LSERs and molecular descriptors with varying success.[20,61,62] One such study utilised the solvatochromic equation (Equation 1.8).[21] There were two issues with this. Firstly, KT parameters can only be determined for substances which are liquids at room temperature, and secondly, KT solvent descriptors will translate accurately to solute descriptors only for liquids which are unassociated as solvents (no significant self-interactions). Abraham *et al*. proposed a model, known as the solvation parameter model (Equation 1.10),[59] which uses five solute descriptors to describe the cavity theory of solutions (Figure 1.7).[63]

Equation 1.10. $$SP = c + eE + s'S + a'A + b'B + vV$$

The cavity theory of solution is based on the rationale that for a solute molecule to migrate into a liquid phase, a cavity of suitable size must first be prepared by the rearrangement of solvent molecules in the receiving liquid phase to accommodate the solute molecule (Figure 1.7), which requires an energy contribution due to the disruption of solvent-solvent interactions.[63,64] The solvent molecules around the cavity must then align themselves in such a way as to interact with the incoming solute.[59] The free-energy change is negligible in this step as enthalpic and entropic energies cancel each other out. Finally, the solute molecule moves to occupy the cavity, forming solvent-solute interactions, and releasing energy.[59] If the donating solvent is a liquid (as opposed to a gas), the closure of the cavity in which the solute molecule resided also releases energy as solvent-solvent interactions are re-established. For a solute to transfer from one phase to another, an overall net release of energy over the course of the process is necessary.[59]

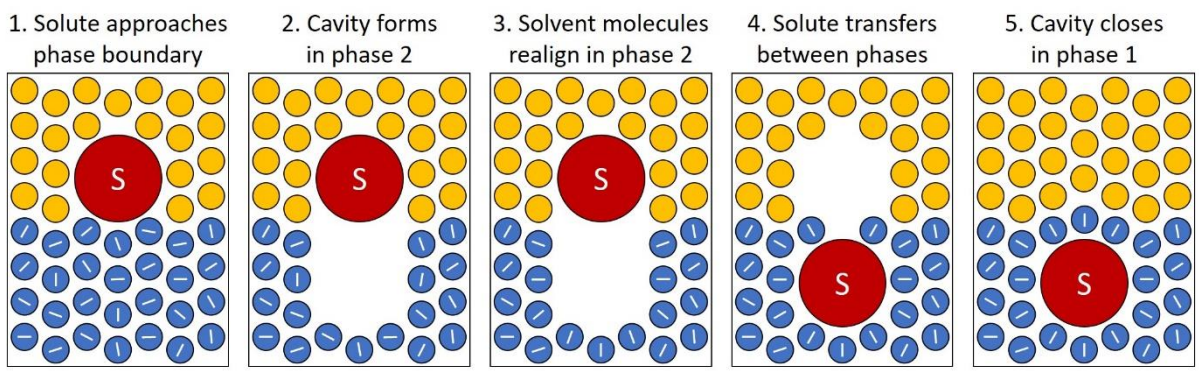

Figure 1.7. A simplified image showing the cavity theory of solution.[65]

In the solvation parameter model (Equation 1.10), the molecular descriptors are shown in upper case letters while their coefficients in lower case letters are the system constants. *SP*, the dependant variable can be any free-energy related property of a series of solutes.

The *E* descriptor is defined as the excess molar refraction of a solute, *x*, of a given McGowan's volume, MR_x, minus the molar refraction of an alkane with the same McGowan's volume, MR_{alkane}, as shown in Equation 1.11.

Equation 1.11. $$E = MR_x - MR_{alkane}$$

MR_x, can be found using Equation 1.12, where η is the refractive index of a pure liquid at 20 °C, while Equation 1.13 gives MR_{alkane}. It can also be described as a measure of the polarisable

electrons in a solute. If the McGowan's volume of the solute and alkane are equal, E can be found using Equation 1.14.

Equation 1.12. $$MR_x = 10V\left(\frac{\eta^2-1}{\eta^2+2}\right)$$

Equation 1.13. $$MR_{alkane} = 2.83195V - 0.52553$$

Equation 1.14. $$E = 10V\left(\frac{\eta^2-1}{\eta^2+2}\right) - 2.83195V + 0.52553$$

The McGowan's volume descriptor, V, can be easily found by subtracting the number of bonds, B_N, in a molecule from the sum of the atomic volumes, $\Sigma_{atomic\ volumes}$, of that molecule, as shown in Equation 1.15. Division by 100 is necessary to scale the V descriptor to a value more comparable to the other descriptors. The number of bonds can in turn be found using Equation 1.16, where N_a is the number of atoms in the molecule and R_g is the number of ring systems.[66] Combining the two equations gives Equation 1.17.

Equation 1.15. $$V = \frac{\Sigma_{atomic\ volumes} - 6.56B_N}{100}$$

Equation 1.16. $$B_N = N_a - 1 + R_g$$

Equation 1.17. $$V = \frac{\left(\Sigma_{atomic\ volumes} - 6.56\left(N_a - 1 + R_g\right)\right)}{100}$$

The S, A and B descriptors represents dipolarity/polarisability, hydrogen-bond acidity and hydrogen-bond basicity respectively, in a similar way to the π^*, α and β parameters of Kamlet and Taft. The difference between the two sets of descriptors is that while the KT parameters are obtained by solvatochromic means, S, A and B are determined using chromatographic means in which the retention times on polar stationary phases relate to polarity.[65,67–70] S, A and B descriptors can be subsequently determined by regression analysis of water/solvent partitioning based on a known set of solutes.[71]

Summary of solubility theories

Each of the four methods of classifying solvents in terms of their solvation power have their own advantages and disadvantages (Table 1.1). The three parameter HSP scale is an improvement upon the single Hildebrand parameter as it considers hydrogen-bonding, dipolarity and dispersion forces separately. The three parameters allow easy visualisation of the solubility

Table 1.1. Advantages and disadvantages of HSP, KT parameters and Abraham's solvation parameter model.

	Advantage	Disadvantage
HSP	• Easily visualised on three axes using designated software • Dipolarity and polarisability are considered separately • Can be applied to solvents and solutes • Can be quickly calculated	• Not 100% experimental • Hydrogen-bond accepting and donating abilities combined into one overall hydrogen-bonding parameter
KT parameters	• Can be quickly illustrated on solvent polarity maps • Hydrogen-bond accepting and donating abilities are represented separately • Choice of standard dyes minimises experimental work	• Can only be applied to solvents that are liquids at room temperature • Polarisability and dipolarity are combined into one parameter
Abraham solvation parameter model	• Five descriptors provide the most in-depth description of solubility • Can be applied to both solvents and solutes • Solute descriptors experimentally measured • Dipolarity and polarisability are represented separately • Hydrogen-bond accepting and donating abilities are represented separately • Solute partitioning between two phases can be predicted	• Requires significant experimental work covering a wide range of solutes • Cannot be easily visualised due to its five-dimensional nature

properties of solvents and solutes and can be quickly predicted using task-specific software (HSPiP). Therefore, they are very useful for solvent screening. The KT parameters use a different three parameter scale which separates hydrogen-bonding into donors and acceptors. To compensate, dipolarity and polarisability are merged into one parameter. The KT parameters are an empirical correlation based on solvatochromism using probe dyes and can be used in LSERs. However, they can only be measured for liquids at room temperature and not solutes. LSERs can provide a mechanistic insight in into a solvents interaction with solutes a significant number of reactions in a selection of solvents are required. Abraham's five-parameter solvation model provides the most in-depth description of both solvents and solutes based on the cavity theory of solution, but a large amount of experimental work is required, and five parameters cannot easily be visualised. When all three solubility theories are used together, a detailed description of solubility is obtained.

1.2.3 Toxicity measurements

Toxicity is a major issue with many traditional solvents, but full toxicity testing is expensive and difficult to fully understand due to the many modes of action. Knowledge of toxicity levels are required to register new substances with REACH for sale and use in the EU.[3] To avoid different research labs testing the same substance on animals, data sharing between research groups and companies as well as the use of predictive methods, such as TEST by the EPA,[72] are encouraged.[73] The Ames mutagenicity test does not rely on animal testing but instead uses bacterial strains.[74] Rat liver extracts are optional but will give more comprehensive results.

Toxicity Estimation Software Tool (TEST)

TEST is a computer program developed by the EPA, which estimates different toxicity properties of an inputted chemical using a variety of predictive QSAR methods.[72] LC_{50} fathead minnow (96 hour), LC_{50} *Daphnia magna* (48 hour), LD_{50} rat (oral), IGC_{50} (median growth inhibition concentration) Tetrahymena pyriformis, BCF, Developmental toxicity and Ames mutagenicity can all be estimated.[72] Several QSAR methods are available to estimate toxicity, each with their own advantages and limitations. The model type predictions are described below and all information has been obtained from the User's Guide for TEST.[75]

- The "Hierarchical method" clusters structurally similar molecules together and uses the weighted average of the predictions from several pre-determined models to predict properties. The advantage of this is that more reliable predictions can be obtained due to the use of multiple models. However, external validation is not possible in this method.[75]

- The "FDA method" models the properties of a single cluster of chemicals that are similar to the test compound only. The benefits of this is that a bespoke training cluster is used to predict the properties of the test chemical. Additionally, external predictions can be made using the FDA method as the test chemical is never present in the cluster used to make the model. However, a new model has to be generated on each run which is computationally demanding.[75]
- The "Single-model method" which uses multilinear regression using molecular descriptors based on a single training set of data. As the entire training set is used, the model validation may be subject to overfitting.[75]
- The "Group contribution method" which uses the data from a training set, and predicts toxicity in a similar manner to that described in Section 1.2.2. Again, isomers are an issue in group contribution predictions.[75]
- The "Nearest neighbour method" takes an average of the three chemicals in the training set that are most structurally similar to the test chemical. While this is a quick method that gives external predictions, it does not consider subtler structural differences between the test chemical and the training set chemicals.[75]
- The "Mode of action method" uses a two-step process to predict aquatic toxicity. First, linear discriminant analysis is performed to predict the mode of action. Linear regression is then implemented, using a model associated with that mode of action. The disadvantage of this is that the training set is often small which leads to inaccuracies.[75]
- The "Consensus method" takes the average of the estimated toxicities from each of the above methods. It was shown to give the best predictions out of all the methods in TEST in an external validation.[75]

Toxicity estimations should not be relied upon to classify solvents for toxicity, but instead can indicate substances which are likely to be of high toxicity. Any results must be experimentally verified by full toxicity testing.

Ames mutagenicity test

Even though mutagenicity does not automatically imply carcinogenicity, there is a strong correlation between the two.[76–78] The Ames mutagenicity test is a simple preliminary test of toxicity which tests two mutated *Salmonella typhimurium* (His-) strains for mutagenicity in different concentrations of a test chemical.[74,79] The bacterial strains have been mutated to an auxotrophic state, meaning that they are unable to synthesise the histidine they need to grow and therefore, should not survive in histidine-free environments. Different concentrations of a test chemical are added to the bacterial strains, along with an indicator dye. Sufficient concentrations

of mutagenic test chemicals can mutate the bacterial strain back to its original prototrophic state (His+), allowing it to grow in the absence of histidine and causing a colour change in the dye indicator. Non-mutagenic substances can metabolise into mutagenic substances in the liver.[76,79] As the liver is the organ responsible for the breakdown of ingested material in mammals, rat liver extracts are often added to the Ames test, thus providing a more comprehensive test for mutagenicity of a test chemical.

The advantages of the use of the Ames test are that it is cheap, and results are obtained in three days, making it a useful preliminary test for toxicity. Substances which fail the Ames test could be further tested for toxicity, or if other toxicity issues are present, it might not be worth committing extra time and money into development.

Octanol/water partition coefficient (Log $P_{o/w}$)

The octanol/water partition coefficient (Log $P_{o/w}$) represents the distribution of a solute between immiscible layers of octanol and water. In terms of the environmental fate of solvents, knowledge of the Log $P_{o/w}$ of substances has uses in estimating the BCF.[80–82]

High correlations are observed between the partitioning of solutes in octanol/water mixtures and the lipids of organisms,[81] although some specific molecular interactions may be ignored.[80] Additionally, organisms are often assumed to be single, homogeneous bodies, but in this simplified approach, the possibility of varying concentrations in different parts of the organism is disregarded.[81] More specific BCF measurements can be taken but at the consequence of increasing complexity and mechanistic studies can be performed which consider different mechanisms of uptake and clearance of substances in organisms, but this comes with added complexity. All approaches to BCF are satisfactory as long the approach that has been used in a given study is disclosed.[80]

1.3 Green chemistry

The definition of green chemistry is "the design of chemical products and processes to reduce or eliminate the use and generation of hazardous substances."[83] The 12 principles of green chemistry provide guidelines as to how to achieve greenness. The 12 principles are:[83]

1. Prevention of waste as opposed to retrospective treatment or clean up after it has been created.
2. Atom economical synthetic methods should be utilised to maximise the amount of process materials in the final product.

3. Less hazardous chemical syntheses should be utilised to manufacture chemicals of low toxicity and environmental impact.
4. Designing of safer chemicals that maintain performance levels while minimising toxicity.
5. The use of safer solvents and auxiliaries or their avoidance altogether.
6. Designing for energy efficiency to reduce environmental and economic impacts. Ambient temperatures and pressures should be used where possible.
7. Use of renewable feedstocks where technically and economically practicable.
8. Reduction of derivatives (blocking groups, protection/deprotection, temporary modification of physical/chemical processes) should be minimised or eliminated where possible to reduce synthetic steps and waste.
9. Use of catalysis instead of stoichiometric amounts of reagents.
10. Designing products for degradation so that products do not persist in the environment but instead break down into innocuous degradation products at the end of their lifetime.
11. Real-time analysis for pollution prevention before the formation of hazardous chemicals.
12. Use of inherently safer chemistry for accident prevention to reduce the risk of chemical releases, explosions, and fires.

The replacement of hazardous solvents with a safer alternative is a good example of principles 4 and 5 being applied. Where a solvent cannot be avoided, the replacement of a hazardous solvent with a less hazardous solvent improves the greenness of the process. The use of clean synthetic technologies, such as solvent-free reactions[84] and reusable catalysts with energy efficiency in mind is also vital to achieve greenness.[85] Due to the high levels of solvent release into the atmosphere by evaporation, solvents should be developed which break down innocuously in the environment, thus adhering to principle 10. Many of the principles of green chemistry can be adhered to if clean synthetic technologies are used effectively.

Solvent-free chemistry helps reduce the amounts of auxiliaries required in a process (principle 5).[84] Although solvents offer many benefits to a process, such as lowering viscosity, absorbing heat and facilitating the interaction of reactants, they are not always necessary and in such cases process greenness can be significantly improved.[84] It seems imprudent to use solvents to make solvents so this should ideally be avoided.

Catalysts lower the activation energy of a reaction and accelerate the reaction rate (without affecting the overall Gibbs energy), resulting in reduced energy requirements (principles 9 and 6 respectively).[86] The use of suitable catalysts can increase yields and selectivities, thus avoiding the production of waste or stoichiometric amounts of by-products from the use of reagents.[87,88]

They should ideally be easy to produce, low-toxicity, non-corrosive and highly reusable.[88] Catalysts can be classified into two main types: homogeneous and heterogeneous.

1.3.1 Homogeneous catalysts

Homogeneous catalysts are soluble in the reaction medium which can lead to separation issues at the end of the process. In the case of acid catalysts, corrosion of stainless steel reactors and piping can occur unless coated with acid-resistant material such as glass or a fluorinated polymer. Neutralisation is often required to retrieve products, which results in the loss of the catalyst, and generates large amounts of waste.[89] However, not all homogeneous catalysts are highly corrosive (*e.g.* metal catalysts) and neutralisation is not always necessary.[90] In fact, solvent production is an area which is particularly suitable for homogeneous metal catalysts. Solvents tend to be small, volatile molecules which can be separated by reactive distillation,[90] potentially allowing high catalyst reusability.

1.3.2 Heterogeneous catalysts

Heterogeneous catalysts are porous materials such as zeolites, clays, doped carbon materials, silica and metal oxides. The material itself can catalyse some reactions (such as silica)[91] but catalyst centres can also be doped onto the surface (such as palladium on carbon).[92] Heterogeneous catalysts tend to be highly reusable and non-corrosive, although leaching or deactivation of the active sites can be an issue with some catalysts.[92] In addition, different pore sizes, surface areas, hydrophobicity/hydrophilicity, acid/base strengths and acid/base types (Lewis or Brønsted) can be obtained in heterogeneous catalysts, allowing more control over selectivities.[93]

Zeolites

Synthetic zeolites are highly tuneable porous materials, most commonly aluminosilicates although other heteroatoms can be used instead of aluminium. Due to the difference in valency between Si and Al (or another heteroatom), the solid has an overall negative charge. The negative charge is balanced by positively-charged cations within the pores. Ion exchange of the ammonium or metal cations in the pores with protons generates an acidic surface.

Aluminosilicate zeolites are synthesised by many methods, but usually involve the mixing of a silica source, an alumina source, and a templating agent in controlled conditions.[94,95] A wide range of structural frameworks with different pore sizes can be produced by varying the synthesis conditions, such as the silica and alumina sources and ratios, the templating agents, reaction temperatures, times and pressures.[95] The different pore sizes can influence the selectivities of

reactions when used as catalysts and as such, they are of huge importance in the field of catalysis.[96] Increasing Si/Al produces a zeolite with fewer, but stronger, acid sites and higher hydrophobicity.[96] Some common zeolites and their properties are shown in Table 1.2.

Table 1.2. Pore sizes of several zeolites with different frameworks. Data taken from the International Zeolite Association Structure Commission (IZC-SC).[97]

Zeolite	Framework	Pore dimensions (Å)	No. of atoms in ring
Faujesite[98]	FAU	7.35 x 7.35 x 7.35	12, 6, 4
Beta[99]	BEA	5.95 x 5.95 x 5.95	12, 6, 5, 4
Mordenite[100]	MOR	1.57 x 2.95 x 6.54	12, 8, 5, 4
ZSM-5[101]	MFI	4.7 x 4.46 x 4.46	10, 6, 5, 4

Montmorillonite clay

Montmorillonites are layered, two-dimensional aluminosilicate structures composed of tetrahedral Si and octahedral Al bridged by O atoms.[102] The presence of other metal centres such as Fe^{2+} or Mg^{2+} in place of Al^{3+} results in an overall negative charge on the solid.[103] Like in zeolites, this is countered by interlamellar cations such as Na^{+} or K^{+} which can be exchanged with protons by acid treatment to produce solid acid catalysts.

Table 1.3. Properties of the K-series of montmorillonite clays produced by Süd Chemie.

Clay	Si/Al	Number of sites (mmol m^{-2})	Distribution of 0-140 Å pores (mL g^{-1})	Surface area BET (m^2 g^{-1})
K5	7	0.27	0.18	200
K10	10	0.20	0.26	240
K20	12	0.19	0.30	240
K30	16	0.18	0.38	330

Süd Chemie produced a series of montmorillonite clay catalysts called the “K series”, in which neutral clay was treated with boiling hydrochloric acid for various times and concentrations.[104] It

was found that increased acid exposure caused more breakdown of octahedral Al from the solid structure which resulted in increased porosity and surface area (Table 1.3).[104] As the octahedral Al^{3+} centres are responsible for Lewis acidity, their removal results in an overall reduced number of acid sites but a higher number of stronger Brønsted acid sites.[104]

KSF montmorillonite is another acid treated clay, but instead of hydrochloric acid, concentrated sulfuric acid is used instead. The surface area of KSF is generally smaller than the K-series clays, ~10 m^2 g^{-1} compared to 200-330 m^2 g^{-1} for the K-series (Table 1.3).[102] In addition, sulfuric acid is known to leach from KSF, resulting in homogeneously catalysed reactions and thus limiting its use.[105]

Nafion-H

Nafion-H is an acidic form of a perfluorinated resin first produced by DuPont in the 1960's.[106] It is prepared by the copolymerisation of tetrafluoroethylene with perfluorinated vinyl ethers containing terminal sulfonyl fluoride groups to form a branched polymer. Treatment with sodium hydroxide followed by ion exchange with dilute acid yields a perfluorinated polymer with use as a heterogeneous Brønsted acid catalyst.[107,108]

Amberlyst 15

Amberlyst 15 is a solid acid resin which is produced from the copolymerisation of vinylbenzene and divinylbenzene followed by sulfonation.[109] It has a rigid macroporous structure with an average surface area of 42.5 m g^{-1} and pore size of 288 Å.[109] Brønsted acidity comes from the sulfonate groups on the polymer chain.

Sulfated zirconia

Sulfated zirconia is sulfated crystalline zirconium oxide, produced by mixing zirconium gel with sulfuric acid and calcining in air.[110] Depending on the sulfate loading during preparation, the acid sites can be exclusively Brønsted (at higher loading) or a mixture of Lewis and Brønsted (at lower loading), and the hydrophilicity solid acid can be altered.[111] However, in general, sulfated zirconia is more hydrophilic than zeolites of montmorillonites. The crystalline structure contains a mixture of micropores and mesopores[112] Increasing calcination from 400 °C to 800 °C results in reduction of surface area and sulfate sites.[110]

1.3.3 Green metrics

Chemical processes, including synthetic pathways to solvents, should be chosen so that they are atom economical.[113] Atom economy (AE) is defined as the molar mass of the products as a percentage of the total molar masses of the starting materials (Equation 1.18).[113]

Equation 1.18. $$AE = \frac{\sum Molar\ mass\ of\ products\ (g\ mol^{-1})}{\sum Molar\ mass\ of\ starting\ materials\ (g\ mol^{-1})} \times 100\%$$

However, AE is not the only metric used to assess the greenness of synthetic procedures. Other metrics, such as yield, selectivity, E factor,[114] reaction mass efficiency (RME)[115] and process mass intensity (PMI) should be used in combination with atom economy to give a more complete evaluation. Yield and selectivity are vital, as highly selective processes reduce waste and can eliminate the need for separation steps.[116] The E-factor is the mass ratio of waste to products (Equation 1.19).[114] Waste includes all chemicals used throughout the process that are not the final product, including solvents, reagents and process aids except for water.[114] The larger the E-factor, the more waste that has been generated.

Equation 1.19. $$E\ factor = \frac{\sum Mass\ of\ waste\ (g)}{\sum Mass\ of\ products\ (g)}$$

PMI is similar to the E-factor but is the ratio of the mass all materials used to the mass of all products.[117] While PMI is useful in assessing batch reactions, reactions carried out in flow are not assessed fairly as the amount of product produced can be significantly increased against the amount of catalyst used. In addition, recycling of solvent is not considered. PMI can be calculated using Equation 1.20.

Equation 1.20. $$PMI = \frac{\sum Mass\ of\ all\ materials\ (g)}{\sum Mass\ of\ products\ (g)}$$

RME is the mass of products as a percentage of the total mass of starting materials (Equation 1.21).[115]

Equation 1.21. $$RME = \frac{\sum Mass\ of\ products\ (g)}{\sum Mass\ of\ starting\ materials\ (g)} \times 100\%$$

1.3.4 Bio-based platform molecules

The use of renewable feedstocks (principle 7) ensures a sustainable supply of resources for chemical production. Fifteen molecules were identified by the US Department of Energy in 2004 which can be sourced from biomass and can be subsequently converted into higher value chemicals.[118] These bio-based molecules were later termed "bio-based platform molecules"[119] and

were envisaged to supplement or replace the base chemicals of the petroleum industry. The original bio-based platform molecules were highly functional C-1 to C-6 compounds which could be derived from lignocellulose, starch, protein and triglyceride material and were not already super-commodity chemicals.[118] The top candidate molecules were three 1,4-diacids (succinic, fumaric and malic), 2,5-furandicarboxylic acid, 3-hydroxypropionic acid, aspartic acid, glucaric acid, glutamic acid, itaconic acid, levulinic acid, 3-hydroxybutyrolactone, glycerol, sorbitol, xylitol and arabinitol.[118]

The list was revised in 2010 and several other molecules were added to the list and some were removed based on more recent technological advances since the first list.[120] The new platform molecules were ethanol, furfural, hydroxymethylfurfural (HMF), lactic acid, derivatives of glycerol and bio-based hydrocarbons such as isoprene. Those that were removed were fumaric, malic, aspartic, glucaric, glutamic and itaconic acids.[120]

More recently, bio-based platform molecules have been defined as "a chemical compound whose constituent elements originate wholly from biomass (material of biological origin, excluding fossil carbon sources), and that can be utilised as a building block for the production of other chemicals."[119] Based on this definition, bio-based platform molecules are not limited to those listed by the US Department of Energy but instead, any molecule which can be easily produced from biomass is considered a bio-based platform molecule. Many other examples which have received attention in recent years are listed in a book chapter by Farmer and Mascal, such as isosorbide, levoglucosenone, small alcohols, aromatics from lignin, syngas ($CO+H_2$), amino acids, terpenes such as D-limonene and pinene and waxes.[119] A key consideration in the use of platform molecules vs. petrochemical base chemicals is the significant increase in the presence of heteroatoms in former. Many of the proposed platform molecules contain oxygen or nitrogen and

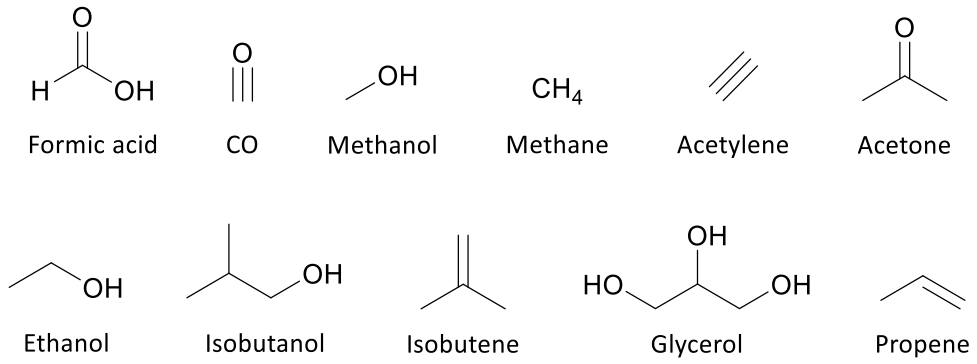

Figure 1.8. A selection of bio-based platform molecules relevant to this work.

these result in functional groups that allow for further chemical modification, something very relevant to the synthesis of new solvents.[119] A selection of bio-based platform molecules relevant in this work are shown in Figure 1.8 and are discussed in the following sections.

Formic acid and CO

Formic acid is a product of the Biofine process along with levulinic acid, furfural and char.[121,122] The Biofine process involves the treatment of lignocellulosic biomass with dilute sulfuric acid at 190-220 °C for short reaction times. This hydrolyses cellulose and hemicellulose to their constituent sugars. Xylose is subsequently converted to furfural while glucose is converted, first to HMF, which in turn breaks down to levulinic acid and formic acid.[121] The lignin fraction produces char. The advantage of the Biofine process is that it does not rely on fermentation processes unlike some of the other platform molecules used in this work. Formic acid is a very useful platform molecule as it can be used for the *in-situ* production of CO,[123,124] which is a key platform molecule used in this work, by treatment with acid. Additionally formic acid can be used to produce H_2.[125]

Methanol and methane

Syngas ($CO+H_2$) is an important platform for the production of bio-based chemicals. While syngas has traditionally been produced by the gasification of coal, biomass can also be used a raw material.[126] Syngas is an alternative source of carbon monoxide (CO) which can be purified and used directly. Alternatively, methanol can be produced from the same platform by the reaction of the two main components syngas ($CO+2H_2$).[126] Methane can also be produced by gasification of biomass waste to form syngas ($CO+H_2$) which in turn can be converted to methane by steam reforming.[127,128] However, technical and economic barriers exist for the gasification route at present which must be overcome.[129] Another source of methane is by anaerobic digestion of biomass, municipal waste and landfill waste.[130–132] However, hydrolysis of the lignocellulosic component is an ongoing issue for all fermentative processes, including anaerobic digestion.[131] Another attractive route to bio-based methane is by the fast pyrolysis of biomass, which is predicted to be comparable to the gasification in terms of efficiency.[133]

Acetylene

Acetylene is currently produced from petroleum sources, usually by steam cracking or partial pyrolysis of hydrocarbons.[134] Methane is a particularly appealing source of acetylene production due to its relatively facile production from biomass, as described above. The partial oxidation of methane gives acetylene, CO and hydrogen and is known as the Sachsse process.[135] methane pyrolysis using high temperature steam (1200 °C) yields acetylene as well as three equivalents of

hydrogen.[134] Both CO and hydrogen gas are two important by-products which are highly important in bio-based chemical production and compliment acetylene production.

Acetone and ethanol

Acetone can be produced by the acetone-butanol-ethanol (ABE) fermentation process,[136] a well-established fermentation process which was a significant source of acetone early in the 20th century.[137] ABE fermentation mainly uses *Clostridium acetobutylicum* or *Clostridium beijerinckii*. Interest in the ABE fermentation process has been growing in recent times due to the interest in bio-based butanol as a fuel.[138] As well as the issue of lignocellulosic biomass hydrolysis, separation of the individual product components is difficult and hinders the commercialisation of ABE fermentation.[139] Ethanol from fermentation is already well-established and produced at a large scale. It is used as a fuel and as a building block for chemicals. It is produced mainly by *Saccharomyces cerevisiae* or *Escherichia coli* and has been extensively reviewed in recent years.[140,141]

Isobutanol

Isobutanol production by fermentation has recently been scaled-up by Gevo,[142] and this year, a second producer, Butamax, have announced plans for its production.[143] The aim of Gevo is to make fuel blends and polyethylene terephthalate (PET) for the production of drinks bottles in collaboration with Coca-Cola. Isobutanol itself can be used as a blendstock for fuel, but Gevo also produce isobutene, another platform in this work, by the dehydration of isobutanol. Isobutene is dimerised to produce isooctane, a branched alkane which can be used as a main fuel component. However, Gevo use corn for the production of isobutanol at present, which is not ideal due to competition with food supplies and indirect land use change.[144] The use of biomass waste, as in all fermentation processes, would make isobutanol an attractive platform for the production of chemicals.

Isobutene

Isobutene can be produced directly by fermentation and has been scaled up by Global Energies.[145] The advantage of isobutene production by fermentation compared to many other fermentation products is that isobutene is a hydrophobic gas, thus, readily separates from the aqueous fermentation broth. In addition, its vapour pressure is very high (2.6 bar at 20 °C)[146] and its boiling point is very high (-7 °C) which allows and efficient separation from carbon dioxide and water.[147]

Glycerol and propene

Finally, glycerol can be produced by the acid or base esterification of triglycerides. Triglycerides are the main component of used cooking oil (UCO) and break down upon acid or base treatment into one equivalent of glycerol and three equivalents of fatty acid esters. Fatty acid esters have uses as fuel or solvents[148] but glycerol, as well as being used as a solvent itself,[149] can be derivatised to produce many other chemicals,[150] solvents being of particular interest in this work. Glycerol can also be hydrogenated and then dehydrated to produce propene.[151] Propene can also be synthesised from metathesis between ethene and butene.[152–154] Ethene can be made from the dehydration of ethanol[155,156] while butene is the product of dimerisation of ethene.[157]

1.4 Bio-based solvents

Bio-based solvents must contain a certain minimum amount of bio-based carbon.[158,159] In Europe, the minimum amount is 25%,[160] and in the US, different thresholds of bio-based carbon are placed on different solvent products. All bio-based products and their bio-based carbon content is added to the "BioPreferred" catalogue whose aim is to encourage the use of bio-based products.[161] Bio-based carbon is that which has been sourced from biomass, ideally from waste streams from the biomass production/consumption industries such as agriculture and food industries, so as not to compete with food sources.[159] Examples are used cooking oil waste,[162,163] citrus peels[60,163] and lignocellulosic waste such as wheat straw, wood or sugarcane bagasse.[164] The renewability of bio-based carbon means it can provide a sustainable raw material supply for chemical production into the future. It also closes the carbon-cycle resulting in no net increase in carbon dioxide emissions.[165]

Bio-based solvents are a sub-category of "green solvents" which is a term that covers bio-based solvents, some ionic liquids, some supercritical fluids and other safer solvents (low toxicity/flammability/ozone depletion),[166] and should adhere to the twelve principles of green chemistry in their synthesis and use.[83,167] Although the perfect solvent which adheres to all twelve principles of green chemistry does not exist, a balance must be struck which takes into account the application for which it is to be used and the risk of human or environmental exposure.[168] Bio-based solvents should have low toxicity, low flammability (high flash point, LEL and AIT), should not form peroxides in ambient storage conditions or deplete the ozone layer.[16,168] Their production from biomass must also be atom-efficient, minimise waste and energy losses, avoid the use of auxiliaries and toxic derivatives, and use catalysts as opposed to stoichiometric amounts of reagents where possible.[168] The benefit of many bio-based solvents (with the exception of D-limonene and *para*-cymene) is that their oxygen content remains high, meaning

mass loss during synthesis from the raw biomass is reduced.[169] In addition, as biomass is already oxygenated, few synthetic steps to add or remove functionality are needed. In contrast, petrochemicals consist almost entirely of carbon and hydrogen (with small amounts of sulphur and nitrogen), thus requiring extra synthetic steps to add functionality.

In summary, bio-based solvents can be an improvement on traditional solvents in all aspects. Many traditional solvents could potentially be sourced from biomass, but the bio-based version will retain the hazards associated with its petroleum-based equivalent, and will therefore deviate strongly from the twelve principles of green chemistry.

1.4.1 Current state-of-the-art in bio-based solvents

There has been huge interest in the development of bio-based solvents in recent times, reflected in the many review articles[168–171] and legislation[158,160] covering the topic as well as the many bio-based solvents that have been proposed.[162,172–174] The range of bio-based solvents must be comparable to what is currently available for conventional solvents; a wide range of physical and solvent properties must be represented.

HSP maps of δ_H versus δ_P are a useful tool to help visualise solvent properties in two dimensions. δ_D is often omitted from HSP solvent polarity maps as the variation between solvents is not as large as the other two axes, so a designated axis on a two-dimensional map is not warranted.[35] If a more in-depth examination is required to separate two solvents/solutes that are placed in close proximity on the two-dimensional map but behave differently, δ_D can then be considered either by the use of two maps (one containing high δ_D molecules and one containing low δ_D molecules) or different labels for molecules with high δ_D (triangles or squares instead of circles). Certain classes of molecules tend to have high δ_D (chlorination hydrocarbons, aromatic hydrocarbons and cyclic carbonates) and thus, the placement of molecules on the δ_D axis is relatively predictable.[35] Plotting bio-based solvents on a HSP solvent polarity map of δ_H versus δ_P shows the variety of solvent properties represented by bio-based solvents, but also highlights some gaps (Figure 1.9).

When the physical properties of bio-based solvents (boiling point, viscosity, etc.) are analysed, it is clear that some combinations of solvent/physical properties have not seen the same high level of progress as others. For example, an easy-to-remove, bio-based dipolar aprotic solvent remains elusive.[57] Additionally, easy-to-remove non-polar solvents are in short supply and safety (peroxide formation) is an issue for those that have so far been developed.[172] The challenge with the development of non-polar solvents from biomass is that biomass is highly functionalised with

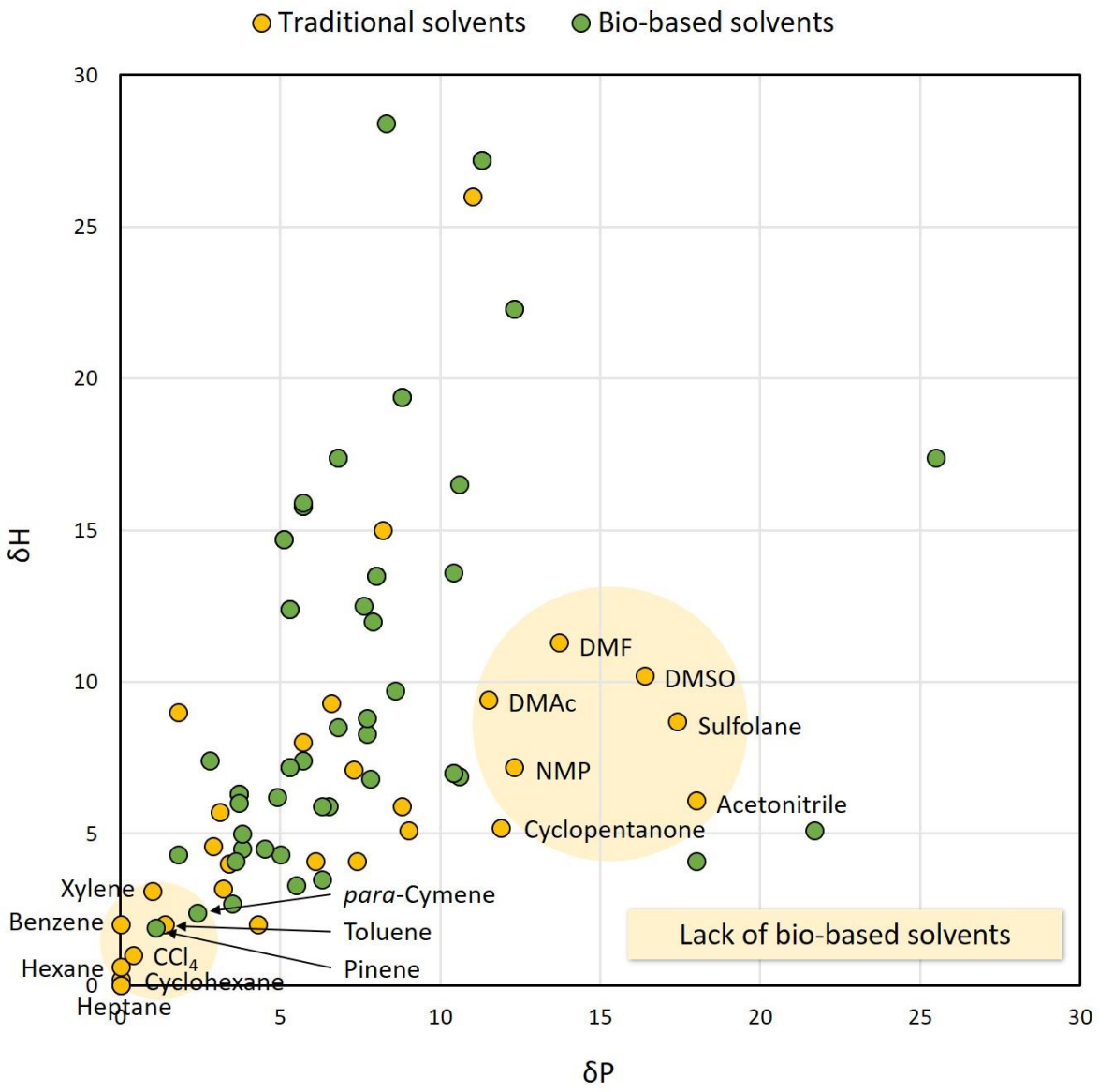

Figure 1.9. HSP solvent map showing bio-based solvents (green circles) and petroleum-based solvents (yellow circles). The areas in pale yellow are regions with a lack of representation by bio-based replacement solvents.

electronegative O atoms whereas traditional non-polar solvents tend to be either hydrocarbons or chlorinated hydrocarbons (Figure 1.9). Removing functionality from biomass is possible but what is left often closely resembles the target traditional solvents for replacement, *e.g.* removing all functionality from glucose yields hexane. Ethers tend to have the required low polarity but suffer from peroxide formation in ambient conditions. On the other side of the HSP map, the opposite problem exists. In this region, amides and sulfur-containing solvents appear, but they suffer from high toxicity and the potential emission of NO_x and SO_x into the atmosphere.

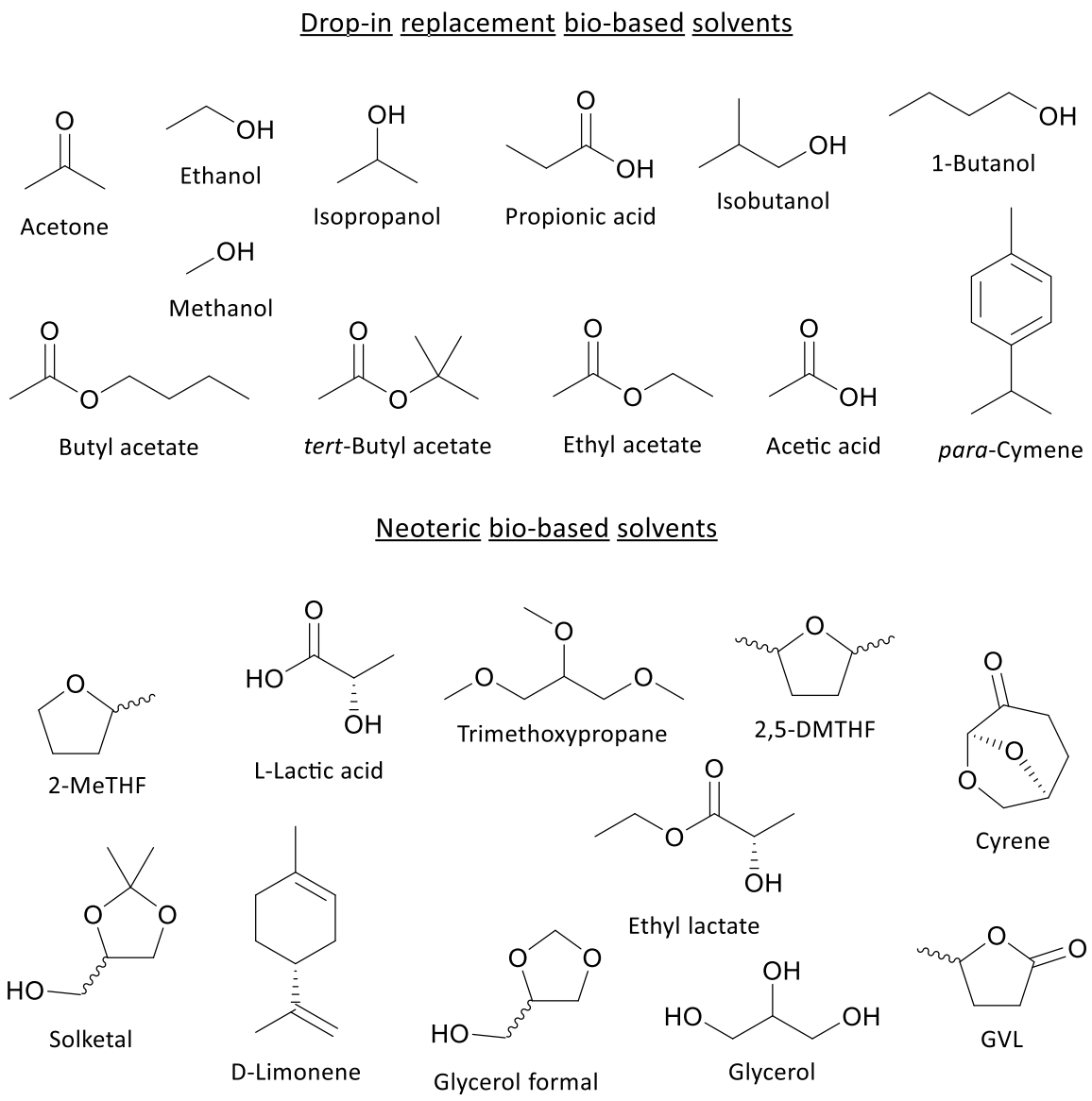

Figure 1.10. Neoteric and drop-in replacement bio-based solvents.

Eliminating N and S leaves only electronegative O to add the required polarity and limits the possible functionality. Ketones and esters are not polar enough to replace many dipolar aprotic solvents whereas lactones and cyclic carbonates possess the necessary polarity but are susceptible to nucleophilic attack, limiting their use. Bio-based solvents can be further grouped into two main categories. Many names have been assigned to different categories of bio-based solvents but in this thesis "neoteric" bio-based solvents and "drop-in replacement" bio-based solvents will be used. "Neoteric", is used as they are structurally different from traditional solvents and refer to solvents which are sourced almost exclusively from biomass. Examples are D-limonene, 2-methyltetrahydrofuran (2-MeTHF) and glycerol. Drop-in replacement solvents refer

to solvents which are structurally identical to traditional solvents but which have been produced using bio-based platform molecules. An example is ethyl acetate which is primarily manufactured from petroleum but which is also produced from bio-based ethanol.[175,176] Bio-based ethanol can of course be used as a drop-in replacement solvent too. Figure 1.10 shows examples of both neoteric and drop-in replacement solvents. [177]

Neoteric solvents

Many neoteric bio-based solvents have been recently proposed and some are shown in Figure 1.10.[118–120,178,179] L-Lactic acid can be produced by the fermentation of biomass[180] and can be used as a solvent in its free acid form.[181] Ethyl lactate has also recently been proposed as a solvent with unique solvent properties due to the combination of ester and hydroxyl functionality.[170,173] Used cooking oil can be treated with acid or base to produce glycerol and fatty acid methyl esters (FAME), both of which can be used as solvents.[148,182,183] Reacting glycerol with formaldehyde or acetone produces the solvents glycerol formal[184,185] and solketal[186] respectively. Terpenes have long been used as solvents in paint thinners, for example in turpentine where pinene isomers are the major component. More recently, D-limonene has gained a lot of attention recently as a replacement for hydrocarbon solvents for synthetic chemistry.[179] Isomerisation and dehydrogenation to give *para*-cymene is preferred, as the use of D-limonene in many applications may be limited due the presence of chemically reactive alkene groups.[187,188] Carbon dioxide is another bio-based platform molecule which can be utilised to produce green solvents. Recently, propylene carbonate has received much attention as a bio-based dipolar aprotic solvent, for example, in the Heck reaction[189] and peptide synthesis.[190] There are a range of solvents that can be produced from the HMF platform such as γ-valerolactone (GVL), also a dipolar aprotic solvent,[191,192] while 2-MeTHF[172] and 2,5-dimethyltetrahydrofuran[193] are low-polarity ether solvents. 2-MeTHF is an example of a bio-based solvent which is produced on a commercial scale.[194,195] Cyrene and its derivatives[196] are neoteric solvents which are produced commercially from cellulose-derived levoglucosenone.[174]

Drop-in replacement solvents

Drop-in replacement solvents are traditionally used solvents whose starting materials can be easily switched to a bio-based drop-in replacement for their traditional petrochemical starting materials.[119] Shown in Figure 1.10 are a range of common esters, acids, alcohols and ketones for which methanol, ethene, propene and isomers of butene are the petrochemical starting materials. A drop-in replacement for methanol can be produced from bio-based syngas,[197,198] and many acids and alcohols can be produced by fermentation.[136,199,200] Many more traditional solvents can be

synthesised using bio-based drop-in replacement starting materials but only those which scored well in the CHEM21 solvent selection guide have been shown.[201]

The advantage of using drop-in replacement solvents over neoteric bio-based solvents is that they can easily replace their petrochemical equivalents in downstream applications with no changes to infrastructure, legislation or process.[119,202]

1.4.2 Challenges facing bio-based solvents

There are many challenges for neoteric bio-based solvents: manufacturing processes must be optimised to compete economically with traditional solvents: downstream uses of bio-based solvents may require new infrastructure; markets for new products and processes, which use bio-based platform molecules and neoteric and drop-in bio-based solvents must be established and matured; toxicology data and regulatory approval (for example REACH) must be obtained for neoteric solvents;[3] and consumer acceptance must be earned.[119] However, these challenges are offset by the long-term benefits of the bio-based economy, which are sustainable supplies of resources, less-toxic products, potential economic benefits and the huge research and business opportunities it presents.[119]

1.5 New solvent selection

Solvent selection has become one of the most important topics in green chemistry in recent years due to the large volumes in which solvents are used (over 80% of the total mass in a batch-type synthesis in the pharmaceutical/fine chemical industry in 2007/08,[117,203] although this may have fluctuated in recent years). Simply switching to a greener process solvent can have huge environmental, health and safety benefits. Since the 1960s, new knowledge of the toxicity and environmental issues of chemicals has led to shifts from one solvent to another. Legislation has also assisted in forcing chemical manufacturers to choose safer solvents,[3] but often the replacement solvent is just a short-term solution until it, in turn, is also subject to scrutiny. For example, toluene was typically used as a replacement for the carcinogenic benzene,[204,205] only for toluene to be later found to be damaging for the unborn child.[1,2] It is only in recent times that proactive efforts have been made to not only use alternative solvents but also to find bio-based neoteric solvents which can totally overhaul traditionally used solvents with the environment, health and safety in mind from the outset.[166,206]

Many tools and approaches are available which aim to assist with solvent substitution, such as solvent guides and computer software. Solvent guides provide useful information about greener

and safer solvents which are currently available and are a good place to start in the search for greener solvents.[201,207–211] However, a full investigation is required to discover new molecules which can be used as bio-based solvents, for which computer software can be of assistance.[44,212] A stepwise method of solvent selection has also recently been published which uses a combination of computer software and experimental work.[213]

1.5.1 Solvent selection guides

The pharmaceutical companies Pfizer,[214] GlaxoSmithKline (GSK)[207,215] and Sanofi[208] have each published solvent guides in recent years. Other groups have also proposed their own guides such as the American Chemical Society Green Chemistry Institute's (ACS-GCI) Pharmaceutical Roundtable.[209] Each guide is presented differently and takes different factors into account, which results in conflicting scores for many solvents.

The CHEM21 guide is the most recent guide,[201] and harmonises the guides of GSK, AstraZeneca (unpublished) and ACS-GCI[210] into three environment, health and safety (EHS) categories. In general, solvent guides consist of several categories by which a solvent is assessed (for example, environment, health, safety, flammability, waste). Scores are assigned in each category and a traffic light system is usually employed to quickly identify green solvents, hazardous solvents, and those in between. An overall assessment of greenness is then assigned based on the scores in each category. Each guide prioritises different categories depending upon their processes, experience and policies.

The advantage of solvent guides is that they are easy to use and greener solvents can be quickly identified. Some useful solvent properties which further help in the choice of solvent substitute, such as boiling point and melting point, are also displayed in many guides. The reduction of hazardous solvent use in chemical labs demonstrates the value of solvent guides. For example, Pfizer achieved a 50% reduction in the use of chlorinated solvents and a 97% reduction in the use of dangerous ethers in just two years.[211]

However, there are limitations to solvent guides. One is that the guides can be over-simplified, and specific positive or negative aspects of solvents in certain applications can be hidden. In addition, different factors are taken into account in each guide and the importance of each factor is weighed differently. This is shown in a recent review of solvent guides where the scores for dipolar aprotic solvents in each guide are compared[211] The variance in scores for acetonitrile is particularly wide with GSK classing it as problematic, AstraZeneca classing it as hazardous (in an unpublished guide), Sanofi and the ACS GCI classing it as recommended and CHEM21, who analysed the other

guides as part of their assessment, classing it as problematic. The reason for this variance is simply contrasting company policies. To add to this problem, many solvent guides do not publicise the calculations from which solvent assessments are based. The CHEM21 guide is an exception to this.

Solvent guides are also limited to solvents for which data is currently available and therefore neoteric solvents are not shown. The CHEM21 guide includes some less-classical solvents and provides a free-to-use spreadsheet, into which some physical properties and global harmonised system (GHS) hazard statements can be inputted to generate evaluations of greenness. However, the problem of available data remains as GHS hazard statements must be available, which is not always the case for emerging neoteric solvents. The CHEM21 consortium have also published a free-to-use metrics toolkit which consists of two spreadsheets. The first spreadsheet can make preliminary assessments of flammability, health and safety based on GHS codes which can be obtained from datasheets.[201] However, often even GHS codes are unavailable for new molecules and therefore the assessment is not always useful. The second spreadsheet assesses the greenness of the synthetic route to new molecules using yield, conversion, selectivity, AE, RME and PMI as metrics.[216] It also draws attention to any highly hazardous solvents, reagents and critical elements used in the synthesis by highlighting them with red flags. The use of these two spreadsheets in combination provides an excellent initial assessment of new molecules.

Finally, none of the guides contain a category which considers whether a solvent is bio-based or not. GSK includes a "cradle-to-gate" life-cycle assessment (LCA) category which scores solvents based on their production. However, details of how conclusions were reached were not disclosed solvents do not appear to be scored better if they are bio-based.

1.5.2 ICAS ProPred/ProCAMD

The ideal replacement for a hazardous solvent often does not exist in a guide. In this case, new solvents must be proposed, and this is where computer software is useful. ProPred[217] and ProCAMD,[218] developed at the Technical University of Denmark (DTU), are two pieces of software which were used in this work.

ProPred works in the "forward" direction,[217] meaning that a structure of interest can be drawn into the program and its properties predicted using group contribution theory. This is useful when new bio-based molecules have been discovered but their properties are unknown. A quick prediction of their properties allows easy identification of potential applications. For example, for a compound to be used as a solvent it must be a liquid at ambient temperatures and must be inert

in a range of conditions. Other properties such as polarity might indicate it can be used as a solvent in specific applications.

ProCAMD works in the "reverse" direction; desired properties are inputted and molecular structures which fit the criteria are generated.[218] First, target properties must be identified (*e.g.* boiling point, melting point, functionality, etc.). Molecular structures are then built by combining first and second-order groups until feasible, complete molecules are formed.[218] As molecular structures are generated, group contribution theory predicts their properties and all suggested molecules are screened for their suitability against the inputted constraints.[218] Finally, a list of molecules which fit all criteria is produced. Further analysis and screening steps can be done *in silico* using a variety of programs however, this is not necessary unless the list of candidate molecules is so large that to obtain experimental data would be time and resource consuming. In addition, the margin of error will increase as more computational steps, which are based on predictions, are added.[218] In cases where the number of candidate molecules is small, a more efficient final screening method is to manually search databases to find any relevant experimental data. The best candidates can then be identified.

This is a very quick and easy way of finding new solvents for a given process, however it is not without limitations. As previously stated, inaccuracies in predictions exist which means that any predicted properties must be confirmed experimentally.[218] Additionally, group contribution theory struggles to differentiate between isomers and account for intramolecular interactions.[44] This does not mean that computer-aided molecular design is useless; it saves time, materials and cost by reducing the number of possible candidate molecules for a given purpose with a high degree of accuracy. Another limitation is that the program must be able to generate all functional groups based on a finite set of first-order groups. This is not always the case, as will be demonstrated in Chapter 2.

In the case that no suitable molecules are suggested by ProCAMD, a manual search for new solvents can be carried out. This can be a beneficial exercise because of the aforementioned limitations of computer-aided molecular design: the software will not predict every molecule correctly and the relevant groups may not be included in the software. Despite exact property values not being accurately predicted all the time, trends will emerge among different classes of molecules (ketones, esters, ethers, etc). For example, it could be observed that ethers tend to be close to the target properties while ketones, esters and alkanes do not. In such cases, a manual investigation into ethers may reap rewards. This includes searching databases such as

Chemspider[219] and PubChem[220] for their experimental properties as well as checking for specific issues with ethers and ways to prevent them.

1.5.3 GRASS and the "top-down" approach

GRASS (GeneratoR of Agro-based Sustainable Solvents) is a computer program, developed at Université Lille Nord de France by Moity *et al.*, which can suggest new bio-based molecules and synthetic routes to them.[212] 53 chemical transformations can be applied to a chosen bio-platform molecule using a selection of reagents. Chemical transformations and reagents are specifically chosen so that only those which adhere to the principles of green chemistry are included. This generates a list of "first generation" products from which potential solvents may be identified. Moreover, the first-generation products can undergo additional chemical transformations and form further generations of products. Due to the large number of generated products, a screening process must be carried out to find the best candidates. No specific screening method is required; the only limitation on which methods can be used are the expertise of the chemist and/or availability of computer software.

In one example, the bio-based platform molecule, itaconic acid, is selected as the target molecule.[212] The co-reactants with which it can react are the inorganic O_2, O_3, H_2, H_2O, H_2O_2, NH_3, and SO_3, as well as the organic carbon dioxide, carbon monoxide, formaldehyde, methanol, glycerol, acetic acid, methylamine, ethylene oxide, acetone and ethene. The target molecule and co-reactants can react by any of the 53 chemical transformations in GRASS. The first generation produced 40 molecules, which were screened based on CAS registry and boiling/melting point (it was established that a potential solvent must be a liquid at room temperature). In the end, 2-methylenebutane-1,4-diol was the only candidate to fit all requirements.

Another application of GRASS is in a "top-down" approach,[221] where the solute is first identified and classified by its HSPs. GRASS is then run using a selection of bio-based platform molecules and co-reactants to generate a list of products. In this case, the products must be assessed for their HSPs and any other pre-established criteria and ranked according to their suitability using predictive software. An example of the top-down approach in practice is the search for a bio-based solvent for nitrocellulose.[221] Five candidates were suggested after screening, 1,2-diactetin, 1,3-diacetin, triacetin, triproprionin and 3-methylamino-1,2-propanediol, which were all able to dissolve nitrocellulose.

The GRASS method is an excellent method of investigating potential solvents from a given bio-based platform molecule, using clean synthetic pathways. Like other predictive methods, results

must be experimentally verified, but the use of the software provide a thorough and quick search for synthetic routes to new solvents. the top-down approach provides a focussed method of finding solvents to fit a pre-defined purpose.

1.5.4 Mixed method

The approach of Jin *et al.* consists of ten steps which are described below.[213] Simpler steps are undertaken earlier in the process to avoid wasting time and resources, with more complicated assessments carried out later.

1. The properties of the subject solvent such as the KT parameters, volatility, and flammability, must be determined. These properties are available in chemical databases such as ChemSpider[219] and PubChem[220] for many traditional solvents.
2. Potential replacement solvents should be identified either using computer aided molecular design or using chemical intuition to derivatise bio-platform molecules.
3. Unknown properties of each candidate solvent should be calculated *in silico* to allow fast screening. HSPiP is suggested as a method of calculating solubility properties to assist with this.[40]
4. Synthetic routes to the best candidates, which adhere to the principles of green chemistry, must be proposed. The literature can be searched to help identify synthetic routes and their greenness should be properly assessed using published metrics toolkits.[216]
5. Proposed routes must be experimentally verified and optimised. Scale-up of production to 1 L is suggested to provide material for further testing and to demonstrate its feasibility.
6. Physical properties must be experimentally verified, as inaccuracies often exist in predicted values using computer modelling software.
7. Several model reactions have been proposed in recent years to help classify solvents and these should be carried out.[60,174,222] The Ames mutagenicity test[74] is recommended as a preliminary toxicity test as it is quick and cheap.
8. A techno-economic assessment should be carried out. However, it is acknowledged that this is not always possible as lab-scale data can be misleading. Therefore, the assessment should be based on larger scale production. This is not available in most university labs so collaboration with industrial partners is encouraged.
9. The synthesis should be assessed for its greenness, also using large-scale manufacturing data where possible. The CHEM21 solvent selection guide tool can assist in this and facilitates comparisons with traditional solvents.
10. A life-cycle assessment of the solvent should be carried out which considers its emissions and social implications over the course of its lifetime.[223,224]

This approach provides a comprehensive method of discovering new solvents, classifying them and determining their greenness. It does not rely on one method, but instead, uses any tools available to a chemist, ensuring a wide-ranging search and assessment is carried out. It acknowledges the difficulties in techno-economic assessments and life-cycle assessments by proposing them in the final steps, and encourages collaborative efforts between industry and academic research groups.

1.6 Introduction to the solvent selection process carried out in this thesis

A mixed method of solvent selection, similar to that of Jin *et al.*, has been proposed and implemented in this work.[213] It uses aspects from each of the methods described in Chapter 1 and is illustrated in Figure 1.11.

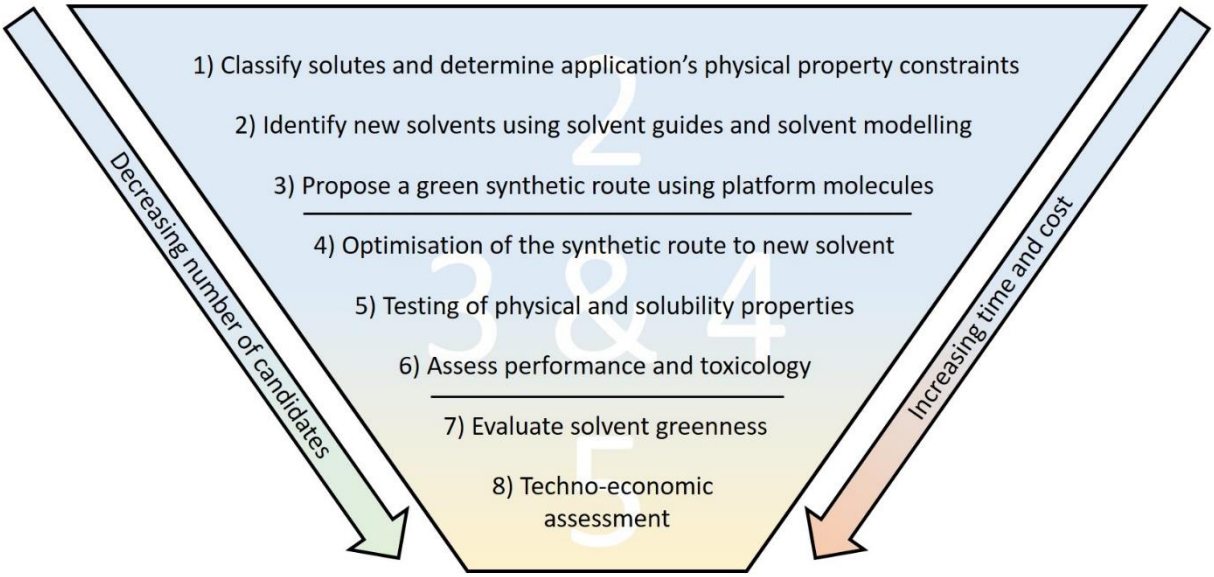

Figure 1.11. Flow chart showing the proposed steps for developing new solvents and the chapters in which they are described. The method is similar to that of Jin *et al.*[213]

In Chapter 2, the polarity requirements of a new target solvent are identified by determining the target solute polarities using HSPs and desired physical properties are established. As the goal of this project was to find a suitable replacement for toluene in synthesis of adhesive polymers, a range of representative polymers were selected as target solutes. A search for new solvents is then carried out using solvent guides and computer aided molecular design software (ProCAMD).[218] A manual search using chemical intuition is also carried out due to limitations in accuracy of computer-aided molecular design. Once candidate solvents have been identified, synthetic routes

from biomass are proposed. At this point, greenness is targeted but not fully assessed until a later stage. Reactions should adhere to the principles of green chemistry as much as possible.

Once a synthetic route to a candidate solvent has been proposed, it must be carried out experimentally and optimised. Sufficient solvent must be prepared to test its properties and evaluate its performance in several processes (described in Chapters 3 and 4). Physical properties such as boiling point, melting point and density can be easily measured in the laboratory but flammability properties such as LEL and AIT are also very important and should be determined where possible. However, speciality equipment and high costs can be a barrier for the determination of some properties.

Solubility properties should be obtained using KT parameters. Abraham's solvation model should be employed where possible although these require significant experimental work to determine. LSERs using different model reactions can help characterise a solvent and can assist in finding applications for new solvents. Toxicity should be estimated using QSAR methods, such as TEST by the EPA.[72] Predictions must be confirmed experimentally where possible so the Ames mutagenicity test should be undertaken.[74]

Finally, in Chapter 5 the overall greenness of the candidate solvents is assessed using two methods, one of which was proposed in this work and one which uses the CHEM21 metrics toolkit. Combining the data that has been obtained based on the previous steps, a preliminary assessment of greenness can be made. A comparative assessment of the greenness of new solvents is difficult due to the lack of data available at the early stages of development. Data from lab-scale synthesis can be used but this is not representative of large-scale production which has been optimised by chemical engineers in terms of energy efficiency. Therefore, comparisons cannot be made with traditional solvents. However, preliminary assessments of greenness will highlight any obvious issues with new solvents.

A techno-economic assessment is required before large-scale commercialisation to ensure its production is economically feasible. However, techno-economic assessments are very difficult and likely to be inaccurate based on lab scale data. It is more appropriate to carry out this assessment upon pilot scale manufacturing to provide more reliable predictions. Hints about the costs of new molecules are given by their synthesis, and therefore, economic viability should be considered in the early stages of planning. Some synthetic routes are known to be difficult and expensive and these should be avoided. The use of cheap catalysts which have high reusability and simple separation steps go a long way to ensuring an economic synthesis. In addition, wasted

materials tend to result in wasted money, so high yielding, highly atom economic processes should be targeted.

Overall, the intention is to find a solvent which can replace toluene in the polymerisation and coatings industry which adheres to several physical and solubility property criteria. Crucially, it must be safer than toluene, whose use has been restricted under REACH, and it must be sourced from abundant renewable resources. Finally, it must be cheap!

2 Solvent selection process

2.1 Introduction

In this chapter, the process of solvent selection is described. The physical property requirements as demanded by the manufacturing process are first highlighted. Next, the top-down approach of Moity *et al*. is utilised, in which solutes are characterised by their solubility properties to establish polarity requirements for a new solvent.[221]

Using the newly established physical and solubility property constraints, the search for greener solvents began. Solvent selection guides were first consulted to identify potential candidates from those which are already commercially available.[201,208,209,215,225,226] As the list of commercially available solvents in common use is limited and the likelihood of finding a suitable candidate was low, the search then focussed on the generation of new solvents using computer aided molecular design software.[218] A manual search for new solvents using chemical intuition was also carried out, as also recommended by Moity *et al*.,[221] to ensure all possible candidates were generated. Finally, synthetic routes to the top candidates from bio-based platform molecules and using clean synthetic methodologies which adhered to the principles of green chemistry were proposed.[83,119]

Although, a wide range of property data is available for the most common solvents in the literature, often very little is available for "new" molecules and in many cases, conflicting data is provided across different sources. As such, during the solvent search and throughout this thesis, all solvent properties such as boiling points, melting points were obtained from the ChemSpider[219] or Pubchem[220] databases. Both databases display all available data and provide references for the source of the data. Where data was not available from either of these databases, it was predicted using solvent modelling software. Data which has been predicted is highlighted as such.

2.2 The pressure-sensitive adhesive (PSA) manufacturing process and solvent property requirements

The following paragraphs describe specifically Nitto's manufacturing process and not the polymer coating industry in general. All data was provided by Nitto Belgium.

The pressure-sensitive adhesives (PSA) that Nitto produce require a polymer molar mass greater than 30,000 g mol^{-1}. Chain transfer from the polymer to the solvent during the polymerisation reactions must be avoided to achieve these high molar masses.[227] Therefore, a solvent which is to be used in radical-initiated polymerisations must not be susceptible to attack in the radical reaction conditions. The dissolved polymer is then transferred from the polymerisation tank to the coating line.

The carrier is unwound from rolls and coated with the dissolved polymer using rollers. Once the dissolved polymer has been applied to the carrier the solvent must be removed, so the PSA is passed through drying ovens. The solvent must have a sufficiently high vapour pressure to be easily removed in the drying ovens, but not too high to avoid bubbling of the adhesive layer of the PSA. As the vapour pressure is often unknown or incomparable, the boiling point is used to classify the volatility of potential replacement solvents. Toluene's boiling point (111 °C) was taken as the upper limit and ethyl acetate's boiling point (77 °C) was taken as the lower limit respectively for a potential replacement solvent.

The high temperatures in the drying oven, the presence of gaseous organic solvent and the flow of air mean a risk of explosion is inevitable. However, this risk can be reduced using solvents with a suitable LEL. Again, toluene was taken as the reference and any potential replacement should ideally have an LEL equal to or greater than that of toluene (1.1%). There are exceptions to this which will be discussed in Chapter 3.

The solvent can be retrieved after removal and mostly recycled. Any unrecycled solvent is burnt in an afterburner to provide energy for the production plant. The high temperatures in the inlet lines of the afterburner require a sufficiently high AIT (>250 °C).

Losses of solvent to the atmosphere throughout the process and the burning of solvent for energy result in the potential formation of NO_x, SO_x and ozone depleting compounds.[228] As such, the solvent must only contain carbon, hydrogen and oxygen and the presence of other heteroatoms in the solvents molecular structure is prohibited.

The solvent is stored in tanks on site which are not heated, nor are the pipes to move the solvent around the plant. As such, the melting point of a potential replacement solvent must be below -15 °C to reduce the risk of the solvent freezing in cold conditions.

The physical property constraints are summarised in Table 2.1.

Table 2.1. Physical property criteria for a new solvent as described by Nitto. (a) Data obtained from https://pubchem.ncbi.nlm.nih.gov/. (b) Data measured in this work.

Property	Upper limit	Lower limit	Toluene	Ethyl acetate
Boiling point / °C	111	77	111[a]	77[a]
Melting point / °C	-15	n/a	-93[a]	-84[a]
AIT / °C	n/a	250	417[b]	445[b]
LEL / %	n/a	1.1	1.1[b]	2.0[b]

2.3 Determination of the polymer HSPs and solvent polarity requirements

A representative set of acrylic polymers (P1, P2, P3 and P4) and rubbers (R5 and R6) were chosen for solubility testing. Solvation of all polymers and rubbers is difficult due to the variation in polarity between the acrylic polymers and rubbers; acrylic polymers are polar, while the rubbers are non-polar. Toluene is ideal due its low dipolarity but high polarisability, which allows it to respond to the higher polarity of the acrylic polymers.

2.3.1 Testing method

HSPs were employed to classify the polymers' solubility properties. However, as group contribution theory cannot be used to calculate the HSPs of polymers,[35] an indirect method was employed. The polymers were tested for their ability to dissolve in a range of solvents with known and varying HSPs. Each mixture is scored based on whether dissolution occurred after mixing for at least 24 hours. The results are inputted into HSPiP,[40] which generated solubility spheres for each polymer. An example of a solubility sphere can be seen in Figure 2.1. Small blue spheres represent solvents which dissolved the polymers, while small red cubes represent the solvents which did not. The large green sphere represents the area where solvents that are likely to dissolve the polymer are located and is known as the "solubility sphere". The centre of the solubility sphere is taken to be the HSPs for the polymer being tested.

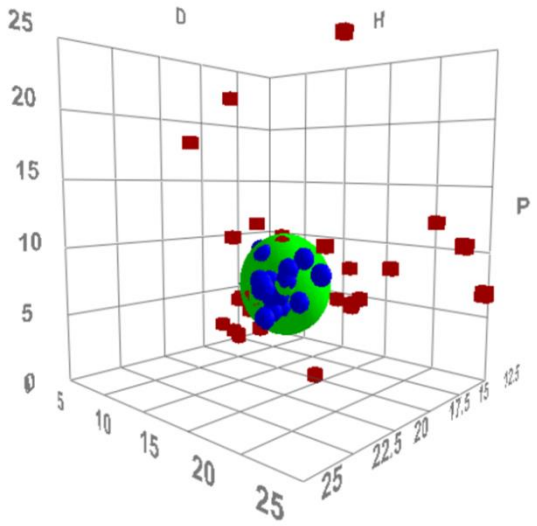

Figure 2.1. A sample HSP map showing blue spheres, red cubes, and the green region in which potential solvents are located.

A solvent which is to be used by Nitto should ideally be able to dissolve all six polymers, so a total solubility sphere which took the data for all polymers into account was generated. Only solvents which dissolve all polymers are located in this region. The coordinates of this total solubility sphere were used as the solubility criteria in Section 2.4.

2.3.2 Scoring of polymers and rubbers

The scoring system is shown in Figure 2.2 and is the method of scoring recommended in HSPiP.[40] Those solvent/polymer mixtures in which one homogeneous phase was observed after mixing were scored from 1 to 4. A clear solution was given the best score of 1, with the score increasing to 4 as turbidity increased. No observable mixing was given the worst score of 6, while slight dissolution was given a score of 5.

The turbidity of a polymer solution is due to its solubility.[229] A polymer which is completely dissolved will move freely around in the solvent, as the free energy of interaction of the polymer with the solvent are at least equal to the free energy of interaction of the polymer self-interactions.[35,229] When solubility is reduced, the polymer self-interactions begin to compete with the polymer-solvent interactions and crystalline regions in the polymer chains are observed.[35] It is these crystalline regions of the polymer chains which fall out of solution and create the turbidity.[230] No dissolution is observed when the free energy of the polymer self-interactions is greater than the free energy of the polymer-solvent interactions.[35] The spectrum of these free energy differences is what is seen in Figure 2.2. Upon quality testing the polymers which were produced from turbid mixtures at Nitto, it was found that the turbidity of the polymer-solvent

mixture did not negatively affect the adhesion and tack of the finished PSA, so a score of 4 was considered to be acceptable. Scores of 5 and 6 were considered unacceptable. The scores of each solvent can be seen in Table 2.2.

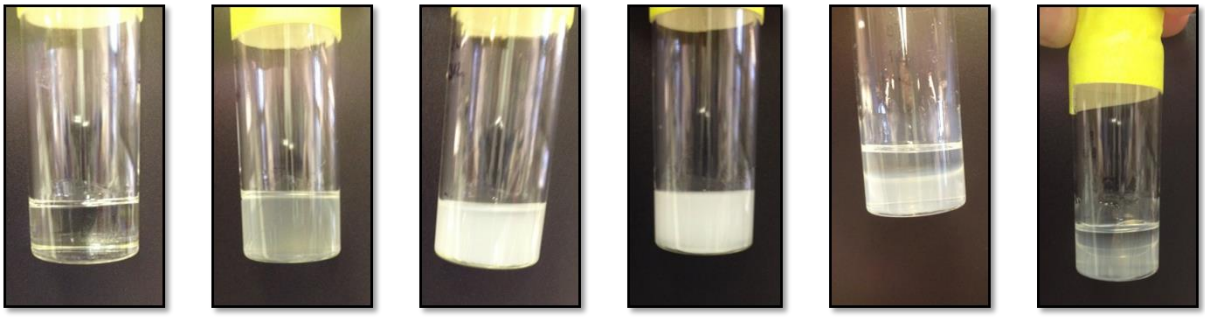

1 2 3 4 5 6

Figure 2.2. Scoring system for polymers mixed with solvents. Scores of 1-6 were given to mixtures depending on the level of dissolution observed.

Table 2.2. Scores for each solvent for their ability to dissolve each polymer.

Solvent	P1	P2	P3	P4	R5	R6
1,1-Diethoxyethane (Acetal natural)	1	2	1	1	6	1
Lactic acid	6	6	6	6	6	6
Propionic acid	1	4	5	1	6	6
Dimethyl carbonate	1	5	1	3	6	6
Diethyl carbonate	1	4	3	1	6	6
Ethyl methyl carbonate	1	4	3	1	6	6
1-Butanol	1	5	5	1	6	6
Ethanol	1	5	6	3	6	6
Isobutyl alcohol		5			6	6
Methanol	4	6	6	6	6	6
1-Propanol	1	5	6	1	6	6
Glycerol	6	6	6	6	6	6
Cyclohexane	1	2	2	2	1	1

Heptane	1	1	1	1	1	1
Anisole	1	1	2	1	6	1
Chlorobenzene	2	2	2	2	1	1
para-Cymene	1	3	1	2	1	1
Cumene	2	3	1	2	1	1
Toluene	1	4	1	2	1	1
Xylene	1	4	2	2	1	1
Propylene carbonate	6	6	6	6	6	6
1,3-Dioxolane	1	4	3	1	6	6
2,2-Dimethyl-1,3-dioxolane	1	3	1	1	6	1
2,2,4-trimethyl-1,3-dioxolane					6	1
Acetonitrile	4	6	6	6	6	6
Dimethyl sulfoxide (DMSO)		6			6	6
Dimethyl Formamide (DMF)	1	5	6	5	6	6
N,N-Dimethyl acetamide (DMAc)	4	5	6	1	6	6
gamma-Valerolactone (GVL)	1	6		6	6	6
N-Methyl-2-pyrrolidone (NMP)	1	2	6	5	6	6
Ethyl levulinate	1		6		6	6
Ethyl lactate	1	5	6	3	6	6
Ethyl acetate	1	4	3	1	6	6
Isopropyl acetate	2	4	1	2	6	5
Methyl butyrate	1	3	1	2	6	1
Propyl propanoate	1	3	1	2	6	6
Propyl acetate	1	3	1	1	6	5
tert-Butyl acetate	2	4	1	2	6	6
tert-Butyl propionate	1	1	1	1	6	5

Chloroform	2	4	2	2	1	1
Dichloromethane	1	3	2	2	6	5
Acetone	1	5	4	1	6	6
Cyclopentanone	1	3	5	1	6	1
Cyclohexanone	1	2	5	1	6	1
MEK	1	4	3	1	6	6
Methyl isobutyl ketone (MIBK)	2	3	1	2	6	6
Citral	1	2	5	5	6	6
D-Limonene	4	2	2	2	6	1
alpha-Pinene	2	3	2	2	1	1
Triethylamine	2	2	1	2	1	1
Cyclopentyl methyl ether (CPME)	2	3	2	2	1	1
1,4-Dioxane		4				
2,5-Dimethyltetrahydrofuran (DMTHF)	1	1	1	1	1	1
Diethyl ether	1	2	2	1	6	1
Di-tert-butyl ether (DTBE)		1	1	1	1	1
Ethyl tert-butyl ether (ETBE)	1	2	2	2	1	1
Isopropyl ether		3	4			
2-Methyltetrahydrofuran (2-MeTHF)	1	2	1	3	1	1
Methyl-tert-Butyl Ether (MTBE)	2	3	1	3	1	1
Tetrahydrofuran (THF)	1	3	5	3	1	1
2,5-dimethylfuran					6	6
2-Methylfuran	2	2	1	2	6	1

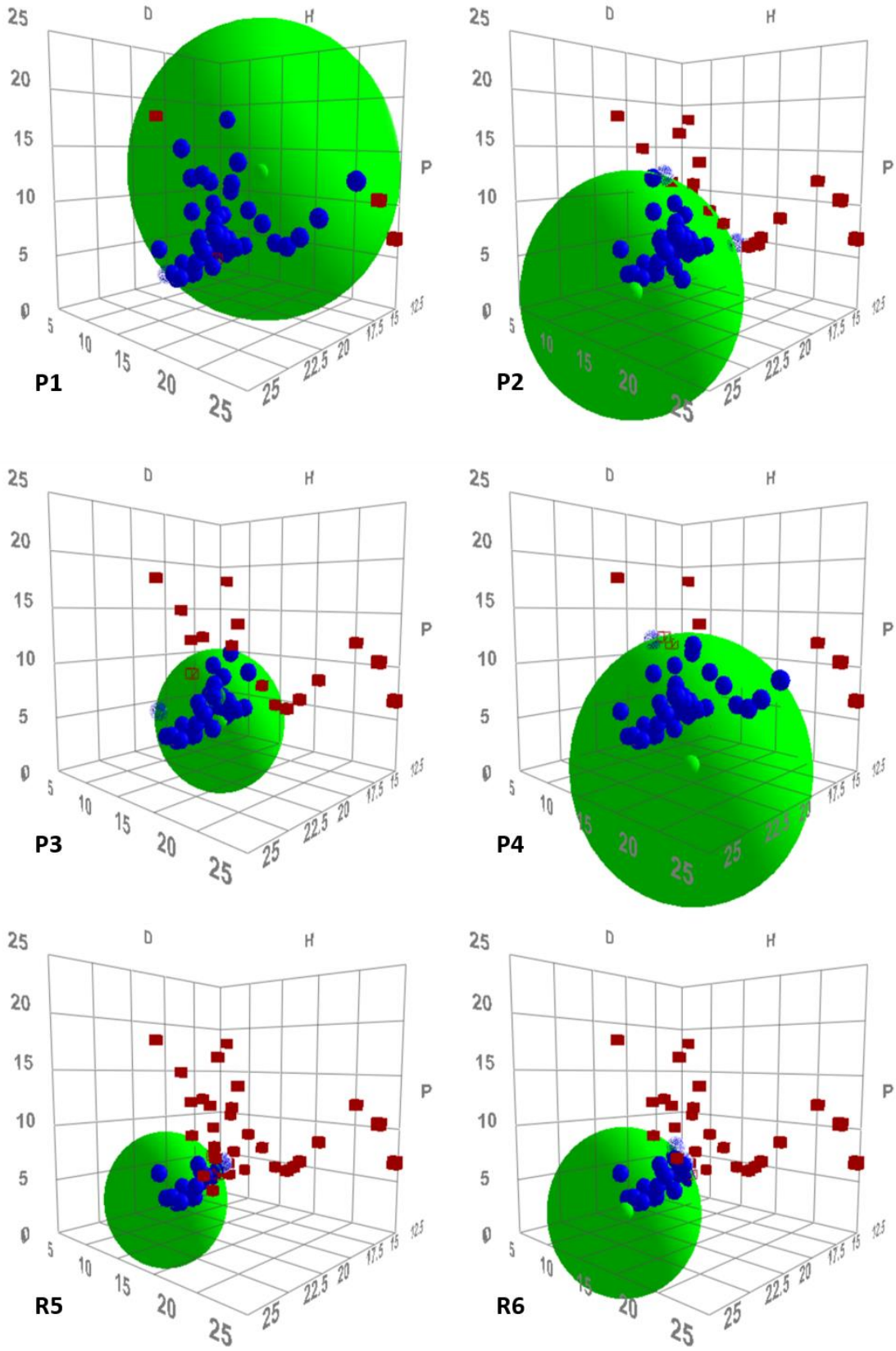

Figure 2.3. HSP spheres for each of Nitto's polymers and rubbers.

Table 2.3. The HSPs and sphere radius of Nitto's polymers and rubbers.

Polymer	δ_D / MPa$^{0.5}$	δ_P / MPa$^{0.5}$	δ_H / MPa$^{0.5}$	Radius / MPa$^{0.5}$
P1	12.0	12.3	6.1	17.1
P2	19.4	0.9	5.6	11.5
P3	15.3	2.7	4.9	8.0
P4	18.1	0.1	11.2	12.9
R5	17.5	0.8	0.0	7.5
R6	18.4	0.0	1.6	9.1
TSS1	16.9	0.2	0.5	6.3
TSS2	17.4	0.6	1.4	7.0

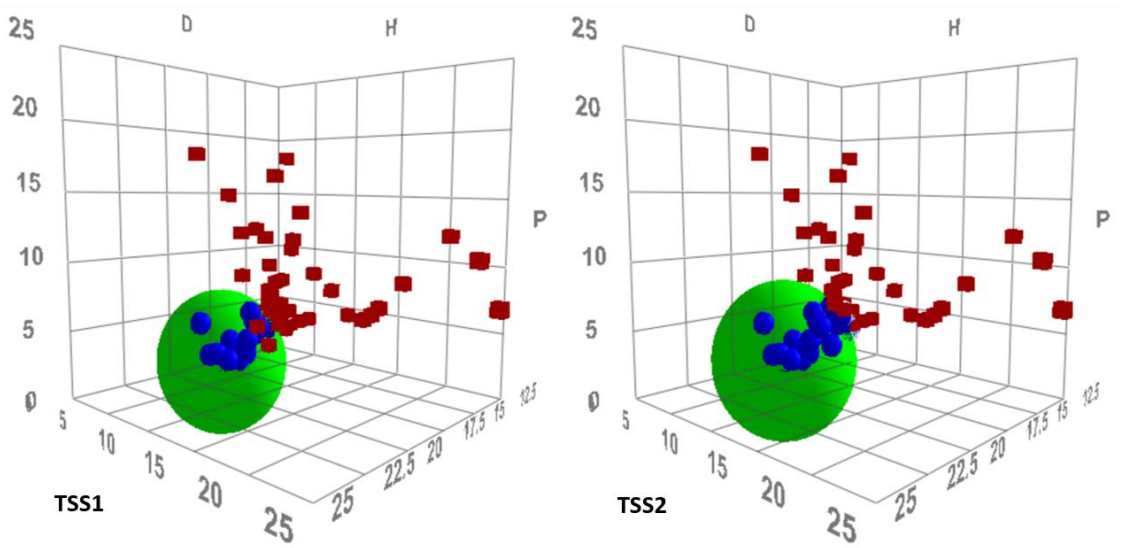

Figure 2.4. HSP maps showing TSS1 and TSS2.

The scores of each solvent were inputted into HSPiP and spheres were generated which can be seen in Figure 2.3. The coordinates of the centre of each sphere were taken as the HSPs for that polymer and can be seen in Table 2.3 along with their radii. Polymers with larger radii were dissolved by a larger number of solvents and vice versa. During the solubility tests, rubber R5 was found to be particularly difficult to dissolve, as illustrated by its small radius (7.5 MPa$^{0.5}$) and lack of hydrogen-bonding ability (0.0 MPa$^{0.5}$). Therefore, it was decided that it was no longer

considered essential for a new solvent to be able to dissolve R5, but it was a bonus if it could. As such, two total solubility spheres were generated: one which considered all polymers and rubbers (TSS1); and another in which rubber R5 was not considered (TSS2). The coordinates and radii of both TSS1 and TSS2 can be seen in Table 2.3 and the spheres can be seen in Figure 2.4. The effect of R5 on the total solubility sphere can be seen in the differences between TSS1 and TSS2. The radius of TSS2 (7.0 $MPa^{0.5}$) is larger than TSS1 (6.3 $MPa^{0.5}$) and its hydrogen-bonding ability is greater (1.4 $MPa^{0.5}$ versus 0.5 $MPa^{0.5}$).

2.4 The search for new solvents

2.4.1 Solvent guide search

The CHEM21 solvent guide was initially searched for potential candidates. First, solvents classed as "Hazardous" were discarded, while those classed as "Recommended" and "Problematic" were considered. Boiling points of solvents displayed in the guide were taken into account. Solvents with boiling points above 111 °C and below 77 °C were omitted. Water was known to be unsuitable and was therefore not included. A list of the remaining potential candidates can be seen in Table 2.4.

Table 2.4. Solvents in the CHEM21 solvent guide with suitable boiling points and which are classed as "Recommended" or "Problematic".

Solvent	Bp / °C	Ranking	Solubility tests
Ethanol	78	Recommended	Fail
Isopropanol	82	Recommended	Fail
Isobutanol	107	Recommended	Fail
Isopropyl acetate	89	Recommended	Fail
MEK	80	Recommended	Fail
Dimethyl carbonate	80	Recommended	Fail
2-MeTHF	80	Problematic	Pass
(TAME)	86	Recommended	Assumed pass
Acetonitrile	82	Problematic	Fail

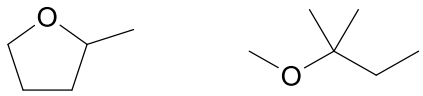

2-MeTHF TAME

Figure 2.5. The two candidates from the CHEM21 solvent selection guide.

All of the solvents in Table 2.4 were tested during the solubility tests, except for *tert*-amyl methyl ether (TAME). The alcohols were all found to be unable to dissolve the polymers and rubbers. 2-Butanone (MEK) was able to dissolve the polymers but not the rubbers and acetonitrile and dimethyl carbonate were unable to dissolve the polymers and rubbers (Table 2.2). Therefore, only two solvents remained from the CHEM21 solvent selection guide, 2-MeTHF and TAME. TAME was not tested during the solubility tests but based on the performance of other ethers with similar solubility properties, it was predicted to be able to dissolve the all polymers and rubbers. Both molecules (shown in Figure 2.5) were considered as candidates but were subsequently discarded for reasons which will be discussed in Section 2.4.2.

2.4.2 Solvent modelling

Solvent modelling software was run three times and a list of molecules was generated each time (Run A, Run B and Run C, shown in Table 2.5). The criteria were loosened with each run to ensure all possible candidates were generated; Run A was the most stringent while Run C was the least stringent. Different families of molecules could also be selected or omitted (shown in Table 2.6). Carboxylic acids, alcohols, aldehydes, phenols and non-aromatic olefins were omitted due to their reactivity in the polymerisation process. Amines and amides were omitted due to the potential formation of NO_x gases upon incineration. Similarly, sulphur containing solvents were omitted due to the potential formation of SO_x gases upon incineration, silicon containing solvents were omitted due to ash formation upon incineration and halogenated solvents were omitted due to the risk of release of ozone layer depleting compounds upon incineration.[231] The remaining families were alkane, aromatic, ester, ether and ketone solvents. Derivatives of these families could also be suggested, for example, dioxolanes have ether functionality and lactones have ester functionality. In total, 165 molecular structures were generated and can be seen in Figures 2.6, 2.7 and 2.8. Each molecule is colour coded for reasons which will be explained in the following paragraphs.

Table 2.5. The criteria entered into ProCAMD for each run.

	Run A		Run B		Run C	
	Min	Max	Min	Max	Min	Max
Bp / °C	77	111	77	111	77	120
δ_D / $MPa^{0.5}$	10.6	23.2	10.4	24.4	10.4	24.4
δ_P / $MPa^{0.5}$	0.0	6.5	0.0	7.6	0.0	7.6
δ_H / $MPa^{0.5}$	0.0	6.8	0.0	8.4	0.0	8.4

Table 2.6. Molecule families which were included and omitted.

Families included	Families omitted
Alkanes	Carboxylic acids
Aromatics	Aldehydes
Ethers	Compounds with double bonds
Esters	Amines
Ketones	Amides
	Halogen-containing
	Sulphur-containing
	Silicon-containing

Results of Run A using TSS1 sphere

Run 1

Ethers

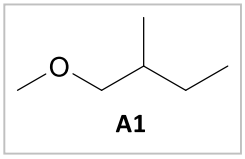
A1

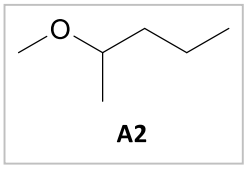
A2

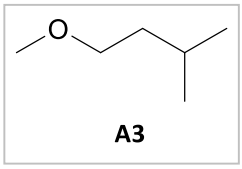
A3

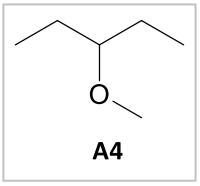
A4

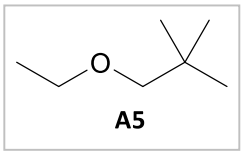
A5

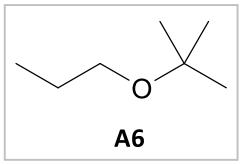
A6

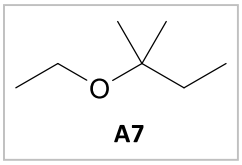
A7

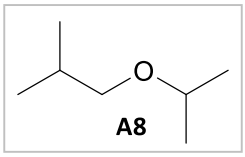
A8

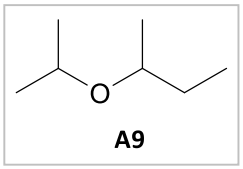
A9

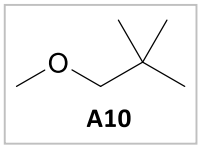
A10

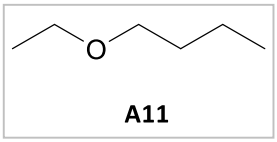
A11

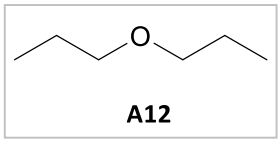
A12

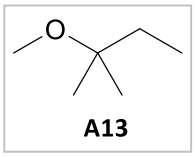
A13

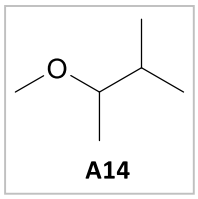
A14

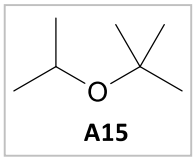
A15

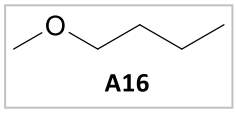
A16

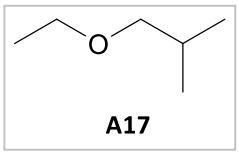
A17

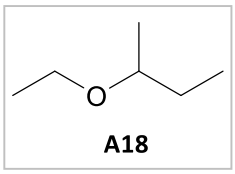
A18

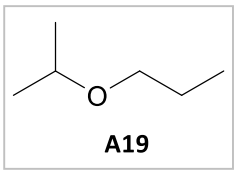
A19

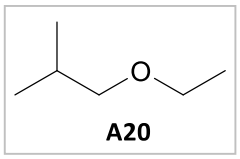
A20

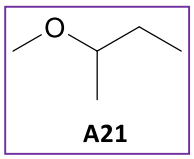
A21

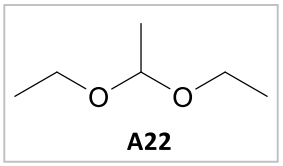
A22

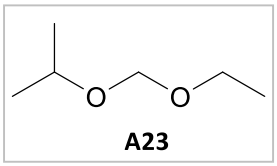
A23

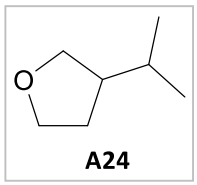
A24

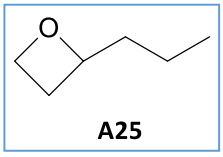
A25

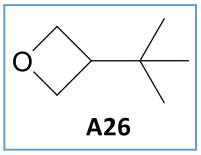
A26

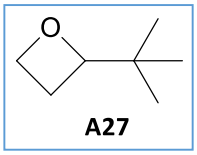
A27

A28

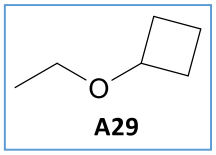
A29

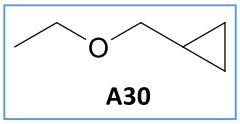
A30

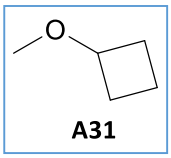
A31

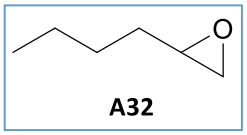
A32

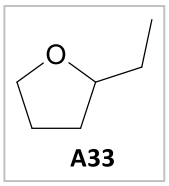
A33

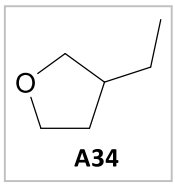
A34

Run 1 cont.

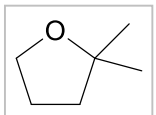
A35

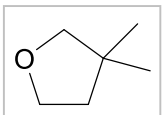
A36

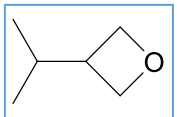
A37

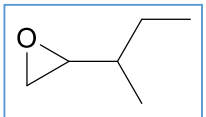
A38

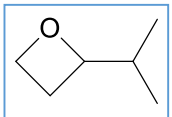
A39

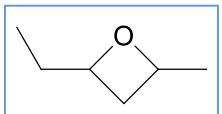
A40

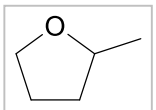
A41

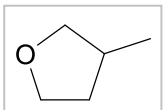
A42

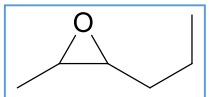
A43

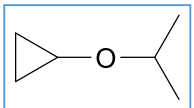
A44

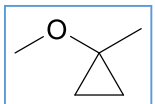
A45

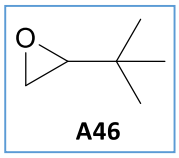
A46

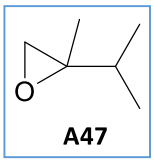
A47

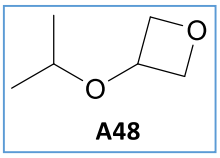
A48

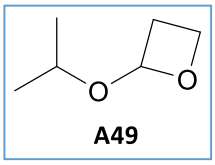
A49

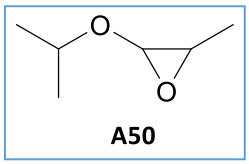
A50

Alkanes

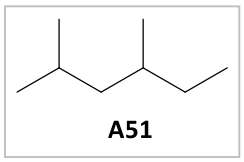
A51

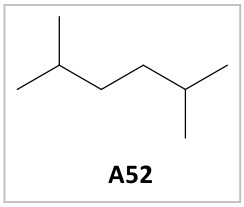
A52

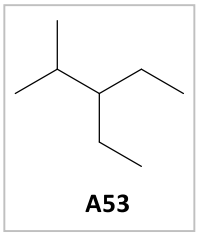
A53

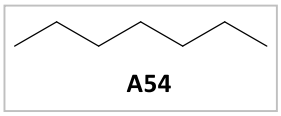
A54

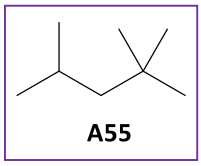
A55

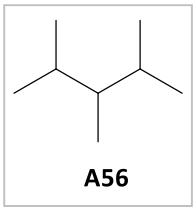
A56

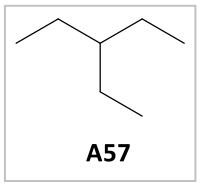
A57

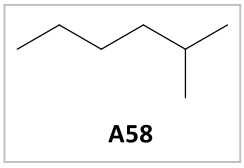
A58

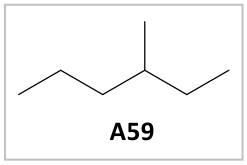
A59

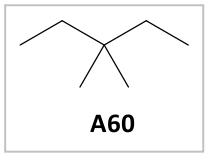
A60

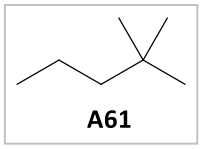
A61

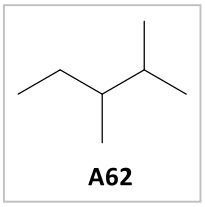
A62

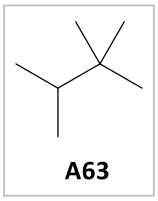
A63

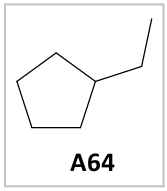
A64

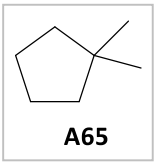
A65

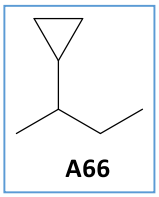
A66

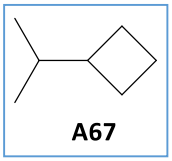
A67

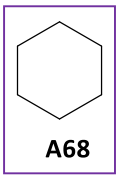
A68

Run 1 cont.

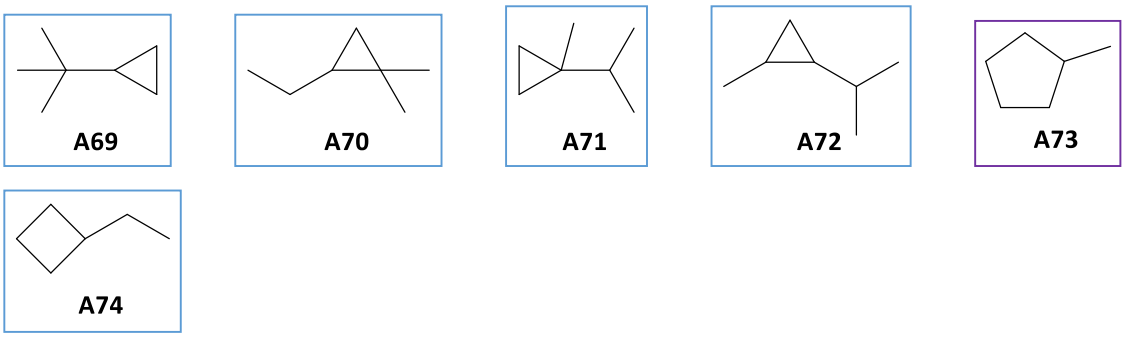

Aromatics

Ketones

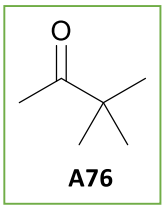

Figure 2.6. Results of the Run A using ProCAMD. Molecules highlighted in green are the top candidates which have been taken forward to the synthesis stage of development. Blue indicates exclusion due to high ring strain, grey indicates ethers and alkanes, purple indicates molecules with properties known to be outside the criteria limits.

The extremities of the TSS1 sphere along each axis were used as the HSP limits, along with the physical property criteria, for Run A (shown in Table 2.5). A total of 76 molecules were generated which consisted of 48 ethers, 25 alkanes, 1 aromatic, 1 ketone and no esters (shown in Figure 2.6. TAME, **A13**, and 2-MeTHF, **A41**, the two candidates from the solvent guide search, were also among the solvents suggested in Run A using ProCAMD.

A fast screen of these 76 molecules involved the removal of 3- and 4-membered ring structures which are likely to be both difficult to make and unstable due to their high ring strain (highlighted in blue). The only proposed aromatic structure was the known carcinogen, benzene, **A75**, which was also removed from the list. The melting point of cyclohexane, **A68**, was considered too high (4 °C), while the boiling points of methylcyclopentane, **A73**, and 2-methoxybutane, **A21**, were too low (72 °C and 57 °C respectively). The boiling point of 2,3,4-trimethylpentane, **A56**, was also too

high (113 °C) (all highlighted in purple in Figures 2.6, 2.7 and 2.8). 44 molecules remained, which consisted primarily of ethers and alkanes, along with one ketone, pinacolone **A76**. Many of the candidates with ether functionality were acetals and ketals. The issues of peroxide formation in ethers[232] and flammability and persistence, bioaccumulation and toxicity (PBT)[233] in alkanes are well established, therefore were not ideal candidates, but, all 44 were retained on the potential candidates list.

Results of Run B using TSS2 sphere

A second run using the extended total solubility sphere (TSS2) was carried out in an attempt to generate some more potential candidates (Run B). Any extra candidates generated in this run would likely not be able to dissolve the rubber R5. The parameters which were entered into ProCAMD for Run B can be seen in Table 2.6. The looser constraints on the HSPs meant an extra 20 molecules were generated and they are shown in Figure 2.7. Four molecules with high ring strain were removed (highlighted in blue), reducing the number of candidates to 16. These molecules consisted of seven esters and nine ethers. Esters tend to be of low toxicity and can be easily synthesised from biomass making them attractive for use as solvents.[234] They also provided an alternative to the alkanes and ethers generated in the first run. After runs 1 and 2 using TSS1 and TSS2, a total of 60 candidates were in contention (14 alkanes, 38 ethers, seven esters and one ketone).

Run 2

Esters

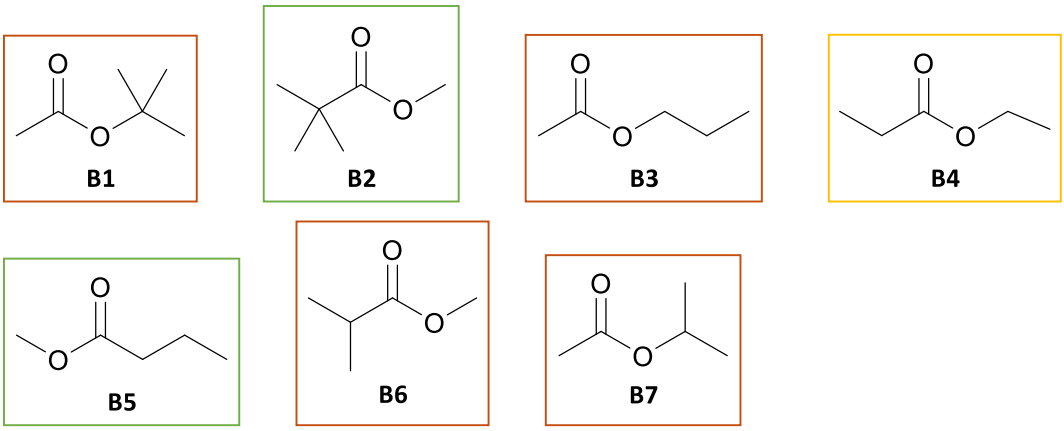

Ethers

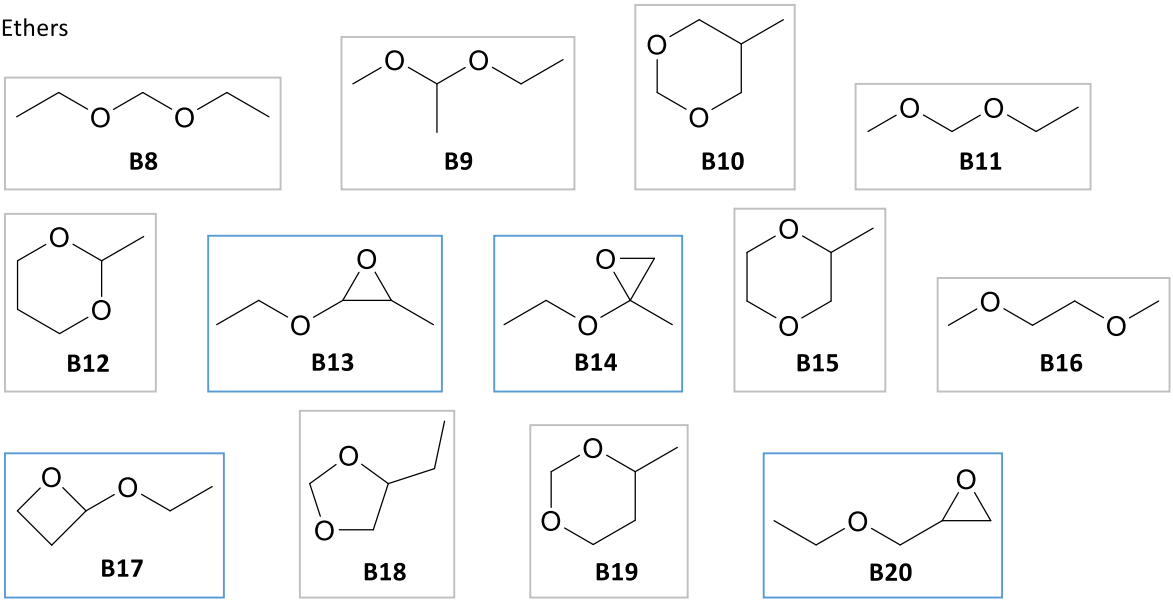

Figure 2.7. Results of the Run A using ProCAMD. Molecules highlighted in green are the top candidates which have been taken forward to the synthesis stage of development. Blue indicates exclusion due to high ring strain, grey indicates ethers and alkanes, orange indicates molecules which passed all criteria but were found to unable to dissolve either rubber and yellow indicates molecules which were predicted to be unable to dissolve either rubber.

Results of Run C using expanded boiling point limit

The upper boiling point limit was increased to 120 °C and the TSS2 sphere was used as the HSP criteria in Run C, the criteria of which can be seen in Table 2.5. An extra 76 molecules were generated and are shown in Figure 2.8 (16 alkanes, 48 ethers, seven esters, four ketones and one aromatic). The molecules with high ring strain were again removed (highlighted in blue), as well as 3,3-Dimethylhexane, **C50**, cycloheptane, **C58**, isobutyl acetate, **C65**, *sec*-butyl acetate, **C66**,

methyl 2-methylbutanoate, **C67**, and methyl isobutyl ketone (MIBK), **C72**, as their boiling points are known to be too high. Toluene, **C76**, (the aromatic) was also removed for obvious reasons (all highlighted in purple in Figure 2.8). This left 104 molecules (seven alkanes, 31 ethers, two esters and three ketones).

Run 3

Ethers

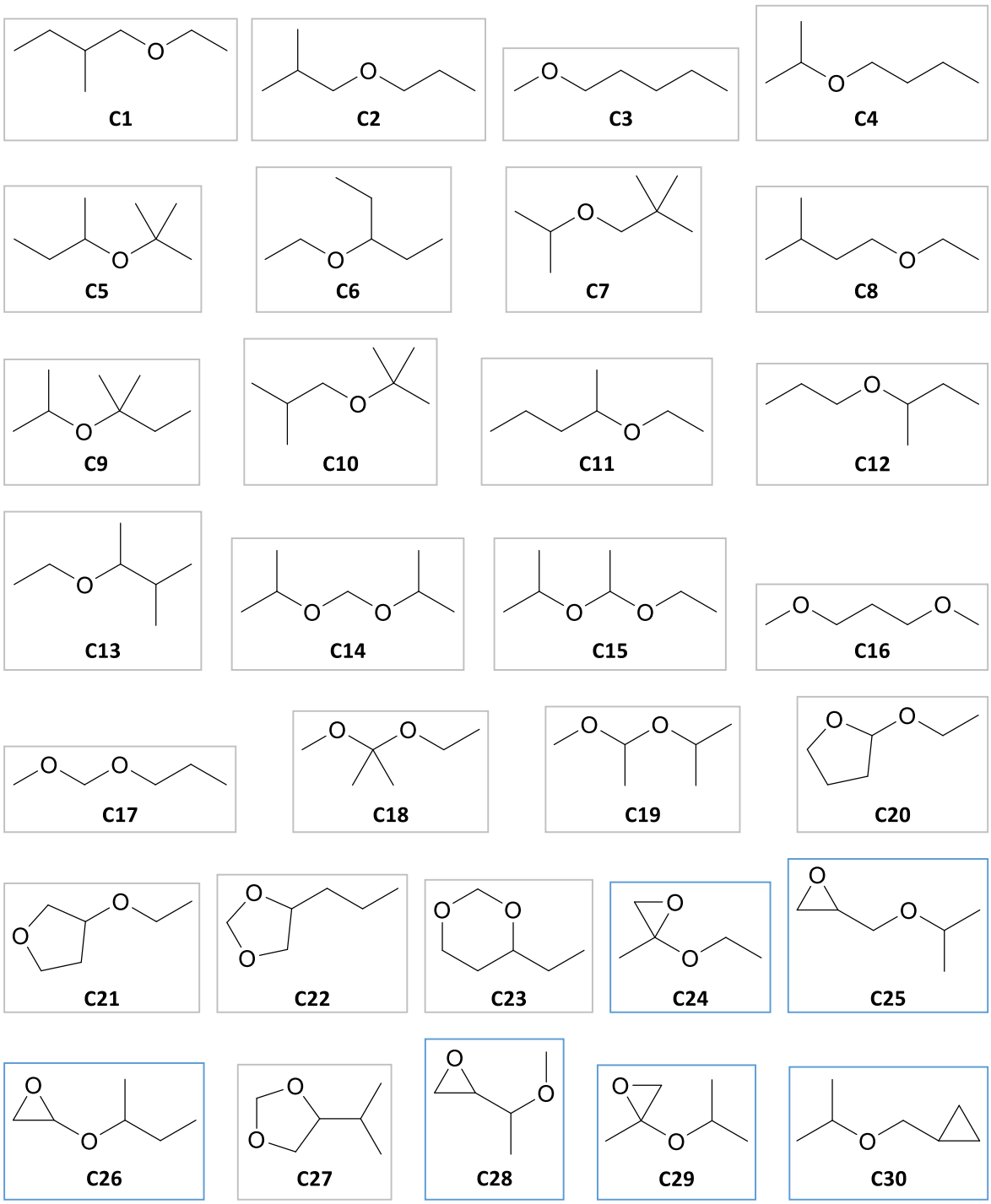

Run 3 cont.

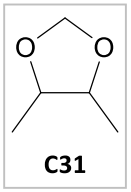
C31

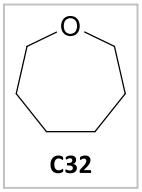
C32

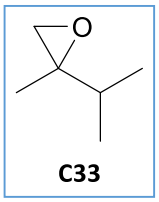
C33

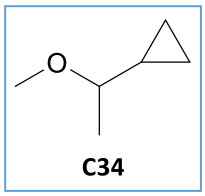
C34

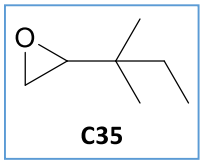
C35

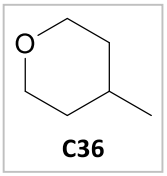
C36

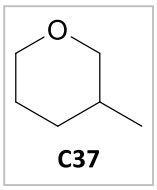
C37

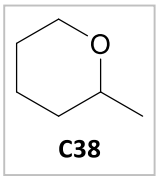
C38

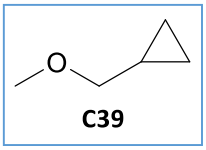
C39

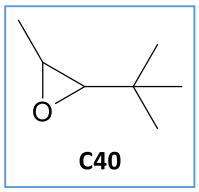
C40

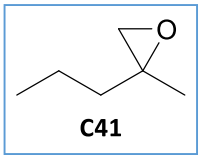
C41

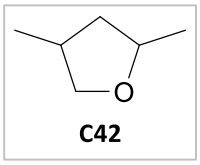
C42

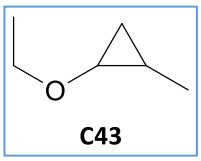
C43

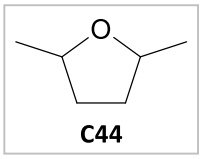
C44

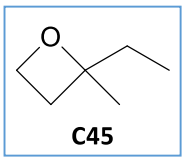
C45

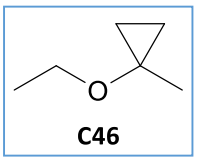
C46

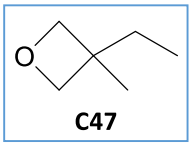
C47

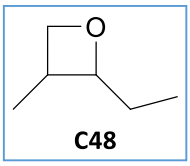
C48

Alkanes

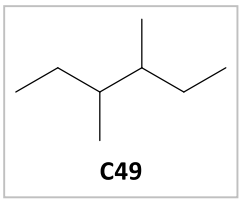
C49

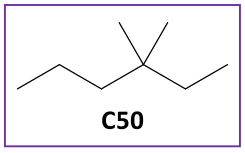
C50

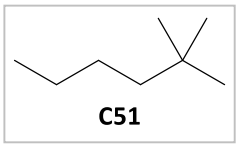
C51

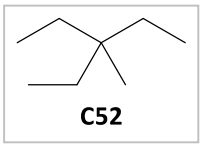
C52

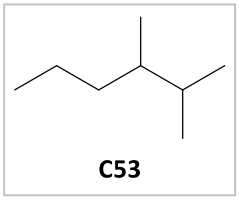
C53

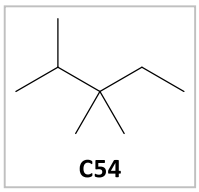
C54

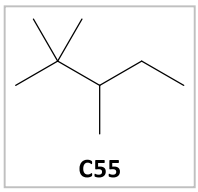
C55

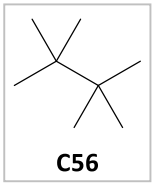
C56

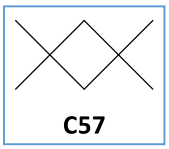
C57

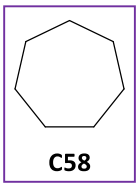
C58

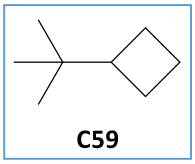
C59

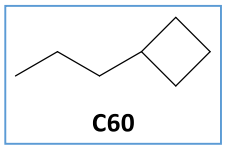
C60

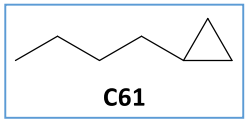
C61

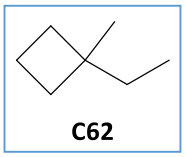
C62

Run 3 cont.

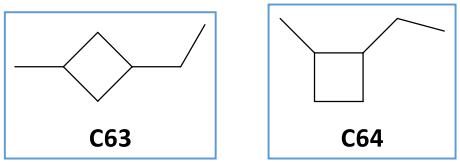

Esters

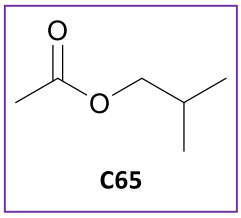

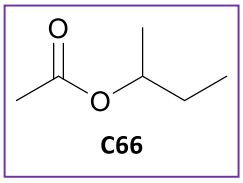

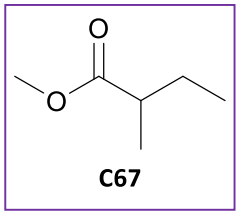

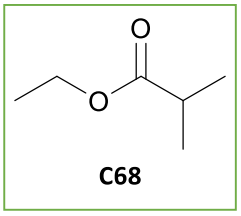

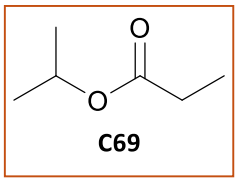

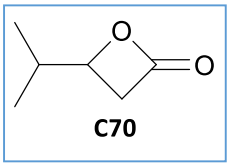

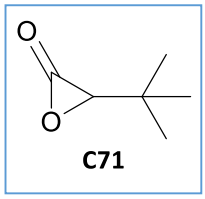

Ketones

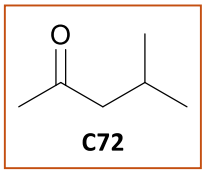

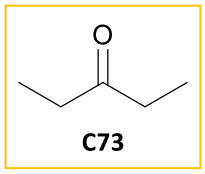

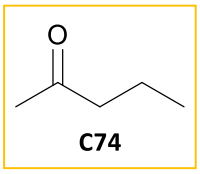

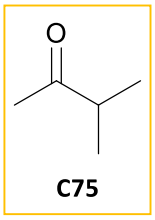

Aromatics

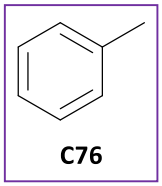

Figure 2.8. Results of the Run A using ProCAMD. Molecules highlighted in green are the top candidates which have been taken forward to the synthesis stage of development. Blue indicates exclusion due to high ring strain, grey indicates ethers and alkanes, purple indicates molecules with properties known to be outside the criteria limits, orange indicates molecules which passed all criteria but were found to unable to dissolve either rubber and yellow indicates molecules which were predicted to be unable to dissolve either rubber.

Screening of ProCAMD candidate solvents

In total, after three runs of ProCAMD, 104 candidates were proposed. TAME, **A13**, and 2-MeTHF, **A41**, which were identified from the CHEM21 solvent selection guide, were among the 104 molecules. Due to the large number of candidates, a screening process was required to find the best candidates. Molecules with high ring strain have already been removed, as well as any molecules with known high toxicity or physical properties which are known experimentally to be outside the acceptable range.

At this point of the search for new solvents, 2-MeTHF was tested for its suitability as a polymerisation solvent, as it had been proposed from an early stage by the CHEM21 solvent selection guide. However, it was found to undergo chain transfer in radical conditions. Consequently, the high molar masses required for PSA polymers (>30,000 g mol^{-1}) could not be obtained. This was assumed to be due to the abstraction of the hydrogen atoms in the *alpha*-position to the ethereal oxygen. hydrogen atoms in this position are known to be easily removed and are the reason for peroxide formation in ethers.[235,236] Therefore, it was decided that due to the combination of the risk of peroxide formation and the expectation that they would undergo chain transfer (based on experiments carried out at Nitto), ethers would not be considered any further. All 69 ethers were removed from contention and are highlighted in grey).

A wide range of C-5 to C-8 alkanes were proposed. All acyclic C5 and C6 alkanes fall outside the lower boiling point limit of 77 °C and no obvious synthetic route could be proposed for the cyclic ethylcyclopentane, **A64**, and 1,1-dimethylcyclopentane, **A65**, so both were excluded. Furthermore, the synthesis of heptane, **A54**, from biomass was not obvious and it too was excluded. The branched C7 and C8 alkanes were unattractive due to concerns about their potential persistent, bioaccumulative and toxic (PBT), and very persistent and very bioaccumulative (vPvB) properties. To qualify as a PBT or a vPvB, a substance must fulfil the relevant criteria shown in Table 2.7. The Log $P_{o/w}$ of branched C7 and C8 alkanes tend to be very high (>4.5).[233] At this Log $P_{o/w}$ region, BCF tends to surpass the threshold of 2,000 (which indicates bioaccumulative) and approaches the threshold of 5,000 (which indicates very bioaccumulative), according to ECHA (Table 2.7).[237] In addition, nephrotoxicity tests on gasoline components, including isooctane, **A55**, 2-methylhexane, **A58**, and 2,3-dimethylpentane, **A62**, showed that branched C7 and C8 alkanes tended to induce nephropathy in the kidneys of male rats. Isooctane, **A55**, was also shown to be resistant to biodegradation due to its high level of branching.[238] Despite the lack of data to explicitly eliminate the alkanes, the combination of all of the above "circumstantial" evidence meant that the potential for alkanes to be classed as PBT or vPvB in the future was considered too

high to be a viable solution. Consequently, all alkanes were removed from contention (all highlighted in grey).

Table 2.7. PBT and vPvB criteria according to Annex XIII to REACH.[237]

Property	PBT criteria	vPvB criteria
Persistent	A substance fulfils the persistence criterion in any of the following situations: • $T_{1/2}$ > 60 days in marine water; • $T_{1/2}$ > 40 days in fresh- or estuarine water; • $T_{1/2}$ > 180 days in marine sediment; • $T_{1/2}$ > 120 days in fresh- or estuarine sediment; • $T_{1/2}$ > 120 days in soil.	A substance fulfils the "very persistent" criterion in any of the following situations: • $T_{1/2}$ > 60 days in marine, fresh- or estuarine water; • $T_{1/2}$ > 180 days in marine, fresh- or estuarine sediment; • $T_{1/2}$ > 180 days in soil.
Bioaccumulative	A substance fulfils the bioaccumulation criterion when: • BCF > 2000	A substance fulfils the "very bioaccumulative" criterion when: • BCF > 5000
Toxic	A substance fulfils the toxicity criterion (T) in any of the following situations: • NOEC* or EC_{10}** < 0.01 mg/L for marine or freshwater organisms; • substance is classified as carcinogenic (category 1A or 1B), germ cell mutagenic (category 1A or 1B), or toxic for reproduction category 1A, 1B or 2); • there is other evidence of chronic toxicity, as identified by the classifications: STOT*** (repeated exposure), category 1 (oral, dermal, inhalation of gases/vapours, inhalation of dust/mist/fume) or category 2 (oral, dermal, inhalation of gases/vapours, inhalation of dust/mist/fume) according to the CLP Regulation.	

*NOEC = No Observed Effect Concentration; **EC_{10} = 10% Effect Concentration; ***STOT = Specific Target Organ Toxicity.

The remaining candidates were nine esters and four ketones. Several trends were observed within these families of molecules (Figure 2.9 and 2.12). First, as the molar mass of esters and ketones increased by adding alkyl groups, polarity decreased, and approached the target region of the HSP space shown in Figure 1.9. Second, increased branching in alkyl groups in esters and ketones resulted in lower boiling point and lower polarity than their linear alkyl equivalents with the same number of carbon atoms, demonstrated by *tert*-butyl acetate and *n*-butyl acetate. The boiling point of *tert*-Butyl acetate is 96 °C, while the boiling point of *n*-butyl acetate is 126 °C. Additionally, *tert*-butyl acetate is less polar. Third, in the case of esters, the carboxylate side of the ester tended to have more influence on the ability to dissolve the rubbers than the alcohol side. For example, the C6 ester with a C3 carboxylate group, propyl propionate, could not dissolve either rubber whereas the C5 ester with a C4 carboxylate group, methyl butyrate, could dissolve rubber R6. The cut-off for carboxylate groups appeared to be C4: butyrates and isobutyrates. Finally, the HSPs of esters and ketones (Figure 2.9 and 2.12) show that esters which are within the boiling point range (< 111 °C) have a lower dipole, but higher hydrogen-bonding ability than ketones. These trends were useful in screening esters and ketones.

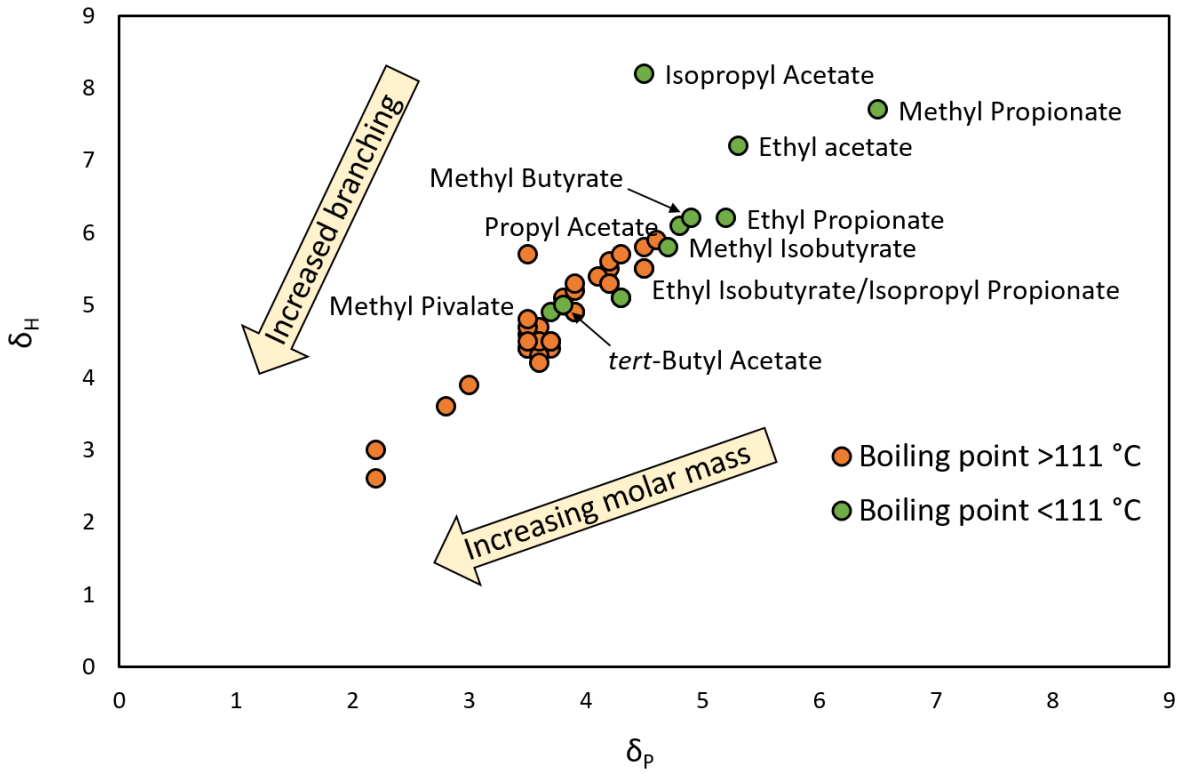

Figure 2.9. HSP map showing the trends of molar mass, branching, boiling point and polarity in esters.

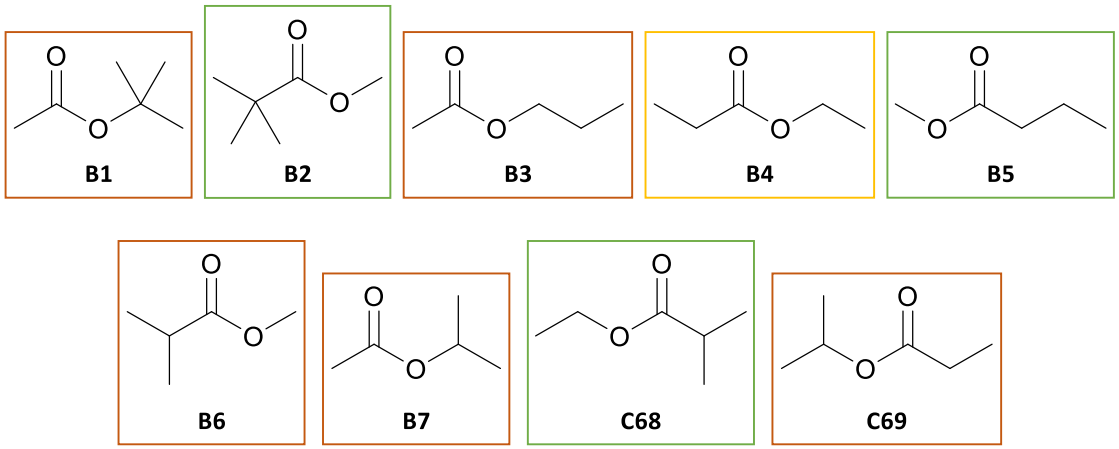

Figure 2.10. The nine ester candidate molecules. The molecules highlighted in green could dissolve rubber R6. Orange indicates molecules which passed all criteria but were found to unable to dissolve either rubber and yellow indicates molecules which were predicted to be unable to dissolve either rubber.

HSPs were obtained for the nine esters (Figure 2.10) using HSPiP and their ability to dissolve the polymers and rubbers was tested. Only methyl pivalate, **B2**, methyl butyrate, **B5**, and ethyl Isobutyrate, **C68**, were able to dissolve rubber R6 and as such were selected for the next screening stage (all highlighted in green). *tert*-Butyl acetate, **B1**, propyl acetate, **B3**, methyl isobutyrate, **B6**, isopropyl acetate, **B7**, and isopropyl propanoate, **B69**, could not dissolve either rubber and therefore were omitted (all highlighted in orange). Based on the trends observed among the other candidates, ethyl propanoate was unlikely to dissolve R6 was therefore not tested (highlighted in yellow). Propyl propionate and isopropyl isopropionate, the other C3 carboxylate esters with lower polarity than ethyl propionate, were unable to dissolve either rubber, it was anticipated that ethyl propionate would also perform poorly in the dissolution of rubbers.

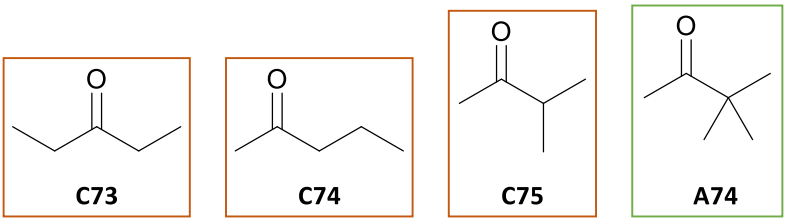

Figure 2.11. The four ketone candidates. The molecules highlighted in green could dissolve rubber R6 while the others could not.

HSP predicted that three of the four ketones (Figure 2.11), 3-pentanone, **C73**, 2-pentanone, **C74**, and methyl isopropyl ketone, **C75**, were unable to dissolve the rubbers (all highlighted in orange, Figure 2.11. The fact that methyl isobutyl ketone (MIBK) is less polar than all three but was found

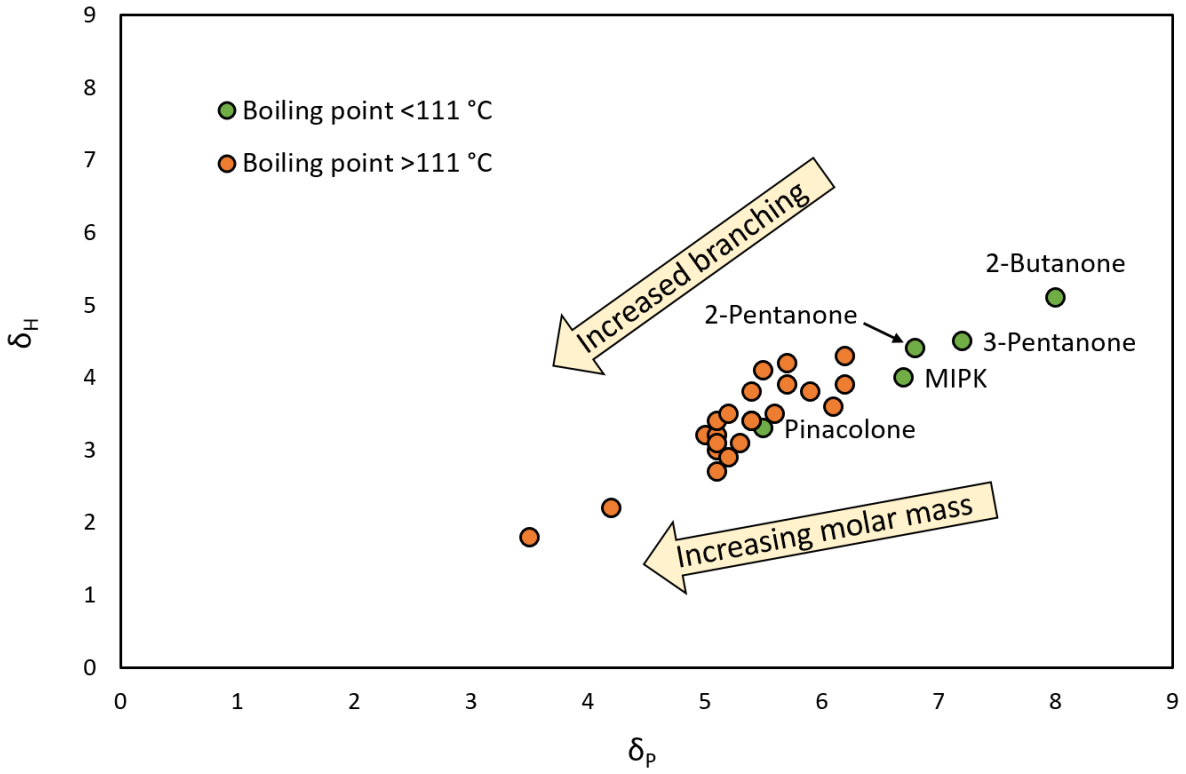

Figure 2.12. HSP map showing the trends of molar mass, branching, boiling point and polarity in ketones.

to be unable to dissolve either rubber during the solubility tests provided further evidence to support these predictions (Table 2.2). Pinacolone, **A76** (highlighted in green), was found to be able to dissolve R6 but not R5 and was taken to the next screening stage.

Overall, four new solvents were proposed, methyl pivalate, methyl butyrate, ethyl isobutyrate and pinacolone (Figure 2.13). However, none were able to dissolve rubber R5. Although this was decided to be acceptable, a final manual search for new molecules was undertaken to ensure that no potential candidates were missed and in the hope that an ideal solvent which could dissolve R5 could be found.

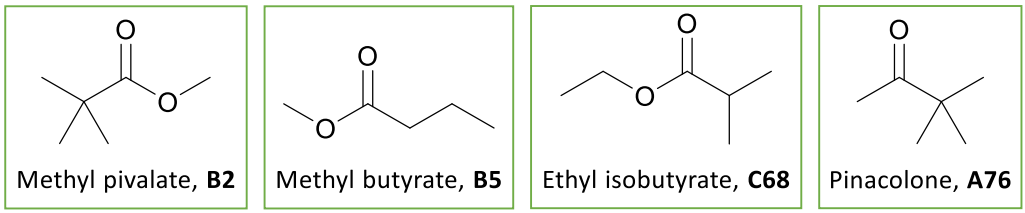

Figure 2.13. The final four candidates generated by ProCAMD.

2.4.3 *Manual search for new solvents*

Due to their high performance in the rubber solubility tests, a manual search focussing on ethers was conducted. However, their major problem was the potential ability to form peroxides.

Ethers are oxidised in ambient conditions in the presence of oxygen. Low molecular weight peroxides are known to be very unstable and can become shock-sensitive explosives when concentrated.[232] Due to the dangers of their instability, very little work has focussed on determining critical concentrations of ethers.[232,239] This is further complicated as each ether can form a range of peroxides and the stability of each peroxide differs from the next.[239] As such, safety thresholds for the concentration of peroxides in chemicals are vaguely defined as 100 ppm.[239] Most ethers, bought from any major chemical supplier, contain antioxidant additives to prevent peroxide formation.[240] For example, butylated hydroxytoluene (BHT) is commonly used in small amounts.[240] However, the use of additives is not ideal for many applications, especially radically induced polymerisations,[241] and their effectiveness decreases over time as they are used up. Thus, inherently non-peroxide forming ethers were targeted in the manual solvent search.

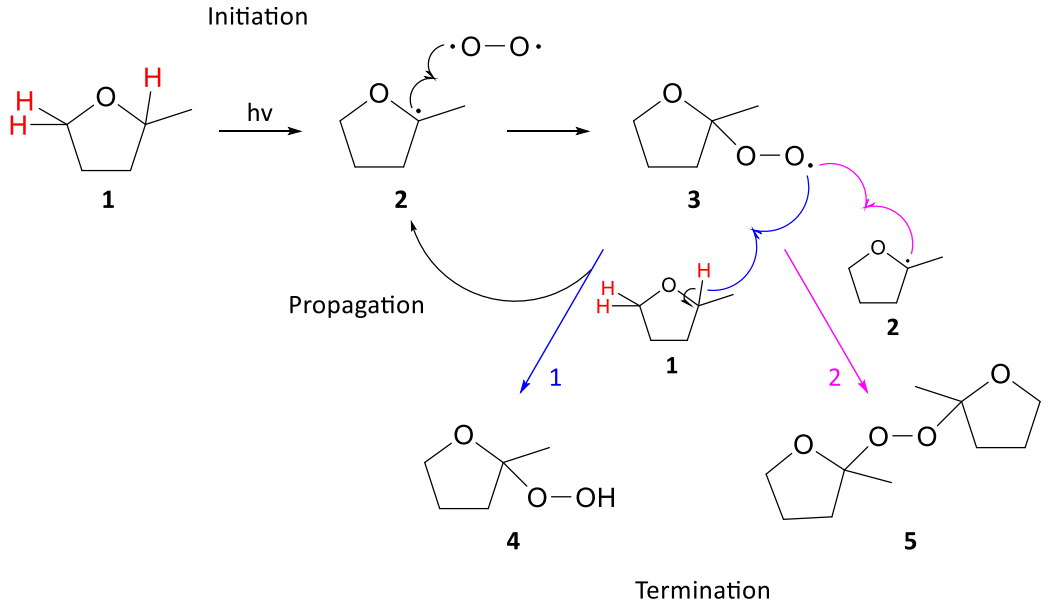

Figure 2.14. Mechanism for the initiation and propagation of peroxides in 2-MeTHF.

The mechanism of peroxide formation was first studied in an attempt to understand its source. An example mechanism of peroxide formation in 2-MeTHF is shown in Figure 2.14. The initiation step of autoxidation in ethers is still debated[235] but it is accepted that hydrogen abstraction occurs at the *alpha*-position to the ethereal oxygen (hydrogen atoms highlighted in red on **1**) to produce

a radical, **2**.[235] The hydrogen abstraction can be achieved with visible or long-wave UV-A light. **2** can react with molecular oxygen to produce **3**.[235] Propagation occurs when **3** abstracts another hydrogen atom from an ether molecule to form **4** and reform **2**.[235] Note that the structures shown in Figure 2.14 are only examples and other similar structures can be formed by abstraction of the other *alpha*-H on **1**. Also, **4** and **5** can potentially undergo further hydrogen abstraction at the remaining *alpha*-H to form heavier peroxides.

As the mechanism showed that peroxide formation proceeds *via alpha*-H abstraction, non-peroxide forming structures which do not contain *alpha*-H atoms were targeted. Two non-peroxide forming basic structures were identified in this work, "quaternary ethers" and "furans", neither of which were suggested by the CAMD software. Both classes of non-peroxide forming ethers are described below, but, why were these structures not generated by ProCAMD? The reason is that there is no group or combination of groups available in the software representative of the two quaternary carbons or two vinyl groups either side of the ethereal oxygen. Different families of molecules can be selected for generation in the CAMD software. Each family has representative groups. For example, when alkanes are selected, the groups CH_3, CH_2, CH and C are the only groups which will be involved in any structures which are generated. Selecting other families adds other groups to the list. So, when ethers are selected as well as alkanes, the groups CH_3-O, CH_2-O and CH-O are also included. However, there is no C-O group in the software available for inclusion. A combination of any of the ether groups (CH_3-O, CH_2-O and CH-O) with the C group can give *tert*-butyl groups on one side of the ether but not on both. For instance, methyl *tert*-butyl ether, ethyl *tert*-butyl ether and *tert*-amyl methyl ether can all be generated but di-tert-butyl ether cannot. Likewise, no groups exist in the software which are representative of two vinyl groups either side of the ethereal oxygen and hence, furan rings could not be generated.

Quaternary ethers

Substituting the *alpha*-H atoms of an ether backbone (C-O-C) with groups which are more difficult to abstract, such as methyl groups, could eliminate the potential to form peroxides. Such ethers are henceforth called quaternary ethers. The four most basic structures, di-*tert*-butyl ether (DTBE), 2,2,4,4-tetramethyloxetane (TMO), 2,2,5,5-Tetramethyltetrahydrofuran (TMTHF) and 2,2,6,6-tetramethyltetrahydropyran (TMTHP) are shown in Table 2.8. The HSPs of the quaternary ethers placed them inside the TSS1 sphere which suggested that they could dissolve both rubber R5 and R6.

TMTHP was ruled out due to its high boiling point. The properties of DTBE were ideal but it cannot not be synthesised by the obvious acid-catalysed route using tert-butanol and isobutene.[242,243]

Alternative routes produce by-products resulting in low atom economies, making the use of DTBE as a solvent less attractive and as such, it was not considered further in this work.[242,244–246] The 4-membered ring structure of TMO was unattractive as it is known to be difficult to synthesise due to the high ring strain.[247] Although TMTHF's boiling point (112 °C) was over the limit of 111 °C, it was deemed to be close enough to the target to be considered further. As its HSPs suggested, it was shown to be able to dissolve both rubbers, R5 and R6. This was significant as none of the other candidates could dissolve rubber R5. Therefore, TMTHF was carried forward for further consideration.

Table 2.8. The four most basic quaternary ether structures, the cyclic TMTHF and the acyclic DTBE.

Property	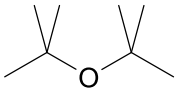 DTBE	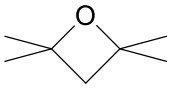 TMO	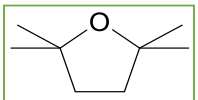 TMTHF	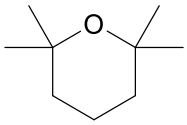 TMTHP
Bp / °C	107[c]	101[a]	112[c]	161[a]
δ_D / MPa$^{0/5}$	14.0[b]	15.1[b]	15.4[b]	15.4[b]
δ_P / MPa$^{0/5}$	2.5[b]	2.8[b]	2.4[b]	2.4[b]
δ_H / MPa$^{0/5}$	1.4[b]	2.0[b]	2.1[b]	1.7[b]

(a) Predicted using ProPred, (b) Predicted using HSPiP, (c) data obtained from PubChem.

Furans

Another method of removing the peroxide forming potential of ethers was by the presence of vinyl groups at the *alpha*-position. The most basic structure with such properties is the furan ring. Table 2.9 shows the structures of three furans (furan, 2-methylfuran and 2,5-dimethylfuran), along with their boiling points and HSPs. The C-H bond on the furan ring and its methyl and dimethyl derivatives has been shown to be very strong, stronger than those in benzene in fact, so that peroxide formation in ambient conditions does not occur.[248,249] Both 2-methylfuran[250,251] and 2,5-dimethylfuran[252,253] can be easily synthesised from biomass *via* the HMF platform.

Although its HSPs looked promising (low δ_P and δ_H), the boiling point of furan was too low to be considered any further (31 °C). In addition, according to the ECHA information on chemicals page, furan is suspected of causing cancer and suspected of causing genetic effects.[254] Adding methyl groups onto the ring increases the boiling point to a more acceptable level. However, 2-methylfuran's boiling point was still too low to be considered any further (63-65 °C) in the current

application. The addition of a methyl group increased its polarity according to HSP. Despite this, it was shown to be non-polar enough to dissolve rubber R6 in the solubility tests. The boiling point of 2,5-Dimethylfuran was high enough to be considered (92-93 °C) but according to HSP, its polarity increased further with the addition of another methyl group as compared to 2-methylfuran (Table 2.9). This was confirmed experimentally when it was found to be unable to dissolve either rubber. This was an interesting observation as in most other families of solvents, adding methyl groups decreases polarity.

Table 2.9. The four most basic furan structures, furan, 2-methylfuran and 2,5-dimethylfuran.

Property	Furan	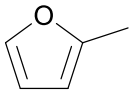 2-Methylfuran	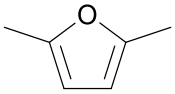 2,5-Dimethylfuran
Bp / °C	31[(a)]	63-65[(a)]	92-93[(a)]
δ_D / MPa$^{0/5}$	17.0[(b)]	17.3[(b)]	16.7[(b)]
δ_P / MPa$^{0/5}$	1.8[(b)]	2.8[(b)]	4.5[(b)]
δ_H / MPa$^{0/5}$	5.3[(b)]	7.4[(b)]	4.5[(b)]

(a) data obtained from ChemSpider, (b) Predicted using HSPiP.

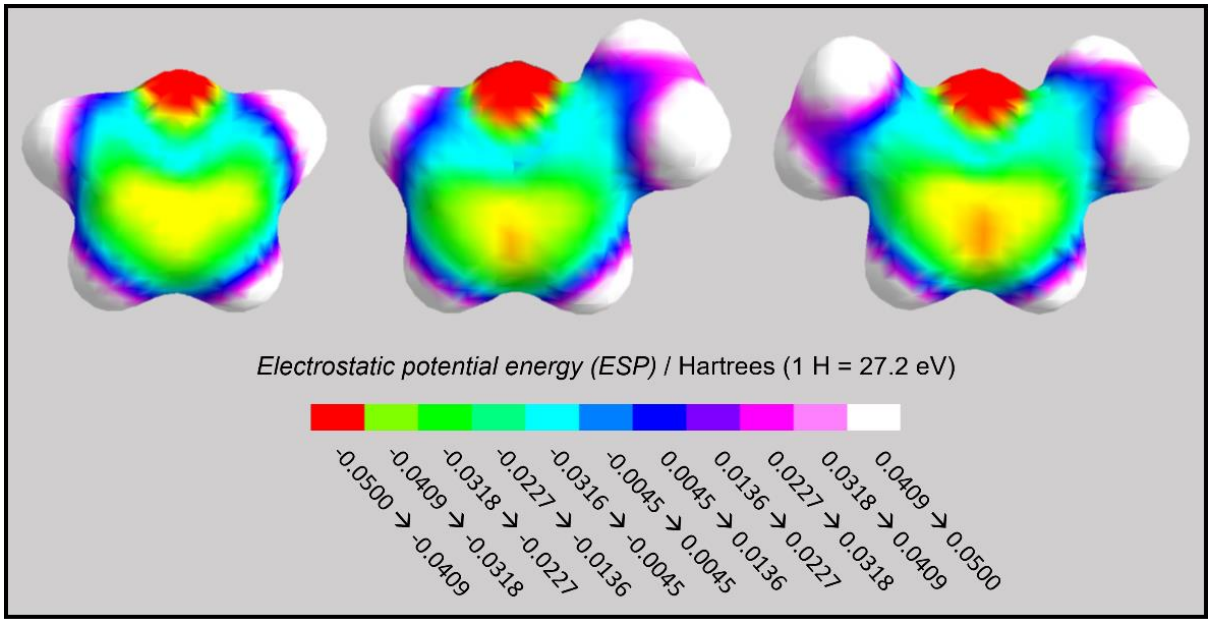

Figure 2.15. ArgusLab mapped surface showing areas of high (red) and low (white) electrostatic potential energy on furan (left), 2-methylfuran (centre) and 2,5-dimethylfuran (right).

The reason for this increase may be due to the conjugated pi-system of the basic furan ring. The electron density on the oxygen is delocalised over the conjugated pi-system, resulting in a ring of low polarity. To help visualise this, the electrostatic surface potential energy (ESP) was mapped using ArgusLab (Figure 2.15).[255] It can be seen that adding electron-donating methyl groups creates regions of relative positivity (white) on the methyl group while the ring system becomes slightly more negative (red), which creates a dipole within the molecule.

2.4.4 Final results of solvent search

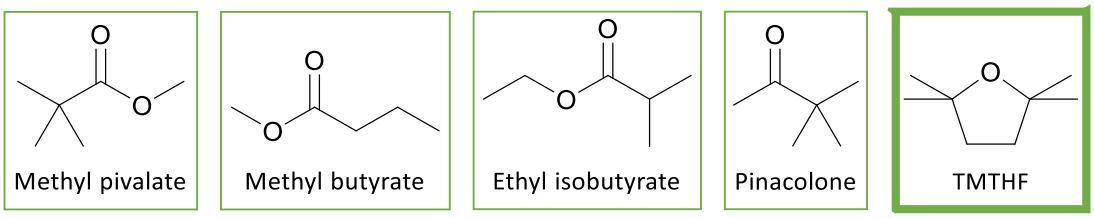

Figure 2.16. The top five candidates after the search for new solvents.

In total, after the different stages of the search for new molecules, five top candidates were identified and are shown in Figure 2.16. TMTHF was the only candidate able to dissolve R5 and is highlighted in bold green, while the other four can dissolve all polymers as well as R6 but not R5 (Table 2.10).

Table 2.10. Scores for each of top five candidates for their ability to dissolve each polymer.

Solvent	P1	P2	P3	P4	R5	R6
Methyl pivalate	1	1	1	1	6	1
Methyl butyrate	1	1	1	1	6	1
Ethyl isobutyrate	1	1	1	1	6	1
Pinacolone	1	1	1	1	6	1
TMTHF	1	1	1	1	1	1

2.5 Synthetic routes to the top five candidates from biomass

At this point, the candidate solvents have been shown to be able to dissolve each polymer and at least one rubber, R6. However, they must also be efficiently synthesised from biomass. Having proposed routes to the five candidates, significant overlap of the bio-based platform molecule starting materials was observed (shown in Figure 1.8). The synthetic routes to all solvents will be discussed in further detail in the relevant chapter (Chapter 3 or 4) and all experimental results will be presented and assessed.

2.5.1 Methyl pivalate and pinacolone

Routes to methyl pivalate and pinacolone were identified (Figure 2.17). Route 1 involves the hydrocarboxylation of isobutene with CO and water. There are two possible methods of doing this: by a metal catalysed process using either palladium, rhodium (like the Monsanto process[256]), iridium (like the Cativa process[90]) or by an acid catalysed Koch reaction.[257] The downside of both the metal catalysed processes are that iridium, palladium and rhodium are scarce and expensive and will reduce the elemental sustainability of the process.[258,259] The upside of the metal catalysts is the extremely high yields obtained (~99% in the Cativa[90] and Monsanto[256] processes).

Sanderson *et al.* have reported the production of pivalic acid from CO, water and isobutene using both solid acid and Lewis acid catalysts.[260,261] The work of Sanderson *et al.* demonstrated that the production of pivalic acid is possible, and while the yields are lower (~90%) than those obtained by the Cativa or Monsanto processes, the use of cheaper acid catalysts could be beneficial if high yields can be maintained.[261]

Due to the dangers of using CO, route 2 is proposed as an alternative. Formic acid is used to generate CO and water in situ by contact with acid catalyst.[123] A H-ZSM-5 zeolite with a silica/alumina ratio of 25:1 was found to be most effective, obtaining a conversion of 75% in batch. CO and water can then react in a similar way to route 1.[123] Another alternative for *in-situ* production of CO is by the reverse water-gas shift reaction (WGSR). CO_2 and H_2 are converted to CO and water which undergo subsequent carbonylation. Rhodium[262] and ruthenium[263] have previously been shown to be able to catalyse both the reverse WGSR and carbonylation steps.

Pivalic acid can then be used to make both methyl pivalate and pinacolone. Simple Fischer esterification with methanol generates methyl pivalate, shown in route 3. Ketonisation of pivalic acid with either acetone[264] or acetic acid[265] gives pinacolone in good yields (~90%), shown in route 4.

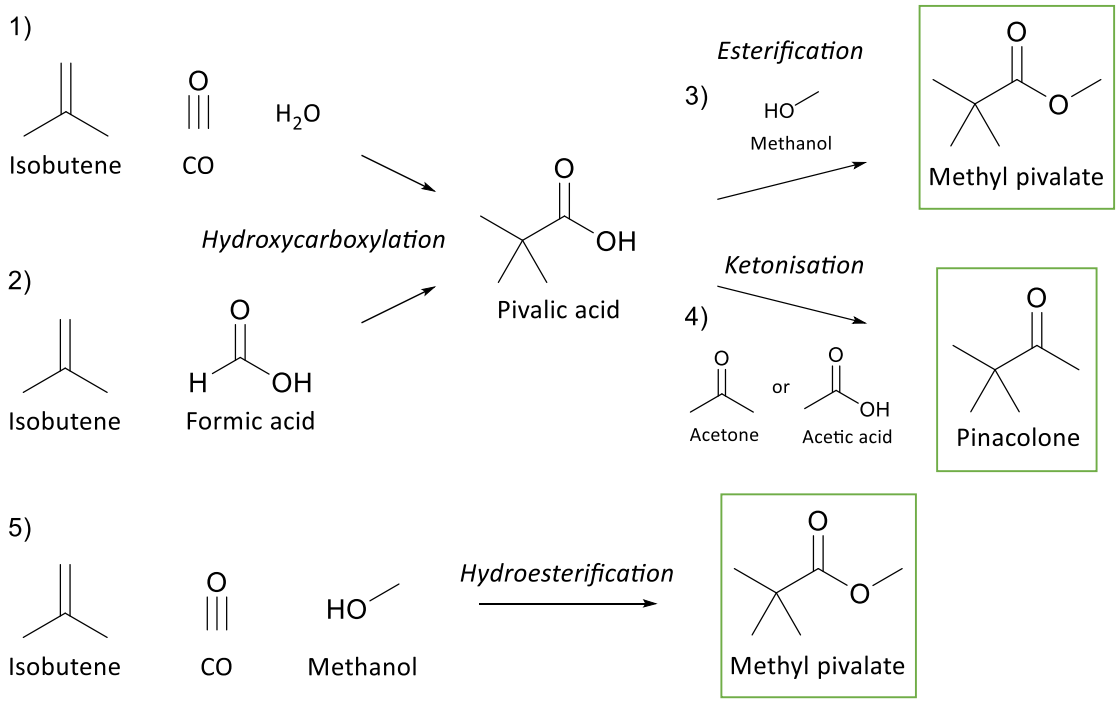

Figure 2.17. Proposed synthetic routes to methyl pivalate and pinacolone.

Route 5 proceeds *via* the hydroesterification of isobutene with CO and methanol. While this route has not been reported before, similar hydroesterifications using a range of alkenes instead of isobutene have been reported. For example, Wu *et al.* used ruthenium catalysts with two equivalents of imidazolium chloride additives and obtained moderate yields (50-80%, for different alkenes).[266] However, the complex and expensive catalyst system is not ideal and it is not compensated with the high yields of the Cativa and Monsanto processes.[266] Brennführer *et al.* published a review of the use of palladium to catalyse hydroesterification reactions.[267] Different ligands, reagents and reaction conditions resulted in different regioselectivities, and this is something which must be considered for the hydroesterification of isobutene.

2.5.2 Ethyl Isobutyrate and methyl butyrate

Ethyl isobutyrate and methyl butyrate are produced in the same process using glycerol as the starting material (Figure 2.18). Wu *et al*. produced propene from glycerol in two steps. Iridium was used as the catalyst for the first step (hydrogenolysis) and a ZSM-5 zeolite was used for the second step (dehydration).[151] Although it was not carried out by the same authors, the hydroxycarbonylation of propene can potentially be done either by the Koch reaction[268] or a metal catalysed reaction,[267] using metals such as palladium, iridium or rhodium.

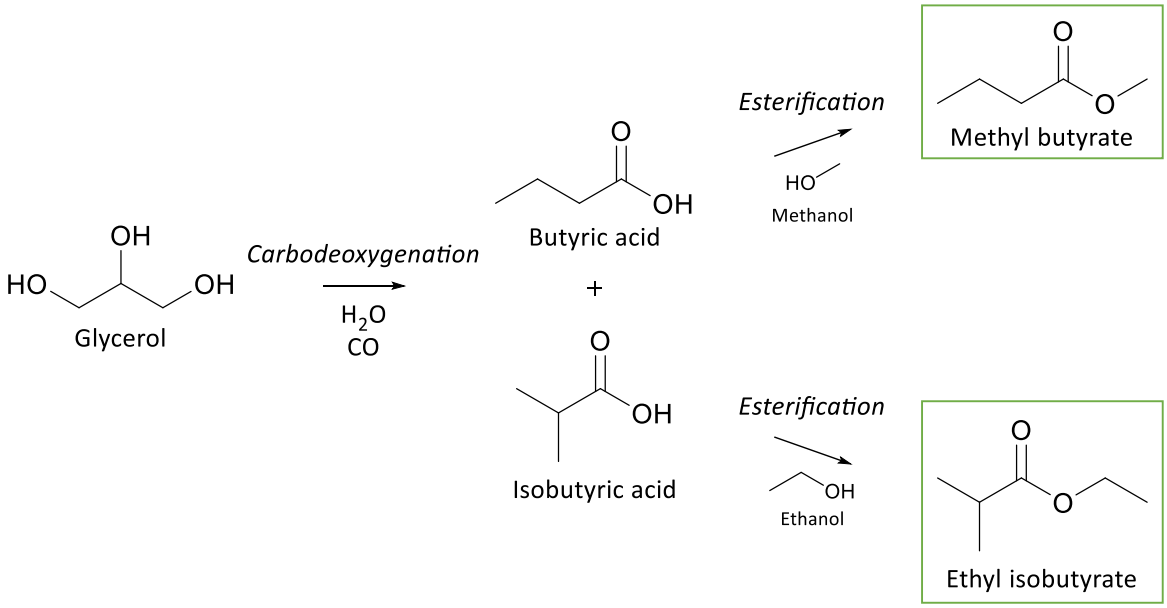

Figure 2.18. Synthetic routes to methyl butyrate and ethyl Isobutyrate.

Coskun *et al*. reported the production of butyric acid and isobutyric acid directly from the carbodeoxygenation of glycerol or triacetin using a rhodium and hydroiodic acid catalyst system.[177] Esterification of each acid using methanol and ethanol respectively is proposed to give the corresponding esters in high yields.

2.5.3 TMTHF

Three routes to TMTHF have been proposed (Figure 2.19). Route 1 involves the cracking of methane, in the same process as its petroleum equivalent, to produce acetylene.[269,270] Acetylene is coupled with two equivalents of acetone in the presence of base to produce 2,5-dimethyl-3-hexyne-2,5-diol (DMHYL). Hydrogenation of DMHYL yields 2,5-dimethyl-2,5-hexanediol (DHL).[271] Dehydration of DHL has been shown to produce TMTHF.[272] There are several advantages of this reaction. The main advantage is that DHL is already produced by BASF for use in polymers and is registered with REACH as a chemical in the 10-100 tonne volume band.[271,273,274] Although the starting materials, methane and acetone, are currently produced from petroleum, they are two of the most established bio-based platform molecules and production from biomass is already quite advanced. In addition, the first two steps of the reaction are additive, resulting in an atom economy of 100% and the only side-product in the last step is one equivalent of water. The potassium isobutoxide base used to couple acetone and acetylene can be regenerated.[271]

Route 2 utilises isobutyraldehyde and isobutene, produced in situ from the partial oxidation and subsequent dehydration of isobutanol respectively, to yield 2,5-dimethyl-2,4-hexadiene (DHN) by

Prins-type chemistry.[275] The isobutanol is dehydrogenated to produce isobutyraldehyde. Gevo, who produce isobutanol by fermentation, have patented this process but they are currently not producing it on a large scale.[275] DHN can potentially be hydrated to generate TMTHF although this has not been previously reported.

In route 3, DHN is synthesised in the same way as described in Route 2, but instead of hydration with water, it is oxidised to form the stable DHN polyperoxide.[276] The DHN polyperoxide is subsequently hydrogenated both at the peroxide O-O bond and the C=C bond to form DHL.[276] DHL is dehydrated as described in Route 1 to produce TMTHF.

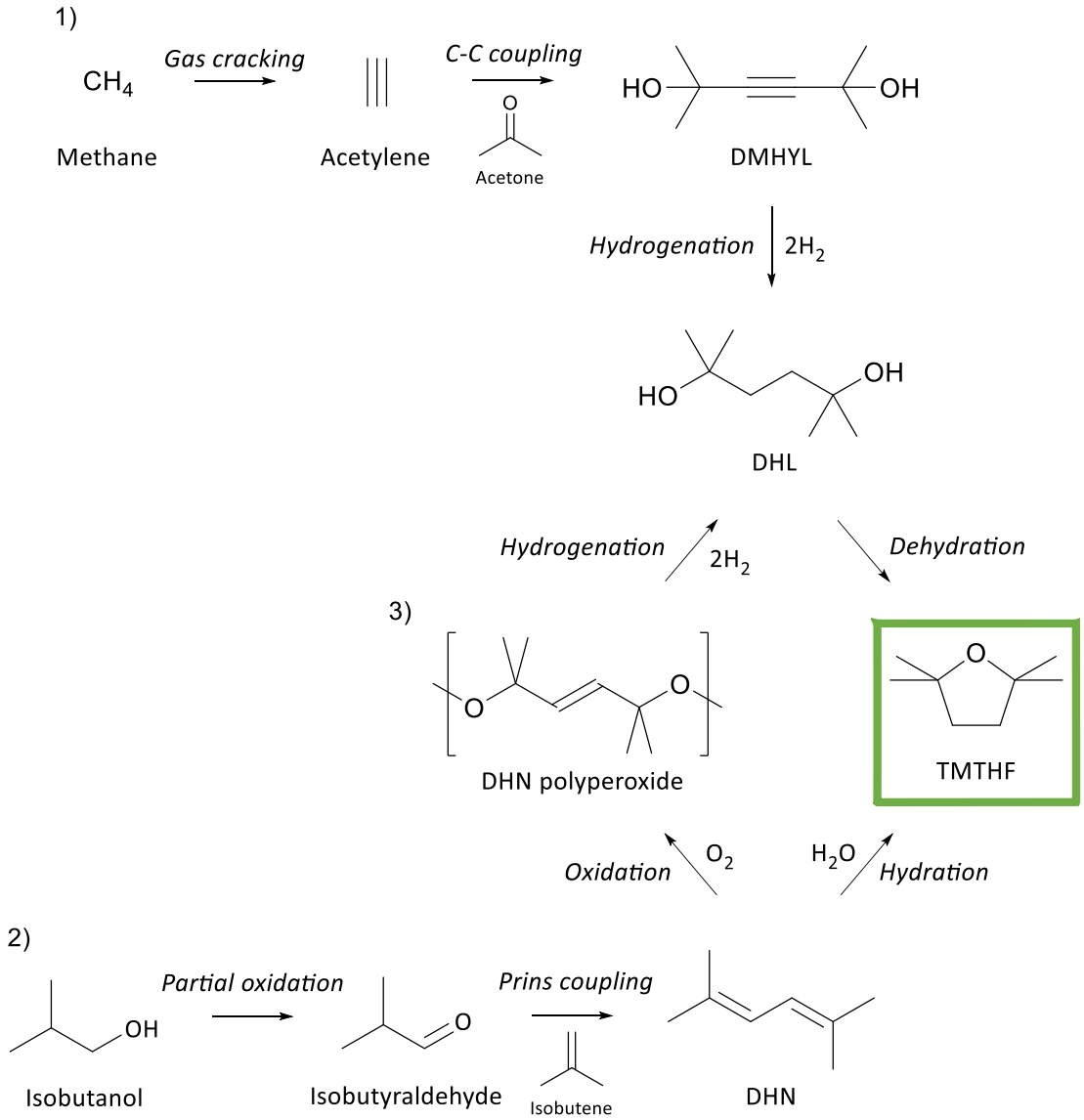

Figure 2.19. Synthetic routes to TMTHF.

2.6 Summary of top candidates

In summary, the three-step solvent selection process was completed successfully, providing five candidate solvents.

1. The HSPs of each polymer and rubber were measured indirectly by testing their solubility in a range of known solvents. This generated a region in the Hansen solvent space where suitable solvents were likely to be situated.
2. A search for new solvents was carried out. An initial search of the CHEM21 solvent guide was carried out which afforded two candidates, TAME and 2-MeTHF, both of whom were later disregarded due to peroxide formation issues.[201] A more in-depth search was then commenced using CAMD software. After three runs using increasingly looser constraints due to the difficulty in dissolving rubber R5 followed by a screening process, four molecules were suggested: methyl butyrate, ethyl isobutyrate, methyl pivalate and pinacolone.

   During this search using CAMD, a strategy for solvent selection was established and was applied to esters, ketones and furans. Different classes of molecules were positioned in the HSP space and molecules with optimal solvent properties within each family could be identified by modifying their structure, chain length and branching.

   However, none of the four candidates could dissolve rubber R5, so a manual search was carried out. A family of ethers which was not generated by the solvent modelling software was discovered. These ethers possessed two quaternary carbons in the *alpha*-positions to the ethereal oxygen and as such, they have been called "quaternary ethers". Unlike traditional ethers, quaternary ethers do not form peroxides. One of the quaternary ethers, TMTHF, was of particular interest as it could dissolve all polymers and rubbers, whilst fitting all of the criteria demanded by Nitto. As such, TMTHF was also taken forward as the fifth candidate.
3. Synthetic routes have been proposed for the five candidates –methyl butyrate, ethyl isobutyrate, methyl pivalate, pinacolone and TMTHF - and each route will be discussed in further detail presented in Chapters 3 and 4 and experimental results will be presented. In Chapter 5 each solvent will be assessed for "greenness" based on its synthesis and chemical properties.

3 Synthesis, characterisation and testing of esters and ketones

3.1 Introduction

The esters and ketones described in this chapter were the four "secondary" candidates proposed in Chapter 2 through solvent selection. These included the esters methyl butyrate, ethyl isobutyrate, methyl pivalate, and the ketone pinacolone. While each solvent had suitable physical properties to replace toluene, none were able to dissolve the synthetic rubber, R5. Due to their similar synthetic routes and bio-based sources, all four molecules will be discussed together in this chapter. Their performance in radical polymerisations, the Menschutkin reaction, and their synthesis and properties are also discussed.

3.2 Application testing of esters and ketones

The four candidates discussed in this chapter could be purchased cheaply from chemical suppliers and therefore, could be tested for their ability to facilitate the radical polymerisation from an early stage. The polymerisation and polymer testing was carried out by Charly Hoebers, Junior Scientist at Nitto Belgium. Due to the susceptibility of esters and ketones to nucleophilic attack, S_N2 reactions such as amidation and esterification as previously used by Sherwood *et al*. could not be used to characterise the esters and pinacolone.[60] Instead, to provide further insight into the solubility properties of each candidate, their performance was tested in the Menschutkin reaction, a reaction known to be influenced by the π^* of the reaction medium.[174,277]

3.2.1 Radical-initiated vinyl polymerisation

A polyacrylate polymer, the details of which could not be disclosed, was produced and its properties were tested. Three of the four solvents, methyl butyrate, methyl pivalate and

pinacolone were able to produce polymers of comparable molecular weight and quality to toluene and ethyl acetate (Table 3.1). TMTHF was also tested in this polymerisation for comparison where it also exhibited a good performance. Although ethyl isobutyrate produced molecular weights of 630,000 kg mol^{-1} (as shown in Table 3.1), polymerisation conditions had to be altered to achieve this. Initially, M_w's were too low to be used as a PSA (like in the case of 2-MeTHF, described in Chapter 2). Altering the conditions for large-scale production was not a viable option for Nitto, and therefore ethyl isobutyrate was removed from the list of potential candidates for polymer production at this point.

Table 3.1. Results of an acrylate polymerisation using the fours candidate esters and ketones in comparison to toluene.

Solvent	M_w (g mol^{-1})	Conversion (%)	Adhesion (cN 20 mm^{-1})	Cohesion (days)	Tack (g)
Toluene	600,000	94.6	1587	>10	900
Ethyl acetate	587,000	93.9	1555	>10	791
TMTHF	600,000	91.5	1445	>10	915
Methyl butyrate	601,000	95.5	1506	>10	655
Ethyl isobutyrate	630,000*	97.6	1641	>10	681
Methyl pivalate	581,000	95.2	1532	>10	727
Pinacolone	589,000	96.3	1646	>10	856

*Chain transfer occurred initially so conditions had to be altered to achieve this molecular weight.

The cause of chain transfer was not investigated further at Nitto but it was thought to involve chain transfer between polymer and solvent, as previously described in Chapter 2.[278,279] Autoxidation in esters[278–280] and ketones[278,279,281] has previously been demonstrated to occur at different rates depending upon the substrate, which suggested that differences in susceptibility to hydrogen abstraction in radical conditions may be observed between each candidate.

A proposed mechanism of radical formation resulting in chain termination in ethyl isobutyrate is shown in Figure 3.1. A hydrogen atom can be abstracted from the solvent molecule which will terminate the chain.[279] The newly formed radical on the solvent molecule can also react with a radical on the polymer, again, terminating the chain.[279] For chain transfer to the solvent to occur,

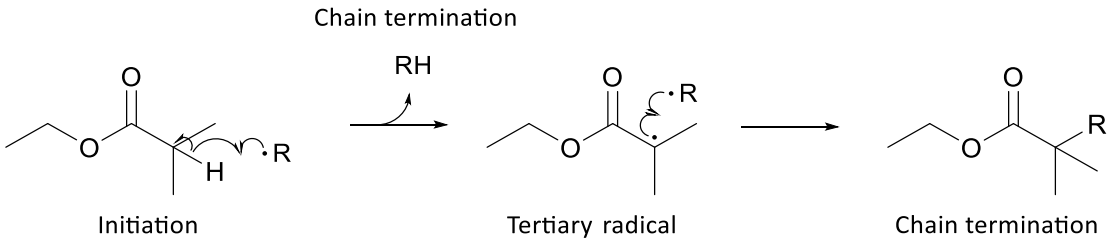

Figure 3.1. Mechanism of radical formation and chain termination in ethyl isobutyrate.

stable radicals must be able to form on the solvent molecules.[279] It was thought that if ethyl isobutyrate was undergoing chain transfer with the polymer, it may also undergo autoxidation to form peroxides, like 2-MeTHF, and that this peroxide formation could be directly proportional to its radical formation. To test this hypothesis, the four candidates were exposed to the same peroxide formation test as the ethers.

3.2.2 Peroxide tests

The abstraction of a hydrogen atom, either by UV light or in the radical-initiated conditions of the polymerisation, forms carbon-radicals and the degree of formation is related to their stability.[278,279] Radicals which form due to abstraction of the hydrogen atom in the *alpha*-position to the carbonyl group of esters are stabilised by delocalisation of the radical over the adjacent pi-orbitals of the carbonyl group (Figure 3.2). As such, both methyl butyrate and ethyl isobutyrate can form radicals at this position due to the presence of *alpha*-H atoms.

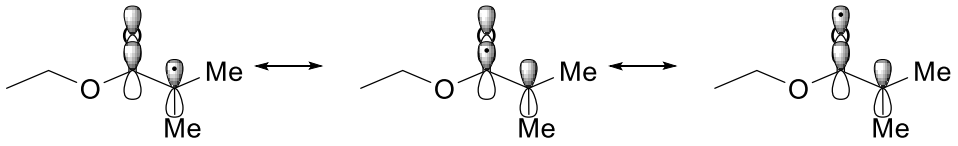

Figure 3.2. Stabilisation by resonance with adjacent pi-orbitals in ethyl isobutyrate.

Radical stability typically increases with increasing substitution, in the order of primary > secondary > tertiary, while the energy barrier for the removal of a methyl group from a quaternary carbon is very large and prevents radical formation at this position.[279,282] As such, the *alpha*-position to the carbonyl group in ethyl isobutyrate gives particular stability to radicals as it is a tertiary carbon, compared to methyl butyrate which has a secondary carbon.[280] Conversely, methyl pivalate does not have *alpha*-H atoms, therefore this pathway to radical formation is not possible, although hydrogen atoms in the *beta*-position could also be abstracted.[280]

An alternative pathway to radical formation is on the alcohol group of the ester and has previously been shown to be more reactive than the carboxylic acid group.[280] Radical stability increases with increasing substitution and as a result, isopropyl or *sec*-butyl groups are most likely to form more stable radicals.[280] On the alcohol side of the ester, ethyl isobutyrate is again the most likely to form radicals due to the secondary carbon on the ethyl alcohol group. Both methyl butyrate and methyl pivalate can form radicals on the alcohol group, but these will not be as stable as ethyl isobutyrate. The expected relative radical stabilities based on structure between methyl pivalate, methyl butyrate and ethyl isobutyrate are shown in Figure 3.3.

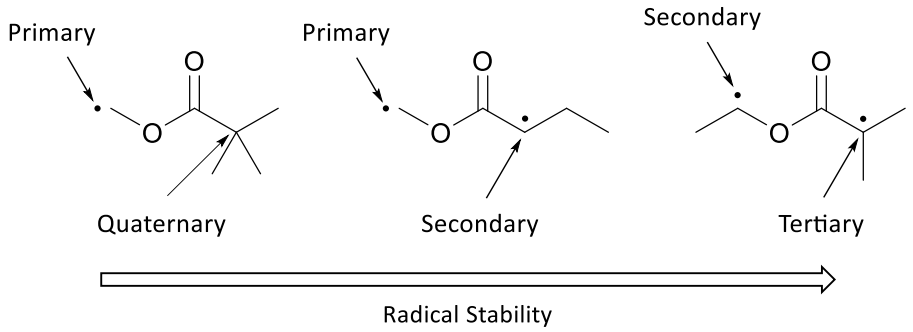

Figure 3.3. Relative stabilities of methyl pivalate (left), methyl butyrate (centre) and ethyl isobutyrate (right).

Table 3.2. Peroxide test results of the esters and pinacolone.

	Solvent	Experiment	T=0 hours (ppm)	T=3 hours (ppm)
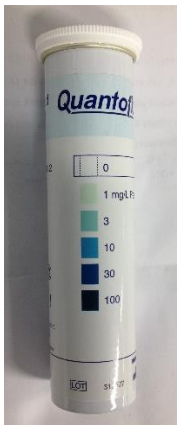	Ethyl isobutyrate	Control	0	0
		Test	0	10-30
	Methyl butyrate	Control	0	0
		Test	0	3
	Methyl pivalate	Control	0	0
		Test	0	3-10
Scale	Pinacolone	Control	3	3
		Test	3	10-30

The results of the peroxide tests are shown in Table 3.2. It can be seen that ethyl isobutyrate formed significant amounts of peroxides (10-30 ppm) after exposure to UV light and bubbling air for 3 hours while less peroxide formation was observed in methyl butyrate (3 ppm) and methyl pivalate (3-10 ppm). Ethyl isobutyrate contains a secondary carbon on the alcohol group and a tertiary carbon in the *alpha*-position, both of which will facilitate radical formation so its quick rate of peroxide formation is not unexpected. Methyl butyrate also contains a primary carbon on the alcohol group which will not provide much stability to radical formation, but the secondary carbon in the *alpha*-position will; its lower rate of peroxide formation is representative of this (3 ppm after 3 hours). Radical formation can only occur on the alcohol group of methyl pivalate due to the quaternary carbon in the *alpha*-position to the carbonyl group. However, the primary radical which could form on the alcohol group is relatively unstable,[279] so its quicker rate of peroxide formation than methyl butyrate is surprising (3-10 ppm). Pinacolone contained some peroxide initially which increased to 10-30 ppm upon exposure to UV light and air.

The combination of the delocalisation over the carbonyl group and the tertiary carbon in ethyl isobutyrate may explain its quicker rate of peroxide formation and could also give enough stability to the radical to undergo chain transfer with the polymer (or react with oxygen to form peroxides), resulting in premature chain termination. In contrast, the lower radical stabilisation in methyl butyrate, methyl pivalate and pinacolone may result in some chain transfer,[279] however, not at a rate that would cause significant chain termination. Due to ethyl isobutyrate's inability to host the polymerisation it was removed from contention as a replacement for toluene in Nitto's radical polymerisation and coating process, but will continue to be discussed in this thesis where work had already been carried out.

3.2.3 Menschutkin reaction

The Menshutkin was the first model reaction to be used to correlate solvent polarity with reaction rate.[56,283] The reaction of triethylamine with iodethane to form the quaternary ammonium salt was the original probe reaction and it was found that solvent dipolarity increased the reaction rate.[283] More recently, a similar reaction between 1-methylimidazole with 1-bromooctane (C8) was exploited for the characterisation of the bio-based dipolar aprotic solvents, Cyrene[174] and *N*-butylpyrrolidinone (NBP),[277] in comparison with a selection of traditional dipolar protic solvents.

Although not dipolar aprotic solvents, the five candidates can be compared to toluene in terms of their π^* using a similar Menschutkin reaction. The Menschutkin reaction between 1-methylimidazole and the longer chained 1-bromooctadecane (C18) was used in this work to compare the esters and ketone with toluene and ethyl acetate due to the insolubility of the C8

product, 1-octyl-3-methylimidazolium bromide, in the lower polarity candidate solvents. The reaction was found to be second-order, as can be seen in Figure 3.4. The integrated second-order rate equation (Equation 3.1) was used to calculate the reaction rate based peak integration using ^{1}H NMR spectroscopy.

Equation 3.1. $$k_2 t = \frac{1}{[A]_0 - [B]_0} \ln\left(\frac{[B]_0([A]_0 - [P]_t)}{[A]_0([B]_0 - [P]_t)}\right)$$

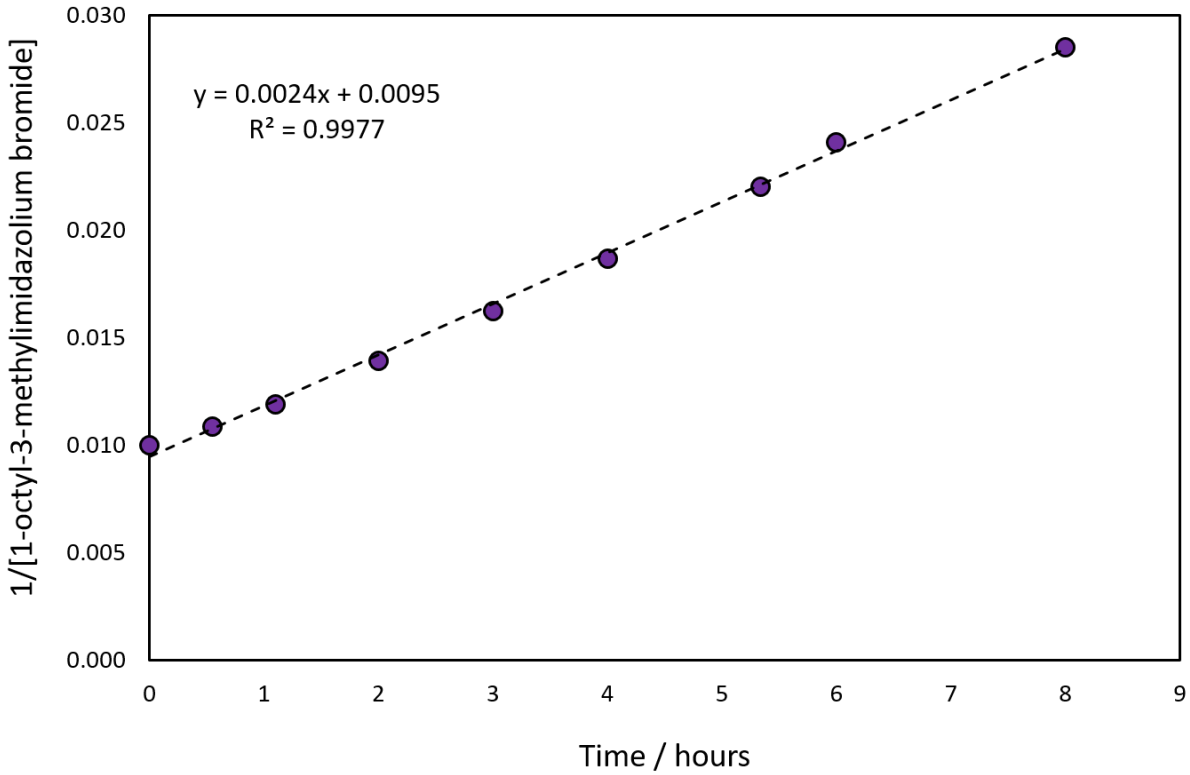

Figure 3.4. Plot of 1/[A] versus time for the Menschutkin reaction between 1-bromooctadecane and 1-methylimidazole.

A selection of other solvents was also used to generate the LSER: NMP, DMF, MEK, acetone, chlorobenzene, THF, triethylamine and limonene. The LSER comparing the reaction rate with π* for each solvent can be seen in Figure 3.5 and product characterisation by NMR spectroscopy can be seen in Figures A21 and A22, Appendix. No protic solvents were used as their effect has previously been discussed in length and is not of relevance in this thesis.[53]

A correlation between rate and π* can be seen in Figure 3.5 among the solvents with π* ≥ ~0.4, which plateaus for solvents with π* < ~0.4 (triethylamine, limonene and TMTHF). The cause of the plateau at low π* is unclear. It was thought that the reaction order may have changed in the

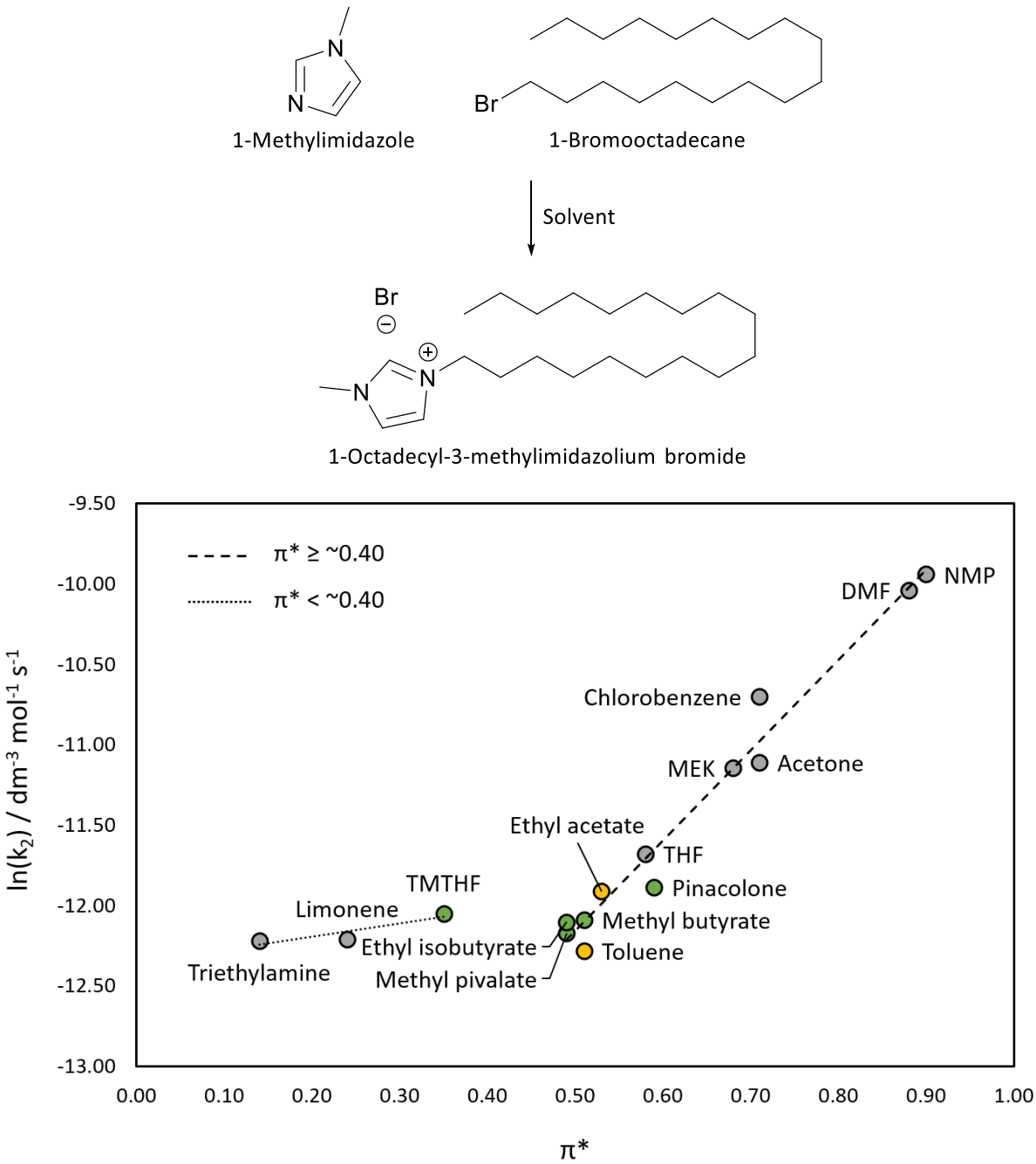

Figure 3.5. The Menschutkin reaction scheme and an LSER showing the relationship between the reaction rate and π*.

solvents of π* < ~0.4 from second-order to first- or zero-order, but plotting the rate versus π* using the first- and zero-order rate equations for the low π* solvents showed that the plateau was still present. Another possibility, in the case of triethylamine is reaction of the solvent with 1-bromooctadecane. However, integration of the peak area for 1-methylimidazole was used to calculate the rate, and therefore any reaction of triethylamine with 1-bromooctadecane would not result in an apparent increase in reaction rate. Stabilisation of the charged product by the lone-

pair of electrons on triethylamine (N) and TMTHF (O) could enhance the reaction rate but this does not explain limonene's high performance.

To investigate this plateau further, the solvatochromic equation was used to investigate whether this deviation could be accounted for by the other solvent descriptors δ^*, β or δ_H^2 (Equation 1.8). Regression analysis generated the coefficients shown in Table 3.3. α was not included in the regression as none of the test solvents were protic.

Equation 1.8. $$\ln(k_2) = c + d\delta^* + s\pi^* + a\alpha + b\beta + h(\delta)^2$$

Table 3.3. Coefficients for regression analysis of the Menschutkin reaction using the solvatochromic equation.

Entry	Solvents	*d*	*s*	*b*	*h*	*c*	R^2
1	Full data set	-0.136	0.474	0.054	0.258	-16.503	0.824
2	$\pi^* > 0.4$	-0.224	5.840	-1.010	0.025	-15.053	0.952
3	$\pi^* > 0.4$	-	5.746	-0.572	0.016	-15.065	0.951
4	$\pi^* > 0.4$	-	6.001	0.600	-	-14.904	0.950
5	$\pi^* > 0.4$	-	4.852	-	0.050	-15.404	0.937
6	$\pi^* > 0.4$	-	5.569	-	-	-14.911	0.934

Blank entries indicate that that parameter was not included in the regression analysis.

It can be seen that by using the full data set and all of the solvatochromic equation parameters (Entry 1), none of the parameters can explain the deviation of the low π^* solvents, demonstrated by their low coefficients (all < 1). When these coefficients are used to test the predictability of the model, a low R^2 of 0.824 is obtained. In contrast, for the solvents with $\pi^* > 0.4$, it can be clearly seen that π^* dictates the rate of reaction, demonstrated by an s = 5.840 and high model predictability (R^2 of 0.952) (Entry 2). In fact, when only π^* is considered in the regression analysis (Entry 6), predictability remains high (R^2 = 0.934), confirming the correlation between π^* and reaction rate, shown in Figure 3.6).

This suggests that the deviation is not caused by any solvent property of the solvatochromic equation, but instead, the reaction proceeds differently in low polarity media. Micelle formation by the product in low polarity solvents is likely due to the highly charged "head" and lipophilic

"tail", and could affect the reaction rate. However, a more in-depth study, which was outside the scope of this work, would be required to shed light on this. Whatever the reasons for the unexpectedly high performance of the low polarity solvents, the motivation for carrying out this set of experiments was to compare the esters and ketone candidates with toluene in terms of their π^* values, and for this it was successful.

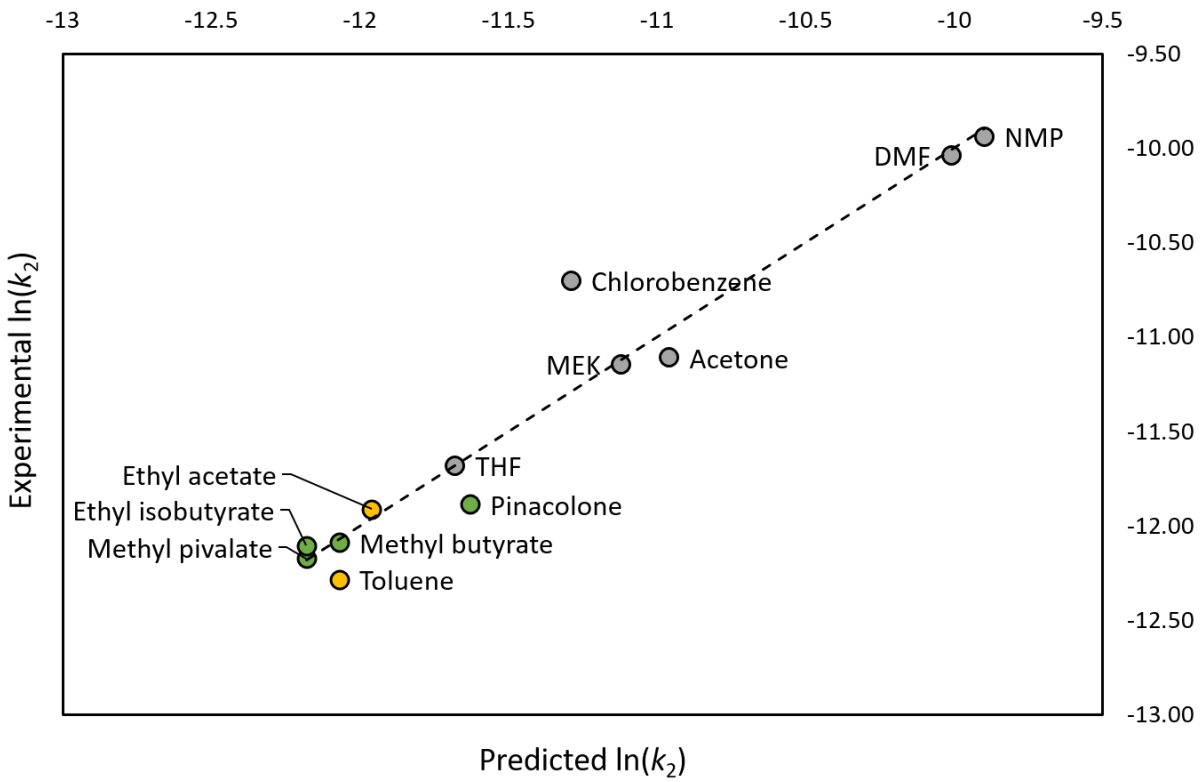

Figure 3.6. Graph showing the predictability of the LSER when only π^* is considered in the regression analysis of solvents with $\pi^* > 0.4$.

The reaction rates in each of the esters was very similar, and all were slightly higher than that of toluene. The reaction rate in toluene was slightly slower than what would be expected in a solvent with $\pi^* = 0.51$ according the LSER in Figure 3.5. This can be explained by toluene's high polarisability concealing its low dipolarity when measured using solvatochromic dyes, but which is revealed when measured in the Menschutkin reaction. The rate of reaction in pinacolone was slightly quicker than the candidate esters, consistent with its higher π^* (0.59), although still slightly slower than what would be expected according to the LSER; the LESR would suggest a rate similar to that of THF. This could potentially be explained by the presence of a small amount of the enol form of pinacolone. Protic solvents are known to inhibit the reaction rate severely due to stabilising interactions with 1-methylimidazole.[53] 1-methylimidazole could in turn stabilise the

enol form of pinacolone just enough to cause the slight reduction in reaction rate observed in Figure 3.5.

Overall, limitations in the use of the Menschutkin reaction to assess the polarity of lower polarity solvents ($\pi^* < 0.4$), it was useful in comparing the esters and pinacolone to toluene in terms of their π^*, and highlighted their similarities. Despite pinacolones higher π^*, it was shown to behave more like a lower polarity solvent such as ethyl acetate.

3.3 Analysis of esters and ketones

The removal of ethyl isobutyrate from the list of candidates based on its poor performance in the polymerisation tests highlighted the importance of obtaining experimental data where possible to confirm any predictions or to uncover unexpected properties.[213] As such, it was important to experimentally determine a range of physical properties for each candidate to ensure its suitability for Nitto's manufacturing plant. Some data had been obtained for ethyl isobutyrate before it was established to be unacceptable and it is also included in the following sections. Table 3.4 highlights the physical and solubility properties of the esters and pinacolone in comparison with TMTHF, toluene and ethyl acetate, and is discussed further in the following sections.

3.3.1 Physical properties of esters and ketones

Boiling points, melting points and densities were available from online databases for each of the remaining candidates and they are shown in Table 3.4. The LEL and AIT of each candidate were measured as part of this work. However, LEL is expressed as a volume percentage, and ideal gas behaviour is assumed. When molar mass and density are considered, it has been found that a larger mass of TMTHF can be present in the air before a flammable mixture is reached. An example calculation of the LEL by mass is shown in the in the Appendix. The boiling point, melting point, AIT and LEL (vol.) were all found to be suitable for each candidate.

All candidates fulfilled the physical property criteria, although the LEL (vol.) of ethyl isobutyrate is noticeably lower than those of the other esters, and only slightly higher than that of toluene (54.02 µl L^{-1} for ethyl isobutyrate versus 52.14 µl L^{-1} for toluene). As combustion is a free-radical reaction, its low LEL (vol.) may be another consequence of its relatively easily abstractable hydrogen atoms. Overall, all four candidates fit the physical property demands of the adhesive polymer manufacturing process.

Table 3.4. The physical and solubility properties of the esters and ketone in comparison with TMTHF, toluene and ethyl acetate.

Property	TMTHF	Methyl butyrate	Ethyl isobutyrate	Methyl pivalate	Pinacolone	Toluene	Ethyl acetate	Limits
M_r / g mol^{-1}	128.25[a]	102.13[a]	116.16[a]	116.16[a]	100.16[a]	92.14[a]	88.11[a]	n/a
Bp / °C	112[b]	100-102[a]	108-110[a]	100-101[a]	105-106[a]	111[a]	77[a]	77 – 111
Mp / °C	< -90[b]	< -85[a]	-88[a]	-70[a]	-53[a]	-93[a]	-84[a]	< -15
Density / g mL^{-1}	0.802[b]	0.898[a]	0.865[a]	0.875[a]	0.803[a]	0.867[a,b]	0.897[a,b]	n/a
AIT / °C	417[c]	428[c]	451[c]	443[c]	428[c]	522[c]	445[c]	> 250
LEL / %	0.91[d]	1.25[d]	0.9[d]	1.25[d]	1.25[d]	1.12[d]	1.75[d]	< 1.1%
LEL (vol.) / µl L^{-1}	64.24[b]	63.4[b]	54.02[b]	74.11[b]	69.64[b]	52.14[b]	76.74[b]	> 52.14
α	0.00[e]	0.00[e]	0.00[e]	0.00[e]	0.00[e]	0.00[e]	0.00	n/a
β	0.77[b]	0.48[b]	0.48[b]	0.45[b]	0.58[b]	0.10[b]	0.46[b]	n/a
π^*	0.35[b]	0.51[b]	0.49[b]	0.49[b]	0.59[b]	0.51[b]	0.53[b]	n/a
δ_D / MPa$^{0.5}$	15.4[f]	15.8[f]	15.4[f]	15.0[f]	15.1[f]	18.0[f]	15.7[f]	n/a
δ_P / MPa$^{0.5}$	2.4[f]	4.9[f]	4.3[f]	3.8[f]	5.5[f]	1.4[f]	5.6[f]	n/a
δ_H / MPa$^{0.5}$	2.1[f]	6.2[f]	5.1[f]	5.0[f]	3.3[f]	2.0[f]	7[f]	n/a
δ / MPa$^{0.5}$	15.7[f]	17.6[f]	16.8[f]	16.3[f]	16.4[f]	18.4[f]	18.1[f]	n/a
Water sat. / %	2.16[b]	2.45[b]	n/a	1.67[b]	2.56[b]	1.22[b]	4.23[b]	n/a
Log $P_{o/w}$	1.92[b]	1.20[b]	1.54[b]	1.74[b]	1.21[b]	2.73[a]	0.73[b]	n/a

(a) PubChem, (b) This work, (c) Work carried out by Chilworth Technology, (d) Work carried out by ITS testing services, (e) Assumed value, (f) Predicted by HSPiP

3.3.2 Solubility properties of esters and ketones

The solubility properties of the esters and pinacolone were determined in comparison with TMTHF, toluene and ethyl acetate. The KT, HSP, Hildebrand parameter, water saturation and Log $P_{o/w}$ have been determined and are shown in Table 3.4. Disparities from toluene and TMTHF are observed in all candidates due to the significant structural differences.

KT parameters

Equation 1.3 was used in combination with the absorbances of *N,N*-diethyl-4-nitroaniline to determine π^* for the esters and pinacolone. π^* was very similar in each ester candidate (0.49-0.51). This was likely due to dipolarity as opposed to polarizability, as there are no significantly polarizable functional groups on the ester molecules (halogen, cyclic carbonate and aromatic groups are particularly polarizable, ester and ketone carbonyl groups are not). π^* was slightly higher for pinacolone (0.59), indicating slightly higher dipolarity in the ketone. The π^* of the esters is very similar to toluene (0.51), however, toluene's high π^* is due to polarizability, whereas as in esters it is due to dipolarity.

Equation 1.4 was used in this work to calculate β, based on the baseline determined by Sherwood[60] and the absorbances of both 4-nitroaniline and *N,N*-diethyl-4-nitroaniline. The absorbances of ten non-hydrogen-bond accepting solvents, cyclohexane, limonene, hexane, octane, chloroform, heptane, decane, 1,2-dichloroethane, dichloromethane and chlorobenzene, were used to create a baseline which is described by Equation 3.3.

Equation 3.3. $$\lambda_{\max}(NA) = 1.00\lambda_{\max}(NN) - 3.44$$

The degree of deviation from the baseline of a hydrogen-bond accepting solvent is proportional to its β. The basicity of pinacolone (0.58) was found to be higher than that of the esters (0.45-0.48) and all were significantly higher than toluene (0.10) but lower than TMTHF (0.77).

As esters are aprotic, α was assumed to be 0.00 in all cases, like toluene. The enol form of pinacolone was suspected of contributing to hydrogen-bond donation so its UV spectrum was measured using Reichardt's dye. However, determination of α was impossible as the dye did not give a useful spectrum. The α values of acetone (0.08) and MEK (0.06) suggest that the value decreases with increasing molecular weight, so the α of pinacolone could be assumed to be negligibly low (~0.00).[21,57] This is consistent with Kamlet *et al.* who have also assumed the larger molecular weight ketones to be aprotic, and assigned an α of 0.00 to all ketones except acetone and MEK.[21]

HSPs

HSPs were calculated for each of the esters and pinacolone and they are shown in Figure 3.7. It can be seen that the esters and pinacolone have a lower polarizability, δ_D, than toluene, which is consistent with their structures: toluene has a polarizable aromatic group while the esters and pinacolone do not. The dipolarity, δ_P, is higher in each of the esters and pinacolone than in toluene due to their oxygen atoms.

Dipolarity decreased with increased branching in the esters, with methyl pivalate being the least dipolar and methyl butyrate being the most. Pinacolone was observed to be more polar than each of the esters, consistent with KT. Hydrogen-bonding ability, δ_H, also decreased with increased

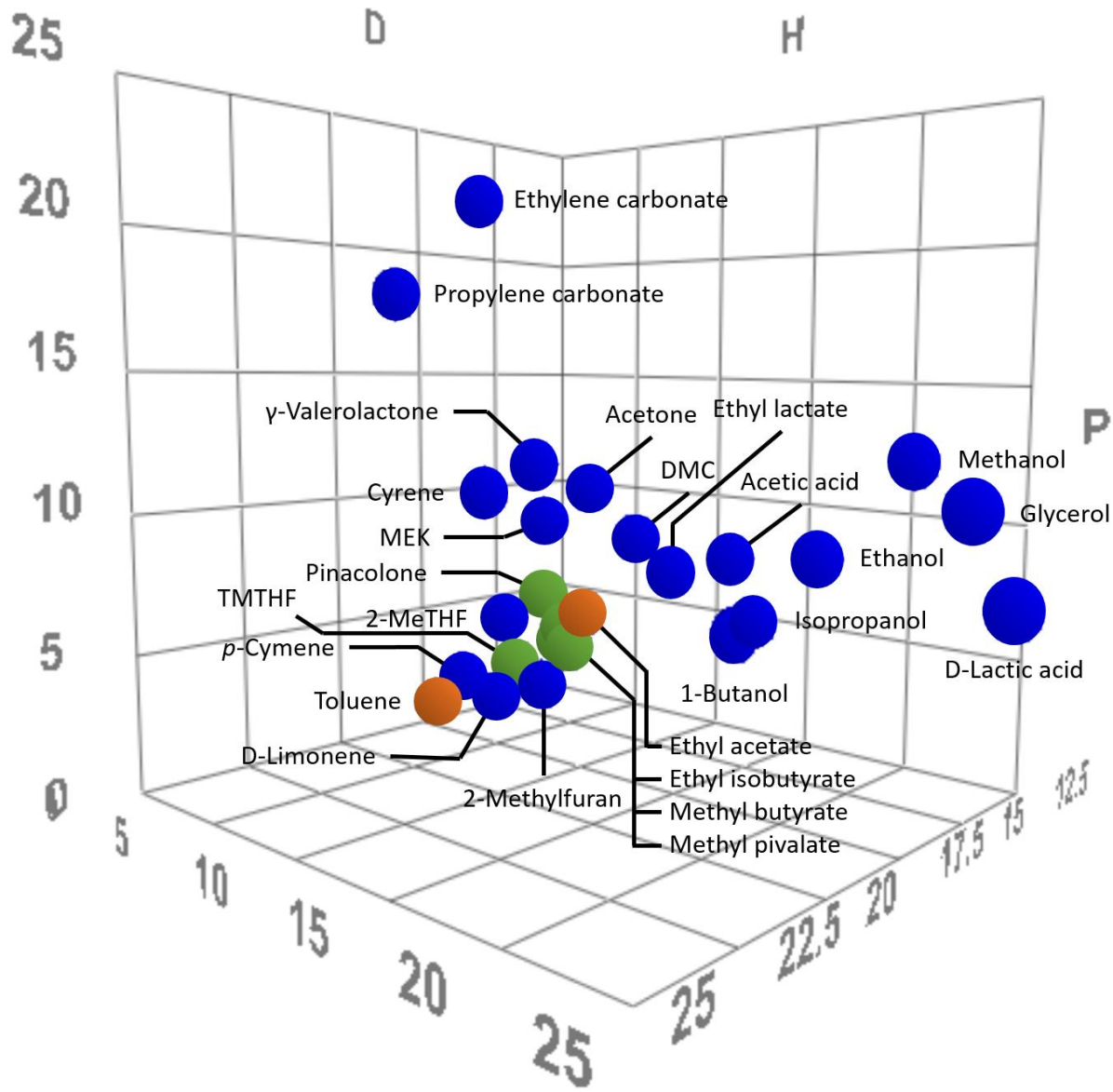

Figure 3.7. HSP map showing the five candidate solvents (green), toluene and ethyl acetate (orange) among a selection of other green solvents (blue).

branching in the esters, while pinacolone's hydrogen-bonding ability was lower than the esters. This is a counter-intuitive prediction as pinacolone's β is higher than each of the esters and the ability of ketones to tautomerize between keto and enol forms. The enol form would be able to both hydrogen-bond donate and accept.

Hildebrand parameter

The limitations of the Hildebrand parameter, δ, are highlighted when comparing the esters with toluene. It suggests that toluene is more polar due its higher δ. However, HSP and KT show that toluene only has a greater polarizability than the esters and pinacolone, but that its dipolarity and hydrogen-bonding ability are much lower.

Water saturation

The water saturation of each solvent was measured by mixing each one with water to form two phases. The water content of the organic layer of each candidate was then measured by Karl-Fischer titration. Methyl pivalate contained the least amount of water (1.67%) and was the most comparable to toluene (1.22%), whereas methyl butyrate and pinacolone contained slightly more (2.45% and 2.56% respectively).

3.3.3 Toxicity properties

Octanol/water partition coefficient (Log $P_{o/w}$)

The Log $P_{o/w}$ in all cases was greater than 1, indicating immiscibility with water (Table 3.4). Methyl pivalate exhibited the best separation from water with a value of 1.74, followed by ethyl isobutyrate at 1.54. Methyl butyrate and pinacolone demonstrated similar water separation with values of 1.20 and 1.21 respectively. The values are consistent with the observations of the water saturation tests described in the previous section and all are lower than toluene (2.73). These results are promising as a lower Log $P_{o/w}$ suggests a lower BCF compared to toluene.[284]

Ames test

Methyl butyrate, methyl pivalate and pinacolone were tested for mutagenicity using the Ames test.[74,79] Ethyl isobutyrate was not tested due to the high cost of the test and the fact that it had been eliminated from the list of candidates after the polymerisation tests. TA98 and TA100 *Salmonella typhimurium* strains were used for the Ames test.[74,79] The optional S9 rat liver extract was not included; thus, mutagenic metabolites could not be detected. DMSO was employed as the solvent and negative control while a mixture of 2-nitrofluorene (2-NF) and 4-nitroquinoline-*N*-oxide (4-NQO) was the positive control. In Figure 3.8, the green bar on the left-hand side of each

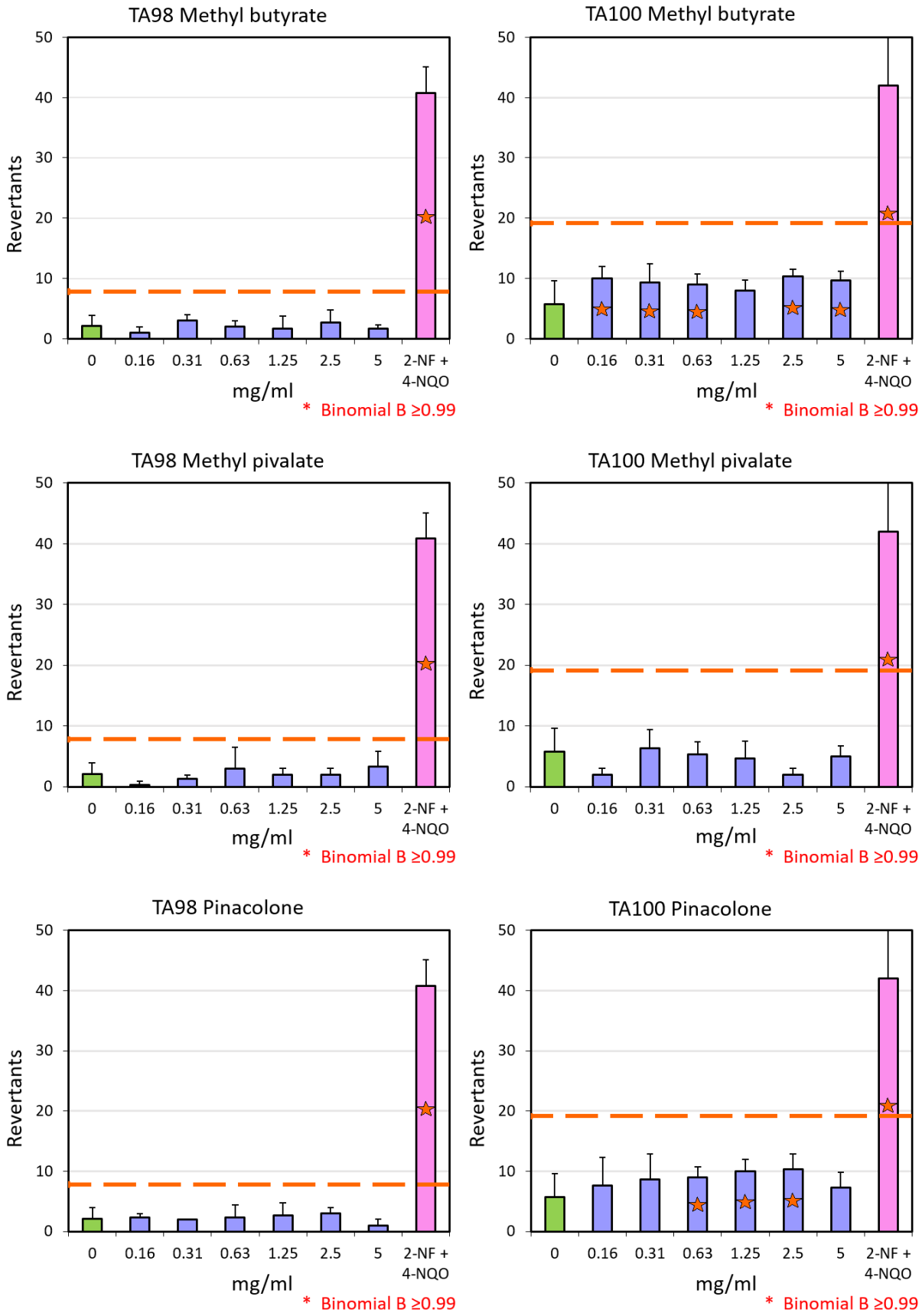

Figure 3.8. Ames test results for methyl butyrate, methyl pivalate and pinacolone.

graph is the negative control (ethanol) and the pink bar on the right-hand side of each graph is the positive control (2-NF + 4-NQO). The various concentrations of the test chemicals are shown as the purple bars.

The two-fold increase over the baseline is represented by the red dashed line while a red star indicates a binomial *B*-value ≥ 0.99. The baseline is calculated as the mean number of revertants in the negative control plus one standard deviation and a binomial B-value ≥ 0.99 indicates that chances are ≤1 that reversion was spontaneous. For a given concentration of test chemical to fail the Ames test, the number of revertants in that concentration must exceed the two-fold increase over the baseline and have a binomial *B*-value ≥ 0.99.

Methyl butyrate, methyl pivalate and pinacolone were all found not to be mutagenic in concentrations up to 5 mg mL^{-1}. In all cases, the positive control failed in both the TA98 and TA100 test strains, as the average number of revertants was above the two-fold baseline (red dashed line), and had binomial *B*-values ≥ 0.99 (Figure 3.8).

3.4 Synthesis of esters and ketones

The four candidates are sourced from similar bio-based starting materials and processes. Carbonylation is required to produce the carboxylic acid precursor for each candidate. Methyl pivalate and pinacolone can be sourced *via* the carbonylation of bio-based isobutene.[260,261] While methyl butyrate and ethyl isobutyrate can be produced *via* carbonylation of glycerol,[177] although butyric acid can also be produced from the fermentation of carbohydrates.[285] The carboxylic acids then undergo subsequent esterification to produce the three esters or ketonisation to produce pinacolone.[265] Due to the difficulties and dangers of flammability and toxicity involved in handling high pressure CO, extra precautions and equipment were required. Although carbonylation could not be carried out in the timescale of this project, future work would involve the carbonylation of alkenes to produce these solvents.

The esterification of butyric acid (BA) and pivalic acid (PA) was carried out in this work. A range of catalysts were first screened in the esterification of BA with methanol. Based on an initial screening step, a narrower selection of catalysts were then used to catalyse the esterification of BA with methanol and PA with methanol in a reactive distillation-type apparatus.

3.4.1 Catalyst screen in the esterification of BA with methanol

The esterification of BA with methanol was chosen for the catalyst screen. 13 catalysts were tested against a control experiment in which no catalyst was used. The reaction was carried out in batch

on a 5 mL scale with a 3:1 molar excess of methanol and 10 wt.% (based on BA) catalyst loading for heterogeneous catalysts and a 10.0 mmol catalyst loading for homogeneous catalysts. The results can be seen in Table 3.5.

The best performing catalysts were the homogeneous catalysts methane sulfonic acid and sulfuric acid which achieved almost full conversion (97% and 96% respectively), followed by the heterogeneous Amberlyst 15 (94%). Methanesulfonic acid is preferable to sulfuric acid as it is less corrosive, but both are toxic and expensive reactors would still be required, as a result neither the methanesulfonic acid nor sulfuric acid are ideal. Amberlyst 15 is an attractive alternative as it is heterogeneous and relatively safe. Therefore, corrosiveness is not a problem and as such, scaling up of production is easier. KSF montmorillonite performed well (84% yield) compared to K10 montmorillonite (31%) but this may be due to homogeneous catalysis caused by leaching of sulfate groups from the KSF clay into solution, although this was not confirmed. Nafion-H and sulfated zirconia produced moderate yields of 69% and 64% respectively while the effectiveness of the zeolites and K10 montmorillonite was poor.

Overall, the homogeneous sulfuric acid and methanesulfonic acid and the heterogeneous Amberlyst 15 were taken forward as the best catalysts to be tested in a reactive distillation apparatus. For comparison, the zeolite H-BEA (25:1) was also tested due to its low cost, ease of synthesis and robustness.

Table 3.5. Results of the catalyst screen for the esterification of BA with methanol.

Catalyst	Conversion of BA	Catalyst	Conversion of BA
Methanesulfonic acid	97	H-BEA (150:1)	50
Sulfuric acid	96	H-BEA (30:1)	44
Amberlyst 15	94	H-ZSM-5 (80:1)	38
KSF montmorillonite	84	H-ZSM-5 (30:1)	36
Nafion-H	69	H-ZSM-5 (280:1)	33
Sulfated zirconia	64	K10 montmorillonite	31
H-BEA (25:1)	52	Control	30

3.4.2 Reactive distillation in the production of methyl butyrate and methyl pivalate

As the boiling point of the product was lower than the BA starting material, a reactive distillation was attempted. Using this setup, as the products formed (methyl butyrate and water) they would distil out of the reaction mixture, leaving behind the less volatile BA and catalyst. As some methanol also distilled out of the reaction mixture before reacting with BA due to its low boiling point, it was topped up at different time intervals. The unreacted methanol can be recycled back into the system. Over time, the amount of BA in the reaction mixture decreased as it was esterified to methyl butyrate and distilled.

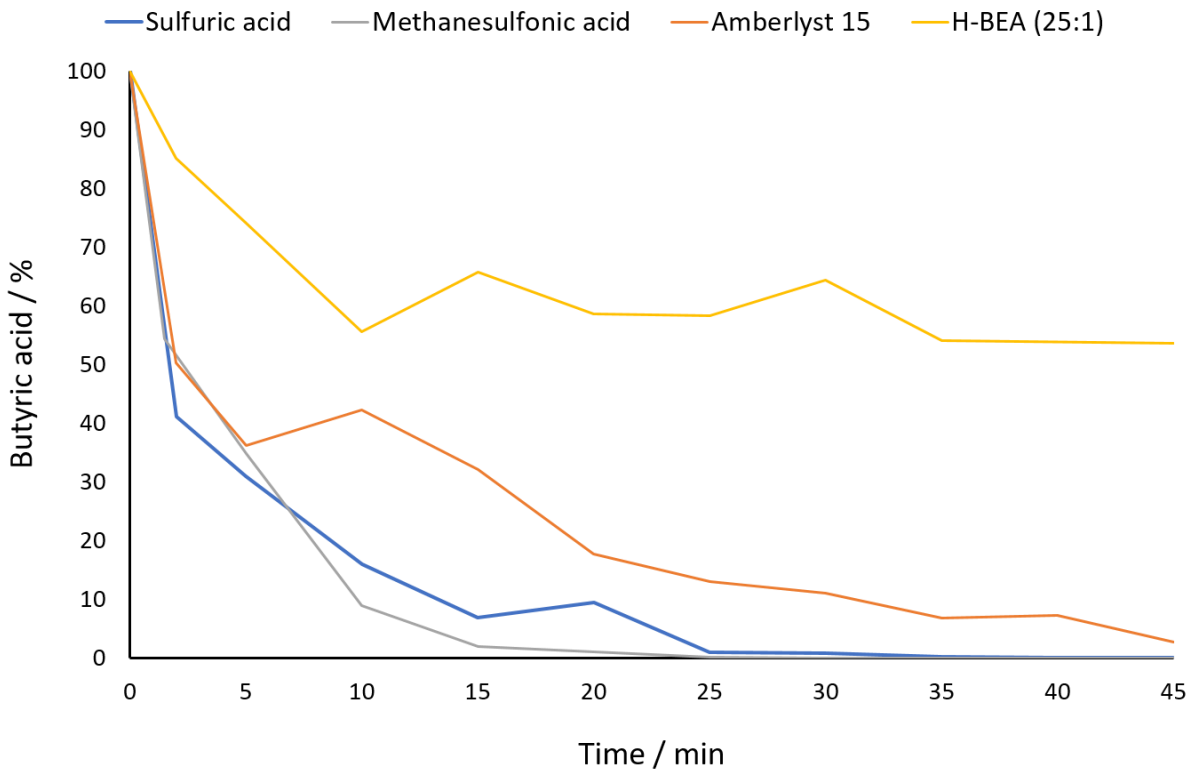

Figure 3.9. Conversion of BA in a reactive distillation-type system using four different catalysts.

The reactive distillation was carried out using a Dean-Stark apparatus. The same amounts of BA, methanol and catalyst as in the batch reactions were used in the reactive distillation. The four catalysts selected from the screening step, sulfuric acid, methanesulfonic acid, Amberlyst 15 and H-BEA (25:1) and their performance can be seen in Figure 3.9. Sulfuric acid and methanesulfonic acid demonstrated full conversion of BA within 25 and 35 minutes respectively. Amberlyst 15 achieved almost full conversion after 45 minutes, at which point the reaction was stopped. Although the rate was not as quick as in the homogeneous acids, this may be compensated for by

its non-corrosiveness, reusability, safety and cost, and presents an excellent alternative to the mineral acids for large-scale production.

The rate of the esterification of PA with methanol was slower with all catalysts compared to the BA esterification (Figure 3.10). This is possibly due to the bulky pivalic group which would be expected to hinder the reaction slightly. The same trends between the performances of the four catalysts remained: sulfuric acid was the most effective, followed by methanesulfonic acid and then Amberlyst 15. In contrast, H-BEA (25:1) was far less effective.

The reactive distillation demonstrated that simple scale-up of the esterification steps in the synthesis of methyl butyrate and methyl pivalate was realistic. Importantly, a safe, non-corrosive, reusable heterogeneous catalyst was identified to be capable of promoting the reaction. an issue with this synthesis is the separation of methyl butyrate and methyl pivalate from water due to their similar boiling points (methyl butyrate = 100-102 °C; methyl pivalate = 100-101 °C; water = 100 °C). For the solvents developed a simple distillation will not be sufficient to purify the organic solvents, therefore complex and more expensive methods will be required, *e.g.* pervaporation using a porous membrane.

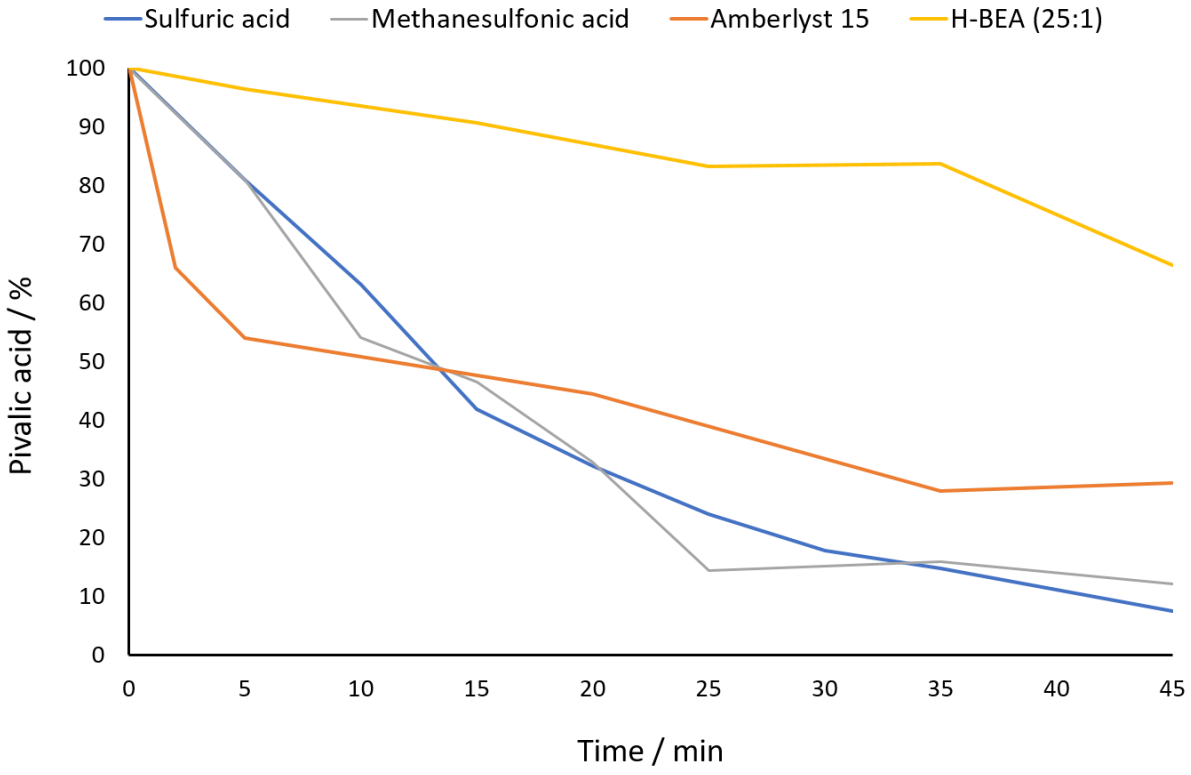

Figure 3.10. Conversion of PA in a reactive distillation-type system using four different catalysts.

3.5 Conclusion

In conclusion, four excellent candidate ester and ketone solvents with the ability to replace toluene in several applications have been identified, characterised and tested. It was found that three of the four candidates, methyl butyrate, methyl pivalate and pinacolone, could host the polymerisation. However, one of the candidates, ethyl isobutyrate, underwent chain transfer to the polymer. Due to its unsuitability, ethyl isobutyrate was removed from the list of candidates.

Physical properties such as boiling point, melting point and density, as well as AIT and LEL were measured and found to be ideal in all cases. From the LEL, a new property which takes into account molecular weight and density of a solvent, the LEL (vol.), was calculated and it too was found to be sufficiently high in all cases. Methyl butyrate, methyl pivalate and pinacolone were all found to not be mutagenic at concentration up to 5 mg mL^{-1}. In addition, all four candidates were found to have a lower Log $P_{o/w}$ which suggests a lower BCF to toluene.

The candidates were characterised by their solubility properties (KT and HSP). It was found that although the esters and pinacolone have an overall low polarity, their KT and HSP solubility properties show that they differ from toluene in hydrogen-bonding ability, dipolarity and polarizability. These differences will affect the ability of the esters and pinacolone from replacing toluene in some applications however, the solubility tests (described in Chapter 2) show that for simple dissolution of solutes, they are capable replacements. The Menschutkin reaction was used to compare each of the candidates with toluene in terms of their π^*. A limitation of the Menschutkin reaction used in this work was discovered; it was unable to characterise low polarity solvents ($\pi^* < 0.4$). However, it was successful in showing the similarity between the esters and pinacolone to toluene.

Finally, esterification of each of the corresponding carboxylic acid precursors for the production of methyl butyrate and methyl pivalate were carried out, where it was shown that a reactive distillation could be successfully carried in out using the heterogeneous catalyst Amberlyst 15 in short reaction times.

4 Synthesis, characterisation and testing of 2,2,5,5-Tetramethyltetrahydrofuran (TMTHF)

4.1 Introduction

TMTHF was the only solvent candidate proposed in the solvent selection process which was able to dissolve all the polymer and rubber samples from Nitto. Although concessions were made regarding the dissolution of rubber R5, the discovery of a solvent which is sufficiently non-polar to be able to dissolve synthetic rubber, while being sufficiently volatile to be easily removed by evaporation is of great significance to Nitto and also for the wider chemical industry.

In this chapter, TMTHF is discussed in more detail. Some synthetic routes proposed in Chapter 2 have been experimentally tested and the results are presented. Some physical properties, solubility properties and toxicity have also been measured to help characterise TMTHF as a solvent. Furthermore, TMTHF's resistance to peroxide formation is shown and it has been tested in a range of model reactions for its suitability as a solvent, addressing a major issue encountered when using ethers as reaction solvents.

4.2 Synthesis of TMTHF

Three synthetic routes to TMTHF were proposed in Chapter 2. The first route proceeded *via* the dehydrative ring-closure of 2,5-dimethyl-2,5-hexanediol (DHL) and the second route proceeded *via* the sequential hydration and ring-closure of 2,5-dimethyl-2,4-diene (DHN). As the production of both DHL and DHN have already been established by BASF[271,273] and Gevo[142,275] respectively, efforts in this work focussed on the final step of each route. Route 1 was scaled up once optimised, while only some preliminary experiments were carried out for the last step of route 2.

4.2.1 Synthesis of TMTHF from DHL

The use of several catalysts for the facile dehydration of DHL to produce TMTHF (Figure 4.1), with varying levels of success, has been reported in the literature: Olah *et al.* reported the use of Nafion-H which gave a 94% yield of TMTHF in a solvent-free reaction at 130 °C after two hours;[272] Gillis and Beck produced TMTHF from DHL, using only DMSO as a solvent in a catalyst-free synthesis, obtaining a yield of 52%;[286] Denney *et al.* described the synthesis of TMTHF from DHL using pentaethoxyphosphorane as the catalyst in DCM, obtaining a yield of 79% with triethylphosphate produced as a side-product;[287] Kotkar *et al.* reported the synthesis of TMTHF from DHL using aluminium-doped montmorillonite clay, obtaining a yield of 65% after one hour at 140 °C;[288] and Vlad and Ungur synthesised TMTHF using a DMSO/$(CH_3)_3SiCl$ reagent at 20 °C for 75 hours and obtained a yield of 75%.[289]

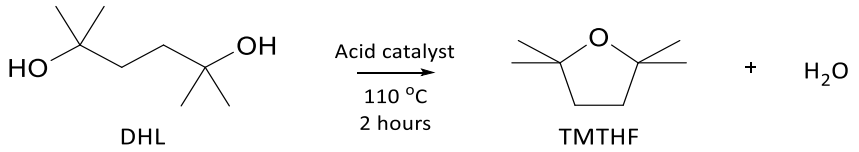

Figure 4.1. The synthesis of TMTHF from DHL.

The process of Olah *et al*. was determined to be the greenest compared to the other methods due to the short reaction time, the absence of a solvent, the use of a reusable heterogeneous acid catalyst and high yield of 94%.[272] However, while yields of 94% are excellent, the low value, high volume nature of solvent production means waste must be minimal. Therefore, the use of other acids to catalyse the dehydration of DHL were studied in this work.

Catalyst screen

An acid catalyst screen was first carried out using fixed conditions. A moderate reaction temperature of 110 °C was used as it was high enough to melt DHL (Mp = 85 °C), but, was not too far above the boiling point of water (100 °C), thus minimising the risk of boil over upon the addition of catalyst. A range of heterogeneous (1 wt.%) and homogeneous (0.9 mmol) catalysts were tested by addition to molten DHL (5 g) in batch reactions over two hours. A range of heterogeneous and homogeneous catalysts were tested which included H-zeolites, clays, Nafion-H, methanesulfonic acid and sulfuric acid. The results of the catalyst screen can be seen in Figure 4.2.

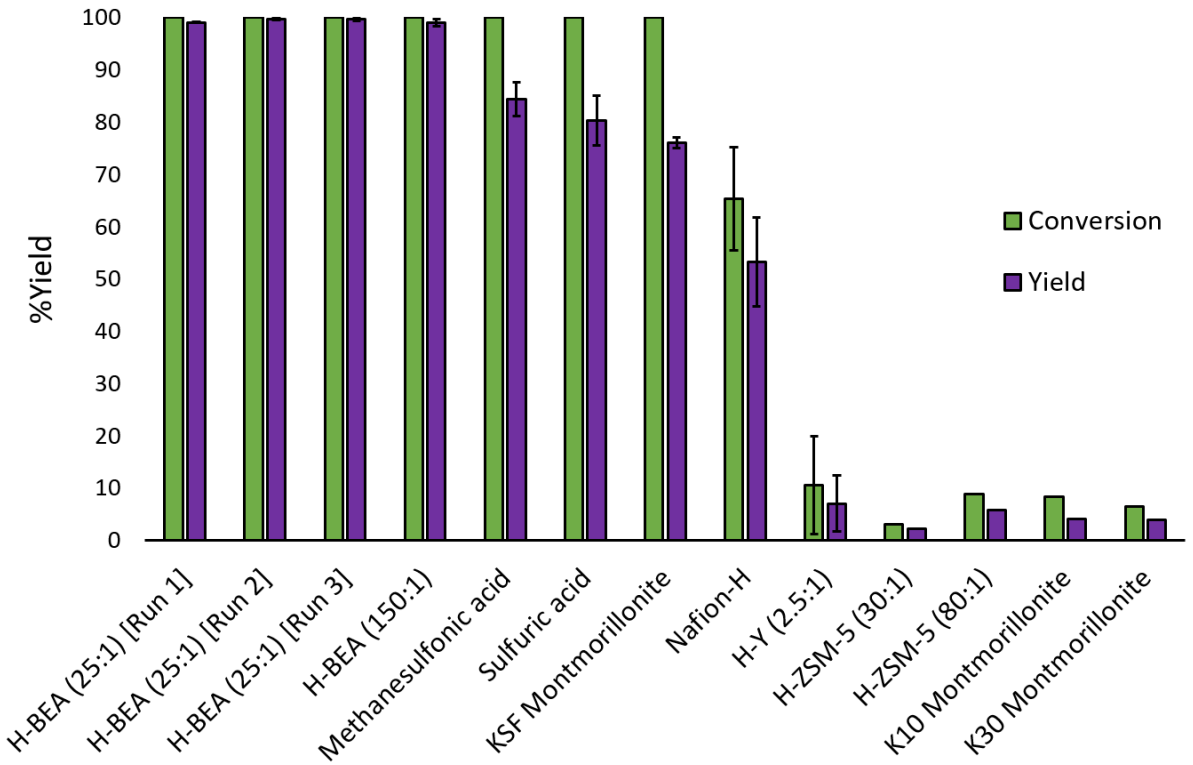

Figure 4.2. Conversions and yields from the catalyst screen for the synthesis of TMTHF from DHL. The numbers in parentheses represent zeolite silica/alumina ratio.

H-BEA-zeolites were found to fully convert DHL with excellent selectivity (>99%) for TMTHF, even at the low catalyst loadings and short reaction times employed (Figure 4.2). Trace amounts of DHN and 2,5-Dimethyl-4-hexen-2-ol (HNL) were produced as by-products. The Si/Al of the H-BEA zeolite did not affect the yield of TMTHF, as demonstrated by the performance of Si/Al ratios of 25:1 and 150:1. Future work would involve using lower catalyst loadings and reaction times in an effort to identify a difference in performance between the 25:1 and 150: Si/Al ratio H-BEA catalysts. H-ZSM-5 and H-Y zeolites were found to be ineffective for the synthesis of TMTHF from DHL. As the Si/Al did not influence the performance of H-BEA zeolites, it is not likely to impact the performance of H-ZSM-5 or H-Y zeolites. The smaller pore size of the H-ZSM-5 zeolite (6.36 x 4.70 Å)[101] could explain its inactivity, but does not explain the inactivity of the large pore sized H-Y zeolite (11.24 x 7.35 Å).[98] As water is released in the synthesis of TMTHF, the difference in hydrophobicities of H-ZSM-5 and H-Y zeolite could be a more likely reason. Commercial H-Y zeolites tend to be of a lower Si/Al ratio[290] and as such, are more hydrophilic,[291] limiting the rate of diffusion of the DHL starting material into the pores and water from the pores after formation. The lower Si/Al also results in weaker acid strengths which may also contribute to the low activity of H-Y zeolite.[96]

Moderate to good yields of TMTHF were obtained using methanesulfonic acid, sulfuric acid, KSF montmorillonite and Nafion-H as catalysts. Yields of TMTHF using Nafion-H were significantly lower in this work than those obtained by Olah *et al,*[272] but in any case, the higher yield of Olah *et al.* (94%) was still lower than those of H-BEA zeolites (>99%). It is suspected that the high conversion of KSF was due to homogeneous catalysis due to leached sulfuric acid from the catalyst, although this was not confirmed.[292] Despite the good yields obtained with sulfuric acid, methanesulfonic acid, Nafion-H and KSF montmorillonite, side-product formation was significantly higher with these catalysts, as can be seen in Figure 4.3. Side-products were proposed based on ^{1}H NMR spectroscopy (Figures A1-A7, Appendix). The formation of the dienes (DHN, DHN2 and DHN3) is more problematic than the formation of HNL, as the dienes do not rehydrate in the reaction conditions and are more difficult to separate from TMTHF by distillation. ^{1}H NMR spectroscopy, MS and IR spectroscopy characterisation data for purified TMTHF can be seen in Figure 4.4.

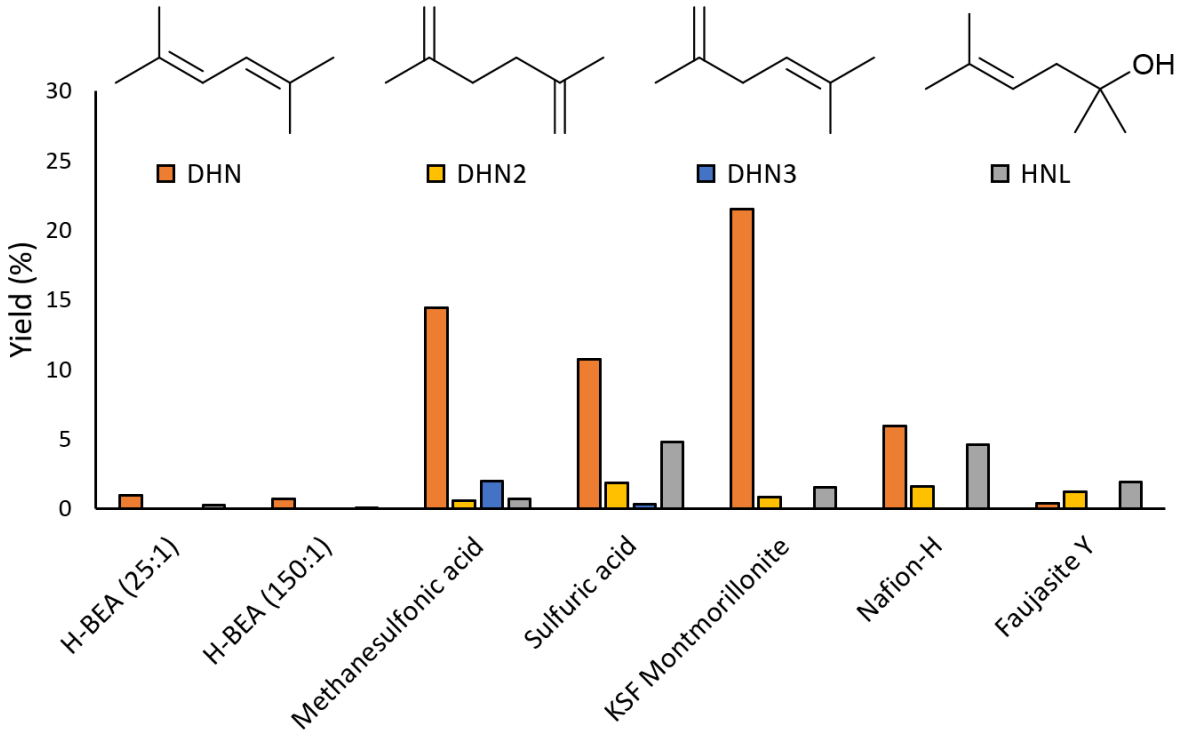

Figure 4.3. Side-products formed during TMTHF synthesis.

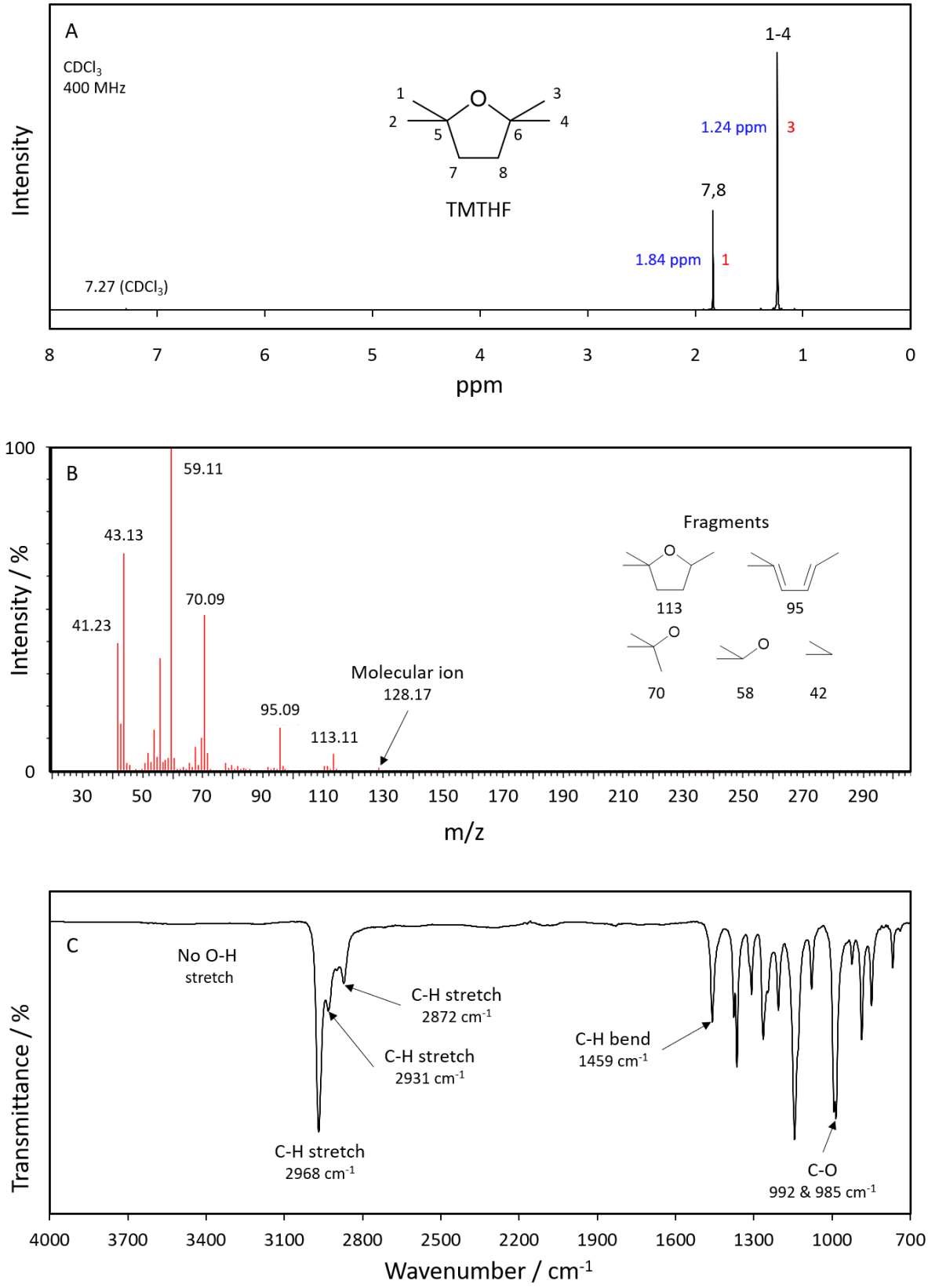

Figure 4.4. (A) ^{1}H NMR spectrum of TMTHF. (B) Mass spectrum showing the fragmentation pattern of TMTHF. (C) IR spectrum of TMTHF.

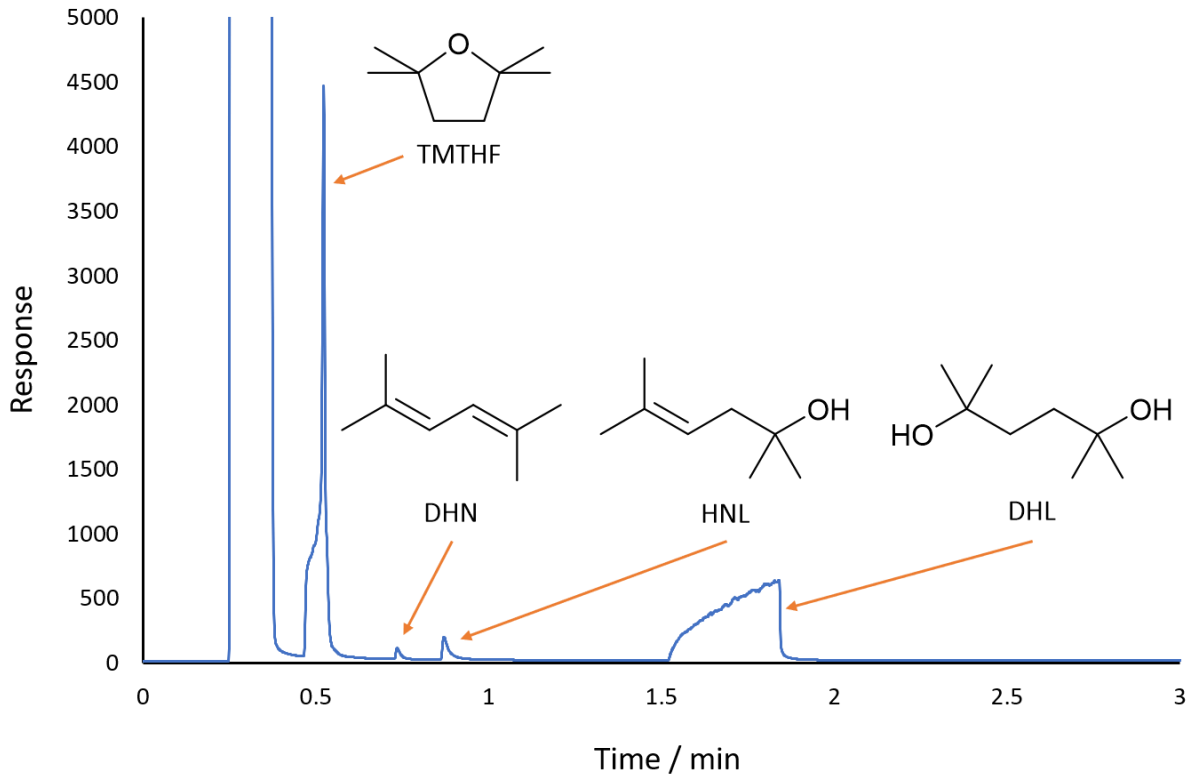

Figure 4.5. GC-FID chromatogram showing the presence of significant amounts of diol after the reaction mixture was allowed to cool to room temperature while stirring.

Interestingly, it was found that TMTHF production from DHL was sometimes reversible, depending upon the source of the starting material (some batches were pelletised, and others powdered). Figure 4.5 shows a GC-FID chromatogram of the reaction mixture after it had been allowed to cool to room temperature (18 °C) while stirring. A significant amount of DHL can be seen as well as smaller amounts of DHN and HNL. Impurities in the starting material are expected to be the cause of the different equilibria obtained, but ^{1}H NMR spectroscopy and ICP analysis were inconclusive in determining what the impurities are.

The mechanism of TMTHF production from DHL is thought to proceed as shown in Figure 4.6. One hydroxyl group on DHL is protonated and subsequently eliminates, generating a carbocation. Attack on the carbocation by a lone pair on the hydroxyl oxygen closes the ring, and subsequent deprotonation yields TMTHF (route 1). Trace amounts HNL could also be formed by deprotonation at the *alpha*-position to the carbocation (route 2). The reverse reaction is likely to be initiated by protonation of the oxygen on TMTHF.

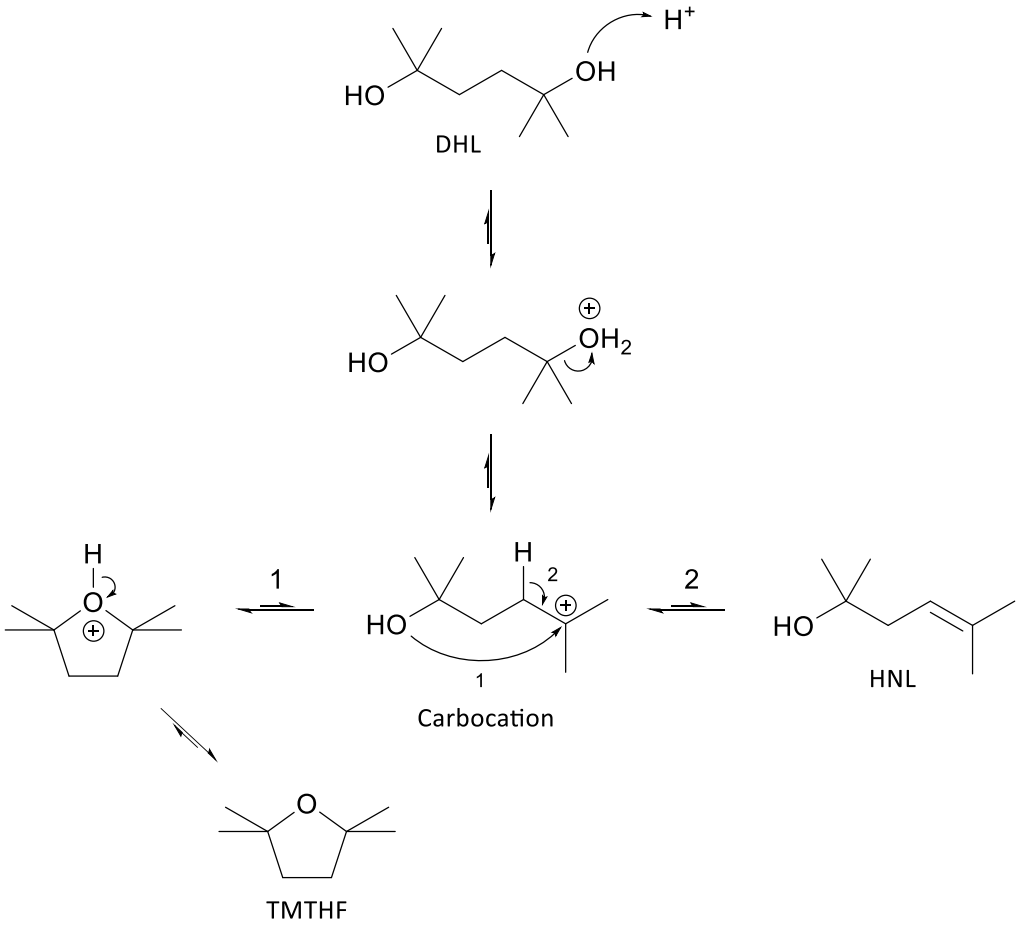

Figure 4.6. Suggested mechanism for the synthesis of TMTHF from DHL *via* HNL.

Larger scale production

The advantages of zeolites as catalysts are amplified in large-scale synthesis. They have extremely high thermal stability, they are reusable and relatively cheap.[291] The high selectivity of H-BEA zeolites in the synthesis of TMTHF maximises the amount of product formed and reduce material loss due to the formation of unwanted side-products.

The synthesis of TMTHF was easily scaled-up to 500 g scale using a 1 L flask fitted with a Dean-Stark condenser. Using this apparatus, a reactive distillation could be carried out (Figure 4.7), simultaneously purifying TMTHF by leaving behind the small amounts of dienes and HNL side-products. This setup allowed for continuous production of TMTHF by simply adding more DHL into the reaction mixture. The zeolite catalyst could be recovered and reused by filtering from the reaction residue and calcining at 600 °C for 4 hours. No noticeable loss of catalyst performance in 500 g scale batches (w.r.t. DHL, therefore 1 g of catalyst) was observed over a six-month period.

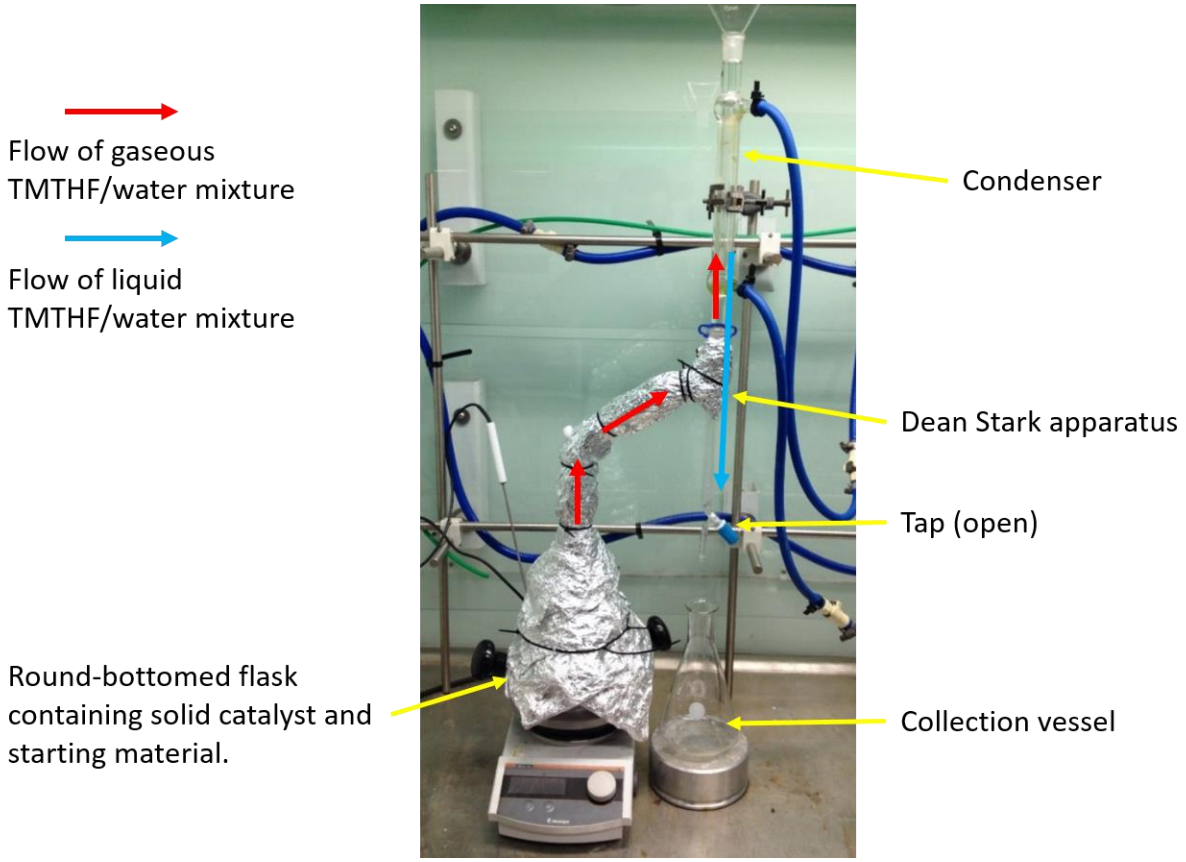

Figure 4.7. Reactive distillation apparatus employed for the 1 L scale production of TMTHF from DHL.

The yields from three successive reactions using the same catalyst can be seen in Figure 4.3, although many more were subsequently carried out with similarly high performance. Due to the simplicity of synthesis, future work would involve the scaling-up the process to a 300 kg scale.

4.2.2 Synthesis of TMTHF from DHN

The synthesis of TMTHF by the hydration of DHN proved to be more difficult in the liquid phase (Figure 4.8). Due to the hydrophobicity of DHN, simply mixing with water and a catalyst meant insufficient contact between two reactants and therefore the reaction was not possible. Several attempts were made using both heterogeneous and homogeneous catalysts. Sulfuric acid and methanesulfonic acid are highly polar and thus, transfer to the organic phase was insignificant. The low polarity, organic trifluoroacetic acid (TFA) and *para*-toluenesulfonic acid (PTSA) were tested in an effort to partition the catalyst into the organic phase with the aim of causing a reaction at the interface of the two phases. However, this was also unsuccessful. Some conversion of DHN was observed in some cases but very low selectivity for TMTHF was observed (~1% generally).

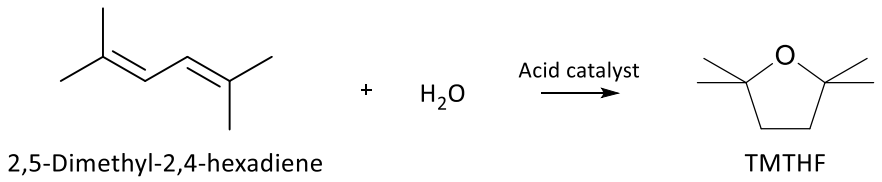

Figure 4.8. Synthesis of TMTHF from DHN.

The experiment was also carried out in a solvent to homogenise the mixture. The choice of solvent was limited, as it needed to be able to dissolve both the hydrophobic DHN as well as the water. Diglyme was employed for this purpose. It also has the benefit of a high boiling point, enabling the use of high reaction temperatures. Although homogeneity was achieved and higher yields of TMTHF were obtained using H-BEA (25) and TFA as a co-catalyst, significant oligomerisation of the diene occurred, in addition to an unidentified product which is more volatile than TMTHF (Figure 4.9). The use of diglyme is not a viable option for large-scale production due to its high reprotoxicity,[293] however, it served as a useful indicator that the reaction is possible. Future work would involve carrying out this reaction in the gas phase using a tube furnace reactor in a similar

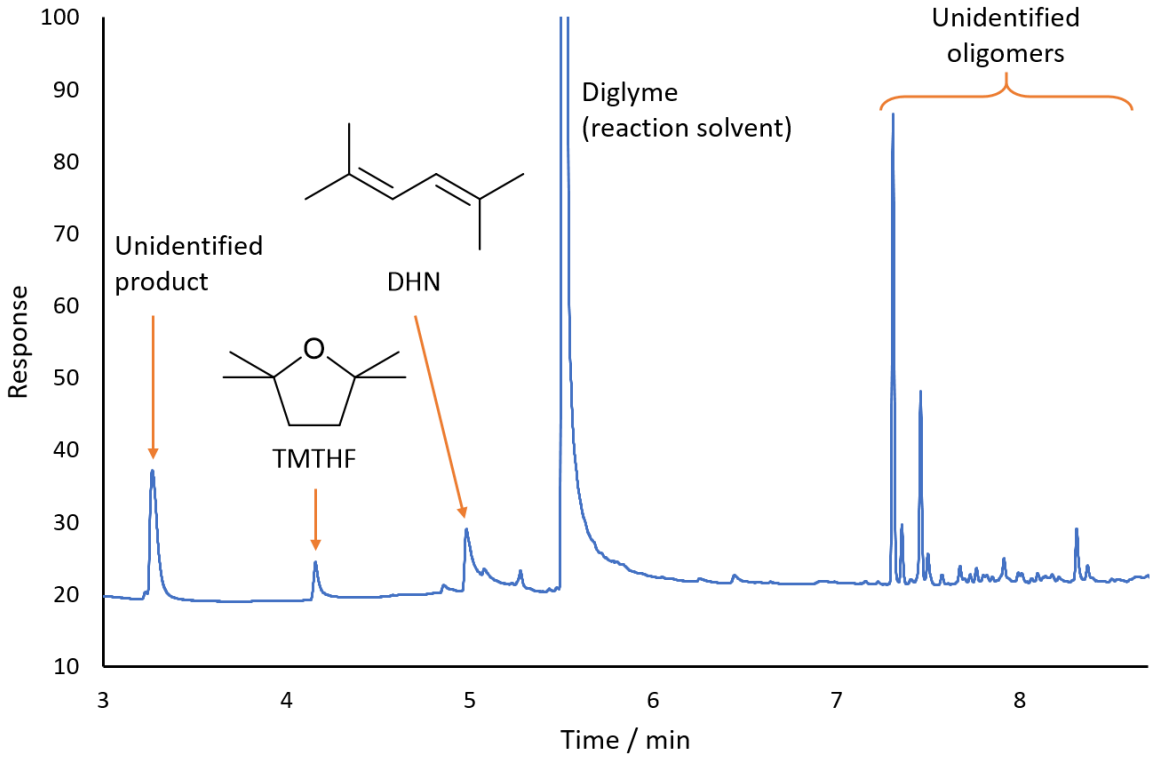

Figure 4.9. GC-FID chromatogram showing the product peaks after reaction between DHN and water.

process to the hydration of ethene.[294] Full mixing of the reagents would be achieved by this method and it is more representative of an industrial process.[294]

An alternative route to TMTHF from DHN is by first producing a polyperoxide by oxidation with bubbling air at room temperature and atmospheric pressure, as reported by Griesbaum *et al*.[276] Liquid-liquid extraction using methanol and heptane was required to separate the polyperoxide from unreacted DHN. Removal of the methanol solvent by evaporation isolated the polyperoxide and subsequently hydrogenation using a palladium-on-carbon catalyst and THF as solvent under 10 bar H_2 yields 90% DHL after 22 hours (Figure 4.10).[276] Unlike peroxides formed by ethers such as THF and diethyl ether,[295] the polyperoxide formed from DHN was reported to be shock resistant. Therefore, the dangers associated with concentrating many smaller peroxides formed from the ether itself do not apply in this case.[276]

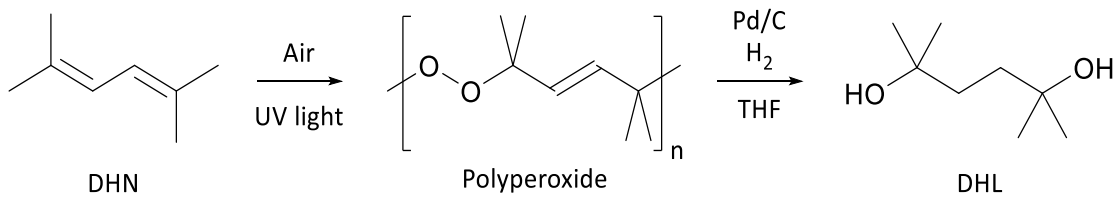

Figure 4.10. Synthetic route to DHL by the peroxidation of DHN.

This procedure was repeated in this work where it was observed that in the absence of a solvent, the increasing viscosity of the mixture as the polyperoxide formed resulted in incomplete conversion of DHN (75%, Figure A8, Appendix). As such, the process was repeated using a solvent in an effort to maintain lower viscosity and hence increase conversion of DHN. TMTHF was chosen as the solvent, as it would allow TMTHF to be both the product and the reaction solvent. 5 mL of DHN was dissolved in 5 mL TMTHF and air was bubbled through with stirring at room temperature. However, the high concentration of polyperoxide was found to be insoluble in TMTHF once conversion of DHN reached 58%. Increasing the amount of solvent to 10 mL resulted in better solubility of the polyperoxide and hence, an excellent conversion of 98% after 5 days was obtained while maintaining low viscosity (Figure A9, Appendix).

Future work in this project would involve treatment of DHN with O_2 instead of air under UV irradiation to potentially reduce peroxidation times. Catalytic hydrogenation of this mixture to yield DHL in high conversions would provide a route from DHN to DHL with no purification required in between each step.

Finally, the non-purified DHL/TMTHF mixture could be used to carry out the ring closure to produce more TMTHF in excellent yields in the same was as described earlier in this chapter. This would allow a high-yielding system for the production of TMTHF using ambient conditions and TMTHF as the solvent. Its greenness is investigated in further detail in Chapter 5.

4.3 Solvent properties of TMTHF

4.3.1 Peroxide formation

As discussed in Chapter 2, autoxidation to form peroxides is known to occur readily in many ethers.[232,281,296,297] TMTHF is not anticipated to behave in the same way due to its lack of a hydrogen in the *alpha*-position, but this must be demonstrated experimentally.

Table 4.1. Peroxide test results for TMTHF in comparison with THF, 2-MeTHF and CPME.

	Solvent	Experiment	T=0 hours (ppm)	T=3 hours (ppm)
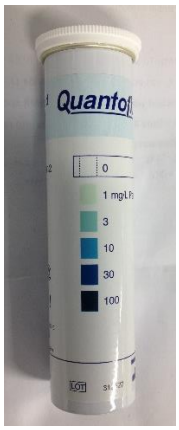	THF	Control	10-30	10-30
		Test	10-30	>100
	2-MeTHF	Control	2	2
		Test	2	>30
	CPME	Control	1	1
		Test	1	3-10
Scale	TMTHF	Control	0	0
		Test	0	0 (Reflux)

A peroxide formation accelerating experiment was designed and TMTHF was tested along with a selection of traditional ethers. In this experiment, the test solvent was placed in a round bottomed flask and stirred. Air was bubbled through using a syringe, and the solvent was exposed to UV light of wavelength 254 nm with the aim of accelerating peroxide formation. Peroxide concentrations in the test solvent were measured using Macherey-Nagel, QUANTOFIX Peroxide-100 test strips. A drop of solvent is placed on the test pad and a colour change is observed when

peroxides are present in the test solvent, shown in Table 4.1. Samples of the test solvent were taken at T=0 hours and T=3 hours. To confirm that these conditions were indeed peroxide formation accelerating, control experiments were undertaken in parallel, in which the test samples were not exposed to UV or bubbling air. A sample was taken from the control solvent at T=0 hours and T=3 hours. No change in peroxide concentration is expected in any of the control experiments. No additives were used in any of the test solvents to prevent peroxide formation and inhibitor-free versions of each of the traditional ether test solvents were bought new from Sigma Aldrich.

It can be seen that peroxides were present in each of the traditional ethers at T=0. This means that peroxides formed over time, even in the sealed bottles. As expected, no increase in peroxide concentrations were observed in the control samples (no exposure to air or UV radiation) during the time of the short experiments. An increase in peroxide concentration was observed in each of the traditional ether test samples. The concentration in THF increased from 10-30 ppm (at higher concentrations it became difficult to distinguish between the colours on the test pad) to over 100 ppm, in 2-MeTHF increased from 2 to >30 ppm and in CPME increased from 1 to 3-10 ppm. However, no peroxide was present in TMTHF at any stage of the experiments, confirming its resistance to peroxide formation. TMTHF was exposed to even harsher reflux conditions, on top of exposure to UV light and bubbling air (bottom right entry, Table 4.1), no peroxide formation was observed.

Note on peroxide formation in crude TMTHF

When crude TMTHF was tested for peroxide formation before it was distilled to remove the diene by-product, DHN, small amounts of peroxide were observed (~1 ppm). However, the source of this peroxide was the diene by-product. As described in the previous section, DHN has been previously shown to oxidise to polyperoxides in air.[276] It is important to emphasise that unlike peroxides formed by ethers such as THF and diethyl ether,[295] the polyperoxide formed from DHN is stable. Thus, the dangers associated with concentrating many smaller peroxides formed from the ether itself are not of concern.

Note on peroxide formation in CPME

The peroxide formation in CPME is particularly striking, as it has previously been claimed that it does not form peroxides.[298,299] The authors measured the peroxide concentration in CPME, diisopropyl ether, MTBE and THF over 30 days. The data presented suggested that CPME did not form peroxides, whereas the other solvents did. However, upon closer inspection of the experimental methods employed in this work, it was noticed that an antioxidant, BHT, was added

to CPME and not to the other ethers it was compared with. Therefore, the claim of Watanabe *et al.* and the Zeon corporation is very dangerous and could result in an explosion.[298,299]

4.3.2 Physical properties of TMTHF

The physical properties of TMTHF were also required to assess its suitability for Nitto's manufacturing plant. The boiling point, melting point, LEL and AIT were determined as part of this work and are shown in Table 4.2. The boiling point of TMTHF was found to 112 °C by refluxing at atmospheric pressure. This is consistent with the boiling point range found by Olah *et al.* of 112-115 °C.[272] Although slightly higher than that of toluene, it was decided that its high performance in the solubility tests compared to all other candidates meant that 112 °C was close enough. Differential scanning calorimetry (DSC) was used to find the melting point. However, no heat flow was observed from 25 °C to -90 °C which suggests that the melting point of TMTHF is below -90 °C, well below the threshold of -15 °C (Figure A23, Appendix). The density of TMTHF was measured to be 0.802 g mL^{-1}, less than of toluene (0.867 g mL^{-1}) and similar to ethyl acetate (0.897 g mL^{-1}).

Table 4.2. Properties of TMTHF in comparison with toluene and ethyl acetate.

Property	TMTHF	Toluene	Ethyl acetate	Limits
M_r / g mol^{-1}	128.25[(a)]	92.14[(a)]	88.11[(a)]	n/a
Bp / °C	112[(b)]	111[(a)]	77[(a)]	77 – 111
Mp / °C	< -90[(b)]	-93[(a)]	-84[(a)]	< -15
Density / g mL^{-1}	0.802[(b)]	0.867[(b)]	0.897[(b)]	n/a
AIT / °C	417[(d)]	522[(d)]	445[(d)]	> 250
LEL / %	0.91[(c)]	1.12[(c)]	1.75[(c)]	< 1.1%
LEL (vol.) / µl L^{-1}	64.24	52.14	76.74	> 52.14

(a) from Pubchem database[220], (b) This work, (c) Carried out by Chilworth Technology, (d) Carried out by ITS testing services.

The AIT was determined using ASTM E659 and LEL was tested using ASTM E681. Toluene and ethyl acetate were also tested as references for both AIT and LEL. It is noteworthy that the values obtained for toluene and ethyl acetate differed from those publicly available in material safety data sheets. The measured LEL for toluene was consistent with the published data (1.1% in both

case), but the AIT was different. The measured AIT was 522 °C while it is reported to be 535 °C. The measured LEL for ethyl acetate was 1.75% compared to the reported value of 2.2% and the measured AIT value was 445 °C compared to the published value to 426 °C.

The AIT value of TMTHF measured as 417 °C, which was well above the threshold of 250 °C set by Nitto, but the LEL value of 0.9% was below the limit of 1.1%. However, the corrected LEL (vol.), which considers molar mass and density, was calculated as described in Chapter 3 where it was found that a larger mass of TMTHF can be present in the air before a flammable mixture is reached. An example calculation of the LEL by mass is shown in the in the Appendix.

4.3.3 Solubility properties of TMTHF

Although TMTHF is an ether by definition, it behaves more like toluene than other widely used ethers such as THF or diethyl ether. Its HSPs, KT parameters, Hildebrand parameter, water saturation and octanol/water partition coefficient are discussed in this section. Table 4.3 shows a selection of solubility measurements of TMTHF in comparison with toluene and THF, a traditional

Table 4.3. The solubility properties of TMTHF in comparison to those of toluene, an aromatic hydrocarbon, and THF, a traditional ether.

Property	TMTHF	Toluene	THF
α	0.00[(a)]	0.00[(a)]	0.00[(a)]
β	0.77[(b)]	0.10[(b)]	0.58[(b)]
π^*	0.35[(c)]	0.51[(c)]	0.59[(c)]
δ_D / MPa$^{0.5}$	15.4[(d)]	18.0[(d)]	16.8[(d)]
δ_P / MPa$^{0.5}$	2.4[(d)]	1.4[(d)]	5.7[(d)]
δ_H / MPa$^{0.5}$	2.1[(d)]	2.0[(d)]	8.0[(d)]
δ / MPa$^{0.5}$	15.7[(d)]	18.2[(d)]	19.5[(d)]
Water saturation / %	2.16	1.22	Miscible
Log $P_{o/w}$	1.92[(e)]	2.73[(e)]	0.46[(e)]

(a) Assumed value, (b) This work using *N*,*N*-diethyl-4-nitroaniline and 4-nitroaniline, (c) This work, using *N*,*N*-diethyl-4-nitroaniline, (d) from HSPiP, (e) This work.

ether. It was found that the HSP description of TMTHF was more accurate than that of the KT parameters.

HSPs of TMTHF

While KT parameters depict TMTHF to be like other ethers such as THF, HSP suggests that the solvation power of TMTHF is more like toluene, an aromatic solvent free of heteroatoms (Table 4.3). The δ_D and δ_P of TMTHF are low (15.4 and 2.4 respectively), consistent with its low π^*. However, the δ_H of TMTHF is low (2.1), which is inconsistent with its high β. Its low δ_H is much more like that of toluene (2.0) than that of THF (8.0).

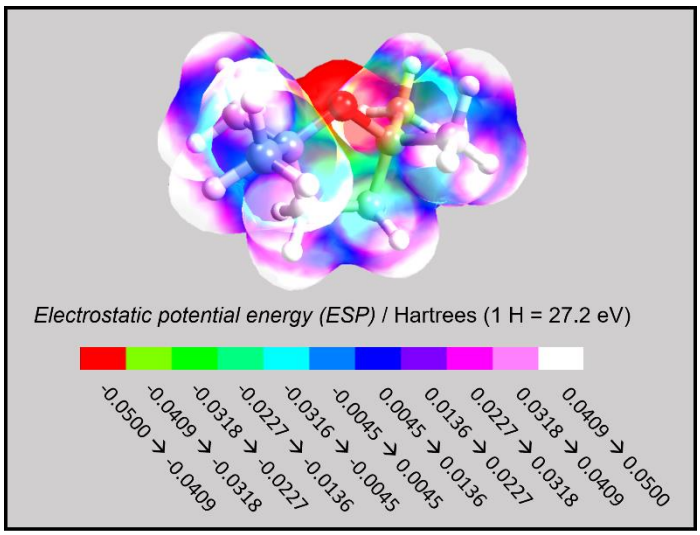

Figure 4.11. TMTHF with mapped surface ESP.

Overall, its KT parameters suggest that TMTHF should behave like a typical ether solvent such as THF but interestingly, its HSPs suggest it will behave more like toluene. It will be shown in Section 3.4 that the HSP description of TMTHF proved more accurate.

An ESP energy map of TMTHF can help to explain the difference between the HSP and KT (Figure 4.11). The areas coloured red on the ESP map are areas of high negative charge density, the areas coloured white are positively charged areas while blue represents neutral regions. Red areas caused by the lone-pairs of electrons on TMTHF's ethereal oxygen, which are the source of its high β, can be seen. However, it can also be seen that access to the lone-pairs is sterically inhibited by the four adjacent methyl groups. This results in reduced hydrogen-bond accepting ability in TMTHF, consistent with its HSPs.

The low Hildebrand parameter, δ, of TMTHF is as a result of both its low δ_H and its low CED (from Equation 1.1). Although CED has not been measured, the lack of polarity and the steric hindrance to hydrogen bonding ability would be expected to be the main causes of its low value.

Overall, while high hydrogen-bond accepting ability is present in TMTHF, shown by its high β, steric hindrance caused by the four methyl groups inhibits this interaction. To confirm its suitability as a replacement for hydrocarbon as opposed to ether solvents, TMTHF has been tested as a solvent in several chemical reactions, described in Sections 3.4, 3.5 and 3.6. Specific reactions were selected where the solvents basicity is known to contribute significantly, both positively and negatively.

KT parameters of TMTHF

Equation 1.3 was used in combination with *N,N*-diethyl-4-nitroaniline to determine π^* for TMTHF. Although *N,N*-diethyl-4-nitroaniline has been reported to suffer from poor band shape in low-polarity solvents,[54] it is one of the earliest dyes used by Kamlet *et al*. to determine the π^* scale.[47] It has recently been utilised by Sherwood *et al*. to classify some green solvents and it is also used in this work.[53,60,222] A λ_{max} = 379 nm was observed for *N,N*-diethyl-4-nitroaniline dissolved in TMTHF which resulted in a π^* = 0.35.

As described in Chapter 3, β was calculated using Equation 1.6 and the absorbances of both 4-nitroaniline and *N,N*-diethyl-4-nitroaniline. A λ_{max} = 360 nm was observed for 4-nitroaniline when dissolved in TMTHF which corresponded to a β = 0.77.

The KT parameters describe TMTHF to be like traditional ethers such as THF, as can be seen in Table 4.3. TMTHF, toluene and THF are aprotic and are assumed to have α = 0. Like other ethers, TMTHF has a high β (0.77) due to the hydrogen-bond accepting lone-pairs of electrons on the ethereal oxygen, whereas toluene has a low β (0.10), more typical of aromatic hydrocarbons. TMTHF has a lower π^* (0.35) than toluene (0.51). π^* is a measure of both dipolarity and polarisability combined, so while dipolarity in toluene is low, its polarisability, caused by the free-to-move electrons in its aromatic ring, is high which results in an elevated π^*. In contrast, TMTHF has very little free movement of electrons but a slight dipole caused by the ethereal oxygen. The dipole in TMTHF is lower than THF due to the four non-polar methyl groups on the *alpha*-position. The same four methyl groups are electron-donating and are also responsible for the enhanced β in TMTHF compared to THF.

Abraham solvation parameter model

The solvation parameter model (Equation 1.10) was used to gain further information about the performance of TMTHF as a solvent compared to toluene.

Equation 1.10. $$Log\ K_P = c + eE + s'S + a'A + b'B + vV$$

The system constants, or partition coefficients, between two water/organic solvent phases are of interest in this work. The system constants describe which solvent-solute interactions are the most significant in that solvent system and their disclosure provides a deeper insight when comparing two solvents with each other, as hydrogen-bond donating and accepting ability, dipolarity, polarisability and molar volume are all considered, unlike the three parameter models of Hansen and KT. A similar method has previously been used to characterise solvents in several organic biphasic systems, such as propylene carbonate with heptane, isopentyl ether and 1-octanol,[300] and dimethylformamide (DMF) with 1,2-dichloroethane, 1-octanol and diisopentyl ether.[301]

In this work, SP is the solute partition coefficient, Log K_P, which describes the distribution of a solute between two phases at equilibrium. Log K_P was measured in a series of solute partitioning experiments between a water/organic solvent biphasic system. The *S*, *A*, *B* and *E* solute descriptors of Jover *et al.*[302] have been used in this work while the *V* values were predicted using HSPiP software. Gas chromatography was used to measure the partitioning of 66 solutes in two biphasic systems, TMTHF/water and toluene/water. All experimental work on the Abraham solvation parameter model was conducted in collaboration with Mr. William Hodds at the University of York, as part of his internship between June-August 2016.

Regression analysis was performed using log K_P as the independent variable, and the known solute descriptors (uppercase) *S*, *A*, *B*, *E* and *V* for the 66 solutes as the dependent variables, to determine the system constants (lowercase) *s'*, *a'*, *b'*, *e*, *v* and *c*. The values of the system constants describe the factors which influence solvation within the systems and allows a comparison between each system.[300,303,304] As the aqueous phase is common to both systems, TMTHF can be compared to toluene with respect to the five solute descriptors of the solvation parameters model.

The 66 solutes were chosen specifically to be representative across a broad area of the "solute space". Molecules containing different heteroatoms and functionality were included in the solute list resulting in a range of *S*, *A*, *B*, *E* and *V* values and combinations. As gas chromatography was the method of analysis used to determine log K_P values, the solutes also had to be sufficiently volatile. In Figure 4.12, Graph A shows *S* versus *B*, graph B shows *S* versus *E* and graph C shows *S*

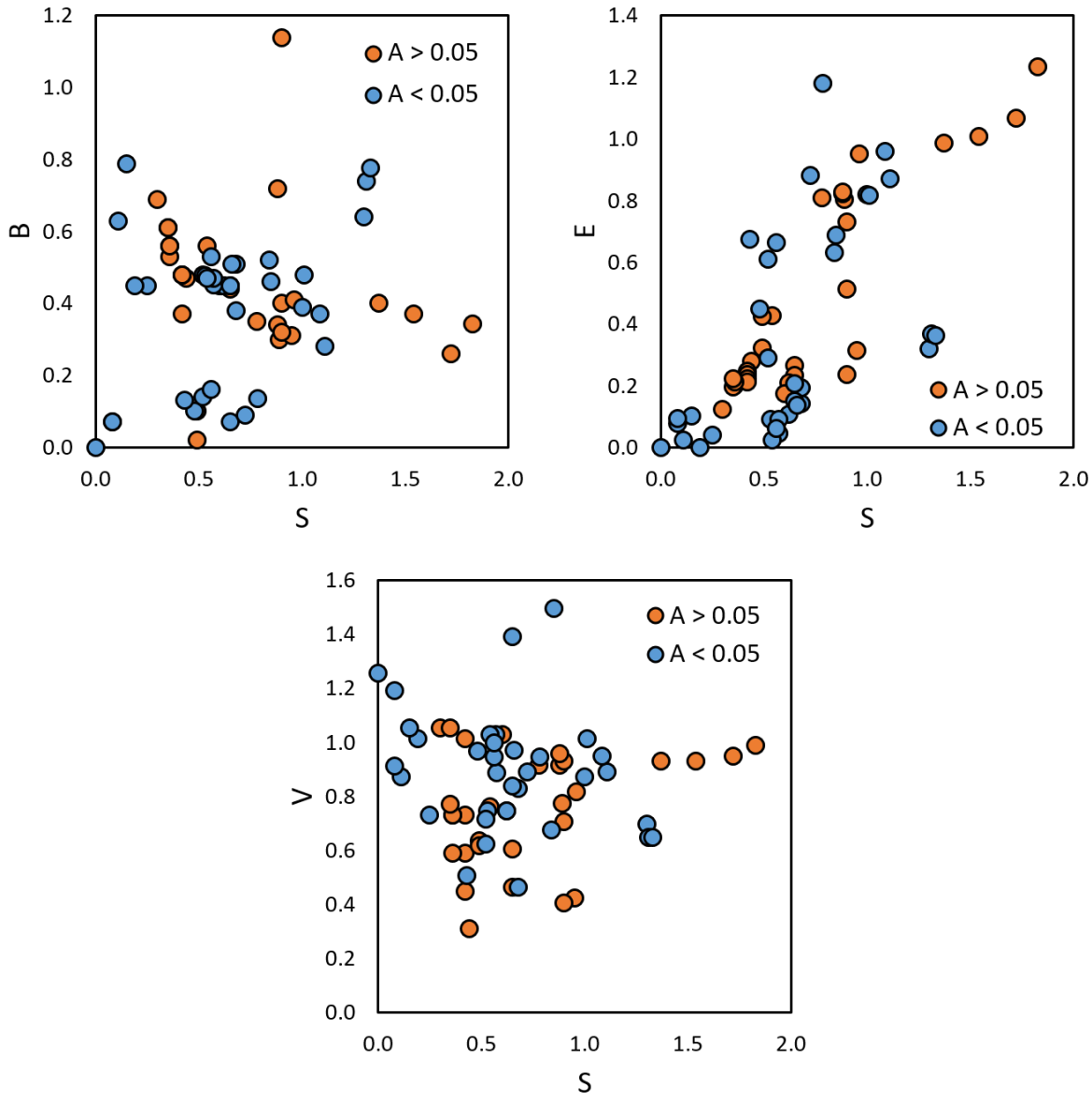

Figure 4.12. Graphs showing the distribution of solutes. S versus B, E and V are shown in three graphs. A > 0.05 is represented by orange circles while A < 0.05 is represented by blue circles.

versus *V*, demonstrating the variety of solute properties. Protic solutes with A > 0.05 are represented by orange circles while aprotic solutes with A < 0.05 are represented by blue circles. The list of solutes, their log K_P values and their descriptor values can be seen in Table A1 (Appendix). Descriptor values were taken from the database of Abraham.[59]

Regression analysis using the data from Table A1 (Appendix) gave the system constants shown in Table 4.4, where *s'*, *a'*, *b'*, *e*, *v* and *c* are the system constants, R^2 is the square of the multiple correlation coefficient, SE is the standard error, the p-value indicates the likelihood of the correlation being due to random noise, and n_s is the number of solutes considered in the model.

The system constants with negative values indicate a preference for the aqueous phase while those with positive values indicate a preference for the organic phase.

The negative *s'* constant (dipolarity) in both systems shows that a solutes dipolarity is a driver towards the aqueous phase, with toluene being slightly less attractive for polar solutes than TMTHF due to its more negative value.

Constant *a'* (hydrogen-bond donating ability), illustrates the main difference between toluene and TMTHF. The ethereal oxygen on TMTHF is capable of accepting hydrogen-bonds and can therefore interact with hydrogen-bond donating solutes. As a result, the *a'* constant of the TMTHF/water system is only slightly negative, indicating only slight preference for the aqueous layer. In contrast, toluene cannot interact with hydrogen-bond donating solutes, so a large negative value is observed. Therefore, hydrogen-bond donating solutes are far more favoured in the aqueous phase in the toluene/water system.

Table 4.4. Regression data showing the system constants, *s*, *a*, *b*, *e* and *v*, as well as the R^2, *SE*, *p*-value and number of tested solutes, n_s, in each model.

Property	Toluene/water	TMTHF/water
s'	-0.767	-0.502
a'	-1.963	-0.257
b'	-2.636	-2.828
e	0.964	0.579
v	2.471	1.637
c	0.278	0.698
R^2	0.794	0.715
SE	0.635	0.524
p-value	< 0.001	< 0.001
n_s	64	55

The *b* constant is negative in both systems, suggesting that solute hydrogen-bond accepting ability it is a driver for the aqueous phase where it can interact with the water protons. Neither toluene nor TMTHF are protic so cannot partake in this type of interaction.

The excess molar refraction (*e*) is a measure of the polarisable electrons in a solute. As there is almost no polarisability in the small water molecule and a high degree of polarisability in alkyl and aromatic molecules, the *e* constant favoured the organic layer in both systems, particularly in the polarisable aromatic toluene layer.

The large positive *v* constant favours the less self-associating phase, which in both cases is the organic layer. Due to hydrogen-bonding in water, its self-association is much higher than the non-polar organic solvents toluene and TMTHF, demonstrated by its higher Hildebrand parameter (32.8 $MPa^{0.5}$ for water compared to 18.2 $MPa^{0.5}$ and 15.7 $MPa^{0.5}$ for toluene and TMTHF respectively). As such, more energy is required to form a large cavity in water to dissolve large solutes compared to toluene and TMTHF.

Table 4.5. Comparison of the toluene/water system constants from this work and the work of Abraham *et al.*[59]

	s'	*a'*	*b'*	*e*	*v*	*c*
This work	-0.767	-1.963	-2.636	0.964	2.471	0.278
Abraham *et al.*	-0.720	-3.010	-4.824	0.527	4.545	0.143

The system constants obtained for the toluene/water system in this work were compared with those of Abraham *et al*. (Table 4.5).[59] Significant differences can be seen between the *a*, *b*, *e* and *v* descriptors. In all cases, the differences were such that the solutes would be predicted to favour the organic layer more in Abraham's work (higher *e* and *v*, lower *a'*, *b'* and *s'*). This is likely to be due to the differences in solutes used between the two systems. Abraham *et al*. primarily used aromatic solutes with many being large conjugated aromatic systems, such as naphthalene and anthracene based molecules, which will have relatively similar solute descriptors and which would strongly favour the organic layer.[59] The lack of diversity among solute descriptors could possibly have skewed the data. In contrast, the solutes used in this work represent a broad area of the HSP space, as shown in Figure 4.12. The data in this work is useful for a comparison of the TMTHF/water and toluene/water systems but for a better comparison with work from other

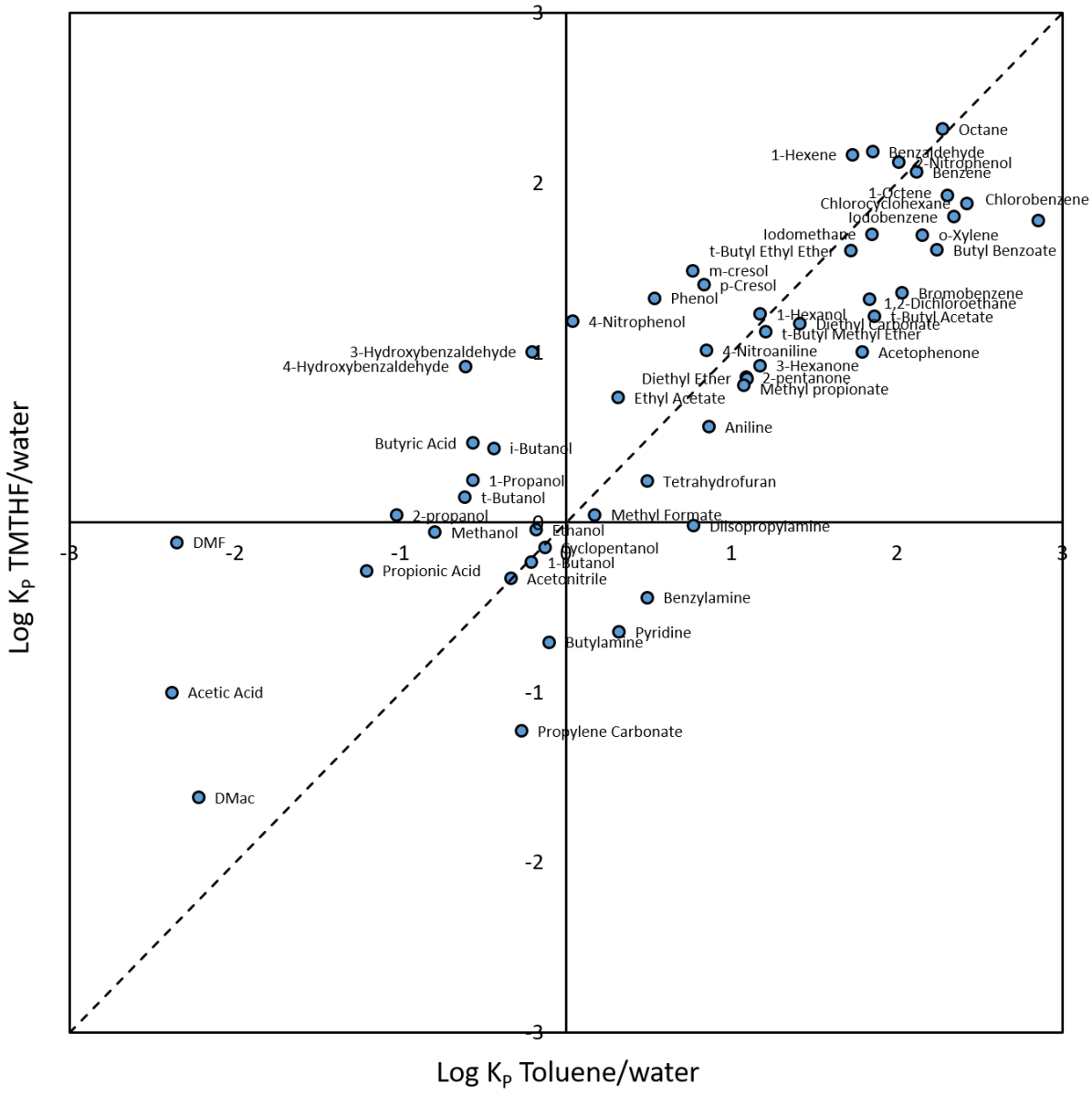

Figure 4.13. Graph comparing the partitioning of solutes in the TMTHF/water system and toluene/water system.

groups, the same solutes should be used in both systems, and the solutes must cover a broad range of the solute space.

Figure 4.13 shows the partitioning in the toluene/water system compared to the TMTHF/water system. Deviations from the dashed line through the origin show the preference of certain solutes for one organic phase over the other. Solutes placed above the dashed line were more comfortable in the organic layer in the TMTHF/water system compared to the toluene/water system and vice versa. It can be seen that protic solutes such as acids, alcohols, phenols were more solubilised in

the basic TMTHF solvent where they can hydrogen-bond, as demonstrated by the weakly negative *a'* system constant in the model (Table 4.4). Amines, ethers, aromatics and haloaromatics tended to favour toluene over TMTHF, consistent with the higher *e* system constant of the toluene/water system. This suggests less lone-pair repulsion in toluene compared to TMTHF. Poole *et al*. previously demonstrated lone-pair repulsion in propylene carbonate using the Abraham solvation parameter model in a propylene carbonate/heptane system, which is consistent with the observations of this work.[300] Propylene carbonate has a strong preference for toluene over TMTHF which suggests repulsion to the lone-pairs in TMTHF. Finally, alkenes, alkanes and ketones tended to be partition similarly in both systems due to the lack of any significant hydrogen-bonding in these classes of molecules.

Table 4.6. System constants of the training set models for the toluene/water and TMTHF/water biphasic systems.

Property	Toluene/water	TMTHF/water
s'	-0.482	-0.158
a'	-2.061	-0.485
b'	-2.571	-2.579
e	0.718	0.222
v	2.570	1.900
c	0.159	0.419
R^2	0.782	0.704
SE	0.607	0.494
p-value	< 0.001	0.001
n_s	52	44

The predictability of the model was tested using a training set and test set of solutes which were chosen by random selection. ~80% of the entire data set was used in the training set and the remaining ~20% of the data was used in the test set. The model was generated using the training set and its predictability was tested using the test set. Some changes in the training model (Table 4.6) compared to the original model (Table 4.4) were observed as expected, as the data used was

different and the number of solutes is reduced. However, the relative differences between the toluene/water system and the TMTHF/water system remained similar.

When the training set model was used to predict the system constants of the test solutes, an R^2 of 0.877 was obtained in the toluene/water system, and an R^2 of 0.818 was obtained in the TMTHF/water system, indicating reasonable model predictability in both systems (Figure 4.14). However, the purpose of this exercise was not to produce a model with high predictability for solute partitioning, but instead to determine the coefficients in each model to allow a comparison between the two systems in terms of Abraham's solvation parameter model, which was achieved successfully.

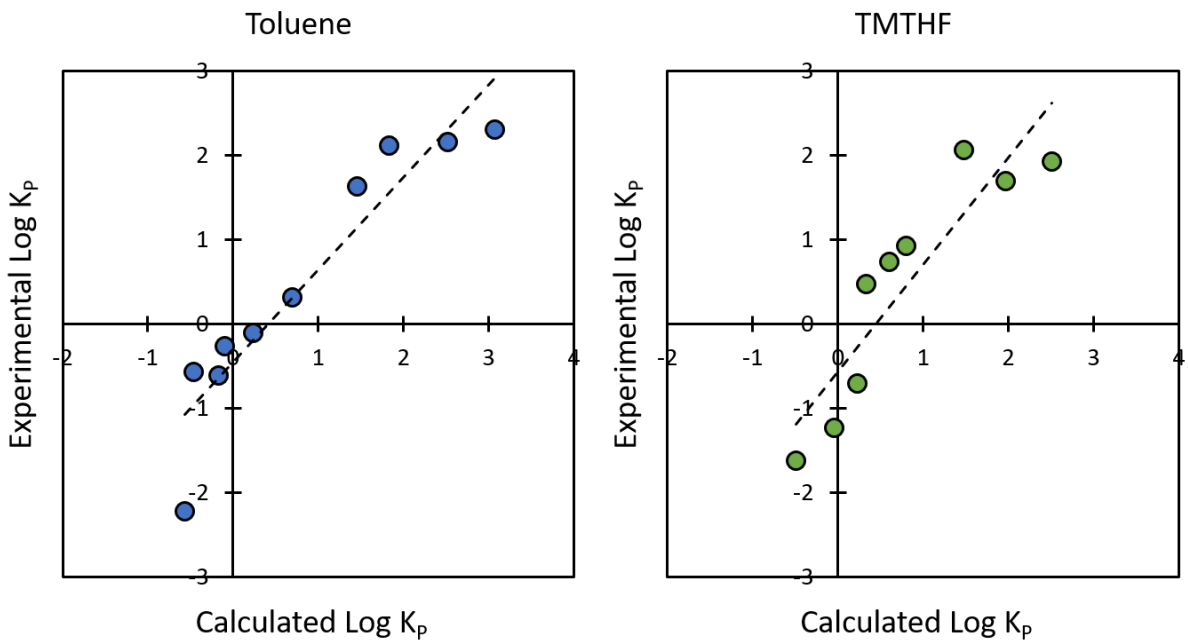

Figure 4.14. Predictability of the solvation parameter models.

Water saturation

TMTHF and toluene were saturated with water, and their level of saturation was determined using Karl-Fischer titration. TMTHF was found to absorb more water than toluene (2.16% and 1.22% respectively), as shown in Table 4.3. This is not surprising as TMTHF can accept hydrogen-bonds from water, whereas toluene cannot. It is also worth noting that under the same experimental procedure THF was found to be fully miscible with water, thus highlighting the significant impact the introduction of the four methyl groups has on TMTHF's interaction with water. In a similar experiment, diethyl ether was previously found to absorb 1.47%,[305] slightly

higher than toluene but lower than TMTHF, indicating lower water miscibility in open chain ethers compared to cyclic ethers.

4.3.4 Toxicity properties

Octanol/water partition coefficient (Log $P_{o/w}$)

The Log $P_{o/w}$ for TMTHF was experimentally determined to be 1.92, compared to 2.73 for toluene and 0.46 for THF, as shown in Table 4.3. Both have values greater than 1, indicating that that they are immiscible with water. The lower Log $P_{o/w}$ for TMTHF is consistent with the observations of the Abraham parameter model in that TMTHF has a greater affinity for protic solutes, including water. The lower value of TMTHF also means that it is less likely to bioaccumulate than toluene.[80–82] The Log $P_{o/w}$ of THF is less than 1, indicating that it is miscible with water.

Ames mutagenicity testing and nearest neighbour toxicity prediction

The Ames mutagenicity test was carried out using TA98 and TA100 *Salmonella typhimurium* strains, which detect frameshift mutations (base pair insertion or deletion) and base pair substitution respectively.[74,79] An optional rat liver extract, S9, was not added due to regulations within our research group regarding animal testing and prevented the detection of mutagenic metabolites.

Due to the insolubility of TMTHF in DMSO, ethanol was employed as the solvent and negative control. The positive control was a 2-nitrofluorene (2-NF) and 4-nitroquinoline-*N*-oxide (4-NQO) mixture. In Figure 4.15, the negative control (ethanol) is shown as the green bar on the left-hand side of each graph and the positive control (2-NF (2 μg mL^{-1}) + 4-NQO (0.1 μg mL^{-1})) is shown as the pink bar on the right-hand side. The various concentrations of the test chemical are shown as the purple bars. The red dashed line represents the two-fold increase over the baseline while a red star indicates a "binomial *B*-value" ≥ 0.99. The baseline is calculated as the mean number of revertants in the negative control plus one standard deviation and a binomial *B*-value ≥ 0.99 indicates that chances are ≤1 that reversion was spontaneous. For a given concentration of test chemical to fail the Ames test, the number of revertants in that concentration must exceed the two-fold increase over the baseline and have a binomial *B*-value ≥ 0.99.

As expected, the positive control failed in both the TA98 and TA100 test strains, as the average number of revertants was 40.8 and 42.0 respectively, both of which were above the two-fold baseline (red dashed line), and both had binomial *B*-values ≥ 0.99 (Figure 4.15). The results also showed that TMTHF was not likely to be mutagenic in either strain in concentrations of up to 5 mg mL^{-1} (40 mM).

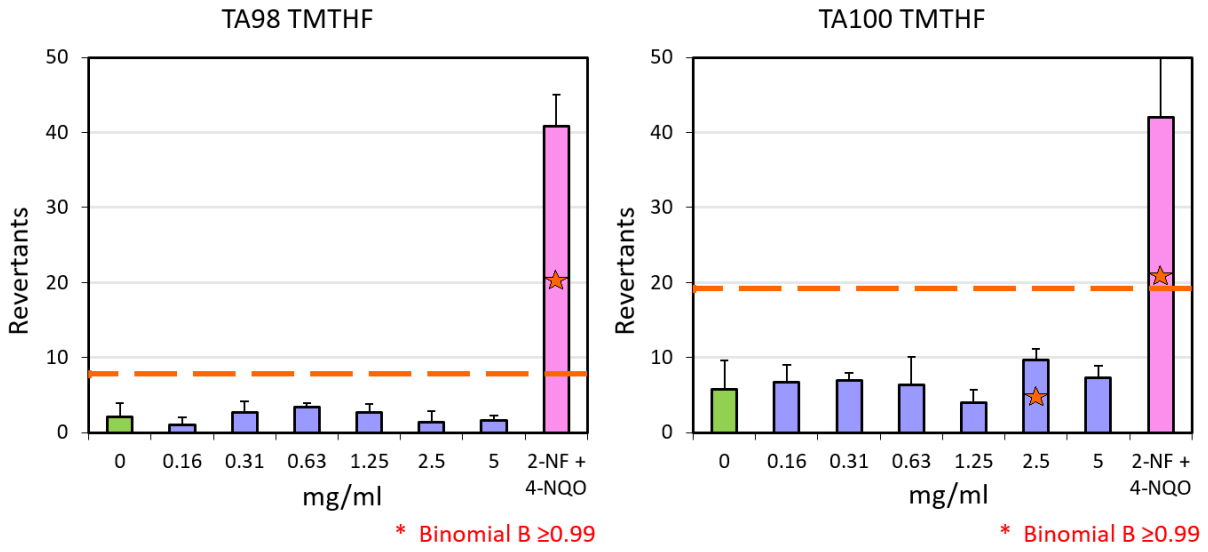

Figure 4.15. Results of Ames test using TA98 and TA100.

4.3.5 Acid stability

As TMTHF is an ether, protonation of the ethereal oxygen is a possibility,[306] so its stability in acidic conditions was also tested. Cleavage of the C-O bond in traditional ethers such as THF is exothermic, which poses a safety hazard that is amplified if any peroxides are present in the ether.[307] While we have previously shown that peroxides are not likely to form in TMTHF, acid stability is of interest when considering potential applications in synthetic chemistry reactions.

To test its stability in acidic conditions, 1 mol% of a selection of acids of varying pK_a's were added to TMTHF and stirred for 24 hours both at room temperature (18 °C on average) and under reflux (~112 °C). The acids tested were acetic acid, PTSA, TFA, hydrochloric acid (37%) and sulfuric acid (98%). No colour change was noticeable after stirring for 24 hours at room temperature and NMR spectroscopy indicated that formation of likely breakdown products was not observed. Small amounts of DHN, DHN2, DHN3 and HNL can be seen but they are in very small amounts (0.5%) and were present before testing. A ^{1}H NMR spectrum showing peaks for such products can be seen in Figure A1 in the Appendix.

At reflux, slight colour change from a clear colourless solution to a pale gold solution was observed in the samples containing PTSA, hydrochloric acid and sulfuric acid. The ^{1}H NMR spectrum of each sample shows some small peaks in each sample although the peak areas are too small to be integrated (Figures A11 and A12, Appendix). Some potential breakdown products are shown in Figure 4.16. It is not known whether the small peaks are due to breakdown of TMTHF or the small amount of impurities initially present. Each of these impurities will be susceptible to protonation

in acidic conditions, resulting in potential carbocation formation and polymerisation, and it is suspected that this is the source of the colour change. A larger unidentified peak can be seen at 4.00 ppm in the sulfuric acid sample which is more likely to be a TMTHF degradation product due to its larger peak area (~5% w.r.t TMTHF). Future work will involve better understanding the acid stability of TMTHF and to identify its breakdown products.

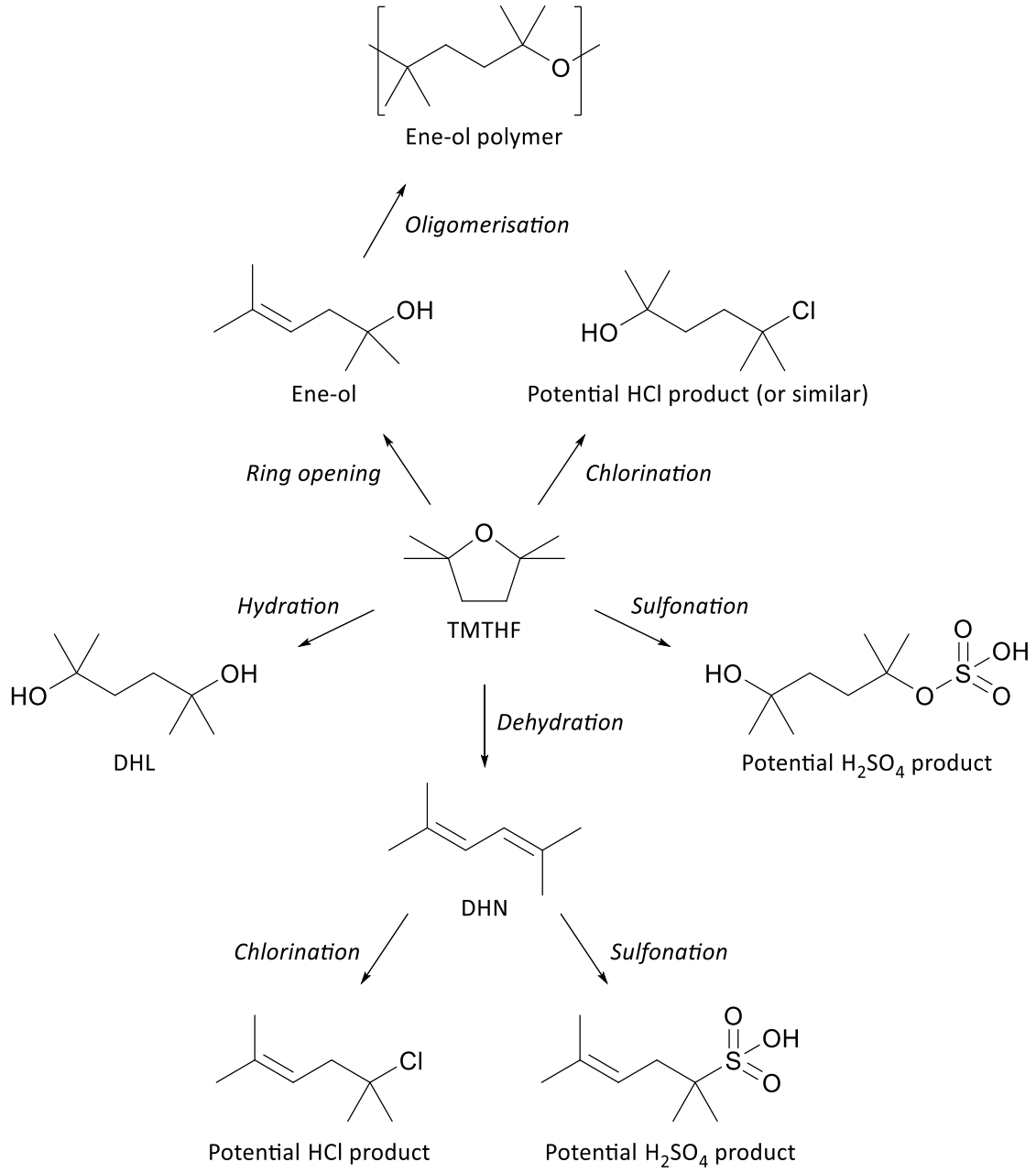

Figure 4.16. Potential breakdown products of TMTHF in acidic conditions.

These results are encouraging as they suggest that TMTHF is suitable for reactions in acidic conditions at room temperature and degradation appears to be minimal in four of the five acids

tested. Some unidentified products can be seen in the sulfuric acid sample, but this is yet to be confirmed. These results present applications for TMTHF in acidic conditions, especially at room temperature but potentially also at higher temperatures. Finally, TMTHF's inability to form peroxides reduces the dangers of exotherms upon cleavage of the ether C-O bond.

4.4 Application testing of TMTHF

TMTHF was tested a several reactions to help characterise it as a solvent and to demonstrate some potential uses. An uncatalysed amidation reaction, an uncatalysed esterification, two Grignard reactions and a radical-induced vinyl polymerisation were used as test reactions and they are described in the following sections.

4.4.1 Uncatalysed esterification reaction kinetic study rationalised by KT parameters

The nucleophilic attack by an alcohol on a carbonyl group (COOH for esterification) results in a protic tetrahedral transition state from which either water (when reacting with a carboxylic acid) or the corresponding carboxylic acid (when reacting with an anhydride) is eliminated (Figure 4.17). The enthalpy of activation ($\Delta H^{\ddagger}$) is lowered by stabilisation of the transition state which is expected to increase the reaction rate (k_2').[60] The reaction of many carboxylic acids or anhydrides with alcohols occurs in the absence of a catalyst[308,309] although the use of a catalyst can improve reaction rates.[308]

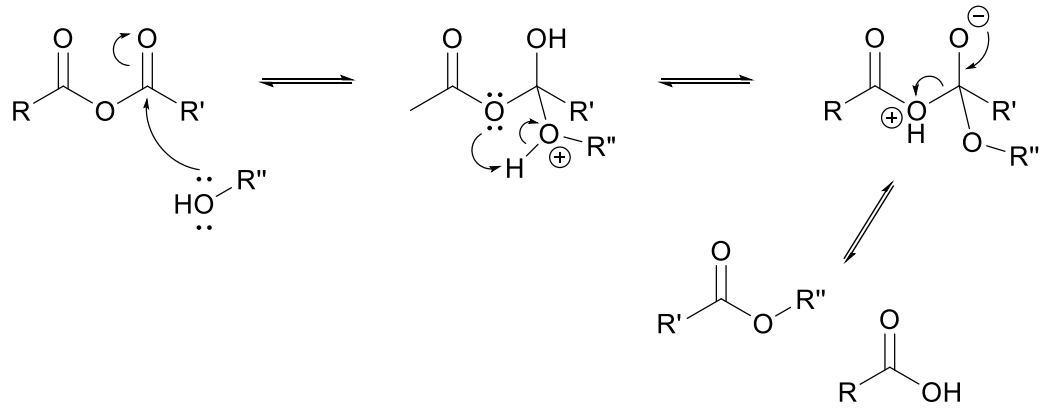

Figure 4.17. Uncatalysed esterification reaction mechanism.

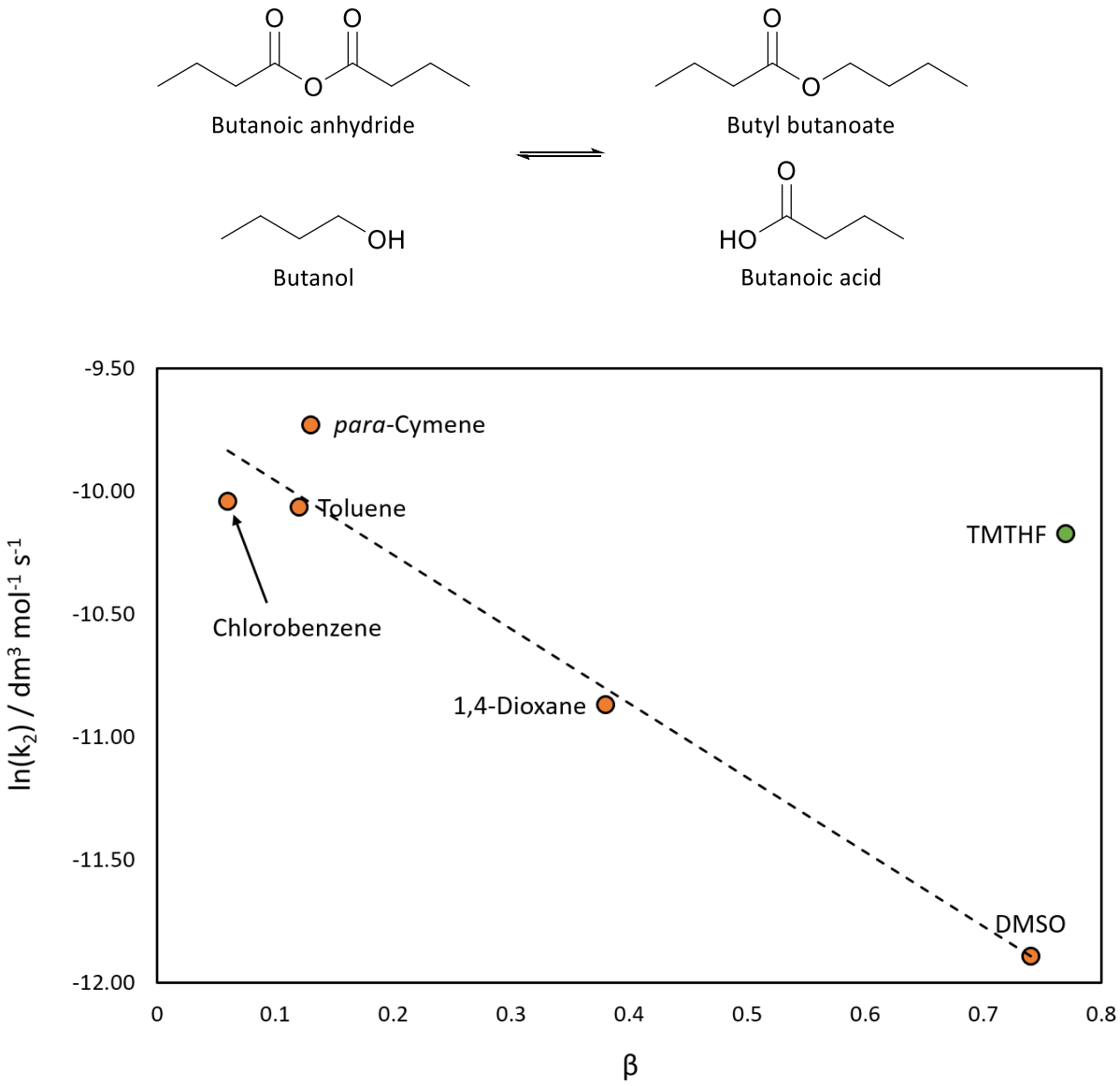

Figure 4.18. Uncatalysed esterification reaction scheme and an LSER showing the deviation of TMTHF from the trend observed in a selection of traditional solvents in the model esterification reaction.

The uncatalysed esterification reaction between butanoic anhydride and butanol was previously used by Clark *et al.* to gauge solubility properties of some bio-based solvents (Figure 4.18). A solvatochromic equation, shown in Equation 1.9, where $\ln(k_2')$ is the second-order rate constant of the reaction, was used to establish which solvent properties determined the reaction rate and could therefore characterise solvents in terms of their polarity.[60]

Equation 1.9. $$\ln(k_2) = Y_0 + b\beta + h(\delta_H)^2$$

Clark et al. found that in most cases β could account for the reaction rate. However, despite the stabilisation of the transition state by solvent lone-pair interactions, solvents with a high β

parameter inhibited the reaction. A slight deviation from the trend was observed in acetonitrile which did not perform as well as would be expected given its β, but this was accounted for by including δ_H^2 in the LSER. This suggests that solvents with a high level of cohesion, represented by high δ_H^2 and β, will prevent the formation of a large cavity and will therefore inhibit the formation of the transition state.

Equation 3.3. $$k_2 t = \frac{1}{[A]_0 - [B]_0} \ln\left(\frac{[B]_0([A]_0 - [P]_t)}{[A]_0([B]_0 - [P]_t)}\right)$$

The reaction was found to be second order so the second order rate equation shown in Equation 3.3 could be used to determine the rate, k_2'.[60] k_2t is the second order rate constant at time t, $[A]_0$ is the initial concentration of reactant A, $[B]_0$ is the initial concentration of reactant B and $[P]_t$ is the concentration of product P after time t. The concentrations of reactants and products were measured using ^{1}H NMR spectroscopy and product characterisation data can be seen in Figure A13 and A14 in the Appendix.

Due to the conflicting description of TMTHF in terms of its hydrogen-bonding ability by KT and HSP, its effectiveness as a solvent was tested in the esterification reaction between butanoic

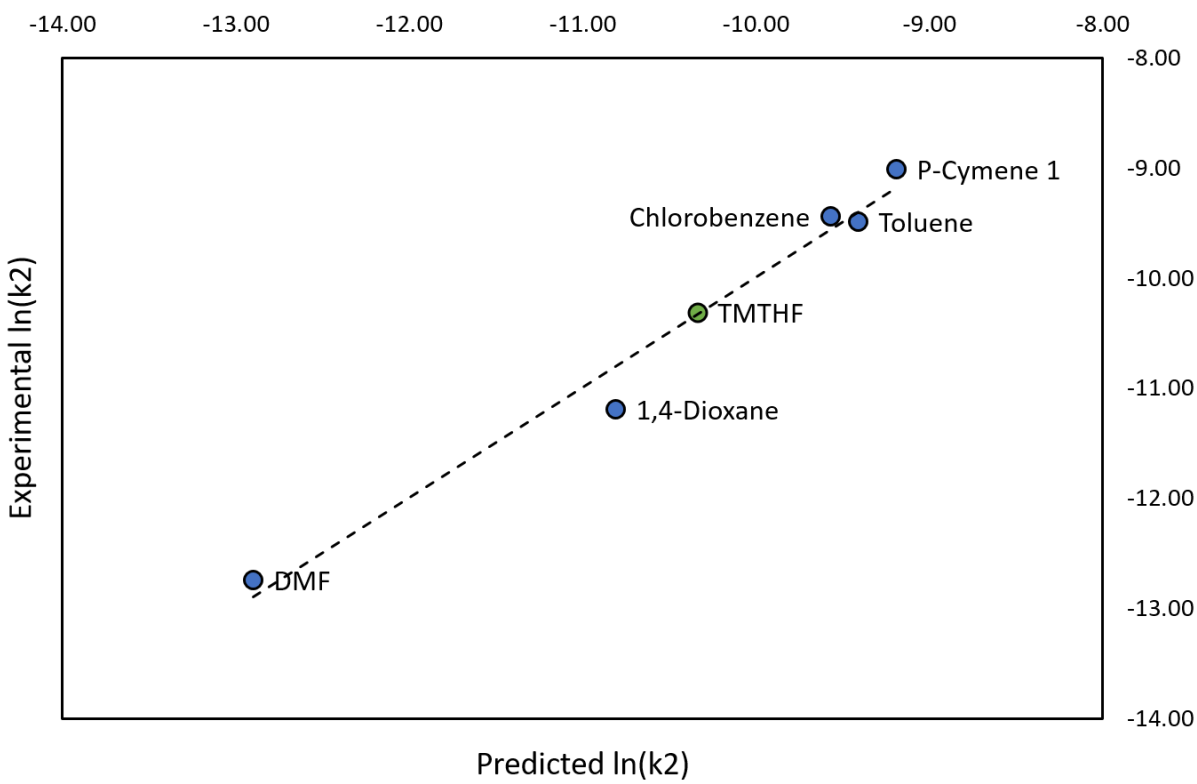

Figure 4.19. Comparison between predicted and experimental ln(k_2') values for the esterification of butanoic anhydride with butanol when both β and δ_H^2 are used to generate the LSER.

anhydride and butanol to shed more light regarding its solubility properties. It was found to deviate from the trend observed by Clark *et al*. in that it was a very effective solvent despite its high β (0.77), as shown in Figure 4.18. Its performance was more comparable to that of toluene, chlorobenzene and *para*-cymene as opposed to that of DMF, another solvent with a high β (0.74), or 1,4-dioxane, another ether.

In an attempt to account for this deviation, δ_H^2 was also included in the LSER which improved the predictability of the model (Figure 4.19). The improvement in predictability is consistent with the observation by Clark *et al*. regarding acetonitrile. Clark *et al*. observed that acetonitrile did not perform as well in the reaction as would be expected based on its β. This observation was reasoned to be due to its small, linear shape, resulting in more cohesion than can be explained by β alone. For similar but opposite reasons, TMTHF performed far better than would be expected due to its four bulky methyl groups blocking access to its β, resulting in lower cohesion than can be explained by β alone.

4.4.2 Amidation reaction kinetic study rationalised by KT parameters

The ideal route to amide formation from an amine and a carboxylic acid is similar to that of the esterification above; by the nucleophilic attack of the nitrogen's lone-pair of electrons on the carbonyl group of the carboxylic acid (Figure 4.20, A). A protic tetrahedral transition state is formed and water is subsequently eliminated, forming the amide. Stabilisation of the transition state lowers the enthalpy of activation ($\Delta H^{\ddagger}$) and therefore, would be expected to increase the reaction rate (k_2").[60] This can be achieved either by the use of catalysts[91] or a suitable solvent.

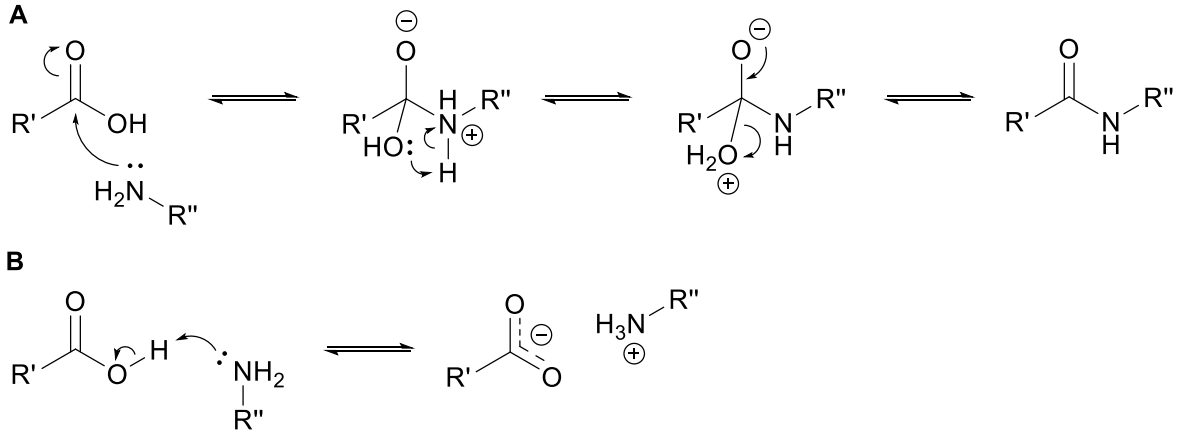

Figure 4.20. (A) Ideal pathway of the amidation reaction between a carboxylic acid and an amine and (B) Formation of a carboxylate salt.

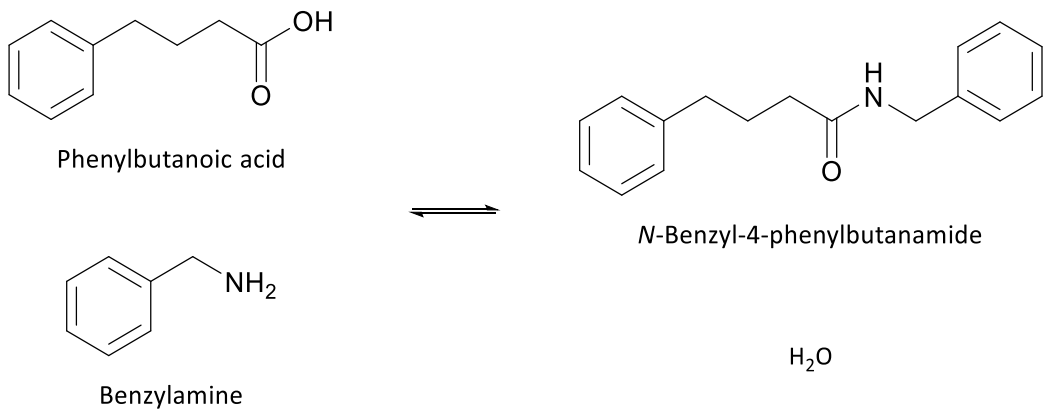

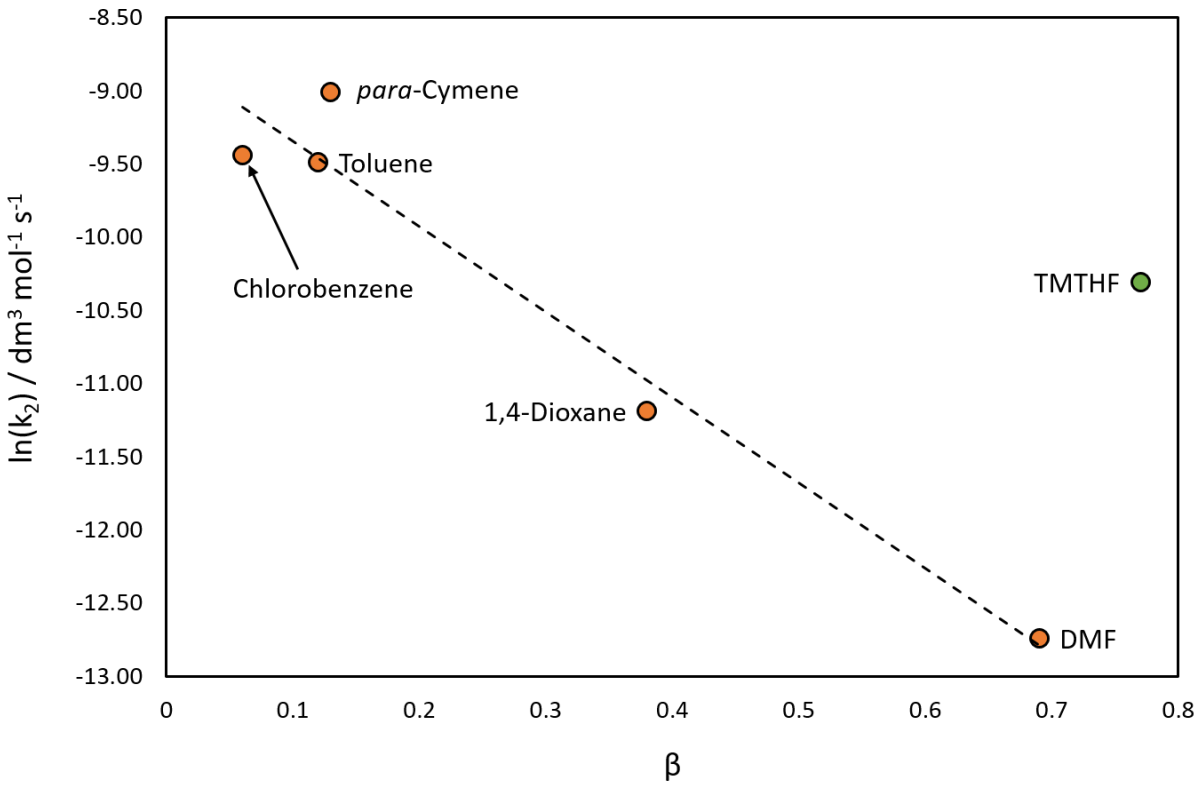

Figure 4.21. The amidation reaction scheme and an LSER showing the deviation of TMTHF from the trend observed in a selection of traditional solvents in the model amidation reaction.

However, due to the high basicity of amines, this pathway is often not possible due to the competing formation of an unreactive amine-carboxylate salt (Figure 4.20, B).

The amidation of phenylbutanoic acid with benzylamine was previously shown to favour the formation of the amide, *N*-benzyl-4-phenylbutanamide, in good yields over the formation of the carboxylate salt with and without a catalyst (Figure 4.21, A).[310] Equation 1.9 was used as an LSER by Clark *et al*. to help characterise the bio-based solvents limonene and *para*-cymene.[60] Clark *et al.* determined this reaction to be second order so Equation 3.3 could again be used to calculate

the rate, k_2''. The concentrations of reactants and products were measured using ^{1}H NMR spectroscopy and product characterisation data can be seen in Figures A15 and A16 in the Appendix.

Clark *et al*. found that β alone was sufficient to account for the reaction rate, but like in the esterification, solvents with a high β parameter inhibited the reaction. The competing entropy ($\Delta S^{\ddagger}$) required to reorganise the molecules of the solvent to form a cavity large enough to facilitate the large transition state, which is amplified at the high reaction temperatures, was again reasoned to be the cause of this.

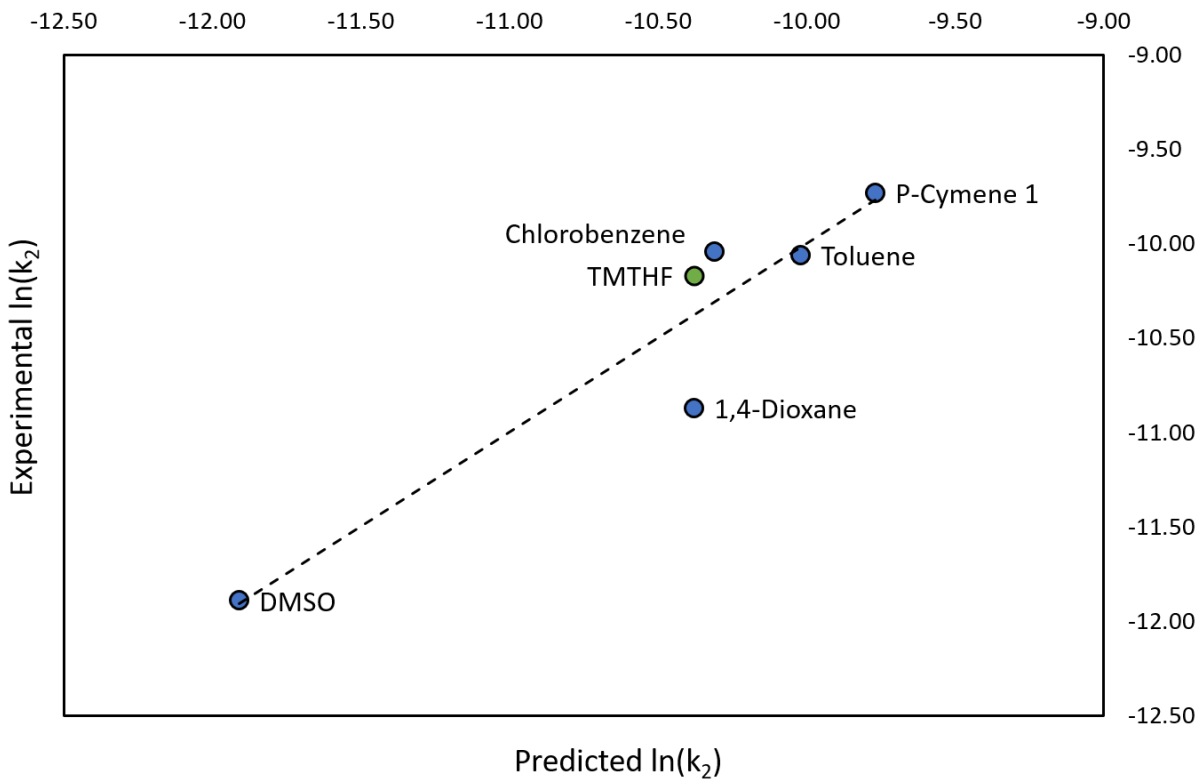

Figure 4.22. Graph showing the predictability of the LSER in which both β and π^* are considered.

TMTHF would not be expected to perform well in this reaction, similar to the esterification reaction. Again, it was found to strongly deviate from the trend when only β was considered in the LSER, being more comparable to that of toluene, chlorobenzene and *para*-cymene, solvents with a low β (Figure 4.21). However, in this reaction, including $\delta_H{}^2$ did not improve the predictability of the LSER. Instead, π^* was included in the LSER which increased the predictability of the model, although a slight deviation was observed for 1,4-dioxane (Figure 4.22). The improvement in predictability when also considering π^* in the LSER also points to high cohesion of the solvent preventing the formation of a cavity to host the large tetrahedral transition state.

The results of both the esterification and amidation were interesting findings as they backed up the hypothesis of HSP which predicted TMTHF to behave like toluene due to the bulky methyl groups around the ethereal oxygen which reduce its expected cohesive energy density.

4.4.3 Grignard reaction testing

Classically, the Grignard reaction is an organometallic reaction in which an alkyl magnesium halide reacts with a carbonyl containing compound such as a ketone, aldehyde or ester to produce a new carbon-carbon bond (Figure 4.23).[311]

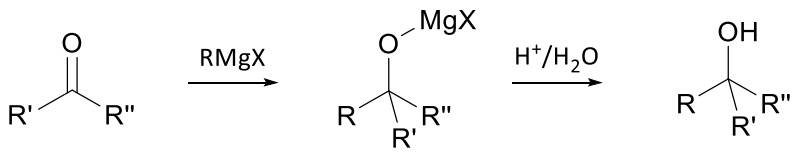

Figure 4.23. General Grignard reaction scheme.

Although commonly expressed as monomeric RMgX, the structure of the Grignard reagent is still uncertain, and is influenced by the solvent and the nature and concentration of the alkyl halide.[312–314] This is demonstrated by the Schlenk equilibrium (Equation 4.1),[315] which results in the precipitation of $MgX_2(1,4\text{-dioxane})_2$ and the suppression of the desired Grignard reaction in some 1,4-dioxane solutions.[316]

Equation 4.1. $$2RMgX \rightleftharpoons R_2Mg + MgX_2$$

The Schlenk equilibrium suggests a more complex solubilised structure than RMgX and indeed, many other dimer and higher oligomer structures which involve halide bridging have been identified.[317,318] However, for most applications, the structure can assumed to be of the form RMgX.[312] The Grignard reagent must be solubilised by a suitable solvent upon formation to allow it to react with the dissolved carbonyl compound.[316] Figure 4.24 shows a simplified solvation of a Grignard reagent by an ether (Guggenberger and Rundle identified this to be the structure of ethylmagnesium bromide solubilised by diethyl ether using XRD).[319] As the Mg centre is two electron-pairs short of its octet of electrons, stabilisation by solvation in ethers is possible due to the donating lone-pairs on the ethereal oxygen.[320] Protic solvent cannot be used as they will destroy the reactive Grignard reagent due to the very high rate of Grignard protonation, although exceptions to this have been reported for certain reactants.[321] Osztrovszky *et al*. exhibited that the rate of reaction of allylmagnesium bromide with acetone was greater than that of the protonation

of allymagnesium bromide by water, by successfully carrying out a Grignard reaction in the presence of protic substrates (water or small alcohols).[321]

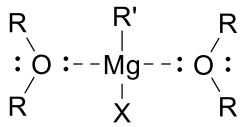

Figure 4.24. Typical solubilisation of Grignard reagents by ethers, although some other complexes are possible, depending upon the nature of the alkyl halide and the concentration in the solvent.

To form the Grignard reagent, magnesium metal is exposed to an alkyl halide where it is inserted into the alkyl halide bond.[322] The Grignard reagent forms on the magnesium surface between the alkyl halide and surface magnesium ions.[323] The surface of the magnesium must be free from oxidation for the reagent to form. Although not always required, activating agents such as iodine and DIBAL-H can be used to prepare the surface of the magnesium metal for the preparation of the Grignard reagent.[324]

While this is a very useful reaction which is employed during the synthesis of active pharmaceutical ingredients such as tramadol,[325] ibuprofen[326] and tamoxifen,[327] stoichiometric amounts of magnesium are required to form the Grignard reagent and hence large amounts of magnesium waste are generated.[328] In addition, there are several safety issues associated with the Grignard reaction such as exotherms during the synthesis of the Grignard reagent and its reaction with the carbonyl compound.

Kadam *et al*. recently reported the use of several ethers to host Grignard reactions, two of which are shown in Figure 4.25, including the "greener" ethers, 2-MeTHF and CPME.[324] However, as has been demonstrated in this work, CPME is not green. The traditional ethers tested were diethyl ether, THF, diethoxymethane, and diglyme. With the exception of diglyme, all were able to facilitate both Grignard reactions to varying degrees. In THF and CPME, the competing Wurtz reaction was favoured. The Wurtz product, **W1**, is the self-reaction between two alkyl groups of Grignard reagent molecules and is usually an undesired competing reaction.

As TMTHF is an ether, albeit one that behaves differently to traditional ethers in many applications, its ability to host a Grignard reaction was of interest. On one hand, the lone-pairs on TMTHF potentially could donate to the electron deficient Mg of the Grignard reagent but on the other hand, the four bulky methyl groups could prevent this interaction.

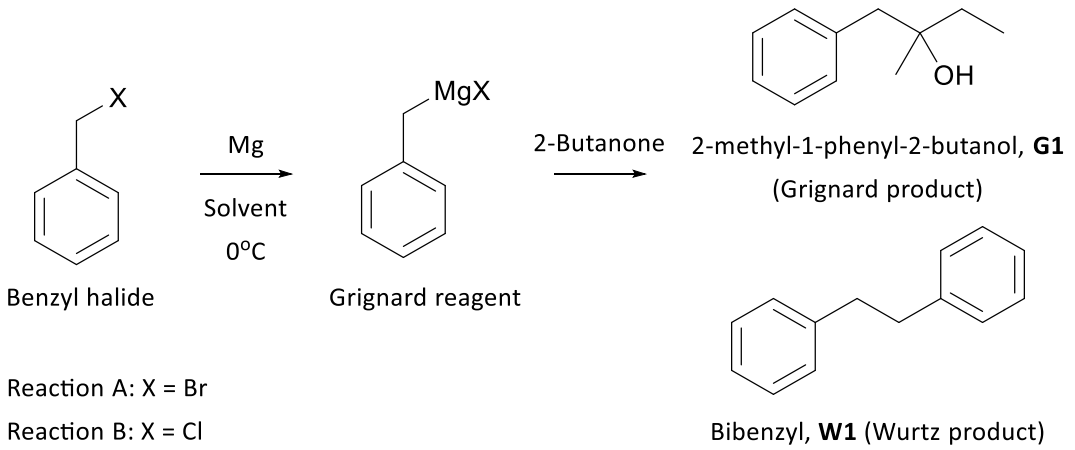

	Reaction A		Reaction B	
Solvent	Conv. (%)	Ratio **1**:**2**	Conv. (%)	Ratio **G1**:**W1**
THF	99	18:82	99	33:66
2-MeTHF	100	87:13	100	97:3
TMTHF	0	-	0	-
Toluene	0	-	0	-

Figure 4.25. Reaction schemes for the two Grignard reactions carried out in this work and a table showing the results of the Grignard reaction. Conversion and product ratios measured by NMR spectroscopy.

In this work, two Grignard reactions were undertaken, one using benzyl chloride and one using benzyl bromide as the alkyl halides. 2-Butanone was the carbonyl moiety in both reactions (Figure 4.25). Both reactions were tested in three ether solvents: 2-MeTHF, THF, TMTHF. Toluene was also used as a comparison for TMTHF. As expected, THF and 2-MeTHF achieved full conversion of the alkyl halide, although in THF the Wurtz product, **W1**, was favoured over the Grignard product, **G1**, which was consistent with the results reported by Kadam *et al.*[324] (Figure 4.25). In contrast, when TMTHF or toluene were used as the reaction solvent, no conversion of the alkyl halide to Grignard reagent was observed. Product characterisation of both products was done using NMR spectroscopy and the spectra can be seen in Figures A17-A20 in the Appendix.

The absence of donating lone-pairs on toluene means it is unable to solvate the electron deficient Mg and the steric hindrance of the four methyl groups on TMTHF is assumed to inhibit access to its lone-pairs. This provides further evidence of TMTHF's disparity from traditional ethers and similarity to toluene.

4.4.4 Radical-initiated vinyl polymerisation

The properties of TMTHF have been demonstrated to be similar to toluene and it exhibits comparable behaviour to toluene in several organic applications. It has also been shown to be able to dissolve a representative selection of Nitto's polymers and rubbers. However, a replacement solvent for toluene has to be able to host the polymerisation reaction to produce polymers of the required quality. In this section, the performance of TMTHF in radical polymerisations is described. All polymerisation work in this section was carried out by Mr. Charly Hoebers, Junior Scientist at Nitto Belgium, while all interpretation conducted by the author.

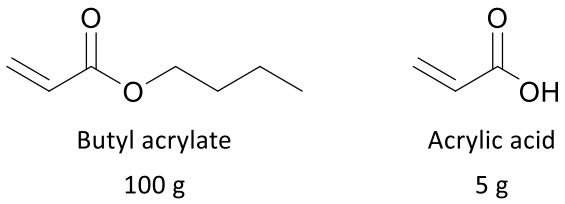

Figure 4.26. The components of the test radical polymerisation carried out in TMTHF (30 g).

It was shown in Chapter 2 that 2-MeTHF, a traditional ether, was unable to achieve the high molecular weights required for Nitto's PSA polymers. The polymerisation of butyl acrylate (100 g) and acrylic acid (5 g) was the test polymerisation reaction (shown in Figure 4.26), in which 2-MeTHF could achieve a weight average molecular mass (M_w) of 9,200 g mol^{-1}. The reason for this appeared to be due to chain transfer from the polymer to the solvent, resulting in chain termination. Two mechanisms termination in 2-MeTHF are proposed, both of which can contribute to premature termination (Figure 4.27). The *alpha*-H is abstracted by the radical at the end of the polymer chain, terminating the polymerisation and producing a reactive solvent radical. The solvent radical can subsequently terminate another polymer chain by reacting with the polymer radical. Further complications could arise by hydrogen abstraction from the other side of the ethereal oxygen, which would reinitiate the polymerisation, but this was not investigated.

Due to the structural difference of TMTHF to traditional ethers, in particular its lack of a hydrogen atom in the *alpha*-position, it was hoped that the same issues of chain transfer would not exist in TMTHF. To test this hypothesis, TMTHF was used in the same polymerisation conditions as 2-MeTHF where it performed comparably to toluene, as can be seen in Table 4.7. GPC showed that an M_w of 501,000 g mol^{-1} was reached in TMTHF compared to 509,000 g mol^{-1} in toluene (Figures A24 and A25, Appendix). The dispersity, *Đ*, of the polymer differed between each system; a narrower molecular weight distribution was observed in toluene compared to TMTHF (Table 4.7). The solid content of TMTHF was 27.25% compared to 31% for toluene. The quality of the polymer

was adequate in TMTHF, with superior adhesion and tack obtained in in-house tests at Nitto. The performance of TMTHF in radical polymerisations gives even more evidence of its disparity to traditional ethers and demonstrates yet another application where it behaves similarly to toluene.

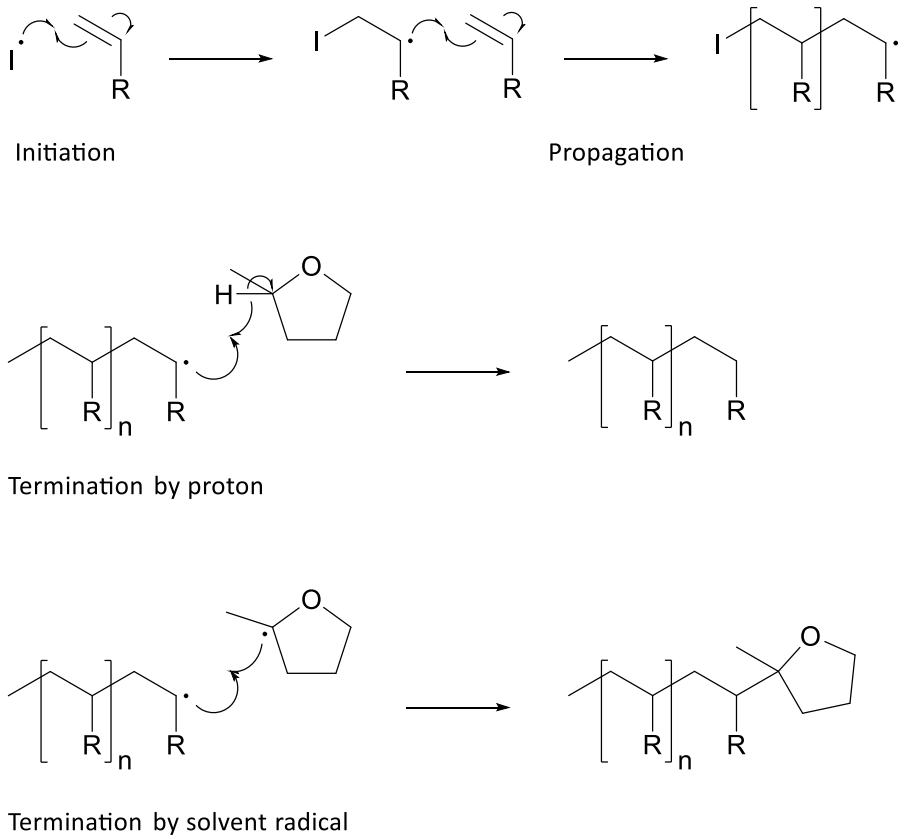

Figure 4.27. Chain transfer by solvent molecules resulting in chain termination.

Table 4.7. Results of the radical polymerisation of butyl acrylate and acrylic acid.

Polymer property	TMTHF	Toluene	2-MeTHF
M_w / g mol^{-1}	501,000	509,000	9,200
Dispersity	7.17	2.58	n/a
Solid content / %	27.25	31.00	31.00
Adhesion / cN/20 mm^{-1}	809	757	n/a
Cohesion / days	>10	>10	n/a
Tack (wt. supported) / g	291	264	n/a

4.5 Conclusion

In conclusion, TMTHF has been shown to be easy to synthesise *via* two different routes using potentially bio-based starting materials, although petroleum based analogues were used in this work. Full conversion and excellent selectivity was obtained from the ring closure of DHL, a diol which is already produced commercially for use in polymers. This reaction has been easily scaled up to 1 L flask, and future work would involve expanding the scale of synthesis to 300 kg.

TMTHF was comparable to toluene based on several physical properties: a boiling point of 112 °C (toluene = 111 °C); a melting point below -90 °C (toluene = -92 °C); high AIT of 417 °C (toluene = 522 °C). Limitations in the LEL measurement were highlighted, upon which it was shown that TMTHF is safer than toluene with regards to its LEL.

The solubility properties of TMTHF were shown to more similar to toluene than traditional ethers such as THF. Although TMTHF has KT parameter typical of ethers, its HSPs suggested it was more comparable to toluene and this was backed-up by two kinetic studies using an uncatalysed esterification reaction and an amidation reaction. It transpired that HSP's description of TMTHF's solvation power was more indicative of its performance than KT's. The Abraham solvation parameter model highlighted a subtle difference between TMTHF and toluene; that is that TMTHF had a greater affinity for protic solutes compared to toluene due to its donating lone-pairs. In addition, TMTHF was unable to facilitate a Grignard reaction, an application for which ethers are usually employed due to their lone-pair donating ability. Finally, TMTHF was able to host a radical polymerisation of vinyl monomers, a role that 2-MeTHF was unable to fulfil. This was assumed to be a result of the absence and presence of acidic *alpha*-H atoms in the former and latter respectively.

TMTHF was found not to be mutagenic to the *Salmonella typhimurium* strains at concentrations up to 5 mg/mL in the Ames test. Its Log $P_{o/w}$ of 1.53 shows that it is not miscible with water but is also not likely to be bioaccumulative, but full testing will be required to determine its toxicity profile.

TMTHF can be a suitable replacement for toluene in many applications. Its synthesis is facile from a cheap and readily available diol, which could potentially be sourced from biomass. However, an assessment of greenness must be carried to determine whether it actually is an improvement upon toluene from an environmental, health and safety standpoint. This assessment will be carried out in Chapter 5.

5 Assessment of greenness and process suitability of the top candidate replacement solvents

5.1 Introduction

Five molecules have been proposed as replacement solvents for toluene. This chapter evaluates the candidates' greenness using a variety of methods. The overall assessment led to a tailored solvent selection guide specific for the manufacturing plant at Nitto. However, unlike many published solvent guides, solvents will not be assigned a numerical rating as such weightings can be subjective and positive/negative aspects can be hidden in such as scoring system.[210] Instead, this assessment will highlight specific issues relating to each candidate, thereby demonstrating their greenness and suitability for not only polymerisation/coatings but others processes as well.

In Chapter 4, ethyl isobutyrate was found to be unsuitable for polymerisation and was discontinued from experimental work, however significant volumes of data had been collected before it was found to be an ineffective solvent and thus is reported in this assessment. An economic assessment has not been carried out as each of the candidates is in the early stages of development and a fair cost estimate cannot be made at this stage.

The assessment will include the use of the CHEM21 solvent guide which generates a rating of "Recommended", "Problematic" or "Hazardous" based on inputted environmental, health and safety (EHS) data.[201] It is currently the only solvent selection guide that provides such a resource for new solvent assessment and it was found to be a very useful tool for the assessment of solvents. However, the main limitation is that the toxicity data must be known for it to produce a useful assessment, and this is often a problem for new molecules, about which little is known. It does acknowledge when very little data is available by asking whether a solvent is registered with REACH or not. If it is not registered, a default rating of "Problematic" is assigned. As none of the

candidate solvents are REACH registered, estimates of their safety, health and environmental data are made based on structurally similar analogues.

To fill any data gaps in the CHEM21 solvent guide, predicted data using the computer modelling software, TEST is also used.[72] Rat (oral) LD_{50} (48 hr), mutagenicity, developmental toxicity, *Tetrahymena pyriformis* IGC_{50} (48 hr), fathead minnow LC_{50} (96 hr), *Daphnia magna* LC_{50} (48 hr) and BCF values were all predicted. Predicted values can be useful as a quick screening tool, but like all predictions, are subject to a certain degree of inaccuracy.

The CHEM21 metrics toolkit is a calculator that provides a range of green metrics such as conversion, selectivity, atom economy (AE),[113] reaction mass efficiency (RME)[115] and process mass intensity (PMI) of synthetic processes and highlights any other issues with respect to the greenness of solvent synthesis.[216] It was utilised to assess the synthetic routes to each of the candidate solvents.

The solvents were assessed for several factors specific to Nitto's PSA production plant, such as LEL, AIT, carbon emissions upon incineration, Ames test results, Log $P_{o/w}$ and water content.

Based on these assessments, the overall greenness of using each candidate to replace toluene will then be discussed. All data has been either determined experimentally as part of this work or taken from the ECHA,[3] Pubchem[220] and Chemspider[219] databases where available. In the cases where data was unavailable, predicted values using solvent modelling software were used.

5.2 CHEM21 solvent guide: CLP assessment of solvents

Table 5.1 shows the classification of each of the five candidates in comparison with toluene based on the CHEM21 solvent guide assessment. It can be seen that as none of the candidates are REACH registered, they all receive "problematic" classification. As such, structural analogues which can be used for a nearest neighbour prediction of each candidate are also shown. 1,8-cineol, ethyl acetate and MIBK which have been used as structural analogues to TMTHF, the esters and pinacolone respectively (shown in Figure 5.1).

The classifications of each of the structural analogues are promising, as all are classed as "recommended" based on good scores in the safety, health and environment categories. The individual scores for each solvent in each category are described in the following sections.

Table 5.1. CHEM21 solvent guide showing the five candidate solvents along with 1,8-cineol and toluene.

Solvent	Safety	Health	Environment	Overall
TMTHF	4	5	5	Problematic
Methyl butyrate	4	5	5	Problematic
Ethyl isobutyrate	4	5	5	Problematic
Methyl pivalate	4	5	5	Problematic
Pinacolone	4	5	5	Problematic
1,8-Cineol	3	2	5	Recommended
Ethyl acetate	5	3	3	Recommended
MIBK	4	2	3	Recommended
Toluene	4	9	7	Hazardous

Table data taken from the CHEM21 solvent selection guide.[201]

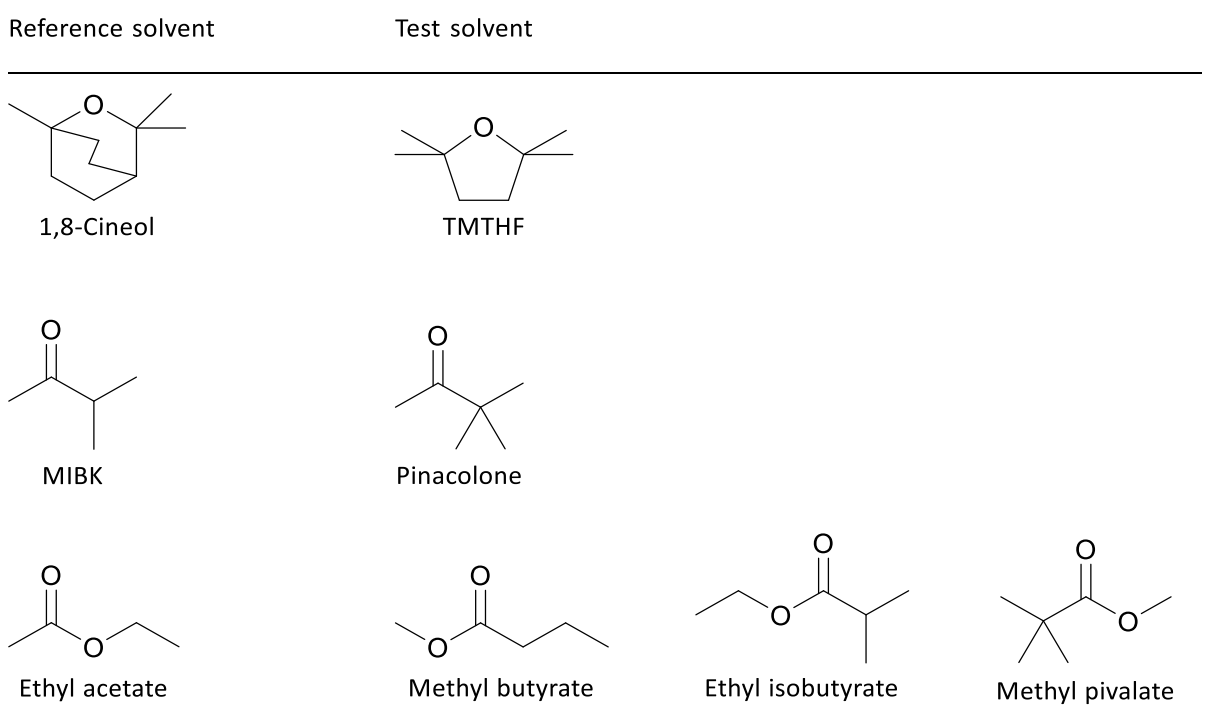

Figure 5.1. Structural analogues for each of the candidate solvents.

5.2.1 Safety

The scoring criteria for the safety category can be seen in Table 5.2. Each of the five candidate molecules as well as toluene, ethyl acetate and MIBK were assigned a score of 4 (yellow) in the safety category as all had a flash point from 0 – 23 °C, an AIT >200 °C and were not resistive or peroxide forming. It must be emphasised that although a yellow rating is not ideal, it is very difficult to find organic molecules which will not have safety issues regarding their flammability. 1,8-Cineol had a higher flash point in the range 24–60 °C and was therefore given a score of 3 (green). While 1,8-cineol outperforms the five candidates in the safety category due to its lower volatility and hence lower flash point, it will be seen in the environment category how this can become a negative property. As such, a yellow rating was expected for each of the five candidates based on the score of their structural analogues.

Table 5.2. Safety criteria scoring.

Basic safety score	Flash pointy / °C	CLP category
1	>60	
3	24 – 60	H226
4	0 – 23	
5	-1 – -20	H224/H225
7	<-20	
Additional safety score		
+1	AIT <200 °C	
+1	Resistivity <10^8 Ω m	
+1	Peroxide formation ability	
10	Energy of decomposition >500 J g^{-1} (*e.g.* nitromethane)	

Table data taken from the CHEM21 solvent selection guide.[201]

5.2.2 Health

The scoring criteria for the health category can be seen in Table 5.3. Each of the five candidates received a score of 5, and hence a yellow rating in the health category. However, this score was assigned due to insufficient data and lack of REACH registration as opposed to concrete data stating that they possess some toxicity.

Toluene was assigned a poor score of 9 due to its reprotoxicity, indicated by its H360 code.[329] Encouragingly for TMTHF, 1,8-cineol was assigned a score of 2 in terms of its health effects. The only health effects associated with 1,8-cineol were lower level hazards such as irritation upon contact with eyes or skin.[330] The esters are not likely to have serious health issues as they are present in flavouring and fragrances and the score of 3 for ethyl acetate is in good agreement with this prediction. Experimental toxicity data was available for pinacolone would result in a green rating in the health category if pinacolone was REACH registered. However, as pinacolone is not fully REACH registered the default score of 5 is assigned. A score of 2 for MIBK also provided encouragement for the toxicity of pinacolone.

Table 5.3. Health criteria scoring.

Basic health score	CMR	STOT	Acute toxicity	Irritation
2		H304, H371, H373	H302, H312, H332, H336	H315, H317, H319, H335
4		H334		H318 (eyes)
6	H341, H351, H361	H370, H372	H301, H311, H331	
7				H314 (skin/eyes)
9	H340, H350, H360		H300, H310, H330	

Additional score	
+1	Bp <85 °C
5	Incomplete data available

Table data taken from the CHEM21 solvent selection guide.[201] CMR: Carcinogen, mutagen, reprotoxin. STOT: Specific target organ toxicity.

5.2.3 Environmental

The scoring criteria for the environment category can be seen in Table 5.4. A score of 5 was assigned to the five candidates due to a lack of available data. Ethyl acetate and MIBK both received scores of 3 which is positive for the esters and pinacolone. 1,8-cineol received a score of 5 due to its H412 classification indicating that it is harmful to aquatic life with long lasting effects, and toluene received a score of 7 due to its H412 classification indicating toxicity to aquatic life with long lasting effects.

It is not clear why 1,8-cineol has been assigned a H412 hazard code, as the available ecotoxicity data does not back this up.[330] According to ECHA's "Guidance on the Application of the CLP Criteria" as of July 2017, for a substance to be assigned a "Category 3" chronic toxicity classification for H412 it must have a $LC_{50} \leq 100$ mg L^{-1} for fish.[331] However, the LC_{50} (fathead minnow) of 1,8-Cineol is 102 mg L^{-1}, which should result in a "Category 4" chronic toxicity rating and hence, no H412 classification.[330] In any case, the LC_{50} (fathead minnow) of TMTHF is 167 mg L^{-1} according to the EPA TEST database[72] and is not assigned a H4XX classification, meaning it would receive a score of 3 or less (green) in the environmental category if it was REACH registered.

Table 5.4. Environmental criteria score.

Environmental score	Bp / °C	CLP	Other
3	70 – 139	No H4XX after full REACH registration	No, or partial REACH registration
5	50 – 69, 140 – 200	H412, H413	
7	<50, >200	H400, H410, H411	

Table data taken from the CHEM21 solvent selection guide.[201] Water score = 1. H420 (ozone layer hazard) = 10.

5.2.4 Overall rating

Using the CHEM21 solvent guide, it could be seen that all five candidate solvents scored as "Problematic" compared to toluene's rating of "Hazardous" (Table 5.1). However, these ratings were only due to a lack of REACH registration. A "nearest neighbour" assessment using ethyl acetate, MIBK and 1,8-cineol as structural analogues to the esters, pinacolone and TMTHF was promising in all cases. 1,8-Cineol, ethyl acetate and MIBK classed were all classed as "Recommended", although full testing would be required for all candidates.

5.3 TEST predictions: Toxicity and ecotoxicity

TEST was employed to give predicted (and some experimental) data for rat (oral) LD_{50}, mutagenicity, developmental toxicity, *Tetrahymena pyriformis* IGC_{50} (48 hr), fathead minnow LD_{50} (96 hr), *Daphnia magna* LC_{50} (48 hr) and BCF for each of the five candidates and are shown in Table 5.5.[72]

Several predictive techniques are available in TEST, each with different advantages and disadvantages (described in Chapter 1). The Consensus method was used for all predictions unless otherwise stated as it was shown to give the best prediction accuracy and coverage.[75] In the Consensus method, the most similar molecules to the test molecule in the training and external test sets are shown, along with their similarity coefficient. The similarity coefficient is a measure of the structural similarity between the test molecule and the molecules in the training and test sets.[75] The closer the similarity coefficient is to 1, the more similarity between the molecules. The mean absolute error or the prediction is also provided which gives an estimation of reliability of the prediction.[75] The results of each category are discussed in the following sections.

5.3.1 Rat (oral) LD_{50}

The values shown for pinacolone and toluene are experimental values (indicated by *) while the others are predicted in the rat (oral) LD_{50} category. Pinacolone was experimentally found to be more toxic than toluene (610 mg kg^{-1} vs. 636 mg kg^{-1}), although a value of 610 mg kg^{-1} only warrants a H302 hazard code.[331] Predicted LD_{50} values for the esters and TMTHF were significantly higher than toluene, indicating lower toxicity. In each case, several molecules with high similarity coefficients (>0.9) and comparable functionality were present in training and test sets, which is likely to produce a reliable prediction.

5.3.2 Mutagenicity

All five candidates were predicted to be non-mutagenic, consistent with the Ames test results presented in Chapters 3 and 4.

5.3.3 Tetrahymena pyriformis IGC_{50} (48 hr) / mg L^{-1}

Tetrahymena pyriformis is a ciliate, which grows at a logarithmic rate in ideal conditions. Inhibition of the ideal rate of growth can be used to indicate toxic concentrations of xenobiotics.[75]

Table 5.5. Predicted toxicity data using the Consensus method in TEST.

Solvent	Rat (oral) LD_{50} / mg kg^{-1}	Mutagenicity	*Tetrahymena pyriformis* IGC_{50} (48 hr) / mg L^{-1}	Developmental toxicity	Fathead minnow LC_{50} (96 hr) / mL L^{-1}	*Daphnia magna* LC_{50} (48 hr) / mL L^{-1}	Log_{10} BCF
TMTHF	3,136	Negative*[(a)]	1,153	Negative[(b)]	167*	118	1.12
Methyl butyrate	7,744	Negative*[(a)]	1,800*	Negative[(b)]	97	102	0.56
Ethyl isobutyrate	7,987	Negative	2,168*	Positive[(c)]	168	83	0.42
Methyl pivalate	2,887	Negative*[(a)]	2,214*	Positive[(c)]	138	34	0.62
Pinacolone	610*	Negative*[(a)]	2,772*	Positive[(c)]	361*	86	0.69
Toluene	636*	Negative*	52*	Negative*	34*	91*	1.82

Dark green = Experimentally found to be better than toluene. Green = Predicted to be better than toluene. Yellow = Predicted to be worse than toluene. Orange = Experimentally found to be worse than toluene. *Experimental data. (a) Experimentally determined as part of this work. (a) Predicted using the Random forest method. (b) Predicted using the Consensus method.

The IGC_{50} values for all of the esters, pinacolone and toluene were experimentally determined, while TMTHF was predicted. The esters and pinacolone are significantly less toxic than toluene in terms of IGC_{50} (1,800-2,772 mg L^{-1} for the esters and pinacolone versus 52 mg L^{-1} for toluene). The predicted value for TMTHF (1,153 mg L^{-1}) is comparable for the esters and pinacolone, although this prediction was carried out using a training set with a maximum similarity coefficient of 0.67, and therefore its reliability is questionable.

5.3.4 Developmental toxicity

Developmental toxicity is determined by animal testing on rats or rabbits.[332] It is defined as "adverse effects induced during pregnancy, or as a result of parental exposure."[333]

Experimental data showed that toluene was a developmental non-toxicant. The Consensus method predicted that the five candidates were all predicted to be developmental toxicants. However, the similarity of the training and test sets to the test solvents was low, therefore the predictions are questionable. The Random Forest method was utilised to provide a more accurate prediction for developmental toxicity.[75] It predicted that TMTHF and methyl butyrate were developmental non-toxicants but it was unable to make a prediction about ethyl isobutyrate, methyl pivalate and pinacolone as the descriptors for these solvents lay outside the descriptor range of the training set.

5.3.5 Fathead minnow LC_{50} (96 hr)

The fathead minnow is commonly used as an indicator of aquatic toxicity.[334] Experimental data for fathead minnow LC_{50} of TMTHF, pinacolone, and toluene were available. Toluene was shown to have the highest toxicity to the fathead minnow with an LC_{50} of 34 mL L^{-1}. TMTHF and pinacolone were shown to be less toxic to the fathead minnow with LC_{50} values of 168 and 362 respectively. The predicted values for methyl butyrate, ethyl isobutyrate, methyl pivalate using the Consensus method were also higher than toluene at 97, 169 and 139 mL L^{-1} respectively, which is promising.

5.3.6 Daphnia magna LC_{50} (48 hr)

Daphnia magna is also commonly used to gauge aquatic toxicity, with the advantage that they can be cultivated all year round and chronic effects of xenobiotics can be measured.[75]

The only experimental LC_{50} data available for *Daphnia magna* was toluene (91 mL L^{-1}). The Consensus method was used to predict the LC_{50}'s of the five candidates. TMTHF and methyl butyrate were predicted to be less toxic to *Daphnia magna* than toluene while ethyl isobutyrate,

methyl pivalate and pinacolone were all predicted to be more toxic. However, in all cases the similarity coefficient of the training set was not strong.

5.3.7 Bioconcentration factor (BCF)

The BCF is defined as "the ratio of the chemical concentration in biota as a result of absorption *via* the respiratory surface to that in water at steady state,"[75,335] and is expressed as a logarithm. No experimental BCF data was available for any of the test solvents and predictions were made using the Consensus method in all cases.

Toluene was predicted to have the highest Log_{10} BCF (1.82). TMTHF was significantly lower (1.12), while the esters and pinacolone were all quite similar and fell in the range 0.56 – 0.62. The predicted Log_{10} BCF results correlate quite well to the Log $P_{o/w}$ values in each of the test solvents (Table 5.6) and all five candidates were predicted to be superior to toluene.

Table 5.6. Comparison of predicted Log_{10} BCF with Log $P_{o/w}$.

Solvent	Predicted Log_{10} BCF	Log $P_{o/w}$
TMTHF	1.12	1.92[(a)]
Methyl butyrate	0.56	1.20[(a)]
Ethyl isobutyrate	0.42	1.54[(a)]
Methyl pivalate	0.62	1.74[(a)]
Pinacolone	0.69	1.21[(a)]
Toluene	1.82	2.73[(a)]

(a) Data obtained as part of this work.

5.4 CHEM21 metrics toolkit: Synthesis of solvents

CHEM21 metrics toolkit was utilised to calculate the AE, RME and PMI for each step of the synthesis.[216] In addition to the reaction metrics, other green factors including the use of hazardous solvents, critical elements, excess energy, flow chemistry and purification requirements are presented.[216] The traffic light scoring system for each category is shown in Table 5.7.

Table 5.7. Metrics toolkit criteria and scoring boundaries.

Catalyst / Enzyme / Reagent	Catalyst or enzyme used, or reaction takes place without any catalyst / reagents.	Use of stoichiometric quantities of reagents	Use of reagents in excess
Recovery	Facile recovery of catalyst / Enzyme	Catalyst/Enzyme not recovered	
Critical elements	+500 years	50-500 years	5-50 years
Reaction temperature	0 to 70 °C	-20 – 0 °C or 70 – 140 °C	<-20 °C or >140 °C
Reflux	Reaction run 5 °C or more below the solvent boiling point		Reaction run at reflux
Flow	Flow	Batch	
Work up	Quenching, Filtration, Centrifugation, Crystallisation, Low temperature distillation / evaporation / sublimation (< 140 °C, atmos. pressure)	Solvent exchange, Quenching into aqueous solvent	Chromatography / Ion exchange, High temperature distillation / evaporations / sublimation (> 140 °C, atmos. pressure)
EHS code	H200, H201, H202, H203, H230, H240, H250 H300, H310, H330, H340, H350, H360, H370, H372 H400, H410, H411, H420	H205, H220, H224, H241 H301, H311, H331, H341, H351, H361, H371, H373 H401, H412	If no red or amber flagged H codes present then green flag is assigned

All data taken from the CHEM21 metrics toolkit.[216]

The assessment was limited to the synthesis of each candidate starting from the bio-based platform molecules described in Chapter 1. Issues and benefits of the production of each bio-based platform molecules will be highlighted but as platform molecule production is currently unoptimized, an accurate comparison cannot be made. However, thermochemical and chemo-catalytic processes are likely to be more cost-efficient than fermentation processes at present due

to the need to pre-treat biomass to free sugars for fermentation.[336] Therefore, chemo-catalytically sourced platform molecules will be preferred unless otherwise stated. Finally, toluene was not assessed in terms of its synthesis due to a current lack of a viable synthetic route from biomass.

5.4.1 Assessment of TMTHF synthesis

Route 1: TMTHF from acetylene

Starting from the potentially bio-based platform molecules acetylene and acetone (bio-based route described in Chapter 1), three steps were considered in the synthesis of TMTHF (Figure 5.2). The first step involved the coupling of acetylene with two equivalents of acetone using potassium isobutoxide to produce DMHYL.[271] DMHYL was subsequently hydrogenated to produce DHL over a palladium on alumina catalyst[271] and finally, dehydration of DHL using a H-BEA-zeolite catalyst yielded TMTHF.

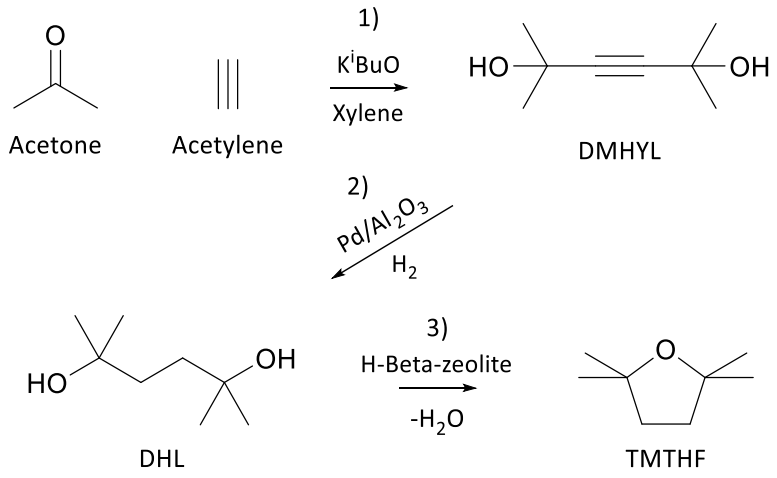

Figure 5.2. Synthesis of TMTHF from acetone and acetylene (Route 1).

The data for Steps 1 and 2 are taken from an example in Gevo's patent US 6,956,141[271] while data for Step 3 was obtained in Chapter 3 of this thesis. The AE, RME and PMI for each step as calculated by the CHEM21 metric toolkit are shown in Table 5.8.[216]

The conversion of the in each step was excellent, 98%, 100% and 100% respectively, and selectivities were also very high at 90.0%, 98.5% and 99.2% respectively. The AE of the first two steps was 100% as all atoms in the reactants ended up in the products. In Step 3, the AE is lower (87.7%), but it should be noted that the only by-product is water. The reaction mass efficiency in the first two steps is also high at 93.4% and 98.5% respectively, but like the AE, the RME is reduced due to the loss of water in Step 3.

Table 5.8. CHEM21 metrics for the production of TMTHF from DHL.

Step	Conv. / %	Sel. / %	AE / %	RME / %	PMI
1[(a)]	98.0	90.0	100.0	93.4	8.3
2[(a)]	100.0	98.5	100.0	98.5	3.3
3[(b)]	100.0	99.2	87.7	87.0	0.9

(a) Data obtained from US patent 6,956,141.[271] (b) Data obtained from work carried out in Chapter 3.

The PMI for each step is also included, but as each step is carried out in flow, the PMI is not representative of the amount of product produced for a given amount of catalyst/solvent/work-up materials. Each step of the process used catalysis as opposed to stoichiometric amounts of reagents, which would further reduce the PMI. This is demonstrated by the PMI in Step 1, which is 8.3. This means that the mass of all reactants, reagents solvents was 8.3 times more than the mass of the product (TMTHF). However, as the process is carried out in flow the amount of product produced can be significantly increased against the same amount of $K^{i}BuO$ catalyst. Therefore, PMI values will be calculated using a much-reduced catalyst mass of 0.01 g for all steps carried out in flow for the remainder of this assessment. In Steps 2 and 3, excellent conversions and selectivities are achieved. AE of Step 2 is 100% while the loss of water (a benign by-product) in Step 3 results in a reduced AE of 87.7%. Both steps use flow chemistry, resulting in more realistic PMIs of 3.3 and 0.9 respectively.

Table 5.9 highlight issues with energy use, waste, the use of critical elements, hazardous substances, using a traffic lights scoring system.[216] Xylene is used in Step 1 which results in a yellow rating while no solvent is used in Steps 2 and 3. However, greener alternatives could be used instead of xylene, such as TMTHF or anisole. Carbonyl group-containing solvents, such as the esters or pinacolone, may be susceptible to reaction with acetylene and cannot be used. Alternatively, the reaction may be successful in the absence of a solvent or in a larger excess of acetone. Reusable catalysts are utilised in all three steps resulting in green colour ratings. $K^{i}BuO$ catalyst is regenerated and can be reused multiple times. All steps receive a yellow score rating in the critical elements category for the use of potassium, palladium and aluminium respectively,[216] however, it has been shown that H-BEA-zeolites with a Si/Al of 150:1 can catalyse Step 3, and the amounts of alumina present in such a zeolite are very small. In addition, the high reusability of the H-BEA-zeolite, as demonstrated in Chapter 3, means a yellow rating is harsh. Step 1 is carried out at 30-35 °C, well below the reflux temperature of xylene and receives a green rating in both

categories while Steps 2 and 3 receive a yellow rating as they are carried out between 70 and 140 °C respectively, but a green rating given that no solvent is used. All steps use flow chemistry and receive a green rating. In the work up category, Step 1 is assigned a yellow rating as the reaction mixture is quenched with water, while Step 2 requires high temperature (140 °C) distillation and is assigned a red rating.

In the EHS category, scores were assigned based on the worst EHS code in that step. Step 1 received a red rating for the use of acetone (H372)[337] and acetylene (H230),[338] Step 2 received a yellow rating for the use of hydrogen (H220)[339] and Step 3 received a green rating as DHL's worst classification was H315 and H318.[23] However, acetone's classification of H372 (damage to organs through prolonged or repeated exposure) is not cited in the ECHA database.[340] In addition, acetone is considered to be "Recommended" in the CHEM21 solvent selection guide so its H372 is questionable.[201] Acetylene also receives a red rating but it has been produced at BASF since the work of Walter Reppe in the 1920's and is handled on a 100,000 – 1,000,000 tonnes scale annually, indicating that its potential explosive hazards are manageable.[273,274]

Overall, Tables 5.8 and 5.9 show that the synthesis of TMTHF from acetylene and acetone is green with some manageable issues regarding the safety of the starting materials.

Table 5.9. Additional assessment by the CHEM21 metric toolkit.

Category	Step 1[(a)]	Step 2[(a)]	Step 3[(b)]
Solvent	Xylene	No solvent	No solvent
Catalyst/Enzyme/ Stoichiometric reagent	Catalyst	Catalyst	Catalyst
Catalyst/Enzyme recovery	Recoverable	Recoverable	Recoverable
Critical elements	P (H_3PO_4)	Pd, Al (Pd/Al_2O_3)	Al (Zeolite)
Reaction temperature	30-35 °C	80 °C	110 °C
Reflux/>5 °C below reflux	>5 °C below reflux	n/a	n/a
Batch/Flow	Flow	Flow	Flow
Work up	Quenching	Distillation (185 °C)	Distillation (115 °C)
EHS (worst)	H372, H230	H220	None

(a) Data obtained from US patent 6,956,141.[271] (b) Data obtained from work carried out in Chapter 3.

Route 2: TMTHF from isobutanol *via* hydration of DHN

The production of TMTHF from isobutanol required four steps (Figure 5.3). First isobutanol is partially oxidised to form a mixture of isobutyraldehyde and isobutanol.[341] Ratios of 33:67 to 67:33 were said to be suitable.[341] The mixture was then passed over an unspecified dehydration catalyst to give an isobutyraldehyde/isobutene mixture.[341] A niobic acid catalyst is employed to couple the isobutyraldehyde and isobutene in a Prins-type reaction to yield DHN[341] which is subsequently hydrated to produce TMTHF using a H-BEA-zeolite catalyst (as described in Chapter 3).

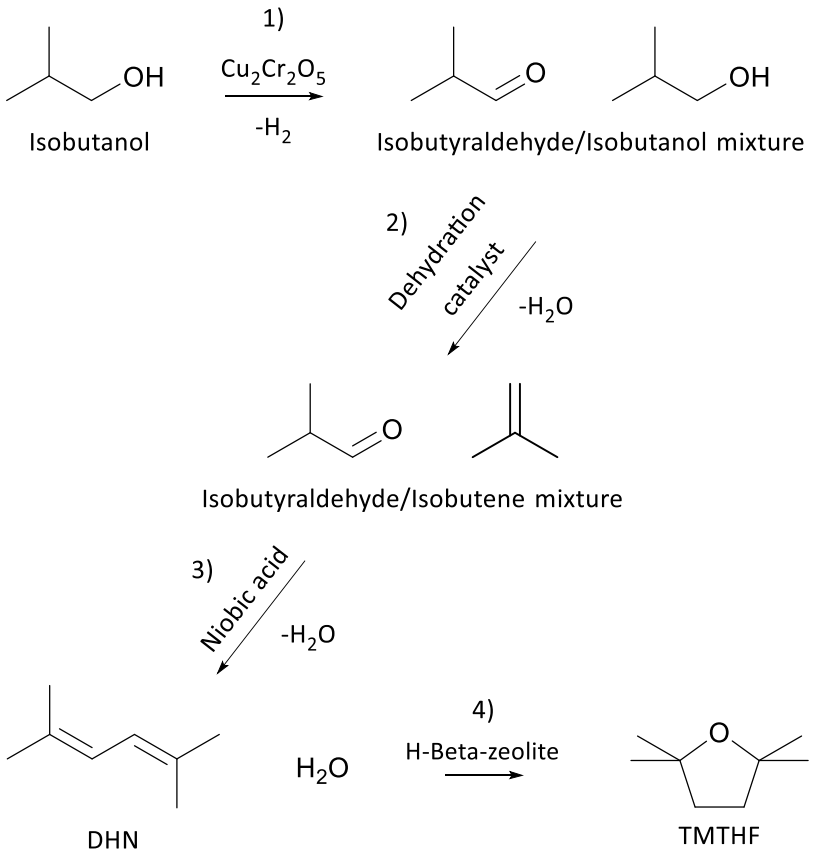

Figure 5.3. Synthesis of TMTHF from isobutanol *via* DHN (Route 2).

The data for Steps 1 and 2 are taken from Gevo's patent US 8,742,187[341] while preliminary experiments have been carried out for Step 3 and are described in Chapter 3 of this thesis. As such, some estimations and approximations had to be made for the calculations in Step 3 and have been highlighted in the relevant sections. AE, RME and PMI for each step are shown in Table 5.10.[216]

Table 5.10. CHEM21 metrics for the production of TMTHF from the hydration of DHN.

Step	Conv. / %	Sel. / %	AE / %	RME / %	PMI
1[(a)]	50.0	100.0	97.3	97.3	1.0
2[(a)]	99.0	96.0	75.7	72.7	1.4
3[(a)]	35.0	95.0	85.9	81.7	1.2
4[(b)]	n/a	n/a	100.0	n/a	n/a

(a) Data obtained from US patent 8,742,187 B2.[341] (b) Data obtained from work carried out in Chapter 3.

Steps 1-3 are carried out in series so no separation is required in between them.[341] Catalyst amount used has been reduced to 0.01 g for the purpose of this assessment to account for the reaction being in flow.

Step 1 involves the partial oxidation of a stream of isobutanol to isobutyraldehyde.[341] Therefore, although a conversion of 50% can be seen in Table 5.10, this is the desired conversion as the remaining isobutanol is dehydrated in Step 2.[341] Conversions of 33-66% are also acceptable. The AE of Step 1 is 97.3%, with recoverable hydrogen gas being the only by-product. The RME is 97.3% and the PMI is a low value of 1.0.

The dehydration in Step 2 can achieve 99% conversion and 96% selectivity for isobutene.[341,342] Due to the loss of water, an AE of 75.7% and an RME of 72.7% are assigned, while the PMI is low at 1.4. The Prins-type reaction between isobutyraldehyde achieved 35% conversion and 95% selectivity of DHN.[341] However, unreacted DHN is recycled and near full conversion is obtained, a fact that is often hidden when only conversion and selectivity are used as reaction metrics. Water is released, resulting in an AE of 85.9% and an RME of 81.7%. In Step 4 water is added again, thus cancelling the loss of water in this step, and maintains an overall high atom economy. Finally, a low PMI of 1.2 is indicative of a catalytic flow reaction.

Relevant data has not yet been obtained for Step 4, it is therefore impossible to calculate the reaction metrics. Preliminary experiments which were described in Chapter 3 show that the reaction is possible, but a gas phase reaction will be required to obtain high conversion and selectivity, and this would be included in future work. Ideally, the hydration would be carried out with the same H-BEA-zeolite that is used to catalyse the ring closure. This would mean that DHN and water could be flowed through the zeolite in the gas phase where the diene is hydrated and ring-closed. As the boiling point of DHN is 132-134 °C, temperatures of ~140 °C would be

required.[343] It has previously been shown that selectivity for the hydration product decreased from 100% at 100 °C to 70-80% at 140 °C[344] in the hydration of propene. Therefore, this may be an issue in the hydration of DHN in the gas phase.

Table 5.11. Additional assessment by the CHEM21 metric toolkit.

Category	Step 1[(a)]	Step 2[(a)]	Step 3[(a)]	Step 4[(b)]
Solvent	No solvent	No solvent	No solvent	No solvent
Catalyst/Enzyme/ Stoichiometric reagent	Catalyst	Catalyst	Catalyst	Catalyst
Catalyst/Enzyme recovery	Recoverable	Recoverable	Recoverable	Recoverable
Critical elements	Cu, Cr ($Cu_2Cr_2O_5$)	Al (Mordenite)	Nb (Niobic acid)	Al (Zeolite)
Reaction temperature	320 °C	180 °C	220 °C	≥150 °C
Reflux/>5 °C below reflux	n/a	n/a	n/a	n/a
Batch/Flow	Flow	Flow	Flow	Flow
Work up	None	None	Distillation (140 °C)	Distillation (115 °C)
EHS (worst)	None	None	H220, H341, H401	None

(a) Data obtained from US patent 8,742,187 B2.[341] (b) Data obtained from planned experiments which would be carried out in future work.

Table 5.11 rates each step of the synthesis in terms of energy use, waste, the use of critical elements hazardous substances, using a traffic lights scoring system. The data shown for Step 4 is based on planned experiments as this method has not been carried out before.

Each of the four steps are carried out using recoverable and reusable solid catalysts and no solvents are required. Therefore, all are highlighted in green for these categories. All four steps use elements which are classed in the 50-500 year of remaining reserves range.[216] However, as the critical elements form part of the catalyst in each step, they can be recycled, thus improving the greenness. All four steps require high temperatures (≥140 °C) meaning energy demand is relatively high, especially in Step 1.[341] All steps are carried out without the use of a solvent, so solvent loss during reflux is not an issue and all four steps are carried out in flow. Steps 1 and 2 are carried out in series and as such, purification is not required in between each step. This is very

significant as purification steps can be difficult.[345] No highly hazardous chemicals are used at any stage of this synthetic route, although isobutene and isobutyraldehyde are given yellow flags.

Overall, compared to the synthetic route to TMTHF *via* DHL, this route displays a less hazardous work up and EHS of the starting materials but a higher energy demand during synthesis. However, it is also shown to be a green synthetic route when all steps are considered together.

Route 3: TMTHF from isobutanol *via* oxidation of DHN

Although not fully carried out in this work, a process for the synthesis of TMTHF *via* the oxidation and subsequent hydrogenation of DHN using TMTHF as the solvent was proposed in Chapter 3 (shown in Figure 5.4). In this section, this potential route to TMTHF will be assessed for greenness based on two assumptions:

1. TMTHF could be used as the solvent in Steps 5.
2. Full conversion of the DHN polyperoxide to make DHL is achieved in Step 5.

If either of the assumptions are not adhered to, the synthesis is highly unlikely to be green, as extra purification steps will be needed in a process which already requires more steps than the other routes.

The synthesis of TMTHF from isobutanol *via* the oxidation of DHN follows the same initial three steps as Route 2.[341] However, instead of a final hydration of DHN, an oxidation in mild conditions is carried out, followed by a hydrogenation (Figure 5.4).[276] It has been shown in Chapter 3 that DHN dissolved in TMTHF can be almost fully converted to the DHN polyperoxide in 5 days (Step 4). Reaction times could be shortened by exposing the thoroughly aerated reaction mixture to UV light in a continuous flow reactor.

Excellent conversions and selectivities for the subsequent hydrogenation have been reported in a paper by Griesbaum *et al*. (Step 5).[276] Yields of 90% DHL were previously obtained under 10 bar of hydrogen using THF as the solvent in a batch reactor.[276] However, the hydrogenation was not optimised and better yields of DHL could potentially be achieved in shorter reaction times. Yields of >99% using TMTHF as the solvent instead of THF would be required for the process to be green (assumptions 1 and 2).

Finally, the ring closure of Route 1 is used to produce TMTHF in excellent yields, as described in Chapter 3 (Step 6).

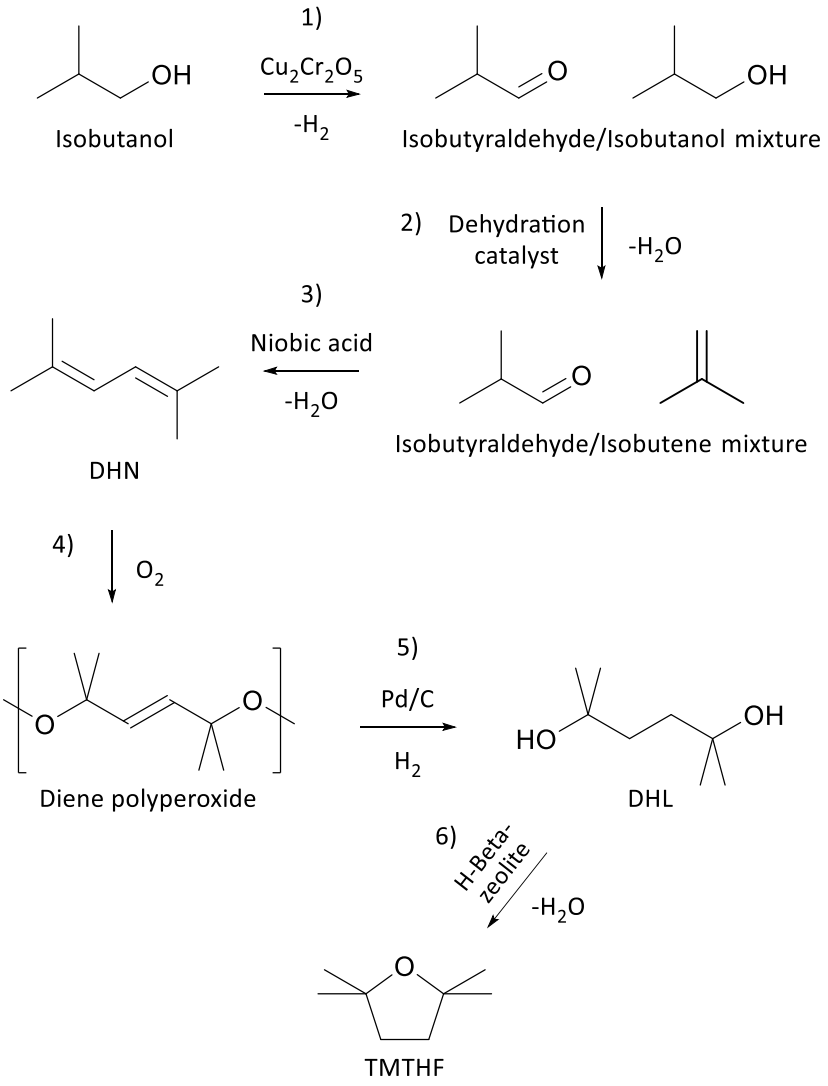

Figure 5.4. Production of TMTHF *via* the oxidation of DHN (Route 3).

The metrics for Steps 4 and the assumed metrics for Step 5 can be seen in Table 5.12. The experimentally determined Steps 1-3 and 6 have been previously discussed in Tables 5.11 and 5.9 respectively, therefore only their colour ratings are shown in Table 5.13. Despite the greater number of steps required in this route to TMTHF, the two additional steps (Steps 4 and 5) have a potentially low environmental impact due to their ambient conditions, while achieving high yields and selectivities. The reactions in both steps are additions, resulting in high AEs of 100% in both cases.

Table 5.13 highlights the potentially ambient conditions required for the synthesis. Assumption 1 states that TMTHF must be used in Step 5 to eliminate the need for a separation step in between.

Table 5.12. CHEM21 metrics for the production of TMTHF from the oxidation of DHN.

Step	Conv. / %	Sel. / %	AE / %	RME / %	PMI
1[(a)]	50.0	100.0	97.3	97.3	1.0
2[(a)]	99.0	96.0	75.7	72.7	1.4
3[(a)]	100.0	95.0	85.9	81.7	1.2
4[(b)]	>98.0	100%	100.0	100.0	1.0
5[(b)]	>99.0	>99.0	100.0	100.0	1.0
6[(c)]	100.0	99.2	87.7	87.0	0.9

(a) Data obtained from US patent 8,742,187 B2.[341] (b) Assumed values based on anticipated improvements upon those values obtained in the un-optimized process reported by Griesbaum et al.[276] (c) Data obtained from work carried out in Chapter 3.

Table 5.13. Additional assessment by the CHEM21 metric toolkit.

Category	1[(a)]	2[(a)]	3[(a)]	Step 4[(b)]	Step 5[(b)]	6[(c)]
Solvent				TMTHF	TMTHF	
Catalyst/Enzyme/ Stoichiometric reagent				None	Catalyst	
Catalyst/Enzyme recovery				n/a	Recoverable	
Critical elements				None	Pd (Pd/C)	
Reaction temperature				RT	RT	
Reflux/ >5 °C below reflux				n/a	n/a	
Batch/Flow				Flow	Flow	
Work up				None	Distillation (>100 °C)	
EHS (worst)				H315, H319, H335 (DHN)	H220 (Hydrogen)	

(a) Data obtained from US patent 8,742,187 B2.[341] Details shown in Table 5.11. (b) Data based on planned experiments which would be carried out in future work. (c) Data obtained in this work. Details shown in Table 5.9.

Accordingly, TMTHF has been entered as a green solvent in this assessment. No catalyst is required for Step 4 while a recoverable and reusable supported palladium catalyst such as Pd/C can be used for the hydrogenation in Step 5.[276] No critical elements would be required in Step 4 while the use of palladium is not ideal in Step 5. Both steps should be carried out in flow at room temperature after which a solution of DHL in TMTHF would be produced. This mixture can pass immediately through to a final reactor containing H-BEA zeolite to convert the DHL into TMTHF as described in Route 1. A portion can then be recycled back into the system at Step 4 and the remainder can be distillation at ~112 °C to increase purity.

Overall, this route is a combination of Routes 1 and 2. It uses the starting material from Route 2 to produce DHN but then proceeds *via* an oxidation to generate DHL as opposed to a hydration. Finally, it uses the H-BEA-zeolite from Route 1 to produce TMTHF from DHL. The advantage of this route is that despite it involving more steps, the extra steps are more benign and "bypass" the red areas shown in the first two routes (Table 5.14). in addition, TMTHF would be used as a green reaction solvent for Steps 4, 5 and 6. However, as previously stated this route it theoretical as Step 5 has not been carried out to date and is based on the assumption that Step 5 can be carried out in flow, achieving quantitative yields using TMTHF as a green solvent.

5.4.2 Assessment of methyl butyrate and ethyl isobutyrate synthesis

Methyl butyrate and ethyl isobutyrate from glycerol

Although ethyl isobutyrate was removed from the list of candidates due to its inability to host radical polymerisation reactions, it can be produced very easily from the same proposed source as methyl butyrate and therefore has been included in this assessment.[177] Starting from the bio-based platform molecules glycerol and CO, one carbodeoxygenation step and one esterification step was considered in the synthesis of methyl butyrate and ethyl isobutyrate (Figure 5.5).[177] This is very similar to the current butyric acid synthesis involving the hydroformylation of propene to produce butyraldehyde, which is subsequently oxidised to butyric acid.[285,346,347] Switching propene for glycerol provides a bio-based alternative synthesis.[177]

Coskun *et al.* have produced a 67:33 mixture of butyric acid and isobutyric acid using a rhodium catalyst and hydrogen iodide (HI) as a co-catalyst.[177] The reaction was carried out in batch under high pressure CO (30 bar). The process is very similar to the Cativa process for the production of acetic acid, as both use high pressure CO and a rhodium/HI catalyst system.[90,347] A proposed flow diagram for the production of butyric and isobutyric acid which is based on a flow diagram of the Cativa process as published in "Chemical Process Technology" can be seen in Figure 5.6.[347] Glycerol dissolved in acetic acid is added to the reactor along with CO. The product stream

undergoes flash evaporation, with unreacted heavier starting material and catalyst being recycled back into the system. The more volatile CO and acetic acid as well as some intermediate products formed *in situ* can be recycled back into the system from the drying column, while the less volatile products are passed through to the product column where they are separated from each other. Potential heavier products are crotonic acid and vinylacetic acid but these were not produced in the work of Coskun *et al*.[177] Table 5.14 shows the reaction metrics for both steps of the process. Full conversion of glycerol was achieved with excellent selectivity for butyric acid (63%) and isobutyric acid (35%). Small amounts of isopropyl acetate (1.0%) and isopropyl iodide (1.5%) were formed as by-products in the batch system.

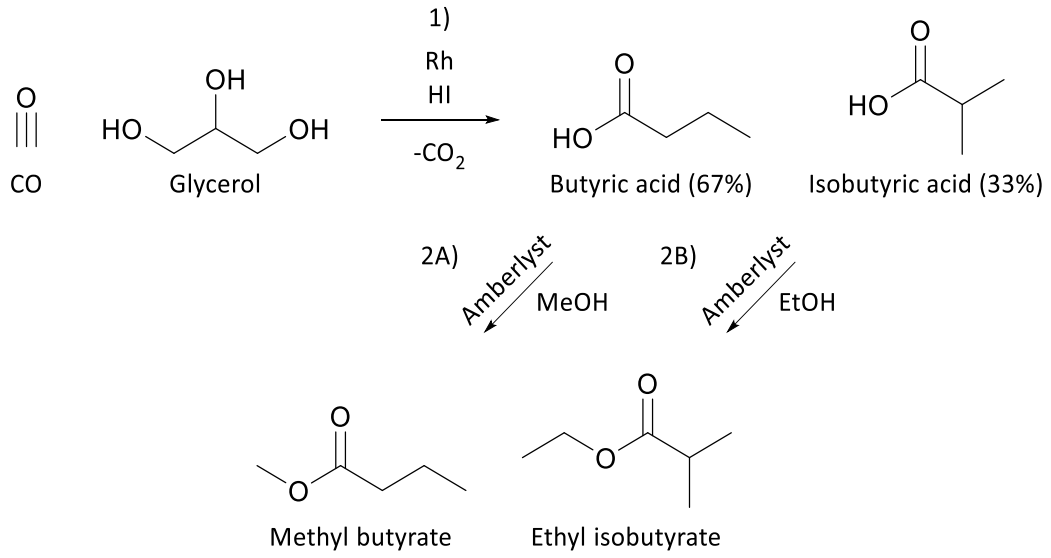

Figure 5.5. Synthesis of methyl butyrate and ethyl isobutyrate from glycerol.

Table 5.14. CHEM21 metrics for the production of methyl butyrate and ethyl isobutyrate from glycerol.

Step	Conv. / %	Sel. / %	AE / %	RME / %	PMI
1[(a)]	100 (both)	63/35 (BA/IA)	73.4 (both)	20.2/11.3 (BA/IA)	11.3/20.1 (BA/IA)
2A[(a)]	100	100	85.0	85.0	1.2
2B[(a)]	100	100	86.6	86.6	1.2

(a) Data obtained from Coskun *et al*.[177]

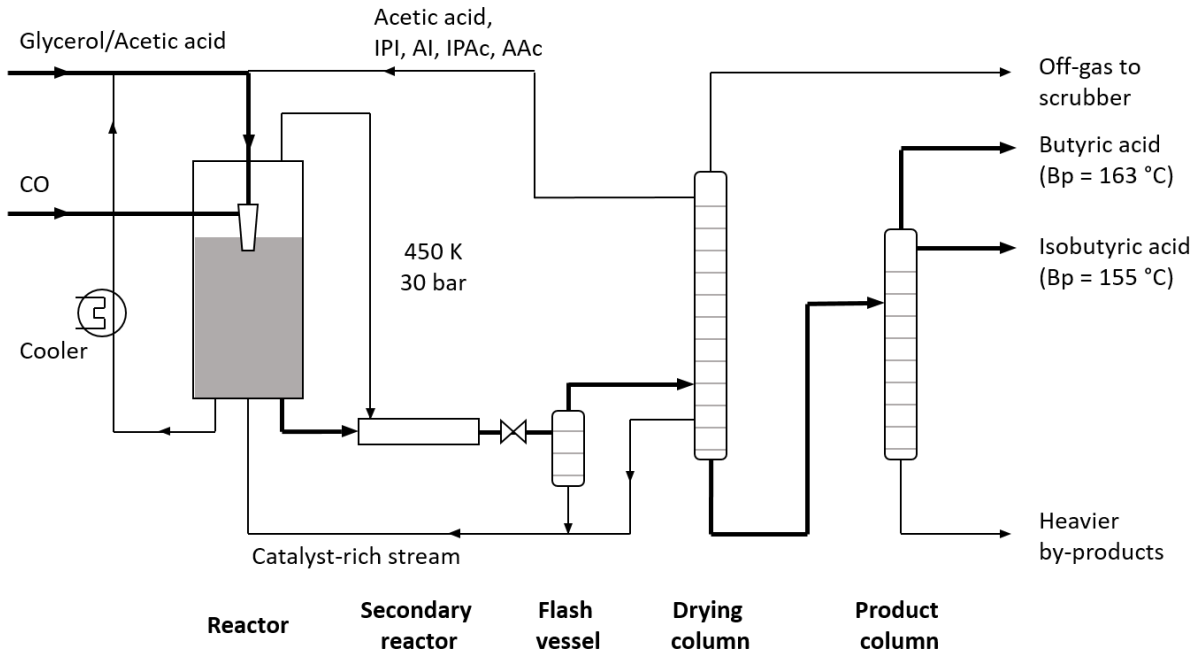

Figure 5.6. Potential flow diagram for the production of butyric acid and isobutyric acid from glycerol. IPI = isopropyl iodide, AI = allyl iodide, IPAc = isopropyl acetate, AAc = allyl acetate. Diagram is an altered version of the flow diagram of the Cativa process shown in Chemical Process Technology.[347]

The AE for both products was 73.4% due to the loss of two equivalents of water from glycerol. The RME for both products is low (20.2% and 11.3% for butyric acid and isobutyric acid respectively) but this is due to the excess CO gas which is almost completely recovered and reused in a flow process (Figure 5.6). Therefore, the low RMEs are not representative of the overall process. When an equivalent amount of CO is used for the calculation, the RMEs of butyric acid and isobutyric acid were 46.2% and 25.8% respectively, a significant improvement and more representative of the process. The PMI is 11.3 and 20.1 for butyric acid and isobutyric acid respectively. This value is overly harsh on the flow process due to the recyclability of the solvent (acetic acid) and CO.

Steps 2A and 2B involve the esterification of the acids. Data has been obtained for the esterification of methyl butyrate in Chapter 3 of this thesis. Although the reaction to produce ethyl isobutyrate was not carried out as part of this work due to its inability to facilitate the polymerisation reaction, the esterification would be expected to proceed in a similar manner to that of butyric acid. The reaction was carried out in flow which allowed all of the butyric acid starting material to be consumed with full selectivity for the ester product and unreacted methanol can be recycled back into the system, as shown in Step 2A, Table 5.14. The AE and RME for methyl butyrate and ethyl isobutyrate production were 85.0% (Step 2A) and 86.6% (Step 2B)

respectively. The loss of water is the reason for the reduction in AE and RME. Using the equivalent amounts of alcohol and acid for the calculation of the PMI, values of 1.2 are obtained for both reactions.

Table 5.15 highlights issues with energy use, waste, use of critical elements and hazardous substances in this synthesis. Acetic acid, which is classed as "Problematic" by the CHEM21 guide,[201] is used as the solvent in the carbonylation of glycerol due to the high viscosity of glycerol.[177] No solvent is used in the esterification step. Both processes are catalytic but the carbonylation requires the very expensive and rare rhodium as catalyst (5-50 years supply remaining) and the corrosive HI as co-catalyst, meaning acid resistant steel is needed for the reactor which will add to capex costs.[177] The carbonylation also requires high temperature (180 °C) and pressure (~90 bar) while the esterification is carried out in refluxing methanol (~60 °C). Both processes can be carried out in flow and distillation is required for purification (Figure 5.6). In terms of EHS of the materials used in the process, the carbonylation requires the highly toxic CO gas and HI acid while the esterification requires methanol for the production of methyl butyrate and ethanol for the production of ethyl isobutyrate.

Table 5.15. Additional assessment by the CHEM21 metric toolkit.

Category	Step 1[(a)]	Step 2A[(b)]	Step 2B[(c)]
Solvent	Acetic acid	No solvent	No solvent
Catalyst / Enzyme/ Stoich. reagent	Catalyst	Catalyst	Catalyst
Catalyst / Enzyme recovery	Recoverable	Recoverable	Recoverable
Critical elements	Rh ($[RhCl(CO_2)]_2$)	None	None
Reaction temperature	180 °C	~60 °C	~60 °C
Reflux / >5 °C below reflux	n/a (high pressure)	Reflux	Reflux
Batch/Flow	Flow	Flow	Flow
Work up	Distillation (165 °C)	Distillation (~100 °C)	Distillation (~110 °C)
EHS (worst)	H360, H372 (CO)	H370 (MeOH)	H350 (EtOH)

(a) Data obtained from Coskun *et al.*[177] (b) Data obtained from experiments carried out in this work. (c) Data obtained from planned experiments which would be carried out in future work.

Several red marks are apparent on Table 5.15, especially in the carbonylation step. However, although rhodium is a rare and expensive metal, in this particular application, it is somewhat compensated by its reusability and excellent selectivity (99.9%) resulting in ease purification and material is not released as waste. In addition, despite the hazard codes of CO (H360 and H372, both red)[348] and HI (H331, yellow),[349] both chemicals are handled safely and on a very large scale in the Cativa process for the production of acetic acid.[90] This demonstrates the overall robustness, greenness and cost effectiveness of the Rh/HI catalysed carbonylation process. The red marks in the esterification step are also slightly deceivable. Refluxing methanol is used but all methanol is recycled back into the system while in the EHS category, the red marks are for ethanol (a unanimously agreed green solvent)[201,208,211,225] and methanol (a bio-based platform molecule with admittedly high toxicity).[350] Overall, based on the above points the carbonylation of glycerol to produce C4 acids and their subsequent esterification could be a viable route to C4 esters.

Methyl butyrate from fermentation

The precursor to methyl butyrate, butyric acid, can also be produced from fermentation of sugars using modified microorganisms.[285,346] If butyric acid from fermentation is considered to be a bio-based platform molecule, this route to methyl butyrate would only require one easy esterification step. However, the production of butyric acid from fermentation requires the difficult initial hydrolysis of lignocellulosic biomass and suffers from low yields.[346] Furthermore, as it is a biochemical route as opposed to a chemo-catalytic route, is susceptible to infection.[285] Just like how the chemo-catalytic synthesis of acetic acid is preferred over the fermentation route, the chemo-catalytic route to butyric acid from glycerol may well be preferred over the fermentation route due to better economics. This is not to say that fermentation will not have a place in the future production of butyric acid, only that it may not be the dominant source.[285]

5.4.3 Assessment of methyl pivalate and pinacolone synthesis

Methyl pivalate and pinacolone from pivalic acid

The synthesis of methyl pivalate and pinacolone both utilise similar carbonylation chemistry as in the production of methyl butyrate and ethyl isobutyrate. The bio-based platform molecules, isobutene and CO, in the presence of water can produce pivalic acid by hydroxycarbonylation (Step 1, Figure 5.7).[260] Formic acid can also be used in place of CO, as it breaks down to CO and water in the presence of acid.[123] However, this route ultimately results in the production of high pressure CO *in situ*, so its benefits are limited to storage and transport.[123] Thus, the use of CO and isobutene will only be discussed in this section.

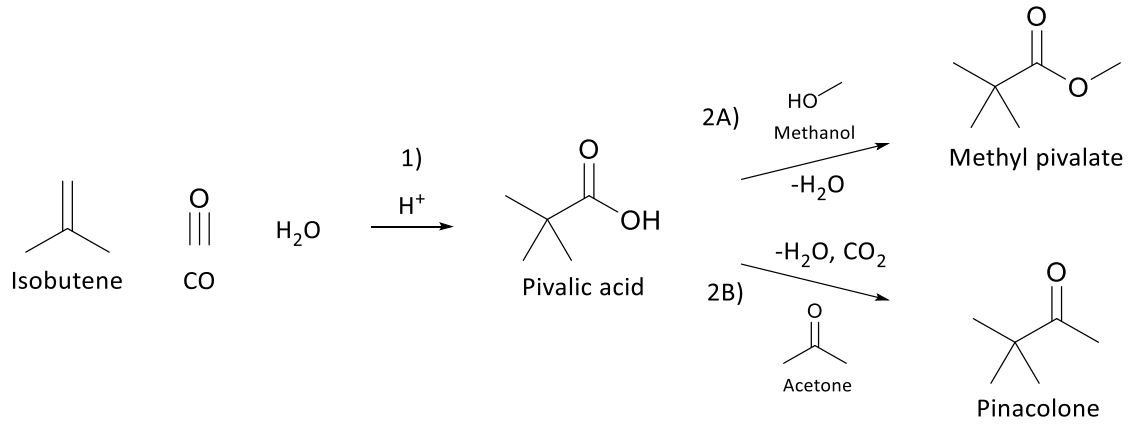

Figure 5.7. Synthetic routes to methyl pivalate and pinacolone from pivalic acid.

Step 1 can potentially be metal catalysed using metals such as palladium,[267] rhodium or iridium (like the Cativa[90] and Monsanto[256] processes respectively) or acid catalysed (Koch reaction).[257,351] Pivalic acid can either undergo esterification with methanol to yield methyl pivalate (Step 2A, Figure 5.7) or ketonisation with either acetone or acetic acid to yield pinacolone (Step 2B, Figure 5.7).

Experimental data for the metal catalysed production of pivalic acid from isobutene has not been reported in the literature and therefore conversion, selectivity, RME and PMI cannot be calculated. While metal catalysed carbonylation of alkenes is well known,[267,352] the less branched product tends to be preferred over the branched product.[267] Careful choice of ligands can improve selectivity for the branched acid.[353,354] However, there are no mentions of the synthesis of *tert*-products using metal catalysts in the literature. Reports of branched selectivity have been limited to *iso*- products and linear products.[267,353–355] This raises a problem for the synthesis of the branched pivalic acid and a deeper investigation would be included in the future work for this project.

In contrast, the acid catalysed Koch reaction favours the branched product as the reaction proceeds *via* the more stable tertiary carbocation (Figure 5.8).[257,356] However, the oligomerisation of the alkene substrate often diminishes yields.[257,356] Efforts to increase the yield of the tertiary alkene and this would form part of the future work of this project.

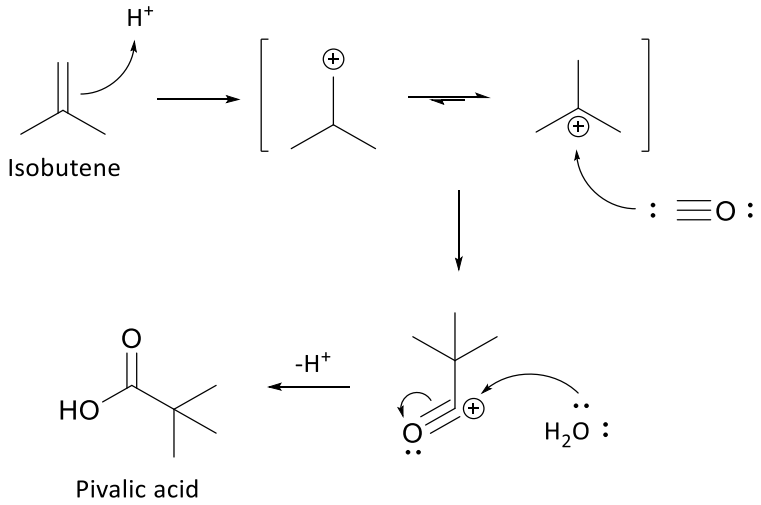

Figure 5.8. Koch reaction mechanism.

The conversion, selectivity, AE, RME and PMI for the acid catalysed route to pivalic acid based on literature data is shown in Step 1, Table 5.16. The use of sulfuric acid has been patented by Du Pont but its selectivity for pivalic acid is low.[257,356,357] Yields of 60-80% were obtained in each case due to oligomerisation of isobutene in the highly acidic conditions. Catalytica Incorporated have patented the production of pivalic acid from isobutene using boron trifluoride as the catalyst in US patent US5227521.[261] Moderate yields of 67% were obtained with significant amounts of higher acids also produced. The yield was increased to 90% by the same inventors in US patent US5241112 by adding $Zr(O_3PCF_2SO_3H)_2$ to the system as a co-catalyst, and it is the results of this system which are shown in Route 1, Table 5.16.[260]

Table 5.16. CHEM21 metrics for the production of methyl butyrate and ethyl isobutyrate from glycerol.

Step	Conv. / %	Sel. / %	AE / %	RME / %	PMI
1[(a)]	100	90	100	90	1.1[(b)]
2A[(c)]	100	100	76.1	76.1	1.3
2B[(d)]	Undisclosed	(90)[(e)]	80.6[(f)]	74.4[(f)]	1.4[(f)]

(a) Data obtained from Sanderson *et al.*[260] (b) Isobutane solvent not included in calculation as it is a gas. (c) Data obtained in this work. (d) Data obtained from Cryberg *et al.*[264] (e) Yield obtained on a single pass through a catalyst loaded tube furnace reactor. (f) Acetic acid is considered as a secondary product.

The reaction is additive resulting in an AE of 100%, but due to the oligomerisation of isobutene a reduced RME of 90% is obtained. A low PMI of 1.1 is due to the use of isobutane gas as the solvent as the CHEM21 guide is unable to include gaseous solvents in the calculation of PMI. To make a more reasonable estimate of PMI which includes the solvent, 100 mL of a hypothetical liquid solvent with a density of 0.70 g mL^{-1} was used in the calculation, upon which the PMI increased to 1.9 which is still a relatively low value. Recovery of the solvent will reduce this value even further.

The data for the production of methyl pivalate from pivalic acid, Step 2A, was obtained in Chapter 3 of this work. Full conversion of pivalic acid and selectivity for methyl pivalate could be achieved using a Dean-Stark apparatus and unreacted methanol could be recycled back into the system. An AE of 76.1% was due to the loss of water during the esterification and an RME of 76.1% was obtained on the assumption that all unreacted methanol was recycled and reacted in the process. Using the equivalent amounts of alcohol and acid for the calculation of the PMI, a low value of 1.3 was attained for both reactions.

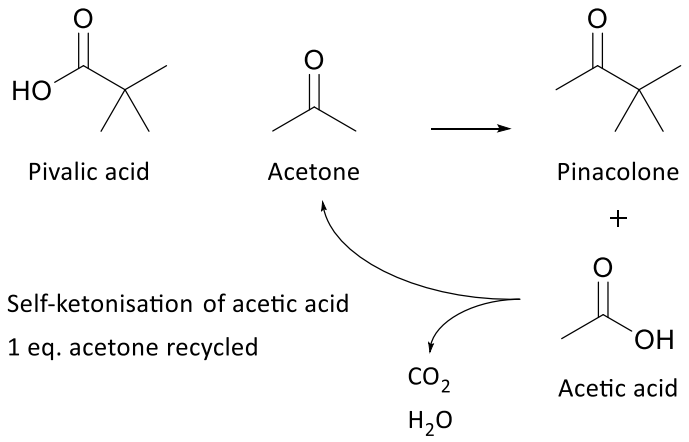

Figure 5.9. Recycling of one equivalent of acetone in the production of pinacolone.

The production of pinacolone from pivalic acid and acetone has previously been patented by SDS Biotech Corporation, and the data for this process is shown in Step 2B, Table 5.16.[264] Two equivalents of pivalic acid react with one equivalent of acetone to yield two equivalents of pinacolone. A yield of 90% was achieved in a single pass through a tube furnace reactor packed with a cerium on alumina catalyst.[264] It is also claimed that this yield can be further improved by recycling unreacted starting material, although data is not provided in the patent.[264] This is a reasonable claim as pinacolone would be the favoured product of this synthesis. Potential side-products could be due to the self-ketonisation product of pivalic acid to form 2,2,4,4-tetramethyl-3-pentanone. However, as an *alpha*-H atom on the carboxylic acid has been shown to be required

for self-ketonisation to occur,[358] the production of 2,2,4,4-tetramethyl-3-pentanone is unlikely. Acetic acid is produced as a secondary product according to the inventors and some CO_2 and water is also observed (Figure 5.9). The CO_2 and water is potentially due to the self-ketonisation of acetic acid upon its formation in the reactor, which would produce one equivalent of acetone along with an equivalent of CO_2 and water.[358]

The AE of the reaction is 62.5%, as a molecule of acetic acid is eliminated. However, two equivalents of acetic acid undergo self-ketonisation to regenerate one equivalent of acetone, CO_2 and water. The regeneration of acetone results in an improved net AE of 80.6%, an RME of 74.4%, and a PMI of 1.4 (Step 2B, Table 5.16).

A second route to pinacolone from pivalic acid has been reported in a patent application by Ignatchenko *et al.*[265] It involves the reaction of pivalic acid with acetic acid instead of acetone. However, when acetic acid is used as the starting material, CO_2 and water are produced as the only by-products, resulting in an AE of 60.1% which is lower than the acetone route (80.6%). Similar results were obtained for RME and PMI. For these reasons, the acetone route was considered a better option for the synthesis of pinacolone.

Table 5.17 highlights issues with energy use, waste, the use of critical elements and hazardous substances using a traffic lights scoring system. Green aspects of the synthesis of methyl pivalate and pinacolone are the absence of a solvent and the use of reusable catalysts in each step. Zirconium is used in the catalyst system for the production of pivalic acid from isobutene (Step 1)[260] and Cerium and aluminium are required for the synthesis of pinacolone (Step 2B),[264] all of which fall into the "50-500 year" category highlighted in yellow. However, these catalysts are recoverable. No critical elements are required in the production of methyl pivalate from pivalic acid (Step 2A) due to the use of Amberlyst 15 as the catalyst. Moderate temperature of 125 °C are required in Step 1 while a lower temperature of 70 °C is required in Step 2A. However, very high temperatures are required for the ketonisation of pivalic acid and acetone (450-500 °C).[264] Steps 1 and 2A are run in the gas phase, while Step 2A is run under refluxing methanol, which is recycled. All three steps are carried out in continuous flow and distillation is used to purify in each step. For the purification of methyl pivalate and pinacolone (Steps 2A and 2B respectively), low temperature distillation is sufficient (~100 °C) due to the low boiling point of the solvents (100 and 106 °C respectively).

The EHS category highlights serious issues in each step. In particular, Step 1 uses CO as a reactant (H360 and H372),[348] isobutane as the solvent (H340 and H350)[359] and BF_3 as co-catalyst (H330).[360] CO is required for the synthesis and its use is unavoidable, but in any case, it is handled

safely and on a large scale in the Cativa process for the production of acetic acid.[90] As BF_3 is corrosive, the correct materials must be used in the reactor system, which can increase capex costs. The highly toxic substance of very high concern (SVHC), isobutane, is reported in the patent as the solvent of choice. However, there are many alternatives to isobutane so its use may be avoidable, which would increase the greenness of the process. Indeed, a solvent may not be required at all.

Table 5.17. Additional assessment by the CHEM21 metric toolkit.

Category	Step 1[(a)] (Pivalic acid)	Step 2A[(b)] (Methyl pivalate)	Step 2B[(c)] (Pinacolone)
Solvent	No solvent	No solvent	No solvent
Catalyst/Enzyme/ Stoich. reagent	Catalyst	Catalyst	Catalyst
Catalyst/Enzyme recovery	Recoverable	Recoverable	Recoverable
Critical elements	Zr (Zr catalyst)	None	Ce, Al (Ceria alumina)
Reaction temperature	125 °C	~70 °C	450-500
Reflux/ >5 °C below reflux	n/a (gas phase)	Reflux	n/a (gas phase)
Batch/Flow	Flow	Flow	Flow
Work up	Distillation (165 °C)	Distillation (~100 °C)	Distillation (~100 °C)
EHS (worst)	H360, H372 (CO), H340, H350 (Isobutane), H330 (BF_3)	H370 (MeOH)	H372 (Acetone)
SVHC	Isobutane	None	None

(a) Data obtained from US patent 5,241,112.[260] (b) Data obtained from planned experiments carried out in this work. (c) Data obtained from US patent 4,570,021.[264]

Methyl pivalate from isobutene

Methyl pivalate can also be produced directly from isobutene by hydroesterification. Hydroesterification is another type of carbonylation reaction which is similar to hydrocarboxylation, except an alcohol is used in place of water to produce esters instead of carboxylic acids (Figure 5.10).[354] Hydroesterification would allow a direct route to methyl pivalate

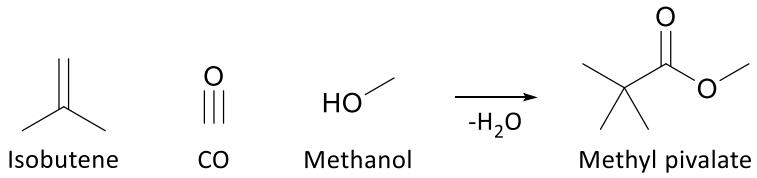

Figure 5.10. Synthetic route to methyl pivalate by hydroesterification.

from isobutene using methanol as the alcohol and would be an improvement upon the two steps required *via* the pivalic acid route in terms of its greenness.

This synthetic route has not previously been reported and no experimental data is available to assess its greenness. Like in the synthesis of pivalic acid, the reaction can potentially be catalysed either using metal catalysts or acid catalysts.[354] The metal catalyst tends to form the linear product although selectivity for the branched product may be increased by altering the ligands used. Acid catalysis may be a better option but run the risk of oligomerisation of isobutene.[257,356] Future work would involve the optimisation of the synthesis of methyl pivalate by one step hydroesterification.

5.5 Process suitability: Application in polymerisation and coating

In this section, the suitability of each solvent for the polymerisation and coating process is assessed. Some of the relevant physical properties which have been presented in Chapters 3 and 4 are discussed here in terms of their effect on the greenness of the process. Each solvent is assessed based on ease of removal in the drying ovens (represented by boiling point), flammability (based on AIT and LEL (vol.%)), ease of recovery (Bp difference from water), ability to dissolve polymers/rubbers, incineration (based on CO_2 release), and other issues.

Table 5.18 shows a range of relevant properties which are assigned a shade of green depending on their suitability. As all candidates have previously been shown to be suitable in each of the categories shown in Table 5.18, the suitability of the candidates is scored relative to each other within each category. Shades of green were chosen as opposed to a traffic light scoring system as a yellow, orange or red rating might appear overly negative. Dark green indicates the best suitability and shades of green fade with decreases suitability.

Table 5.18. Process suitability assessment.

	Bp / °C	Diff. from 100 °C / °C	Ability to dissolve all polymers/rubbers	LEL / vol.%	AIT / °C	CO2 released per mL of solvent / g	Odour
Methyl pivalate	101[(a)]	1	No	1.43[(c)]	443[(d)]	1.99[(e)]	Pass
Methyl butyrate	102[(a)]	2	No	1.22[(c)]	428[(d)]	1.93[(e)]	Fail
Ethyl isobutyrate	108-110[(a)]	8-10	No	1.00[(c)]	451[(d)]	1.97[(e)]	Pass
Pinacolone	106[(a)]	6	No	1.35[(c)]	428[(d)]	2.11[(e)]	Pass
TMTHF	112[(b)]	12	Yes	1.19[(c)]	417[(d)]	2.20[(e)]	Pass
Ethyl acetate	77[(a)]	23	No	1.63[(c)]	445[(d)]	1.80[(e)]	Pass
Toluene	111[(a)]	11	Yes	0.97[(c)]	522[(d)]	2.90[(e)]	Pass

Table Key	**Most suitable**				**Least suitable**

(a) Data obtained from PubChem,[220] (b) Data obtained during this work, (c) Calculations shown in the Appendix based on work carried out by ITS testing services, (d) Work carried out by Chilworth Technology. (e) Calculations shown in the Appendix.

5.5.1 Energy requirements and ease of recovery

The energy required to remove the solvent from the coated polymer was assessed based on boiling point, due to its correlation with vapour pressure and the wider availability of boiling point data (column 1). A solvent with a lower boiling point is easily removed, thus having a lower energy demand. Where the boiling point difference between candidates is 1 °C or less, the same shade of green is assigned, as in the case of methyl pivalate and methyl butyrate.

Table 5.18 demonstrates that ethyl acetate is the easiest to remove from the coated polymer with a boiling point of 77 °C. Of the five candidates, methyl pivalate and methyl butyrate are the easiest to remove, with boiling point ranges of 100-101 °C and 100-102 °C respectively. More difficult to remove are pinacolone (108 °C), ethyl isobutyrate (110 °C), toluene (111 °C) and TMTHF (112 °C). However, despite the lower boiling points of methyl pivalate and methyl butyrate (100-101

°C and 100-102 °C respectively), their recovery by distillation is made difficult by the proximity of their boiling points to that of water (100 °C) (column 2). As the solvent must be dry for use in the polymerisation step, more complicated drying techniques may be required for the separation from water, resulting in reduced greenness overall. A shade of green rating is used where the darkest shade of green is assigned to the solvent with the boiling point furthest away from water. The same shade is assigned to candidates with a 1°C difference or less, as in the case of methyl pivalate and methyl butyrate, both of whom have a boiling point very close to water (1 and 2 °C respectively). Although toluene and TMTHF have higher boiling points (111 °C and 112 °C respectively) which will require greater energy to remove, it may be compensated by the easier recovery and purification. However, this must be confirmed by testing in a pilot scale distillation column where energy input can be measured more accurately.

TMTHF was the only candidate that was able to dissolve all polymers and rubbers (column 3). This allows a one solvent manufacturing process and removes the need to separate two solvents from each other after recovery. Although concessions were made about the solubility of rubber R5, a solvent which can dissolve it would be preferred. As such, solvents which can dissolve all polymers and rubbers are highlighted in dark green while those that can only dissolve rubber R6 are assigned an intermediate shade. As ethyl acetate cannot dissolve either rubber, it is assigned the lightest shade of green.

5.5.2 Flammability

The flammability properties of all solvents were suitable for Nitto (columns 4 and 5). However, the higher the LEL (vol.%) and AIT the lower the risk of fire or explosion. The colour scheme in Table 5.18 again assigns the same shade of green for candidates with an LEL (vol.%) within 0.05% of each other. For AIT, the segmentation was done every 100 °C.

Table 5.18 shows that ethyl acetate has the highest LEL (vol.%) (1.63%) while toluene has the lowest (0.97%), closely followed by ethyl isobutyrate, with a similarly low value of 1.00%. TMTHF and methyl butyrate have comparable values that are better than toluene and ethyl isobutyrate (1.19% and 1.22% respectively), while methyl pivalate and pinacolone have the best LEL (vol.%) at 1.43% and 1.35% respectively.

The AITs of each candidate are similar and all are above 400 °C and fall within the narrow range from 417 °C to 451 °C. Toluene has by far the highest AIT at 522 °C. Interestingly, the two solvents with the lowest LEL vol.% have the highest AITs, toluene (522 °C) and ethyl isobutyrate (451 °C).

5.5.3 Incineration

Some solvent is incinerated to produce energy at Nitto, and therefore, CO_2 is emitted. Different substances emit different amounts of CO_2 and as it is a greenhouse gas, emissions should be minimised. Solvent choice can help with the reduction of emissions.

Solvents in Table 5.18 with emissions of 0.05 g difference or less were assigned the same shade of green. It can be seen that toluene releases the most CO_2 into the atmosphere upon incineration (2.90 g) while ethyl acetate releases the least (1.80 g). The esters all release a very similar amount of CO_2 (1.93 – 1.99 g) while pinacolone and TMTHF release slightly more (2.11 g and 2.20 g respectively). Each of the solvent candidates are composed of only carbon, oxygen and hydrogen, meaning the release of SO_x, NO_x or CFC's to the atmosphere upon incineration is not an issue.

Future work would involve the determination of the calorific value of each of the candidates to assess the energy that can be reclaimed upon incineration.

5.5.4 Solvent odour

Another property of practical importance is the odour of the solvents. Unpleasant odours can be troublesome and unpleasant for workers, so this must be considered when using solvents in open systems. Toluene and ethyl acetate which are currently used have very characteristic odours but neither are particularly unpleasant.

During the course of this work, the odour of methyl butyrate became problematic, to the point that it could no longer be used in the labs at Nitto, so it was discarded as a candidate and is highlighted as such in Table 5.18. It may be found that methyl butyrate is suitable for closed systems where human exposure is minimal but in the coating industry this is not the case. In contrast, ethyl isobutyrate and methyl pivalate gave very pleasant fruity odours. Interestingly, the odour of TMTHF was unlike traditional ethers and instead was pleasant and very similar to 1,8-cineol (eucalyptus), which must be due to the common quaternary *alpha*-carbon functionality. The odour of pinacolone was not particularly unpleasant and was quite like other small ketones such as acetone and MEK.

5.6 Conclusions

In this chapter, a thorough assessment and comparison of each candidate was carried out based on available data in terms of their toxicity, synthesis and application. It was established from the

start that the assessment would not assign a numerical score to each candidate but instead, would aim to simply highlight and hazards associated with their synthesis of use.

The assessment used three freely available resources, the CHEM21 solvent guide spreadsheet, the CHEM21 metrics toolkit and the EPA's TEST predictive software, as well an application assessment aimed specifically for the polymerisation and coating industry. The data obtained from Chapters, 2, 3 and 4 were used to make the assessment of each candidate and where data was unavailable it was highlighted.

Overall, it was found that TMTHF was the best candidate solvent to replace toluene based on its performance in the solubility tests, its similar physical properties and facile synthesis from potentially bio-based starting materials. Full toxicity testing is required before it can be registered with REACH for large-scale manufacturing and use, but predictions of its toxicity are promising.

6 Concluding remarks and future prospects

6.1 Concluding remarks

This project was carried out in collaboration with Nitto Belgium, a PSA manufacturer who currently rely on toluene for their manufacturing process. Toluene is produced from petroleum and is suspected of damaging the unborn child. Therefore, the aim of this project was to find a suitable replacement for toluene. Toluene's useful solvent properties have meant that finding a replacement has proven difficult. It is volatile and non-polar, a combination of properties which is difficult to obtain in safe, bio-based alternatives.

In this work, five potentially bio-based molecules with potential to replace toluene have been identified, synthesised, characterised and application-tested. The five molecules consisted of three esters, methyl butyrate, ethyl isobutyrate and methyl pivalate; one ketone, pinacolone; and the "quaternary ether", TMTHF.

The three esters and pinacolone provided viable alternatives to toluene. Esterification of the corresponding carboxylic acids to produce methyl butyrate and methyl pivalate, was undertaken very successfully in a continuous flow process using a reusable Amberlyst 15 catalyst in a Dean-Stark condenser. Full conversion of the acid was obtained using this easily scalable apparatus. The ketonisation of pivalic acid with acetone in the gas phase to produce pinacolone in high yields has previously been patented and thus was not attempted as part of this work. This too is a relatively simple process to scale-up, although its greenness is affected by the extremely high temperatures required. Synthesis of ethyl isobutyrate was not attempted as it had previously been found to be incapable of facilitating the radically-initiated polymerisations. Although ethyl isobutyrate was unsuitable for the production of PSAs, it has a number of favourable solvent properties such as a low boiling point (108-110 °C), low melting point (-88 °), low polarity and a pleasant odour

(strawberry-like), and could potentially be an excellent solvent in other applications which were outside the scope of this work. Methyl butyrate was found to be unsuitable for the production of PSAs due to its smell, and this could limit its use in other open systems. However, it too has many favourable solvent properties such as low polarity and a low boiling point (100-102 °C) so some closed-system applications could benefit from its use. Methyl pivalate and pinacolone were both successful in PSA production testing and their KAT parameters suggested that they were similar to toluene in terms of dipolarity/polarisability, which was confirmed using a model Menschutkin reaction. In addition, each candidate was tested for mutagenicity using the Ames test, where they were found to be non-mutagenic. This was an encouraging result, but full toxicity testing would be required before REACH registration.

TMTHF was identified as the best candidate to replace toluene. It was synthesised using a potentially bio-based diol, 2,5-dimethyl-2,5-hexanediol (DHL) in excellent yields of >99%. At present, DHL is commercially produced by the coupling of petroleum-sourced acetone and acetylene, but by using bio-based acetone and acetylene, 100% bio-based DHL can be made. Like toluene, TMTHF was non-polar enough to dissolve all polymers and rubbers, as predicted by HSP. TMTHF's boiling point (112 °C) was very similar to toluene's (111 °C), its melting point is below -90 °C and it displayed superior flammability properties compared to many traditional ethers and hydrocarbons, based on AIT and LEL. Most importantly and unusually, as it is a "quaternary ether" it does not form peroxides, and this was demonstrated in peroxide tests in comparison with a selection of traditional ethers. TMTHF has been shown to be stable in acidic conditions at room temperature (1 mol.% of a selection of acids) but some breakdown products were observed under reflux with sulfuric acid. Full testing is required before TMTHF can be registered with REACH for production or use on a 1 tonne scale or more. While very little toxicological data is available, predictions are promising, not least due to its structural similarity to 1,8-cineol, a compound used in flavourings and fragrances.

The performance of TMTHF was found to be comparable to toluene in Grignard, amidation and esterification reactions, in agreement with the predictions of HSP (low dipolarity, low hydrogen-bonding ability). This was significant because in each of the above applications, the KT parameters of TMTHF would suggest otherwise. KT parameters suggest that, like traditional ethers, TMTHF's strongly electron donating lone-pairs would be able to solvate the Grignard reagent. However, the four adjacent bulky methyl groups meant the lone-pairs were inaccessible to the Grignard reagent so instead, TMTHF behaved more like toluene, *i.e.* it did not facilitate the reaction. Similarly unexpected results were observed in amidation and esterification reactions. Solvents with high β had previously been shown to inhibit these reactions, but despite TMTHF's high β it performed

very well in both reactions, like toluene. As HSP and KT parameters provided conflicting description of the solubility properties of TMTHF, a more in-depth study was carried out using Abraham's solubility parameters, where differences between toluene and TMTHF were observed. The partitioning of solutes in biphasic TMTMF/water and toluene/water systems showed that TMTHF and toluene behaved similarly in terms of hydrogen-bond acidity, dipolarity, polarizability and molar volume. A difference was observed in terms of hydrogen-bond basicity, where the lone-pairs on TMTHF resulted in more of an affinity for protic solutes compared to toluene. For the reasons listed above, TMTHF is proposed as the best candidate to replace toluene, not only in the polymerisation and coating industry, but also in many other applications.

Each of the five candidate molecules were assessed for greenness using a combined assessment method. This method drew from the solvent guide and metrics toolkit of CHEM21 as well as the EPA's TEST computer software. As each of the five molecules are "new", very little data is available regarding their toxicity. The experimental data that was available showed that each candidate was less toxic than toluene. An assessment of structural analogues and predictive methods suggested each candidate would be overall less toxic than toluene which was hugely promising. In addition, the Ames test showed that each candidate was non-mutagenic (ethyl isobutyrate was not tested). The metrics toolkit showed that the synthesis of methyl butyrate and ethyl isobutyrate can potentially be produced in a very green process. The three proposed routes to TMTHF were also found to be green, potentially using bio-based platform molecules. The synthesis of methyl pivalate and pinacolone is less simple and their greenness will be dependent upon how well the carbonylation of isobutene can be carried out, for which there is no data available at present. A fourth assessment category was developed in this project which assessed the suitability of each candidate for use in Nitto's polymerisation and coating process and took factors specific to the process into account, such as solvent recovery, carbon emissions, flammability and odour. Methyl butyrate was found to have a particularly unpleasant odour and ethyl isobutyrate was unable to facilitate the radical-initiated polymerisation which may limit their use in the future.

Several observations were made regarding molecular design and solvent selection in this project. Computer-aided molecular design was utilised, during which a limitation was encountered. The software was unable to generate a subcategory of ethers which have been called "quaternary ethers". Quaternary ethers were discovered to have excellent potential for use as solvents due to their inability to form peroxides, unlike traditional ethers such as THF and diethyl ether, even under extreme conditions. This suggests that while computer-aided molecular design is useful as a guideline in the discovery of new molecules, it should not be completely relied upon for product

development. Chemical intuition is difficult to program into computer software so manual screening processes should also be carried out in tandem with computer-aided molecular design.

Trends could be seen among the ketone, ester and furan families of molecules (with no other functionality) that could assist in future molecular design projects.

1. Polarity decreased (HSPs approached 0) with the addition of alkyl groups to esters, ethers and ketones.
2. Adding methyl groups to an unsubstituted furan ring increases the boiling point. However, unlike esters and ketones, its polarity increased according to HSP.
3. Increased branching of alkyl chains in esters and ketones resulted in lower boiling point and lower polarity than their linear equivalents with the same number of carbon atoms, *e.g. tert*-butyl acetate and *n*-butyl acetate. The boiling point of *tert*-Butyl acetate is 96 °C, while the boiling point of *n*-butyl acetate is 126 °C. Additionally, *tert*-butyl acetate is less polar.
4. For esters, the carboxylate side of the ester tended to have more influence on the ability to dissolve natural and synthetic rubbers than the alcohol side, *e.g.* the C6 ester with a C3 carboxylate group, propyl propionate, could not dissolve either rubber whereas the C5 ester with a C4 carboxylate group, methyl butyrate, could dissolve natural rubber. The limit for carboxylate groups appeared to be C4: butyrates and isobutyrates.
5. The HSPs of esters and ketones (Figure 2.9 and 2.12) show that esters which are within the boiling point range (< 111 °C) of this work have a lower dipole, but higher hydrogen-bonding ability than ketones.

In the assessment of greenness in this project (Chapter 5), TEST predictive software was employed to provide predictions of toxicity at the end of the solvent selection process. This could also have been included as part of the initial solvent selection process (Chapter 2). However, due to the complex nature of toxicity, exposure and uptake, inaccuracies with predictions were apparent. Therefore, it was decided not to rely on toxicity predictions early in the screening process to reduce the likelihood of a potentially safe solvent being wrongly eliminated from candidacy.

6.2 Future work

Although excellent conversion and selectivity for TMTHF has already been achieved in a pseudo-flow system, where starting material can be constantly added into the reactor while the product evaporates, further investigations into the catalyst behaviour, optimisation of catalyst loadings

and Si/Al ratios (to optimise catalyst reusability), and improved process design (to improve efficiency) would form part of any future work from this project.

Alternative routes to TMTHF using a bio-based diene (DHN) which is produced by Gevo have also been proposed in this work. It has been shown that DHN can be hydrated to yield TMTHF, but this procedure is far from optimised. Continuous flow in the gas phase is a particularly promising possibility, and optimisation of this route would be of interest for this project going forward. Alternatively, DHN can be oxidised to form a polyperoxide which can subsequently be hydrogenated to produce DHL. DHL can in turn can be ring-closed to yield TMTHF. This process has also not been optimised and its development could potentially be a very easy and green route to TMTHF.

An alternative chemocatalytic route to DHN would be hugely significant due to the difficulties in pre-treating biomass before fermentation. Two approaches to this have been identified: by producing isobutanol or isobutyraldehyde from a non-fermentation source, such as by the carbonylation of waste glycerol, similar to the synthetic route to isobutyric acid and butyric acid described previously; or by sourcing DHN directly by chemo-catalytic means. The discovery of this would not only be valuable for the production of TMTHF, but also hugely significant for the production PET, which is produced on the millions of tonnes scale annually.

To date, an equally high yielding synthesis of pivalic acid, the precursor to methyl pivalate and pinacolone respectively, from isobutene and CO has not been reported. Yields of 90% using strong acid catalysts have been reported in the literature but there is great potential to improve upon these yields using regioselective metal-catalysed carbonylation. Selectivity for tertiary-carboxylic acids and esters from alkenes using metal catalysts has not been reported to date. If this could be achieved it would not only be of significant benefit to the production of methyl pivalate and pinacolone, but also to the wider chemical industry. As such, regioselective metal-catalysed hydroesterification would form an interesting project to follow-up the work reported in this thesis.

Finally, full toxicity testing would be required for all candidates before registration with REACH for production of over 1 tonne per annum.

7 Experimental

7.1 Materials and equipment

7.1.1 Materials

2,5-dimethyl-2,5-hexanediol 97%, methanesulfonic acid ≥99%, Y zeolite, KSF montmorillonite, K10 montmorillonite, Nafion SAC-13, butanoic anhydride 98%, 1-butanol 99%, 4-phenylbutanoic acid 99%, benzyl bromide 98%, benzyl chloride 99%, Magnesium chips 99.98%, 2-butanone ≥99%, anhydrous 2-methyltetrahydrofuran ≥99%, dimethyl sulfoxide 99.9%, 1,4-dioxane 99.8%, toluene 99.9%, para-cymene 99.9%, inhibitor-free anhydrous cyclopentyl methyl ether ≥99.9%, inhibitor free anhydrous tetrahydrofuran ≥99.9%, inhibitor-free anhydrous 2-methyltetrahydrofuran ≥99.9%, Nile red ≥99%, 4-nitroaniline ≥99%, and chloroform-d (CDCl3, 99.8% D) were purchased from Sigma-Aldrich. H-BEA Zeolites were supplied by Clariant. ZSM-5 zeolites were supplied by RS Minerals. K30 montmorillonite was supplied by Fluka. Benzylamine ≥98%, was purchased from Alfa Aeser. Chlorobenzene ≥99% was purchased from Acros Organics. Tetrahydrofuran 99.9% was purchased from VWR. Diethyl ether 99.9%, dimethylformamide 99.9%, and sulfuric acid 95% d=1.83 were purchased from Fischer. QUANTOFIX® Peroxide 100 was purchased from Macherey-Nagel. Ames MPF 98/100 kits, 2-nitrofluorene and 4-nitroquinoline-N-oxide were purchased from Xenometrix. TA98 and TA100 were stored at -70 °C. Anhydrous potassium carbonate was purchased from Fisher Scientific. *N,N*-diethyl-4-nitroaniline was purchased from VWR.

7.1.2 GC-MS analysis

A gas chromatograph-mass spectrometry (GC-MS) proceeded on a Perkin Elmer Clarus 500 GC along with a Clarus 560 S quadrupole mass spectrometer. The equipment was equipped with a DB5HT capillary column (30 m×250 μm×0.25 μm nominal, max temperature 430 °C). The carrier

gas utilised in GC-MS was helium with flow rate at 1.0 mL/min, and the split ratio used was 10:1. The injector temperature was 330 °C. During the GC-MS test, the initial temperature of the oven was at 50 °C for 4 minutes. After that, the temperature increased with a rate of 10 °C/min to 300 °C and held for 10 minutes. The Clarus 500 quadrupole mass spectrum was conducted in electron ionisation (EI) mode at 70 eV with the source temperature and the quadrupole both at 300 °C. The m/z mass scan was in the range of 40 to 640 m/z. The data was collected by the PerkinElmer enhanced TurboMass (Ver. 5.4.2) chemical software. Each GC-MS sample consisted of 20-40 mg product mixture and 1.5 mL DCM or acetone as GC-MS solvent.

7.1.3 1H NMR and 13C NMR analysis

The ^{1}H NMR and ^{13}C NMR spectra in this work were recorded by a JEOL JNM-ECS 400 MHz spectrometer. 16 scans were used for ^{1}H NMR analysis, and 256 scans were used for ^{13}C NMR spectroscopy. The NMR data was processed and analysed by ACD/NMR Processor Academic Edition software (Ver. 12.01).

7.1.4 UV vis. Analysis

The UV vis. spectra were recorded on a JENWAY, 6705 UV/Vis. spectrophotometer in quartz cuvettes at 25 °C.

7.1.5 GC-FID analysis

An Agilent 6890N gas chromatograph with a flame ionisation detector (GC-FID), fitted with a ZB-5HT capillary column (30 m x 250 μm x 0.25 μm nominal, max temperature 400 °C) was used in this work. Helium was used as the carrier gas at a flow rate of 2 mL min^{-1} with a split ratio of 30:1. The initial oven temperature was 40 °C which was held for 1 minute at which point it was increased at a rate of 10 °C/min to 300 °C. Injection temperature was 250 °C and the detector temperature was 300 °C.

7.2 Experimental procedures

7.2.1 General experimental procedures

Peroxide testing

Analysis of peroxide formation was carried out using a peroxide test strip (Macherey-Nagel, QUANTOFIX Peroxide-100). A drop of the test solvent was placed on the test pad of the test strip and allowed to evaporate. Upon evaporation, a drop of water was added to the test pad. The concentration of peroxide present (in ppm) in the solvent was determined by comparing the

colour of the test pad with the peroxide colorimetric card. No colour change indicated no peroxide present. The colour change in the test strips for each solvent at different time intervals can be seen in Tables 3.1 and 4.2.

5 mL of solvent was added to a wide necked 50 mL round-bottomed flask and stirred on a stirrer hot plate. A constant flow of air was bubbled through a syringe with the tip submerged in the test solvent, connected to a compressed air tap via the neck of the flask. UV light (254 nm) was provided using a UVP 95-0007-06 Model UVGL-58 Handheld 6 W UV Lamp, 254/365 nm Wavelength, 115V UV lamp placed above the wide neck of the flask to allow direct irradiation over a three-hour period. Control experiments were carried out by testing each solvent for peroxide formation after three hours without UV irradiation or bubbling air. Tables 3.1 and 4.2 show the peroxide formation in ppm, determined by comparing against the colorimetric card.

TMTHF was further tested under reflux and irradiated with light delivered directly to the sample by a fibre-optic cable which was passed through a septum in a three-necked round-bottomed flask. A condenser was fitted in the middle neck while air was bubbled through a syringe via a septum in the third neck. The light source was a Xenon ILC-302UV lamp. The results of the test of TMTHF under reflux is shown and labelled as such.

Kamlet-Taft solvatochromic parameters testing

The KT parameters were measured by dissolving *N,N*-diethyl-4-nitroaniline (NN) and 4-nitroaniline (NA) dyes in the test solvent (TS) and scanning on the UV vis. spectrophotometer to determine λ_{max}(NA) and λ_{max}(NA). π^* and β were then calculated using equation 1.3 and 1.6 respectively.

The $\lambda_{Baseline\ eq.}$ represents the λ_{max} predicted by a baseline of non-hydrogen-bonding solvents. Deviations from this baseline are proportional to β. Equation 7.1 shows baseline used in this work to find β was that which was determined by Sherwood *et al.*[53] R^2 is shown in Equation 7.2.

Equation 7.1 $$y = 1.0025x + 3.4426$$

Equation 7.2 $$R^2 = 0.9945$$

HSPiP software predictions

HSPiP (4th Edition 4.1.04) is computer modelling software which can predict the Hansen solubility parameters (HSPs) of an inputted molecule. HSPiP was employed to calculate the HSPs of the five candidates which are shown in Figure 3.7 in relation to other common solvents.

ArgusLab surface mapping

ArgusLab (obtainable at http://www.arguslab.com/arguslab.com/ArgusLab.html) is a free software which can be used for molecular modelling and graphics. In this work, ArgusLab was used to map the surface electrostatic potential (ESP) of a selection of molecules. The molecular geometry was optimised using the Austin Model 1 (AM1) and a restricted Hartree-Fock (RHF) calculation.

Ames testing

The experiment procedure was based on manufacturer's guidelines. TA98 and TA100 were tested at 6 different concentrations (0.16 mg/mL, 0.31 mg/mL, 0.63 mg/mL, 1.25 mg/mL, 2.5 mg/mL, 5 mg/mL) of each candidate dissolved in DMSO (TMTHF was dissolved in ethanol due to immiscibility with ethanol), as well as a positive (2 μg/mL of 2-nitrofluorene (2-NF) and 0.1 μg/mL of 4-nitroquinoline-N-oxide (4-NQO)) control and a negative solvent control (DMSO or ethanol depending on the sample). The bacterial strains were allowed to grow for 90 minutes in a medium containing enough histidine to conduct about two cell divisions. After exposure, the cultures were diluted in pH indicator medium without histidine and then aliquoted into 48 wells of a 384-well plate. After 48 hours at 37 °C, a colour change from purple to yellow was observed in wells containing bacteria which underwent reversion to His^+. The number of yellow wells were counted manually for each dose to obtain the average value. A spreadsheet which accompanies the Ames test kit generates the results and plots the graphs shown in Figures 3.15 and 4.8.

Determination of octanol/water partition coefficient (Log $P_{(o/w)}$)

Determination of the log $P_{(o/w)}$ was done by the shake flask method. 1 mL each of octanol and water were mixed in a 2.5 mL vial. 60 μL of the test sample was added and the mixed was shaken for 30 seconds and allowed to stand for at least 1 hour. Samples (50 μL) were taken from both the aqueous and organic layers and dissolved in a standard GC solution (1 mL). The standard solution was made by adding cumene (20 μL) as internal standard (IS) to methanol (20 mL). GC-FID was run according to the method described. Log $P_{(o/w)}$ was obtained using Equation 7.3.

Equation 7.3

$$Log\ P_{(o/w)} = \frac{Area(sample)_o}{Area(sample)_w} \frac{Area(IS)_w}{Area(IS)_o}$$

Water saturation determination

Water and solvent (1 mL each) were added to a 2.5 mL vial, shaken for ~10 seconds and allowed to stand for 24 hours. Karl-Fischer titration was used to measure the water content of the organic layer. Values were taken as the average of samples from three different water/organic solvent mixtures.

7.2.2 Solubility tests

To a known mass of polymer/rubber was added a calculated volume of the chosen solvent in a 25 mL vial. The vials were placed on a roller mixer (Stuart SRT6) and stirred for 1 week or until dissolution occurred. The solubility of each polymer/rubber-solvent mixture was scored by observation.

Dried polymer was added to vials from ethyl acetate solutions by pouring ~10 mL of the polymer solution into a pre-weighed 25 mL vial. Solvent was removed by placing the vial containing the polymer solution in a vacuum oven at 60 °C and 100 mbar for 72 hours. The mass of dried polymer was determined by weighing and subtracting from the pre-weighed vial. Solid bases of each polymer/rubber-solvent mixture are shown in Table 7.1.

Table 7.1. Solid bases of each polymer/rubber-solvent mixture in the solubility tests.

Polymer/rubber	Solid base / %
P1	30
P2	50
P3	60
P4	40
R5	20
R6	20

7.2.3 Catalyst screening for the synthesis of 2,2,5,5-tetramethyltetrahydrofuran (TMTHF) from 2,5-dimethyl-2,5-hexanediol

The chosen catalyst (50 mg for solid catalysts, 0.9 mmol for liquid catalysts) was added to molten 2,5-dimethylhexane-2,5-diol (5 g, 34.0 mmol). The reaction mixture was stirred and heated to 110 °C on a heating plate for 90min. Yields and conversions were calculated by ^{1}H NMR.

[TMTHF]. ^{1}H NMR (400 MHz, $CDCl_3$): δ 1.81 (s, 4H), 1.21 (s, 12H); ^{13}C NMR (400 MHz, CDCl3): δ 29.75, 38.75, 80.75; IR 2968, 2930, 2968, 1458, 1377, 1366, 1310, 1265, 1205, 1144, 991, 984, 885, 849, 767 cm^{-1}; *m/z* (%): (ESI–MS) 128 (40) [M^{+}].

[DHN (2,5-Dimethyl-2,4-hexadiene)] ^{1}H NMR (400 MHz, $CDCl_3$): δ 5.94 (s, 2H); ^{13}C NMR (400 MHz, $CDCl_3$): δ 132.21, 121.31, 26.30, 18.05.

[DHN2 (2,5-Dimethyl-1,5-hexadiene)] ^{1}H NMR (400 MHz, $CDCl_3$): δ 4.68 (s, 4H); *m/z* (%): (ESI–MS) 110 (50) [M^+].

[DHN3 (2,5-Dimethyl-1,4-hexadiene)] ^{1}H NMR (400 MHz, $CDCl_3$): δ 4.84 (t, 1H), 4.65 (m, 2H); *m/z* (%): (ESI–MS) 110 (12) [M^+].

[HNL (2,5-Dimethyl-4-hexen-2-ol)] ^{1}H NMR (400 MHz, $CDCl_3$): δ 5.24 (t, J = 7.79, 1H), 2.18 (d, J = 7.79, 2H), 1.75 (s, 6H), 1.64 (s, 6H); 13C NMR (400 MHz, $CDCl_3$): δ 135.21, 119.68, 71.39, 42.10, 26.11, 17.95; *m/z* (%): (ESI–MS) 128 (25) [M^+].

[DHL (2,5-Dimethyl-2,5-hexanediol)] ^{1}H NMR (400 MHz, $CDCl_3$): δ 1.53 (s, 4H), 1.18 (s, 12H); ^{13}C NMR (400 MHz, $CDCl_3$): δ 29.35, 39.17, 71.37; IR 3269, 2969, 2950, 2936, 2870, 1470, 1403, 1375, 1365, 1286, 1246, 1200, 1139, 1096 cm^{-1}; *m/z* (%): (ESI–MS) 113 (82), 95 (59), 91 (100), 70 (81), 43 (96) [$(CH_3)_2CCH_2CH_2C(CH_3)_2^+$].

7.2.4 Reactive distillation process for the 1 L scale production and purification of TMTHF

H-BEA zeolite powder (150:1 Si/Al ratio) (1 g) was added to molten 2,5-dimethylhexane-2,5-diol (500 g, 3.42 mol) using a Dean-Stark apparatus. The reaction mixture was stirred and heated. The hot plate temperature setting was set to a sufficient temperature to allow distillation over the Dean-Stark apparatus (130 °C, atmospheric pressure when using the experimental set up of the authors. Note that the Dean-Stark apparatus was insulated with cotton wool in aluminium foil). The product formed as two layers, aqueous and organic. The aqueous layer was discarded, while the clear, colourless organic layer was dried over magnesium sulfate, and distilled a further two times.

7.2.5 Synthesis of 2,2,5,5-tetramethyltetrahydrofuran (TMTHF) via the hydration of 2,5-dimethyl-2,4-hexadiene

2,5-Dimethyl-2,4-hexadiene (0.68 mL, 5.0 mmol) and water (0.90 mL, 50.0 mmol) were added to diglyme (5 mL). Catalyst (0.5 mmol for liquid catalyst, 10 mg for solid catalyst) was added and the mixture was stirred for 18 hours at which time an aliquot was removed and analysed using GC-FID chromatography. Comparison were made with chromatographs of pure TMTHF and 2,5-dimethyl-2,4-hexadiene to identify products. An estimation of conversion was made by integrating the peak areas.

7.2.6 Synthesis of 2,5-dimethyl-2,4-hexadiene (DHN) polyperoxide by the oxidation 2,5-dimethyl-2,4-hexadiene

DHN (5 mL) was added to a 25 mL round-bottomed flask equipped with a condenser and magnetic stirring bead along with TMTHF (0, 5 or 10 mL) and allowed to stirred. Air was bubbled through using a syringe needle connected to a compressed air line.

[2,5-dimethyl-2,4-hexadiene polyperoxide] ^{1}H NMR (400 MHz, $CDCl_3$): δ 5.76-5.65 (s, 2H), 1.40-1.26 (s, 12H).

7.2.7 Amidation kinetic reaction procedure

A solution of of 4-phenylbutanoic acid (0.328 g, 2.0 mmol) in 4 mL of test solvent was pre-heated to 100 °C and benzylamine (0.235 g, 2.2 mmol) was added. The reaction vessel was stirred and heated to 100 °C. Conversion of benzylamine to produce *N*-Benzyl-4-phenylbutanamide was determined by taking NMR samples at various time intervals. The integrations of the benzyamine peak at 3.88 ppm and the *N*-Benzyl-4-phenylbutanamide doublet at 4.44 ppm were inputted into equation 7.4 to find the conversion.

Equation 7.4 $$C_t = \frac{[B]_0}{[A]_0}\left(\frac{\frac{I_P}{H_P}}{\frac{I_B}{H_B}+\frac{I_P}{H_P}}\right)$$

[*N*-Benzyl-4-phenylbutanamide] ^{1}H NMR (400 MHz, $CDCl_3$): δ 7.34-7.12 (m, 10H), 4.45 (d, J = 5.5, 2H), 2.67 (t, J = 7.56, 2H), 2.22 (t, J = 7.33, 2H), 2.01 (qn, J = 7.4, 2H); ^{13}C NMR (400 MHz, $CDCl_3$): δ 172.43, 128.75, 128.51, 128.40, 127.89, 127.57, 125.98, 43.64, 35.88, 35.18, 27.11; *m/z* (ESI–MS) 253.1 (10) [M^+].

7.2.8 Esterification kinetic reaction procedure

A solution of butanoic anhydride (0.967 g, 5.5 mmol) in 4 mL of test solvent was pre-heated to 100 °C and 1-butanol (0.373 g, 5.0 mmol) was added. The reaction vessel was stirred and heated to 50 °C. Conversion of 1-butanol to produce butyl butanoate was determined by taking NMR samples at various time intervals. The integrations of the 1-butanol triplet at 2.92 ppm and the butyl butanoate triplet at 3.34 ppm were inputted into equation 7.4 to find the conversion.

[Butyl butanoate] ^{1}H NMR (400 MHz, $CDCl_3$): δ 4.07 (t, J = 6.64, 2H), 2.28 (t, J = 7.33, 2H), 1.65 (m, J = 7.27, 4H), 1.38 (td, J = 7.40, 2H), 0.94 (dd, J = 7.21, 5.72, 6H); ^{13}C NMR (400 MHz, $CDCl_3$): δ 173.90, 64.12, 36.30, 30.73, 19.17, 18.52, 13.73; *m/z* (%): (ESI–MS) 145.1 (8) $[M^+H]^+$.

7.2.9 Grignard reaction procedure

Magnesium turnings (0.23 g, 9.7 mmol) were placed in a warmed (40 °C), argon-purged three-necked flask equipped with a magnetic stirrer, condenser and dropping funnel, along with a small number of iodine crystals (~57 mg, 0.5 mmol). 1 mL of the chosen solvent was added, and the mixture was stirred and cooled to 0 °C while argon was continuously flowed via a septum. ~1 mL of a benzyl halide solution (9.0 mmol benzyl halide in 10 mL of the chosen solvent) was added to the reaction mixture and allowed to stir for 5 minutes, while being kept at 0 °C. The remaining benzyl halide solution was added dropwise over the course of ~30 minutes. The mixture was stirred for a further 30 minutes at which point a solution of 2-butanone (4.5 mmol 2-butanone in 10 mL of the chosen solvent) was added dropwise over the course of 30 minutes. The reaction mixture was stirred at room temperature for 2 hours at which point a sample was taken for NMR analysis to determine conversion and selectivity. The reaction mixture was then poured onto a solution of ammonium chloride (1 g) in 10 mL water. The products were extracted using diethyl ether (3 x 10 mL), dried using $MgSO_4$ and concentrated in vacuo. The Wurtz, 5, (white powder) and Grignard, 6, (colourless oil) products were isolated by column chromatography using 70:30 hexane/ethyl acetate.

[Grignard product] ^{1}H NMR (400 MHz, $CDCl_3$): δ 7.27 (m, 5H), 2.80-2,71 (dd, J = 13.28, 9.16 Hz, 2H), 1.53-1.48 (q, J = 7.63, 2H), 1.14 (s, 3H), 1.00-0.96 (t, J = 7.56, 3H); ^{13}C NMR (400 MHz, $CDCl_3$): δ 137.69, 130.58, 128.16, 126.40, 72.71, 47.59, 34.20, 25.92, 8.33; *m/z* (%): (ESI–MS) 164.1 (2) [M^+].

[Wurtz product] ^{1}H NMR (400 MHz, $CDCl_3$): δ 7.24 (m, 10H), 2.92 (s, 2H); ^{13}C NMR (400 MHz, $CDCl_3$): δ 141.79, 128.45, 128.34, 125.91, 37.97; *m/z* (%): (ESI–MS) 181.7 (80) [M^+].

7.2.10 Synthesis of Poly (butyl acrylate-co-acrylic acid)

In a 500 mL round-bottom three-necked flask, equipped with a condenser and an overhead stirrer, butyl acrylate (100 g) and acrylic acid (5 g) were mixed together with dibenzoylperoxide (0.382 g), and solvent (26.35 g). The mixture was then purged with nitrogen for at least 1 hour, and subsequently heated to 70 °C and stirred under a nitrogen atmosphere. Solvent (219.54 g) was added dropwise once an exothermic reaction was observed. Finally, the mixture was aged at 80 °C for 4-6 hours until a conversion of at least 95% was reached.

7.2.11 PSA preparation

A pressure sensitive adhesive composition was produced using poly (butyl acrylate-co-acrylic acid). a solution of poly (butyl acrylate-co-acrylic acid) (73.39 g, at a solid content of 27.25%) was

mixed with a polyisocyanate solution (1.07 g, at a solid content of 75%) and a melamine resin solution (0.52 g, at a solid content of 58%). The solid content was subsequently reduced to 20%. This composition was applied with a knife coater at a thickness about 25 μm onto a polyester film and the composition was dried to obtain a pressure sensitive adhesive sheet.

7.2.12 Acid stability tests

TMTHF (5 mL, 48.7 mmol) was added to a 25 mL round-bottomed flask and heated to the desired temperature. Acid (1 mol.%) was added and the mixture was allowed to stir for 24 hours. Degradation was measured using ^{1}H NMR, using either methanol-d4 or toluene-d8 as the solvent.

7.2.13 Differential scanning calorimetry (DSC) analysis

The melting point of TMTHF and DTBE were measured by DSC (TA Instruments, Q2000, V24.10) to be <-90 °C. During the testing, a small sample (~5-10 mg) was hermetically-sealed in a Tzero aluminium DSC pan. The cooling rate was 10 °C/min from 30 °C to –90 °C.

7.2.14 Catalyst screen for the synthesis of methyl butyrate

To a mixture of butyric acid (2.29 mL, 25.0 mmol) and methanol (3.03 mL, 75.0 mmol) preheated to 60 °C was added catalyst (110 mg for solid catalysts and 40 μl for liquid catalysts). An aliquot was removed after 18 hours, dried with magnesium sulfate and filtered using cotton wool and conversion was monitored using GC-FID.

Table 7.2. Calibration sample volume calculation data.

	Methanol	Butyric acid →	Methyl butyrate	Water
ρ / g mL^{-1}	0.792	0.96	0.898	1
M_w / g mol^{-1}	32.04	88.11	102.13	18

Calibration sample	Moles	Moles	Moles	Moles
0	0.075	0.025	0	0
1	0.070	0.020	0.005	0.005
2	0.065	0.015	0.01	0.01
3	0.060	0.010	0.015	0.015
4	0.055	0.005	0.02	0.02
5	0.050	0.000	0.025	0.025

Table 7.2. (Continued).

Yield / %	Volume / mL	Volume / mL	Volume / mL	Volume / mL		Total dry volume / mL
0	3.03	2.30	0.00	0.00	Removed using $MgSO_4$	5.33
20	2.83	1.84	0.57	0.00		5.24
40	2.63	1.38	1.14	0.18		5.14
60	2.43	0.92	1.71	0.27		5.05
80	2.23	0.46	2.28	0.36		4.96
100	2.02	0.000	2.84	0.45		4.87

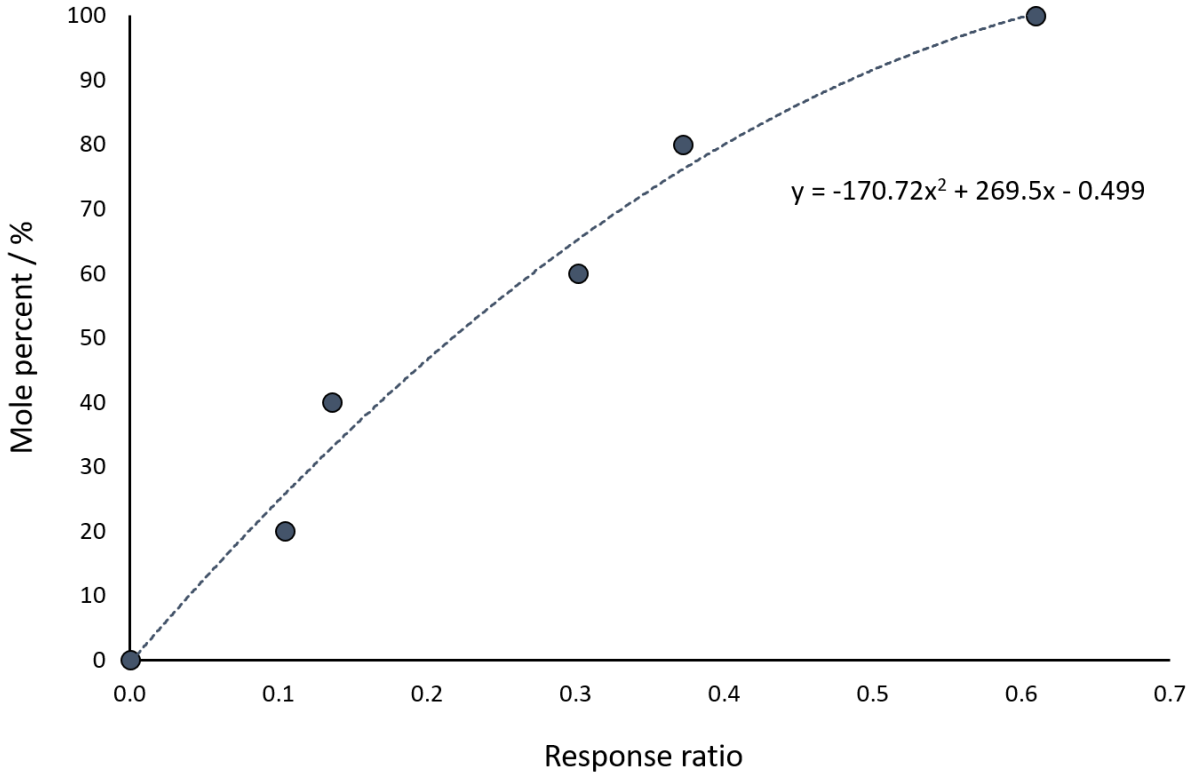

Figure 7.1. Calibration curve and equation for the determination of the yield of methyl butyrate.

A calibration curve was prepared using tetradecane as the internal standard (Figure 7.1). As no solvent was used in the reaction, samples representative of yields of 20%, 40%, 60%, 80% and 100% were prepared using the appropriate amounts of butyric acid, methanol and methyl butyrate (shown in Table 7.2). Water was not added to account for the drying of the aliquots removed from the reaction mixtures prior to GC-FID analysis and hence, the calibration curve is not linear. The relative response factor was calculated using the responses of the IS and methyl butyrate (Table 7.3).

Table 7.3. Table showing the relative response factors for each point of the calibration curve.

Conversion / %	IS Response	Methyl butyrate response	MB/IS
100	5841.15	0	0.000
80	6334.45	650.2	0.103
60	6458.05	1545	0.239
40	6685.7	2533.4	0.379
20	6817.05	3521.7	0.517
0	5915.8	4328.04	0.732

7.2.15 Methyl butyrate and methyl pivalate synthesis using Dean-Stark apparatus

Methanol (12 mL, 0.3 mol) and acid (0.1 mol) were added to a 50 mL two-necked round-bottomed flask equipped with a Dean-Stark apparatus and magnetic stirring bead and heated to reflux. Upon reaching reflux, catalyst was immediately added (440 mg for solid catalysts and 1.9 mmol liquid catalyst). Fresh methanol was added via the second neck of the two-necked flask when 5 mL of a methanol/water/methyl butyrate mixture had distilled from the reaction mixture. The distillate was then released from the trap and this procedure was repeated until full conversion of the acid was achieved. Aliquots were removed from the reaction mixture at various time intervals and analysed by GC-FID. The relative peak areas of the chromatogram were used to assess conversion.

7.2.16 Radical-initiated vinyl polymerisation

In a 500 mL round-bottom three-necked flask, equipped with a condenser and an overhead stirrer, vinyl monomers are mixed together with dibenzoylperoxide (0.382 g, 1.6 mmol). The mixture is then purged with nitrogen for at least 1 hour. Next, the mixture is heated to 70 °C and

stirred under a nitrogen atmosphere. Dropwise addition of solvent takes place once an exothermic reaction can be observed. Finally, ageing of the mixture takes place at 80 °C for 4-6 hours until a conversion of at least 95% is reached.

7.2.17 Menshutkin reaction procedure

1-Methylimidazole (0.328 mL, 4.0 mmol) was added to the chosen solvent (4 mL) and heated to 50 °C. 1-Bromoctadecane (1.503 mL, 4.4 mmol) was added and conversion was monitored by taking samples and various intervals and analysing using ^{1}H NMR spectroscopy.

[1-octadecyl-3-methylimidazolium bromide] ^{1}H NMR (400 MHz, $CDCl_3$): δ 7.28 (s, 1H), 7.23 (s, 1H), 7.20 (s, 1H), 4.28 (t, J = 7.2, 2H), 4.10 (s, 3H), 1.88 (quin, J = 7.6, 2H), 1.68 (s, 3H), 1.30-1.21 (bs, 30H), 0.84 (t, J = 6.9, 3H); ^{13}C NMR (400 MHz, $CDCl_3$): δ 138.62, 123.50, 121.75, 50.75, 37.25, 32.25, 30.25, 29.75, 29.25, 26.50, 23.00, 14.50; IR 3475, 3429, 3083, 3062, 2914, 2849, 1666, 1630, 1573, 1472, 863, 792, 715, 662.

7.2.18 Menschutkin reaction order experiment

1-Methylimidazole (4.0 mmol, 0.328 mL) was added to NMP (4 mL) and heated to 50 °C. 1-Bromoctadecane (1.503 mL, 4.4 mmol) was added and conversion was monitored using ^{1}H NMR spectroscopy at various intervals. Reaction order was determined by plotting 1/[1-octyl-3-methylimidazolium bromide] vs. time.

Appendices

LEL by volume example calculation

A container can hold 1 mole of an ideal gas (22.4 cm^3) and is currently full of air. Toluene and TMTHF are assumed to be ideal gases. The LEL of toluene (1.1%) allows 0.011 moles in the container before an explosive mixture is formed.

- 0.011 moles of toluene = 1.012 g of toluene.
- 1.012 g of toluene = 1.168 mL of toluene allowed in 22.4 L of air.
- = 52.14 µl L^{-1}

The LEL of TMTHF (0.9%) allows 0.009 moles in the container before a risk of explosion.

- 0.009 moles of TMTHF = 1.154 g of TMTHF
- 1.154 g of TMTHF = 1.439 mL of TMTHF allowed in 22.4 L of air.
- = 64.24 µl L^{-1}

64.24 µl L^{-1} TMTHF > 52.14 µl L^{-1} toluene, therefore a larger volume of liquid TMTHF can evaporate into the container before a risk of explosion. Assuming equal volumes of TMTHF and toluene are used to coat the adhesive polymers in Nitto's manufacturing process, fewer moles of TMTHF are available to evaporate into the drying oven and it is less likely to reach its LEL of 0.9%.

This brings into question the usefulness and safety of using LEL as a guide to flammability. Perhaps an adjusted LEL which includes molar mass and density is more appropriate.

CO_2 emissions calculation data.

Table A1. CO_2 emissions data table.

Solvent	Mol (C) cm^{-3} (solvent)	No. of C atoms	Mol cm^{-3} (solvent)	M_w / g mol^{-1}	Density / g cm^3	Mass (C) released cm^{-3} (solvent) / g	Mass (CO_2) released cm^{-3} (solvent) / g	Mass (CO_2) released g^{-1} (solvent) / g
Methyl pivalate	0.045	6	7.5	116.16	0.875	0.543	1.99	2.3
Methyl butyrate	0.044	5	8.8	102.30	0.898	0.527	1.93	2.2
Ethyl isobutyrate	0.045	6	7.4	116.16	0.865	0.537	1.97	2.3
Pinacolone	0.048	6	8.0	100.16	0.801	0.576	2.11	2.6
TMTHF	0.050	8	6.3	128.21	0.802	0.601	2.20	2.7
Toluene	0.066	7	9.4	92.06	0.867	0.792	2.90	3.3
Ethyl acetate	0.041	4	10.2	88.11	0.902	0.492	1.80	2.0

M_w (C) = 12.01 g mol^{-1}; M_w (CO_2) = 44.01 g mol^{-1}

Solute descriptors for Abraham's solvation parameter model.

Table A2. Descriptor values and log KP's for 66 solutes tested for partitioning in a biphasic water/organic solvent system.

Solute	S	A	B	E	V	Log K_P (Toluene)	Log K_P (TMTHF)
2-pentanone	0.680	0.000	0.510	0.143	0.829	1.088	0.858
Benzaldehyde	1.000	0.000	0.390	0.820	0.873	1.852	2.184
3-Hydroxybenzaldehyde	1.370	0.740	0.400	0.990	0.932	-0.203	1.007
4-Hydroxybenzaldehyde	1.540	0.850	0.370	1.010	0.932	-0.609	0.921
Diethyl Ether	0.250	0.000	0.450	0.041	0.731	1.096	0.849
t-Butyl Methyl Ether	0.110	0.000	0.630	0.024	0.872	1.207	1.124
t-Butyl Ethyl Ether	0.190	0.000	0.450	0.000	1.013	1.720	1.601
Diisopropylamine	0.300	0.080	0.690	0.124	1.054	0.771	-0.016
Tetrahydrofuran	0.520	0.000	0.480	0.289	0.622	0.490	0.246
Methyl propionate	0.530	0.000	0.478	0.092	0.747	1.074	0.810
Methyl Formate	0.680	0.000	0.380	0.192	0.465	0.175	0.047
Ethyl Acetate	0.620	0.000	0.450	0.106	0.747	0.315	0.739
Propyl Acetate	0.573	0.000	0.452	0.092	0.888*	1.542	-
n-Butyl Acetate	0.570	0.000	0.470	0.044	1.028*	1.933	-
t-Butyl Acetate	0.540	0.000	0.470	0.025	1.028	1.864	1.215
Butyl Benzoate	0.850	0.000	0.460	0.689	1.495*	2.243	1.605
Diethyl Carbonate	0.560	0.000	0.530	0.061	0.946	1.413	1.172
Propylene Carbonate	1.300	0.000	0.640	0.319	0.697	-0.269	-1.227
Methanol	0.440	0.430	0.470	0.278	0.308	-0.791	-0.054

Ethanol	0.420	0.370	0.480	0.246	0.449	-0.181	-0.042
1-Propanol	0.420	0.370	0.480	0.236	0.590	-0.563	0.251
1-Butanol	0.420	0.420	0.370	0.224	0.731	-0.208	-0.231
i-Butanol	0.360	0.330	0.560	0.217	0.731	-0.436	0.438
t-Butanol	0.360	0.370	0.530	0.200	0.731	-0.610	0.149
1-Hexanol	0.420	0.370	0.480	0.211	1.013	1.174	1.230
Cyclopentanol	0.540	0.320	0.560	0.427	0.763	-0.128	-0.147
Phenol	0.890	0.600	0.300	0.805	0.775	0.535	1.322
m-cresol	0.779	0.672	0.351	0.810	0.916	0.767	1.485
p-Cresol	0.880	0.570	0.340	0.822	0.916	0.833	1.401
Glycerol	0.900	0.700	1.140	0.512	0.707	-1.588	-
Acetic Acid	0.650	0.610	0.440	0.265	0.465	-2.382	-0.999
Propionic Acid	0.650	0.600	0.450	0.233	0.606	-1.206	-0.282
Butyric Acid	0.620	0.600	0.450	0.210	0.747	-0.564	0.471
Benzoic Acid	0.900	0.590	0.400	0.730	0.932	0.499	-
Hexylamine	0.350	0.160	0.610	0.197	1.054	2.292	-
Triethylamine	0.150	0.000	0.790	0.101	1.054	-0.488	-
Aniline	0.960	0.260	0.410	0.955	0.816	0.864	0.566
Pyridine	0.840	0.000	0.520	0.631	0.675	0.321	-0.645
Nitromethane	0.950	0.060	0.310	0.313	0.424	0.252	-
Nitrobenzene	1.110	0.000	0.280	0.871	0.891	2.223	-
2-Nitrophenol	1.086	0.050	0.371	0.962	0.949	2.013	2.122
4-Nitrophenol	1.720	0.820	0.260	1.070	0.949	0.040	1.188
4-Nitroaniline	1.827	0.597	0.343	1.236	0.990	0.849	1.014

1,2-Dichloroethane	0.490	0.100	0.100	0.322	0.635	1.834	1.313
Chloroform	0.490	0.150	0.020	0.425	0.617	1.629	-
Chlorobenzene	0.650	0.000	0.070	0.208	0.839	2.855	1.777
Bromobenzene	0.723	0.000	0.089	0.882	0.891	2.032	1.355
Benzylamine	0.880	0.100	0.720	0.829	0.957	0.491	-0.440
2-propanol	0.360	0.330	0.560	0.212	0.590	-1.025	0.044
Chlorocyclohexane	0.480	0.000	0.100	0.448	0.968	2.421	1.881
Iodomethane	0.430	0.000	0.130	0.676	0.508	1.850	1.699
Dimethylacetamide	1.330	0.000	0.780	0.363	0.647	-2.220	-1.618
Iodobenzene	0.784	0.000	0.135	1.182	0.947	2.344	1.803
Acetonitrile	0.900	0.070	0.320	0.237	0.404	-0.334	-0.326
Octane	0.000	0.000	0.000	0.000	1.258	2.276	2.318
1-Hexene	0.080	0.000	0.070	0.078	0.911	1.733	2.168
1-Octene	0.080	0.000	0.070	0.094	1.193	2.307	1.926
Benzene	0.520	0.000	0.140	0.610	0.716	2.117	2.066
o-Xylene	0.560	0.000	0.160	0.663	0.998	2.155	1.695
3-Hexanone	0.660	0.000	0.510	0.136	0.970	1.172	0.926
Acetophenone	1.010	0.000	0.480	0.818	1.014	1.790	1.003
Butylamine	0.350	0.160	0.610	0.224	0.772	-0.101	-0.702

*Data predicted using ProPred.

NMR spectra

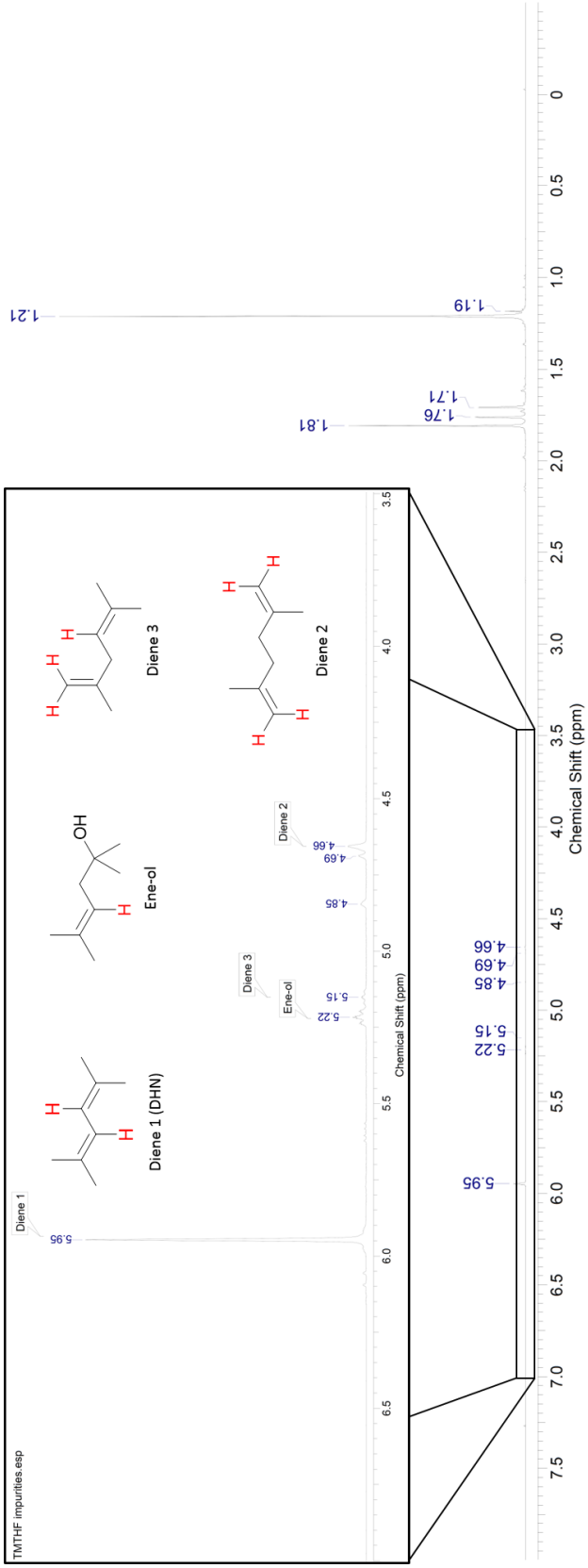

Figure A1. ^{1}H NMR spectrum showing the structures of possible impurities in TMTHF.

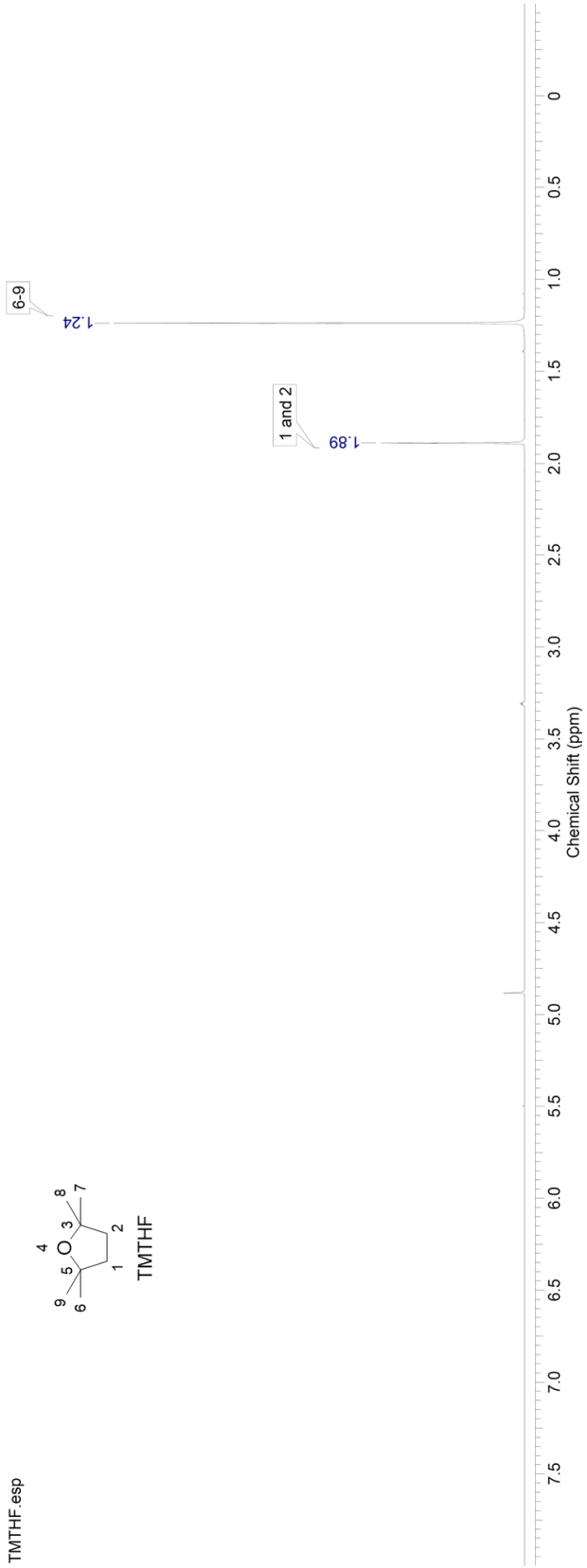

Figure A2. ^{1}H NMR spectrum of TMTHF.

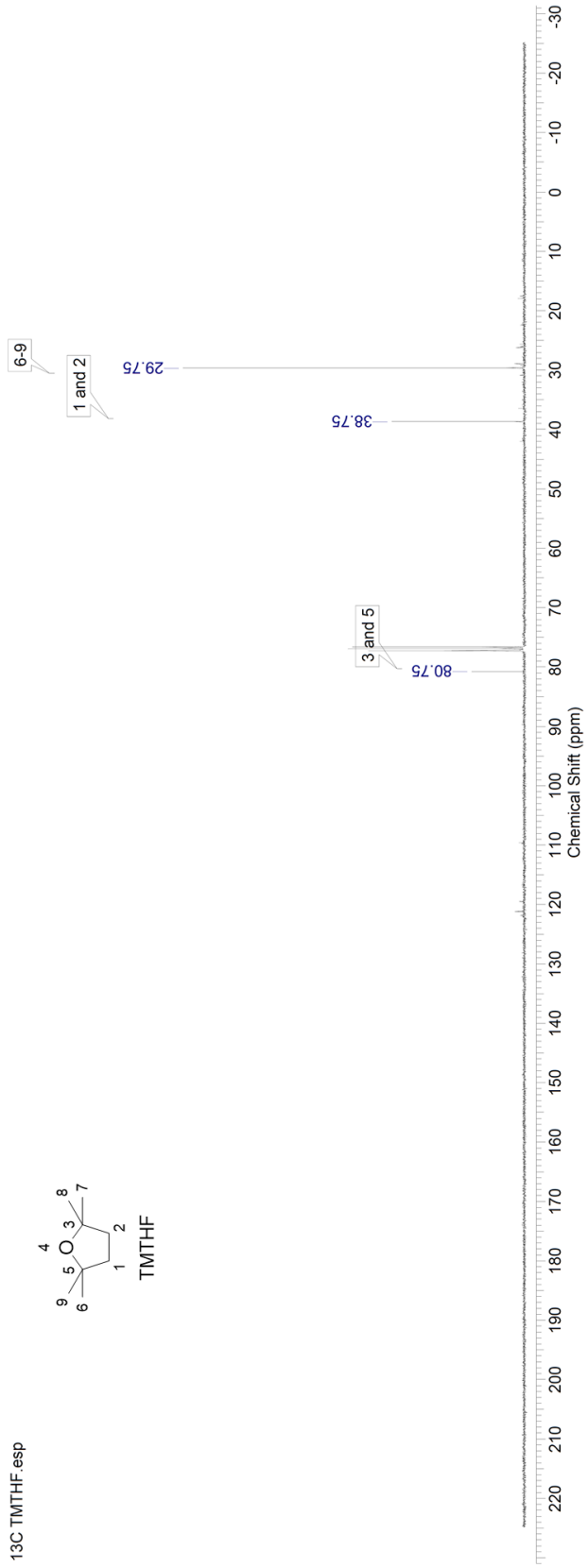

Figure A3. ^{13}C NMR spectrum of TMTHF.

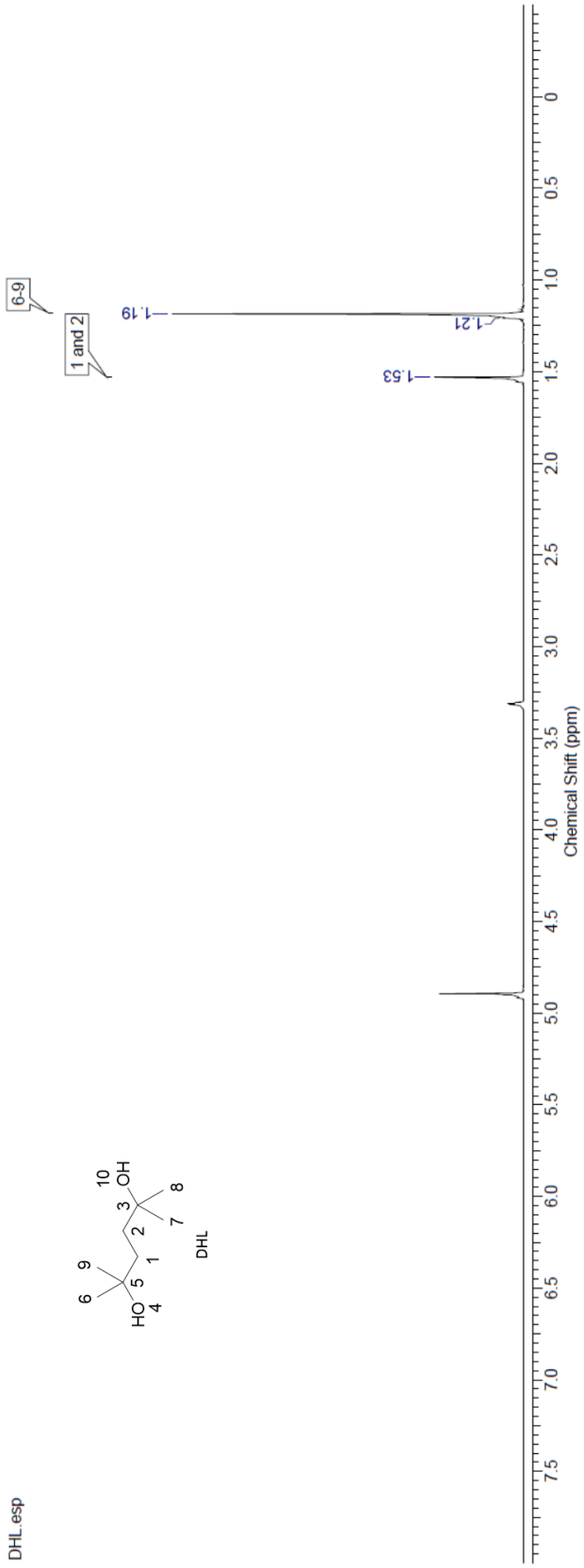

Figure A4. ^{1}H NMR spectrum of DHL.

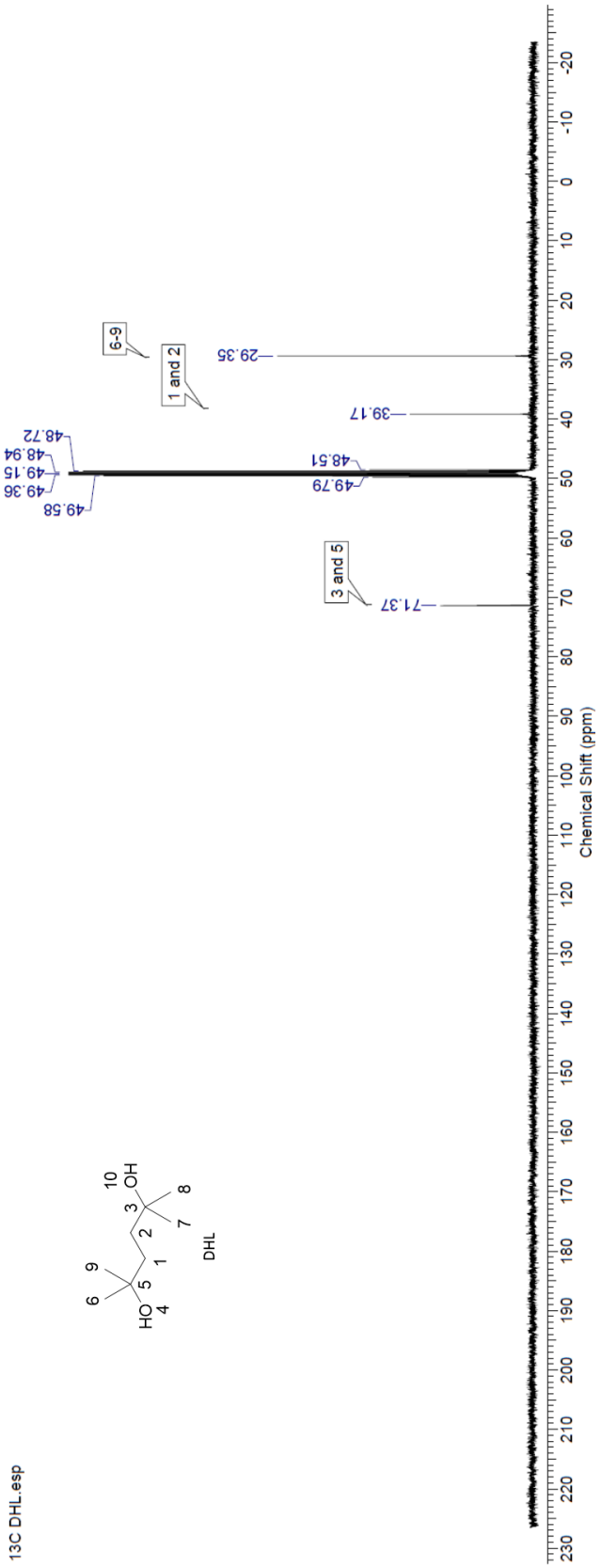

Figure A5. ^{13}C NMR spectrum of DHL.

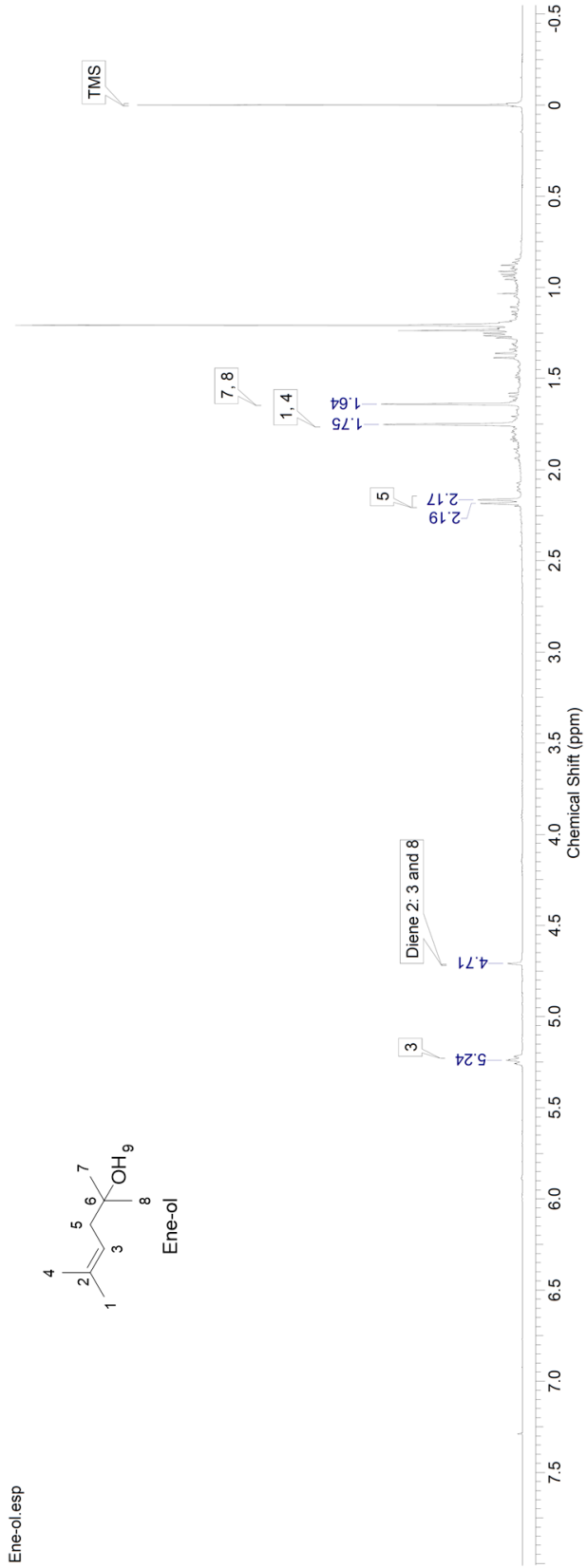

Figure A6. ^{1}H NMR spectrum of HNL.

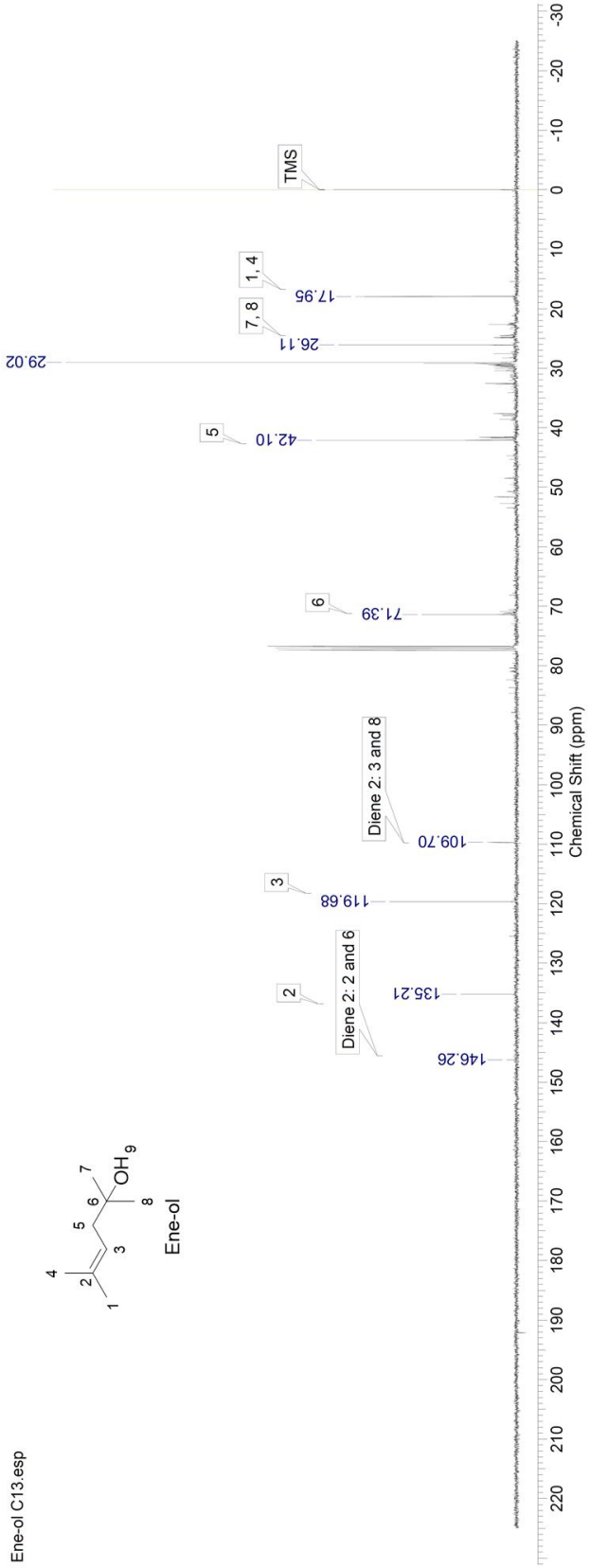

Figure A7. ^{13}C NMR spectrum of the HNL.

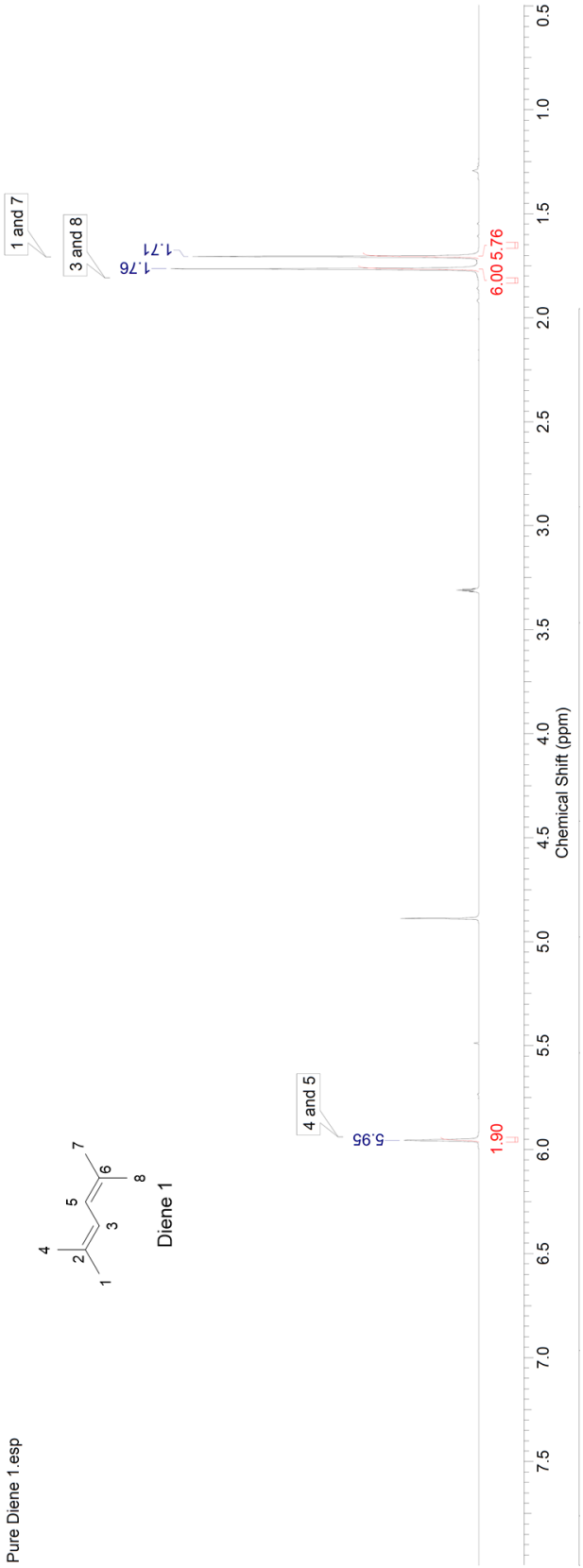

Figure A8. ^{1}H NMR spectrum of DHN.

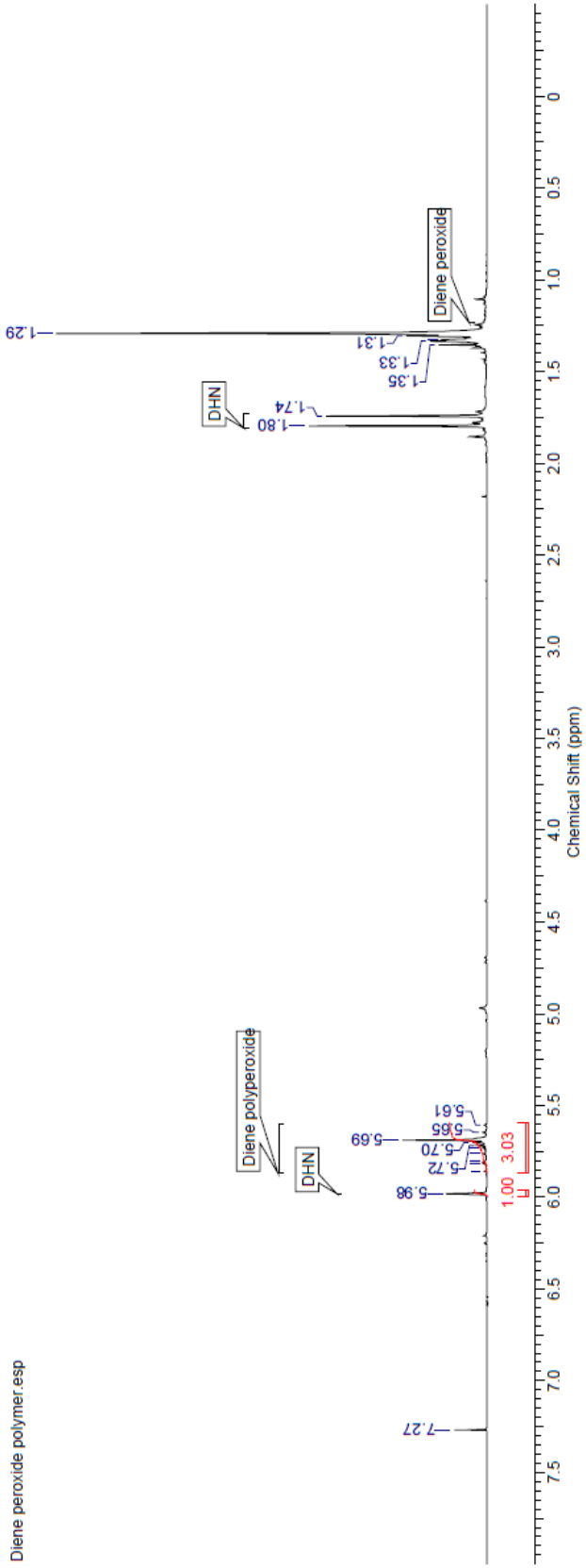

Figure A9. ^{1}H NMR showing the DHN peroxidation after 3 days (no solvent).

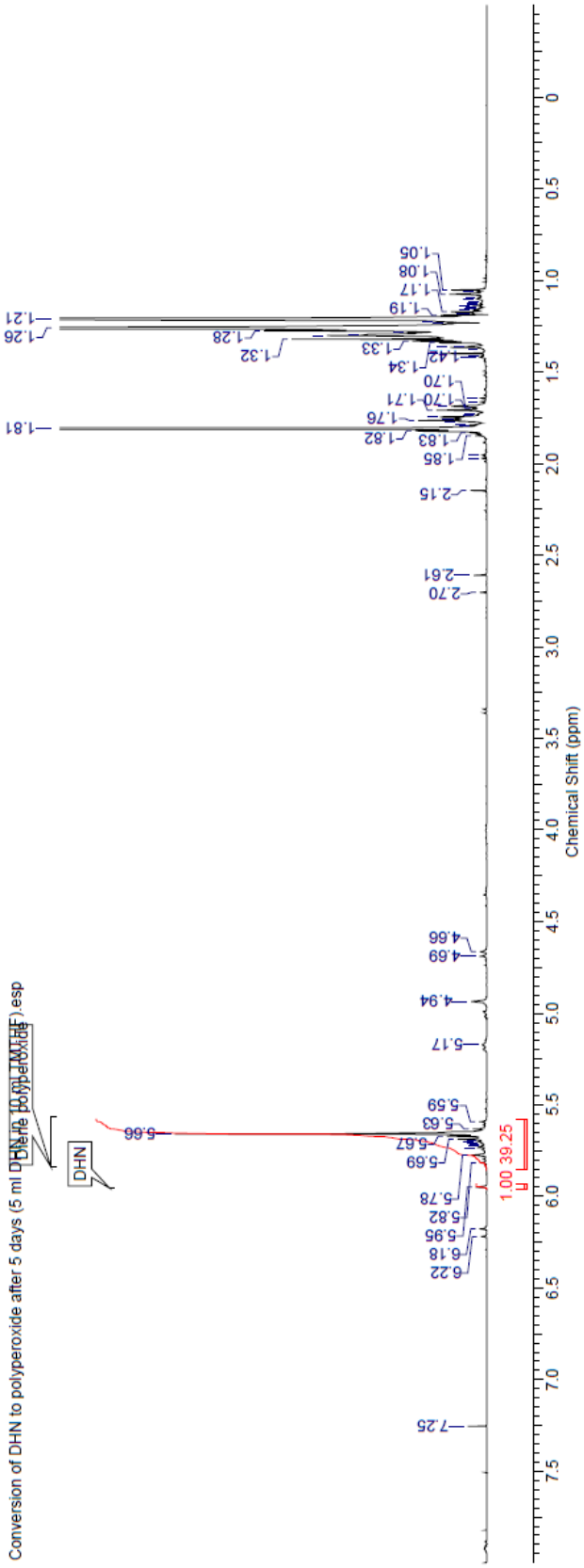

Figure A10. ^{1}H NMR showing the amount of DHN peroxidation after 5 days (5 mL DHN in 10 mL TMTHF).

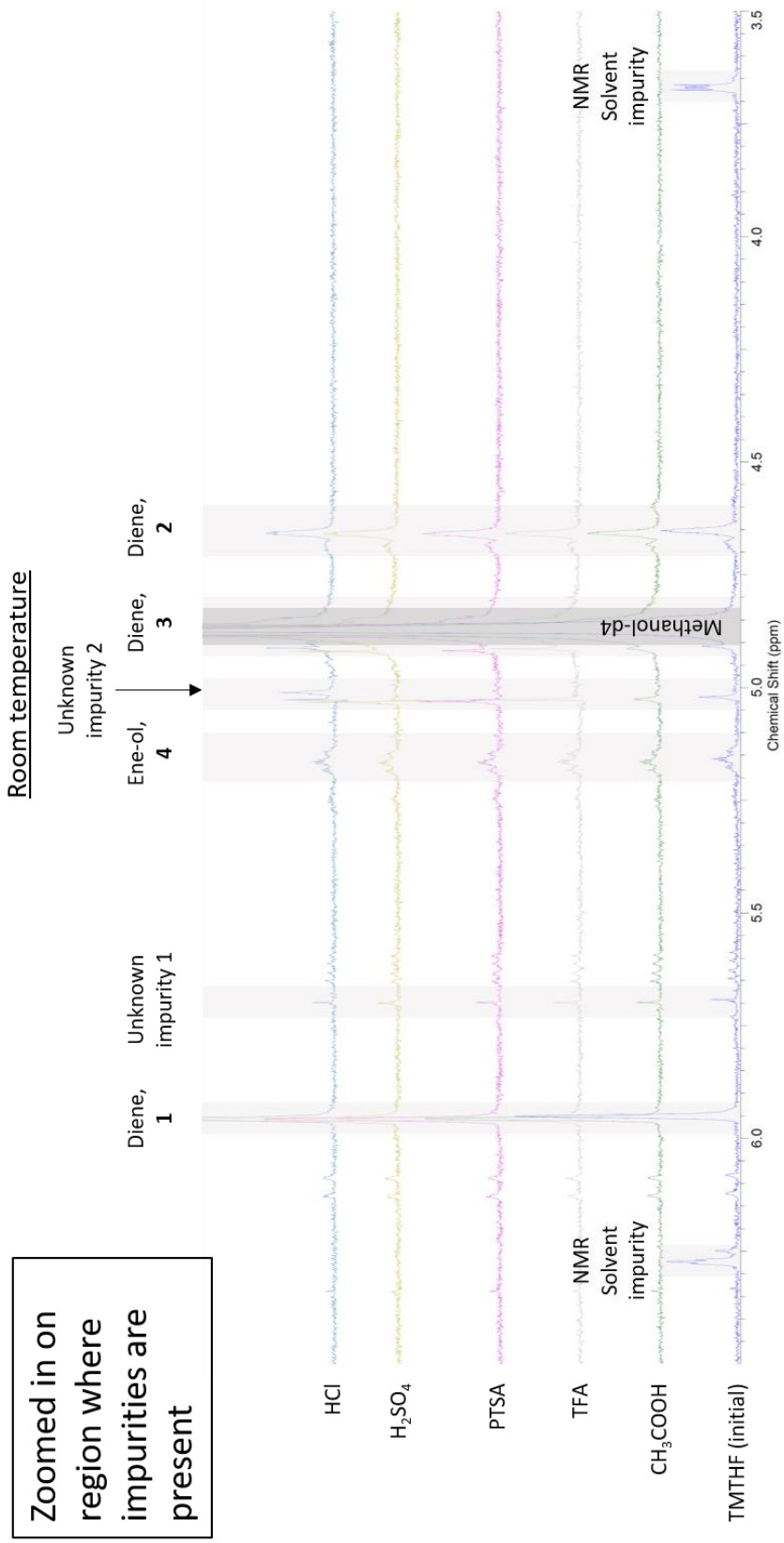

Figure A11. Zoomed in overlayed ^{1}H NMR spectrum showing TMTHF before and after acid tests at room temperature after 24 hours.

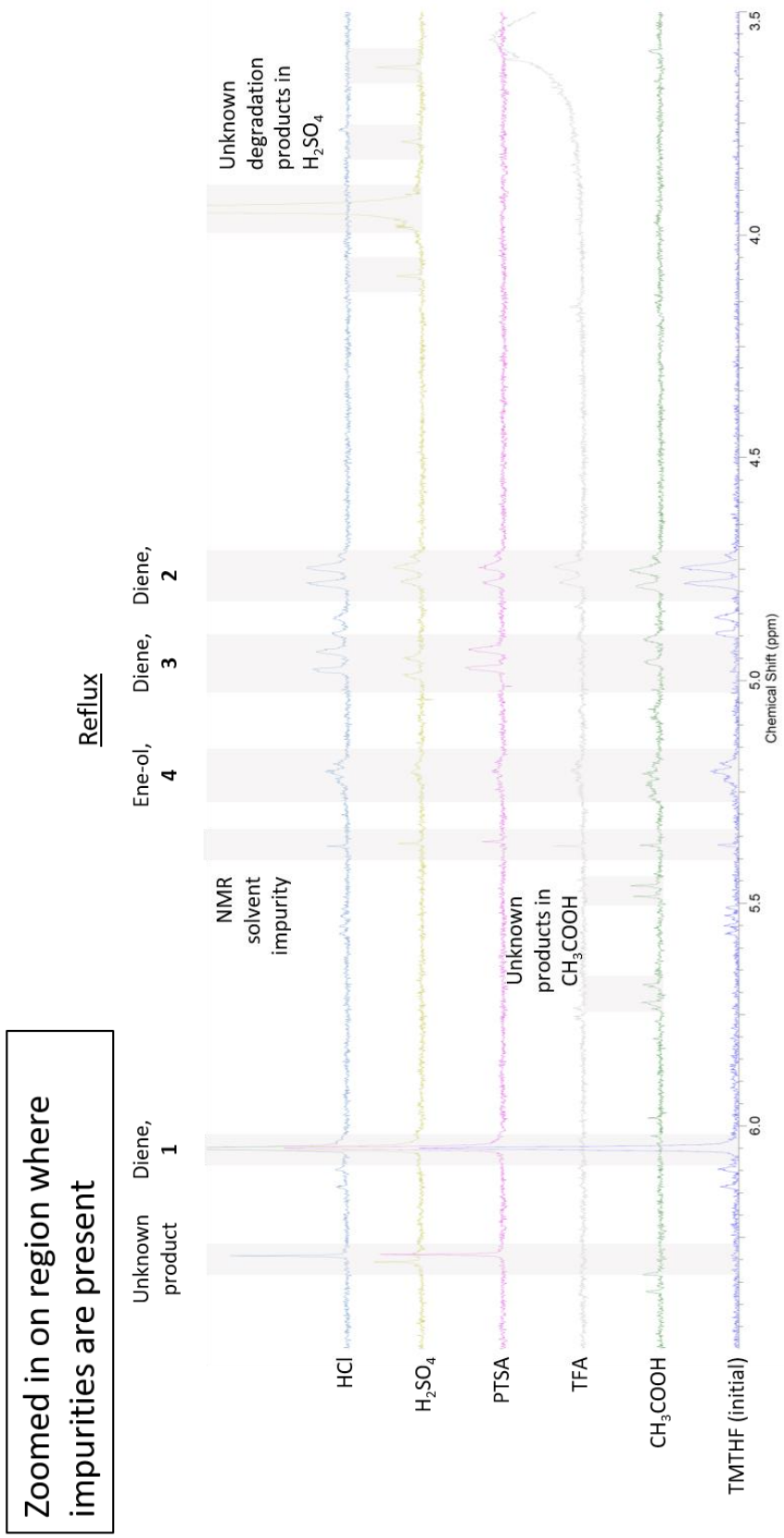

Figure A12. Zoomed in overlayed ^{1}H NMR spectrum showing TMTHF before and after acid tests under reflux (~112 °C) after 24 hours.

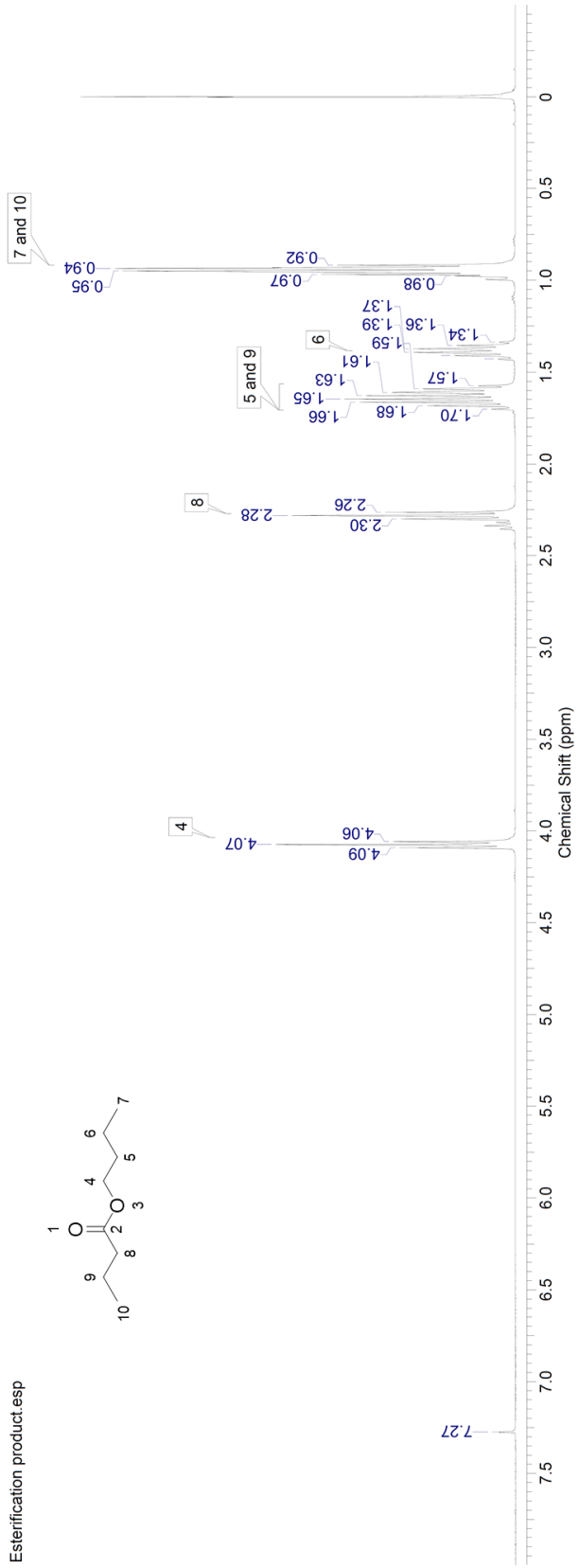

Figure A13. ^{1}H NMR spectrum of the esterification product, butyl benzoate.

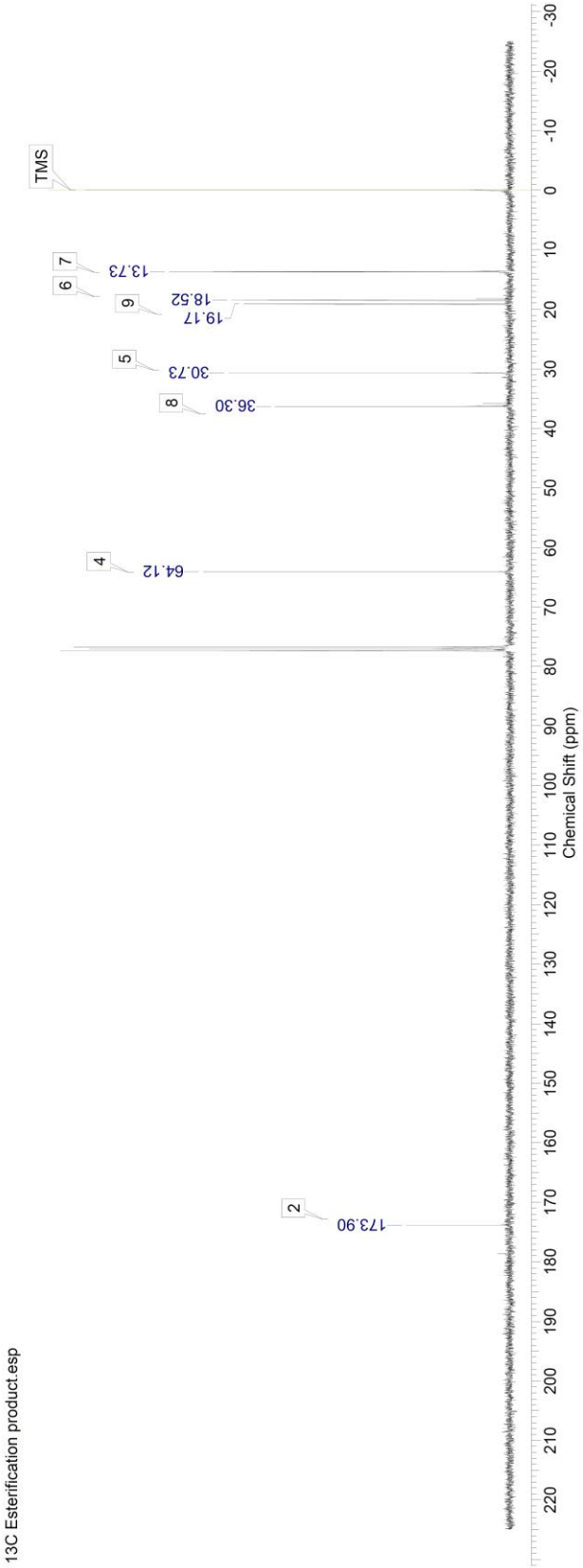

Figure A14. ^{13}C NMR spectrum of the esterification product, butyl benzoate.

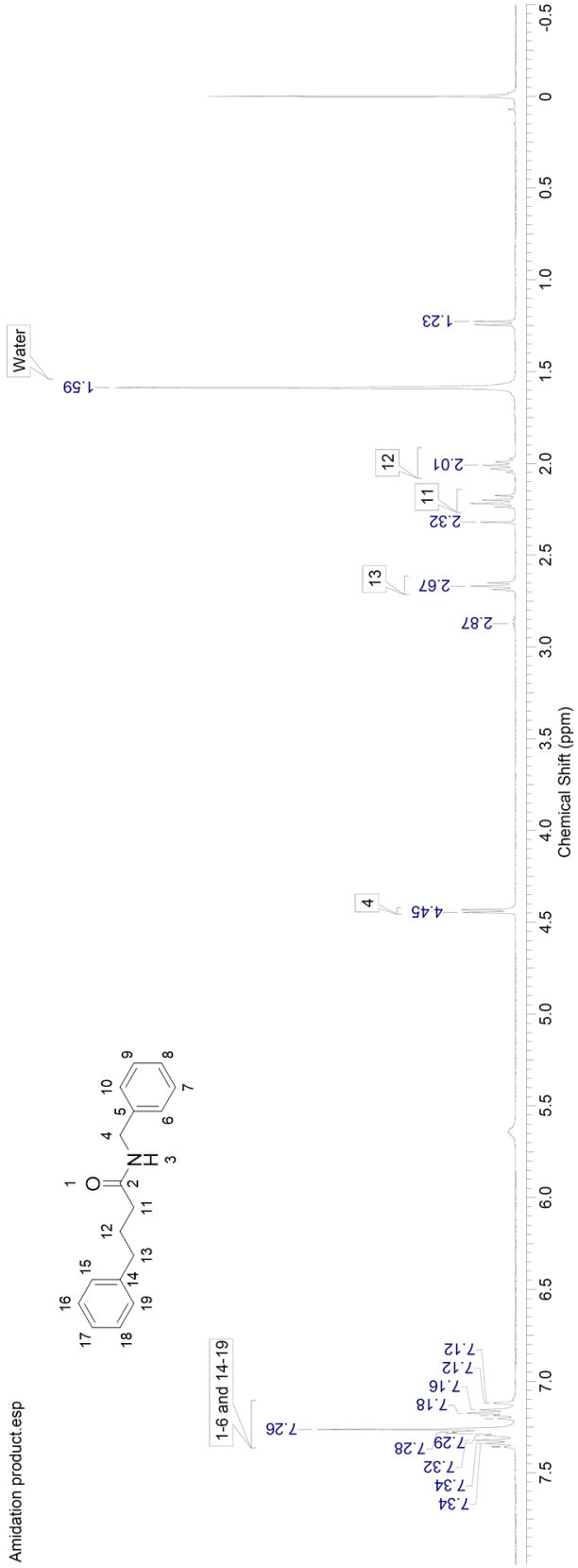

Figure A15. ^{1}H NMR spectrum of the amidation product, *N*-benzyl-4-phenylbutanamide.

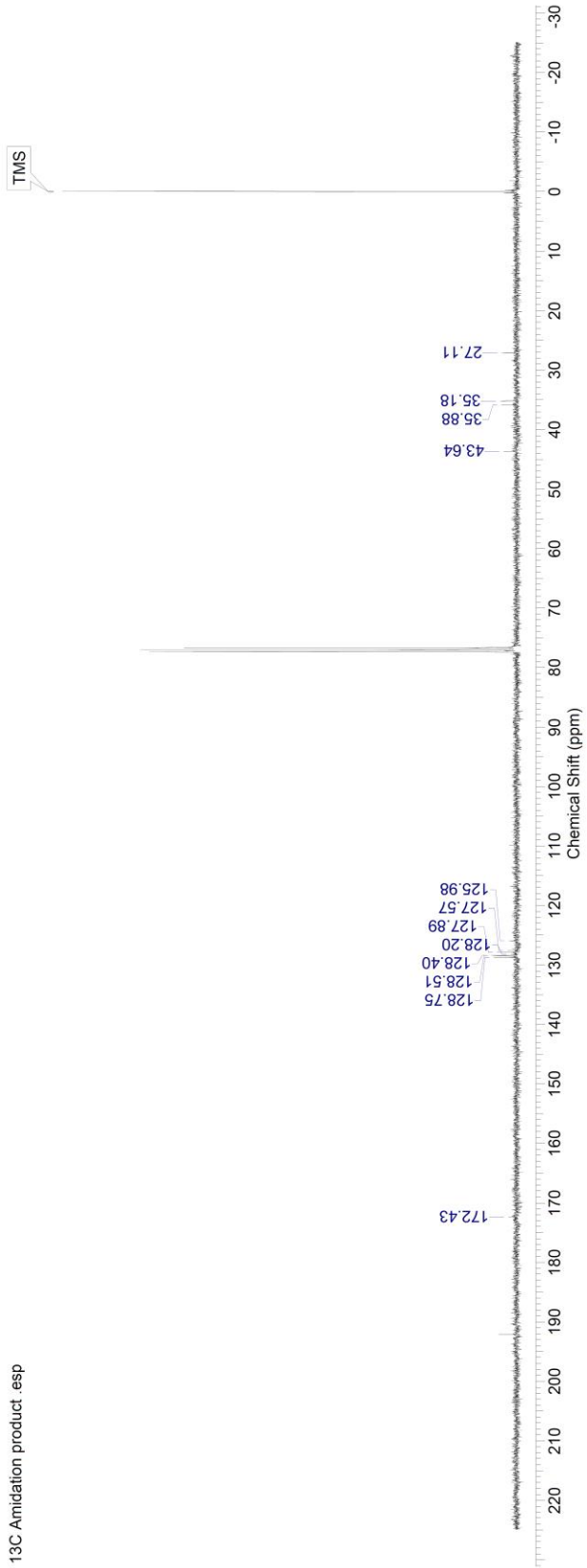

Figure A16. ^{13}C NMR spectrum of the amidation product, *N*-benzyl-4-phenylbutanamide.

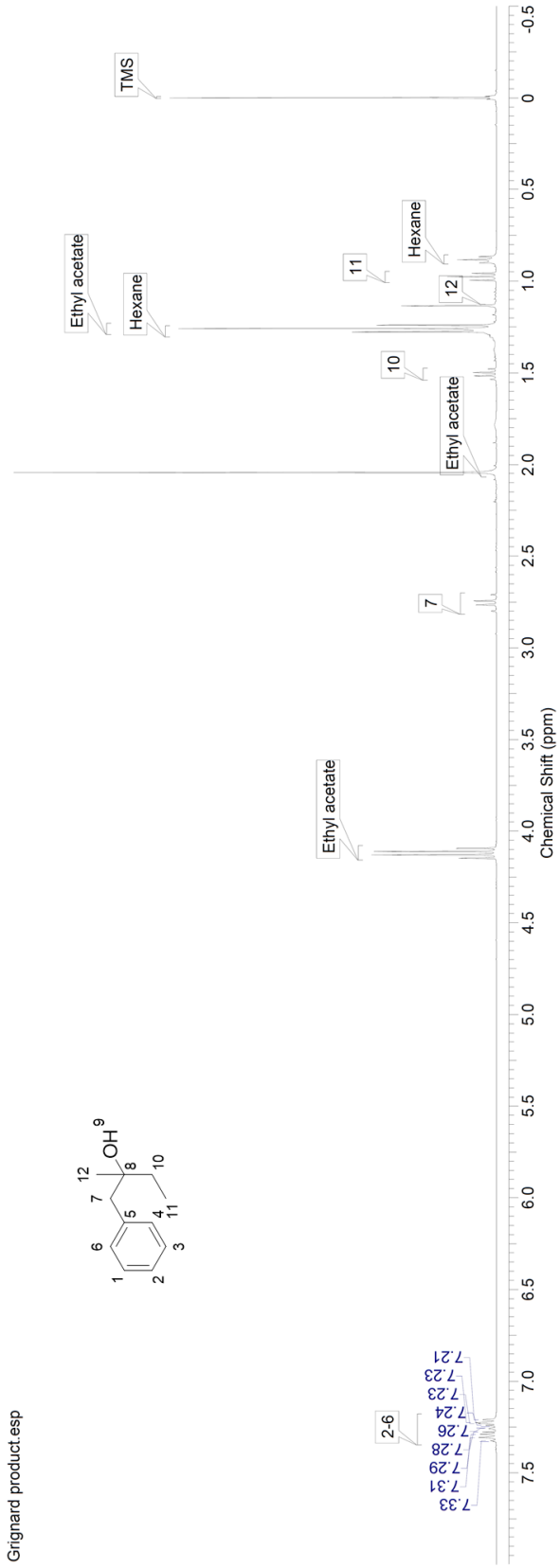

Figure A17. ^{1}H NMR spectrum of the Grignard product, 2-methyl-1-phenyl-2-butanol (**G1**).

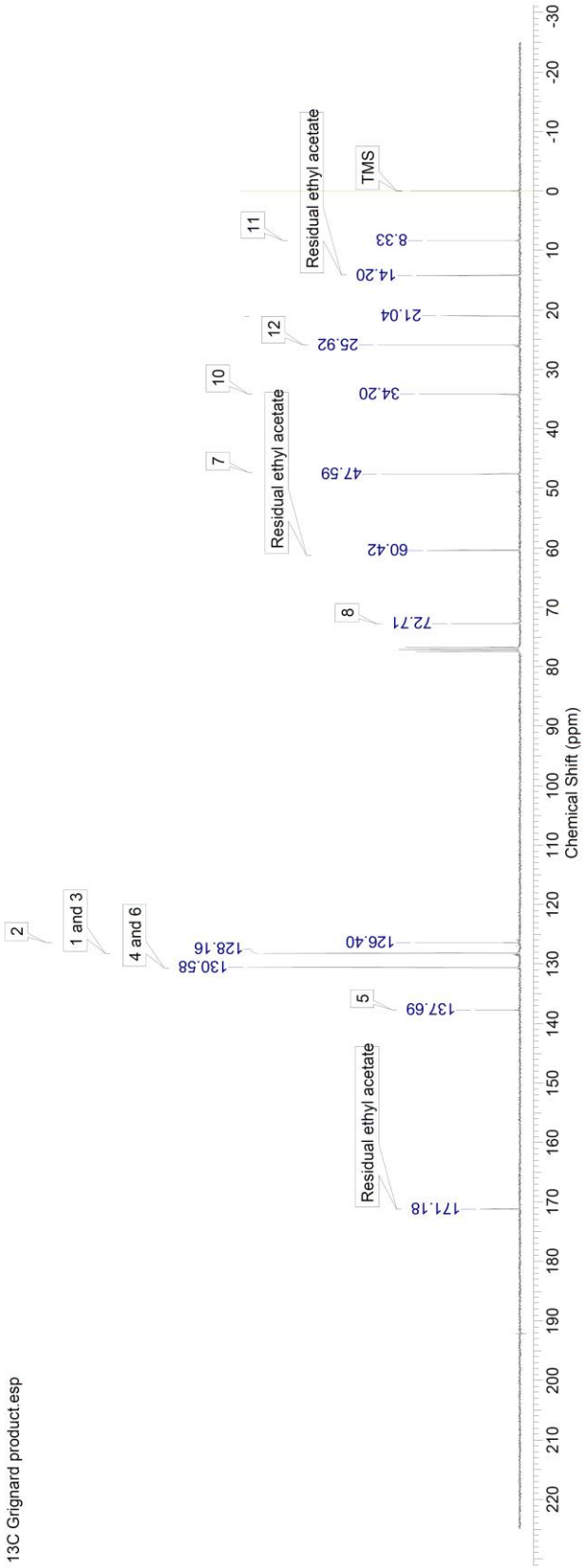

Figure A18. ^{13}C NMR spectrum of the Grignard product, 2-methyl-1-phenyl-2-butanol (**G1**).

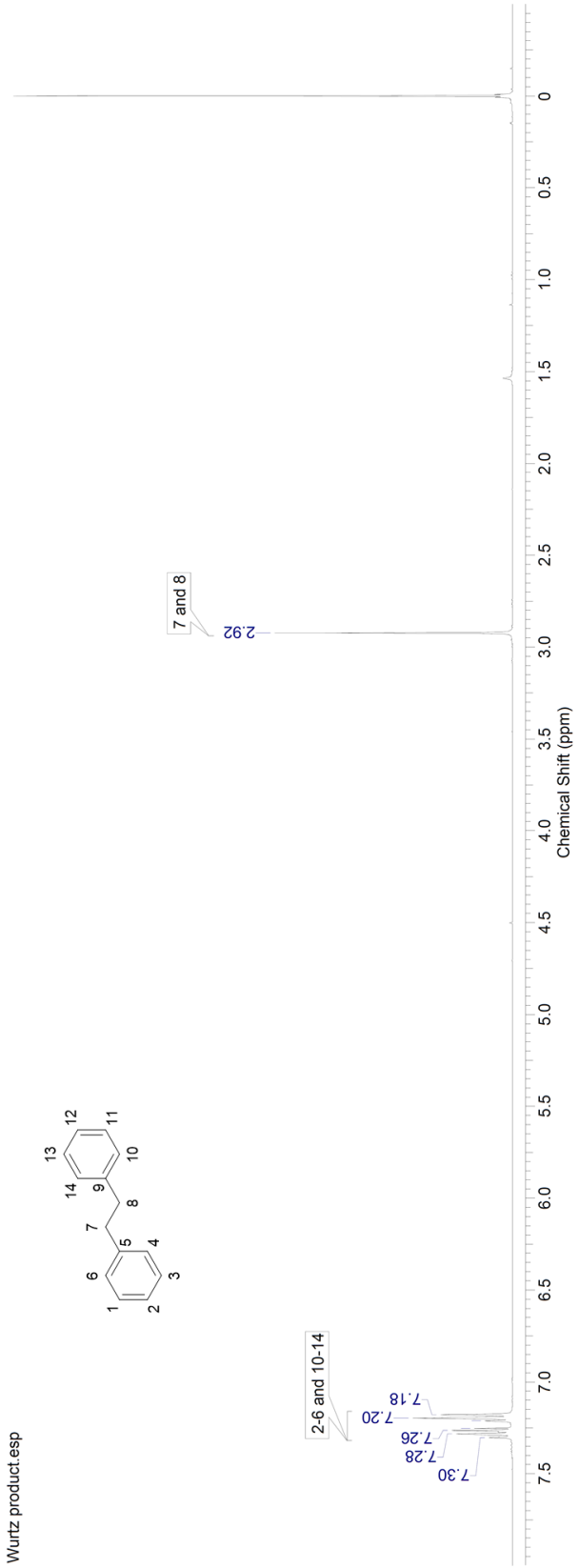

Figure A19. ^{1}H NMR spectrum of the Wurtz product, bibenzyl (**W1**).

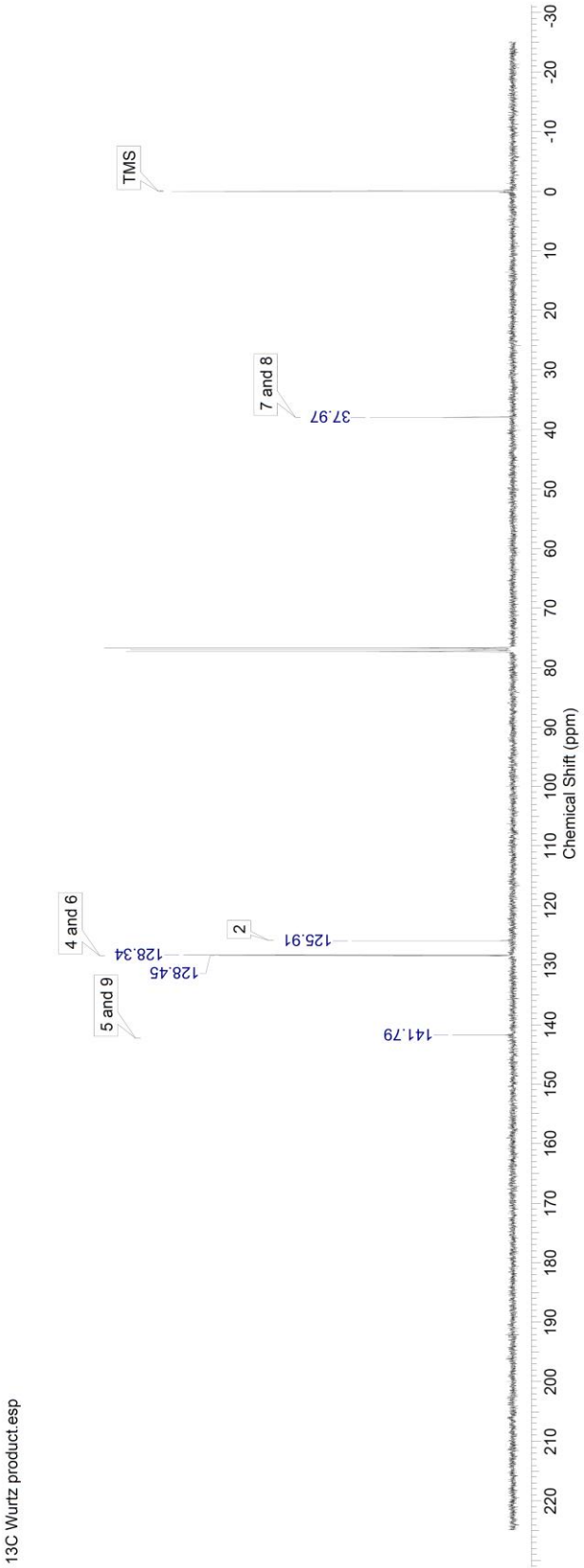

Figure A20. ^{13}C NMR spectrum of the Wurtz product, bibenzyl (**W1**).

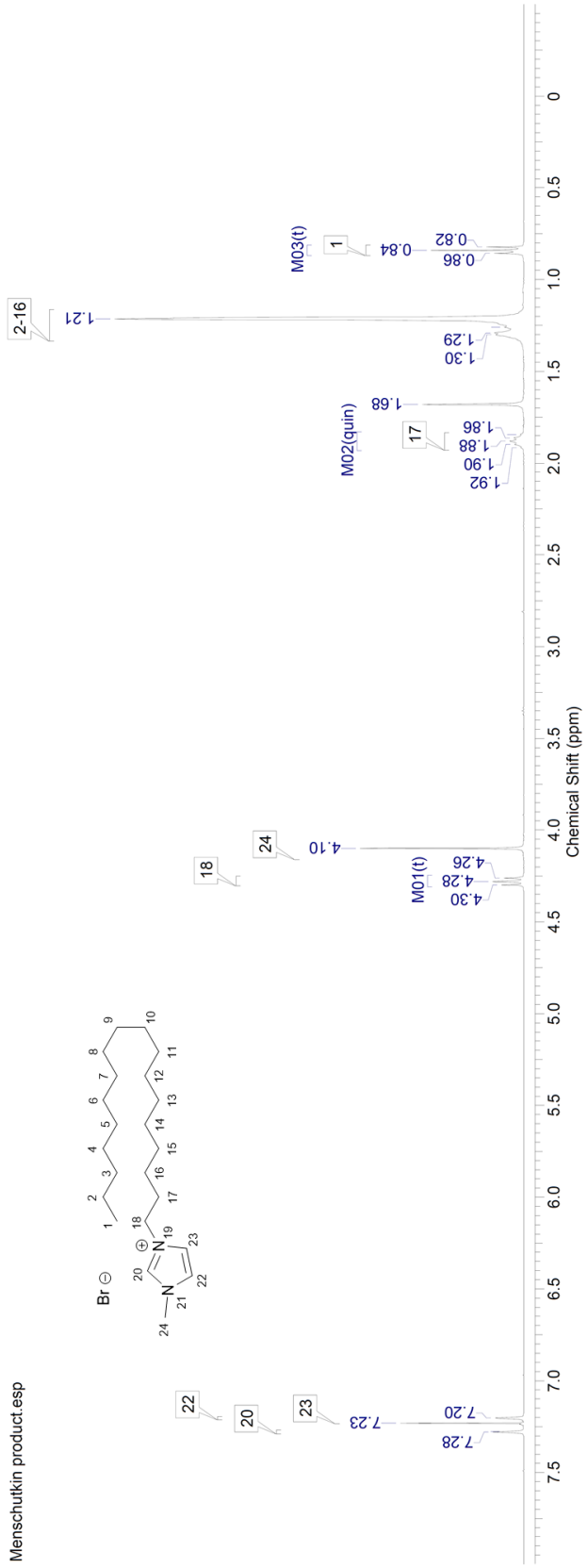

Figure A21. ^{1}H NMR spectrum of the Menschutkin product, 1-octadecyl-3-methylimidazolium bromide.

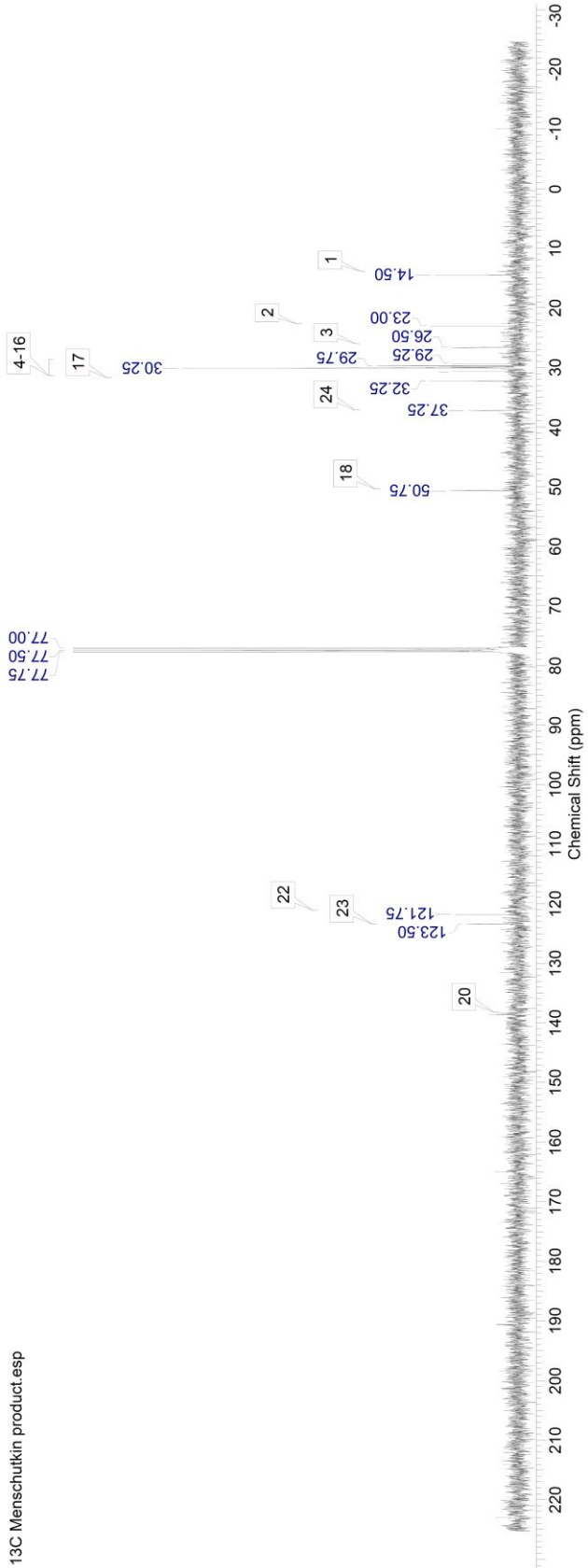

Figure A22. ^{13}C NMR spectrum of the Menschutkin product, 1-octadecyl-3-methylimidazolium bromide.

DSC traces

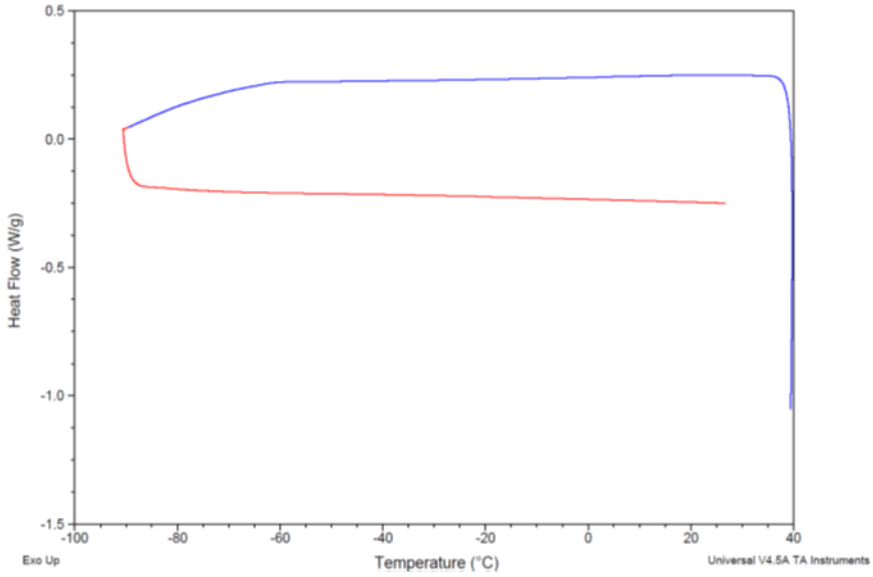

Figure A23. DSC trace of TMTHF.

GPC chromatograms

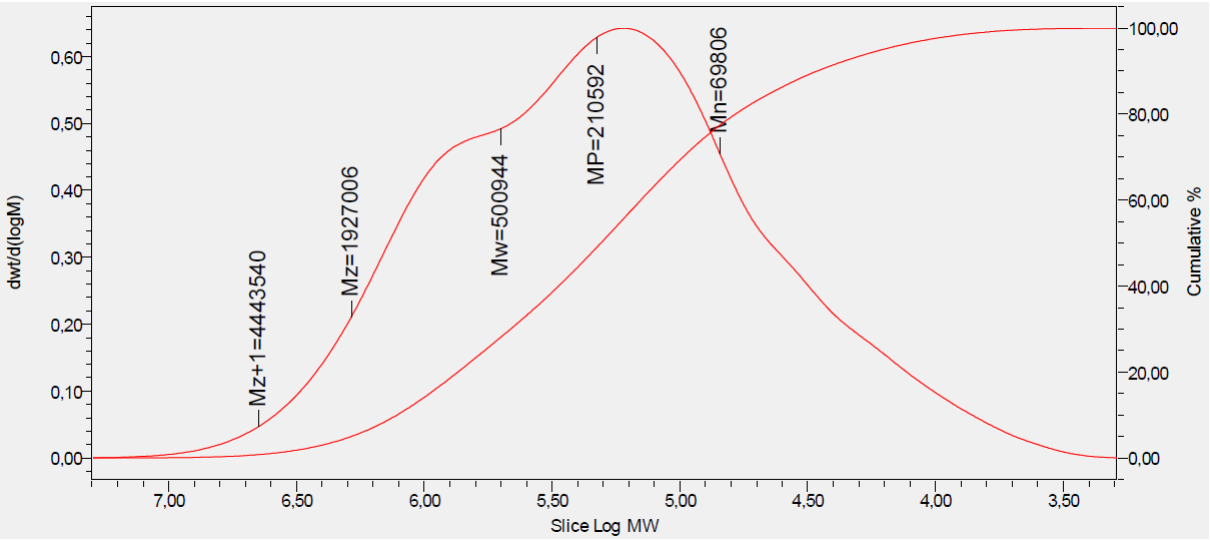

Figure A24. GPC chromatogram of Poly (butyl acrylate-co-acrylic acid) when TMTHF is used as the polymerisation solvent.

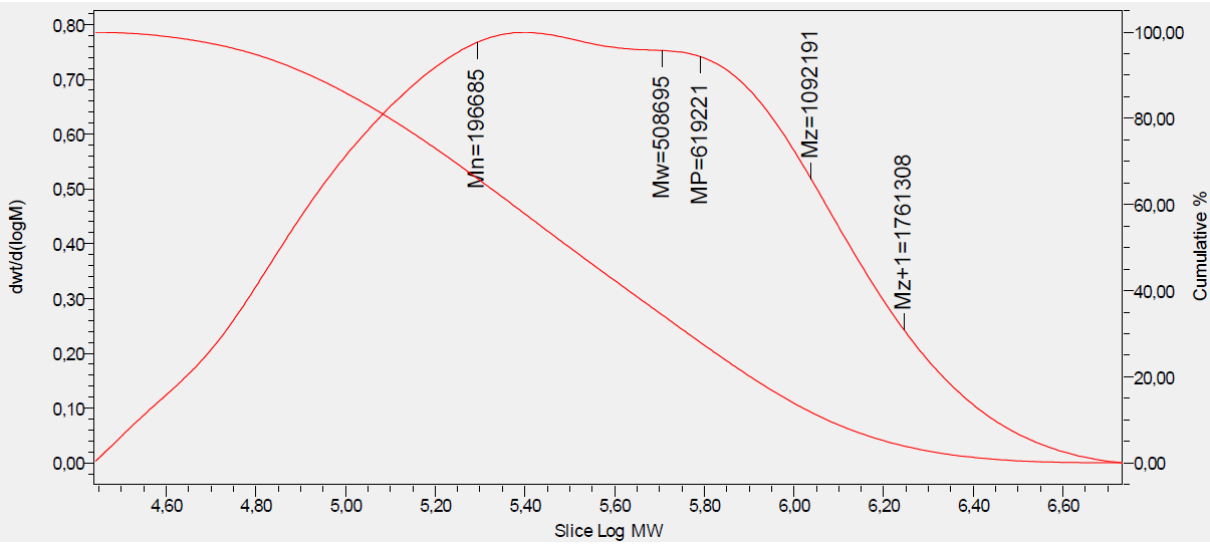

Figure A25. GPC chromatogram of Poly (butyl acrylate-co-acrylic acid) when toluene is used as the polymerisation solvent.

2,2,5,5-Tetramethyltetrahydrofuran (TMTHF) datasheet

M_r / g mol^{-1}	128.25[(a)]
Bp / °C	112[(b)]
Mp / °C	< -90[(b)]
Density / g mL^{-1}	0.802[(b)]
AIT / °C	417[(d)]
LEL / %	0.91[(c)]
LEL (vol.) / µl L^{-1}	64.24
α	0.00(a)
β	0.77(b)
π*	0.35(c)
δD / MPa0.5	15.4(d)
δP / MPa0.5	2.4(d)
δH / MPa0.5	2.1(d)
δ / MPa0.5	15.7(d)
Water saturation / %	2.16
Log Po/w	1.92(e)
Ames test (TA98 and TA100)	Pass
Acid stability	Stable to sulfuric acid and hydrochloric acid in concentrations at least up to 1 mol% at 20 °C. Slight degradation in 1 mol% refluxing sulfuric acid.

[TMTHF]. ^{1}H NMR (400 MHz, $CDCl_3$): δ 1.81 (s, 4H), 1.21 (s, 12H); ^{13}C NMR (400 MHz, CDCl3): δ 29.75, 38.75, 80.75; IR 2968, 2930, 2968, 1458, 1377, 1366, 1310, 1265, 1205, 1144, 991, 984, 885, 849, 767 cm^{-1}; *m/z* (%): (ESI–MS) 128 (40) [M^+].

List of abbreviations

EC_{10}	10% Effect concentration
^{13}C NMR	Carbon-13 nuclear magnetic resonance
^{1}H NMR	Hydrogen-1 nuclear magnetic resonance
2,5-DMTHF	2,5-Dimethyltetrahydrofuran
2-MeTHF	2-Methyltetrahydrofuran
2-NF	2-Nitrofluorine
4-NQO	4-nitroquinoline-*N*-oxide
A	Abraham's scale of hydrogen-bond donating ability term
a	Coefficient of the Kamlet-Taft scale of solvent hydrogen bond donating ability in linear solvation energy relationships
Å	Ångströms
a'	Coefficient of Abraham's hydrogen-bond donating term in the solvent parameter model
AAC	Allyl acetate
ABE	Acetone-butanol-ethanol
ACS	American Chemical Society
AE	Atom economy
AI	Allyl iodide

AIT	Autoignition temperature
ASTM	American Society for Testing and Materials
B	Abraham's scale of hydrogen-bond accepting ability term
b	Coefficient of the Kamlet-Taft scale of solvent hydrogen bond accepting ability in linear solvation energy relationships
b'	Coefficient of Abraham's hydrogen-bond accepting term in the solvent parameter model
BA	Butyric acid
BCF	Bioconcentration Factor
BET	Brunauer–Emmett–Teller
BHT	Butylated hydroxytoluene
B_N	Number of bonds in a molecule
Bp	Boiling point
BTX	Benzene, toluene and xylenes
B-value	Indicator of spontaneity
c	Linear solvation energy relationship proportionality constant for the solvation parameter model
C#	Carbon chain containing # carbon atoms
CAMD	Computer-aided molecular design
CAS	Chemical abstracts services
CCl_4	Carbon tetrachloride
CED	Cohesive energy density
CFC	Chlorofluorocarbon
CLP	Classification, labelling and packaging
cm^{-1}	Wavenumbers
cN	Centinewton

cN 20 mm-1	Centinewton per 20 millimetres
CO	Carbon monoxide
CO_2	Carbon dioxide
Conv.	Conversion
CPME	Cyclopentyl methyl ether
d	Coefficient of the Kamlet-Taft polarisability correction term in linear solvation energy relationships
Đ	Dispersity
DCM	Dichloromethane
DHL	2,5-Dimethylhexane-2,5-diol
DHN	2,5-Dimethyl-2,4-hexadiene
DHN2	2,5-Dimethyl-1,5-hexadiene
DHN3	2,5-Dimethyl-1,4-hexadiene
DIBAL-H	Diisobutylaluminum hydride
DMAc	Dimethyl acetamide
DMF	Dimethylformamide
DMHYL	2,5-dimethyl-3-hexyne-2,5-diol
DMSO	Dimethyl sulfoxide
DSC	Differential scanning calorimetry
DTBE	Di-*tert*-butyl ether
DTU	Technical University of Denmark
e	Coefficient of Abraham's excess molar refraction term in the solvent parameter model
E	Excess molar refraction term
ECHA	European chemicals agency

E-factor	Environmental-factor metric
EHS	Environmental, Health and Safety
EPA	Environmental protection agency
Eq.	Equivalent
ESP	Electrostatic surface potential
$E_T(30)$	Reichardt's dye transition energy
ETBE	Ethyl *tert*-butyl ether
EtOH	Ethanol
EU	European Union
FAME	Fatty acid methyl ester
FDA	Food and drug administration
g	Grams
g mol^{-1}	Grams per mole
GCI	Green Chemistry Institute
GHS	Global harmonised system
GRASS	GeneratoR of Agro-based Sustainable Solvents
GSK	GlaxoSmithKline
GVL	γ-Valerolactone
h	Coefficient of the cohesive energy density term in linear solvation energy relationships
H_2	Elemental hydrogen
H-BEA	Acidic form of the BEA zeolite framework
HI	Hydrogen iodide
HMF	Hydroxymethylfurfural

HMPA	Hexamethylphosphoramide
HNL	2,5-Dimethyl-4-hexen-2-ol
hr	Hour
HSP	Hansen solubility parameters
HSPiP	Hansen solubility parameters in practise software
H-Y	Acidic form of the FAU zeolite framework
H-ZSM-5	Acidic form of the MFI zeolite framework
IGC_{50}	Median inhibition of growth concentration
IPAc	Isopropyl acetate
IPI	Isopropyl iodide
IZC-SC	International Zeolite Association Structure Commission
K	Kelvin
k_2	Second-order rate constant
KT	Kamlet-Taft
kg mol^{-1}	Kilogram per mole
K_P	Solute partition coefficient
L	Litre
LC_{50}	Median lethal concentration
LCA	Life-cycle assessment
LD_{50}	Median lethal dose
LEL	Lower explosion limit
LEL (vol.%)	Lower explosion limit expressed as a volume percentage
ln	Natural logarithm function
Log	Logarithm function of base ten

LSER	Linear solvation energy relationship
m	Metre
m/z	Mass/charge ratio
MEK	2-Butanone
MeOH	Methanol
mg	Milligram
MIBK	Methyl isobutyl ketone
mL	Millilitre
mmol	Millimoles
mol	Moles
Mp	Melting point
Mpa	Megapascals
MR_{alkane}	Molar refraction of an alkane homologue
MR_x	Molar refraction of a solute
MTBE	Methyl *tert*-butyl ether
M_w	Molecular weight
n/a	Not applicable
NA	4-Nitroaniline
N_a	Number of atoms in a molecule
NBP	*N*-butylpyrrolidinone
nm	Nanometre
NMP	*N*-methyl-2-pyrrolidinone
NN	*N*,*N*-diethyl-4-nitraniline
NOEC	No Observed Effect Concentration

NO_x	Nitrogen oxides
NP	4-Nitrophenol
n_s	Number of solutes
O_2	Elemental oxygen
P1	Polymer 1
P2	Polymer 2
P3	Polymer 3
P4	Polymer 4
PA	Pivalic acid
PBT	Persistent, bioaccumulative, toxic
PET	Polyethylene terephthalate
PMI	Process mass intensity
$P_{o/w}$	Octanol/water partition coefficient
ppm	Parts per million
PSA	Pressure-sensitive adhesive
PTSA	*para*-toluenesulfonic acid
p-value	Probability of finding the observed, or more extreme, results when the null hypothesis (H_0) of a study question is true
QSAR	Quantitative structure activity relationship
QSPR	Quantitative structure property relationship
R5	Rubber 5
R^2	Coefficient of determination
R6	Rubber 6
REACH	Registration, Evaluation and Authorisation of Chemicals

R_g	Number of rings systems in a molecule
RME	Reaction mass efficiency
S	Abraham's scale of polarity term
s	Coefficient of the Kamlet-Taft scale of solvent dipolarity/polarisability in linear solvation energy relationships
s'	Coefficient of Abraham's polarity term in the solvent parameter model
SE	Standard error
Sel.	Selectivity
Si/Al	Silica/Alumina ratio
S_N2	Second-order nucleophilic substitution reaction
SO_x	Sulfur oxides
SP	Linear solvation energy relationship dependant variable for the solvation parameter model
Stoich.	Stoichiometric
STOT	Specific Target Organ Toxicity
SVHC	Substance of very high concern
$T_{1/2}$	Half-life
TEST	Toxicity Estimation Software Tool
TFA	Trifluoroacetic acid
THF	Tetrahydrofuran
TMO	2,2,4,4-tetramethyloxetane
TMTHF	2,2,5,5-Tetramethyltetrahydrofuran
TMTHP	2,2,6,6-tetramethyltetrahydropyran
TSS1	Total solubility sphere 1
TSS2	Total solubility sphere 2

UCO	Used cooking oil
US	United States
UV	Ultraviolet
UV-vis	Ultraviolet-visible
v	Coefficient of Abraham's McGowan's volume term in the solvent parameter model
V	McGowan's volume term
V_{mol}	Molecular volume
VNP	Volatile, non-polar solvent
vPvB	very persistent, very bioaccumulative
w.r.t	With respect to
WGSR	Water-gas shift reaction
XRD	X-ray diffraction
Y	Linear solvation energy relationship dependant variable for the solvatochromic equation
Y_0	Linear solvation energy relationship proportionality constant for the solvatochromic equation
α	Kamlet-Taft scale of solvent hydrogen bond donating ability
β	Kamlet-Taft scale of solvent hydrogen bond accepting ability
δ	Hildebrand parameter
δ^*	Kamlet-Taft scale polarisability correction term
δ_D	Hansen dispersion force parameter
δ_H	Hansen hydrogen-bonding ability parameter
$\Delta H^{\ddagger}$	Enthalpy of activation
δ_P	Hansen dipolarity parameter
$\Delta S^{\ddagger}$	Entropy of activation
ΔU_{vap}	Internal energy of vapourisation

η	Refractive index of a pure liquid at 20 °C
µl	Microlitre
ν_{max}	Wavenumber ($1/\lambda_{max}$)
π^*	Kamlet-Taft scale of solvent dipolarity/polarisability
$\Sigma_{atomic\ volumes}$	Sum of atomic volumes in a molecule

References

1 Toluene - Substance Information - ECHA, https://echa.europa.eu/substance-information/-/substanceinfo/100.003.297, (accessed 8 September 2016).
2 J. Kjølholt, J. Maag, M. Warming and S. Hagen, 2014.
3 Understanding REACH - ECHA, https://echa.europa.eu/regulations/reach/understanding-reach, (accessed 12 February 2017).
4 J. A. Kent, *Handbook of Industrial Chemistry and Biotechnology*, Springer Science & Business Media, 2013.
5 J. H. Gary and G. E. Handwerk, *Petroleum Refining: Technology and Economics*, M. Dekker, 1994.
6 W. A. Sweeney and P. F. Bryan, in *Kirk-Othmer Encyclopedia of Chemical Technology*, John Wiley & Sons, Inc., 2000.
7 R. W. Bentley, *Energy Policy*, 2002, **30**, 189–205.
8 N. Abas, A. Kalair and N. Khan, *Futures*, 2015, **69**, 31–49.
9 A. D. McNaught and A. Wilkinson, Blackwell Scientific Publications, Oxford, 2nd edn., 1997.
10 n-Hexane - Substance Information - ECHA, https://echa.europa.eu/substance-information/-/substanceinfo/100.003.435, (accessed 12 September 2016).
11 ATSDR - Toxic Substances - Benzene, https://www.atsdr.cdc.gov/substances/toxsubstance.asp?toxid=14, (accessed 12 September 2017).
12 Dichloromethane - Substance Information - ECHA, https://echa.europa.eu/substance-information/-/substanceinfo/100.000.763, (accessed 7 March 2017).
13 Chloroform - Substance Information - ECHA, https://echa.europa.eu/substance-information/-/substanceinfo/100.000.603, (accessed 7 March 2017).
14 R. Hossaini, M. P. Chipperfield, S. A. Montzka, A. Rap, S. Dhomse and W. Feng, *Nat. Geosci.*, 2015, **8**, 186–190.
15 Tetrahydrofuran - Substance Information - ECHA, https://echa.europa.eu/substance-information/-/substanceinfo/100.003.389, (accessed 11 March 2017).
16 V. Fábos, G. Koczó, H. Mehdi, L. Boda and I. T. Horváth, *Energy Environ. Sci.*, 2009, **2**, 767.
17 Diethyl ether - Substance Information - ECHA, https://echa.europa.eu/substance-information/-/substanceinfo/100.000.425, (accessed 11 March 2017).
18 1-methyl-2-pyrrolidone - Substance Information - ECHA, https://echa.europa.eu/substance-information/-/substanceinfo/100.011.662, (accessed 11 March 2017).
19 N,N-dimethylacetamide - Substance Information - ECHA, https://echa.europa.eu/substance-information/-/substanceinfo/100.004.389, (accessed 11 March 2017).
20 C. M. Hansen, Technical University of Denmark.
21 M. J. Kamlet, J. L. M. Abboud, M. H. Abraham and R. W. Taft, *J. Org. Chem.*, 1983, **48**, 2877–2887.

22 L. Theodore, R. R. Dupont and K. Ganesan, *Pollution Prevention: The Waste Management Approach to the 21st Century*, CRC Press, 1999.
23 Dimethyl sulfoxide - PubChem, https://pubchem.ncbi.nlm.nih.gov/compound/dimethyl_sulfoxide, (accessed 9 May 2017).
24 tert-Butanol - Pubchem, https://pubchem.ncbi.nlm.nih.gov/compound/tert-Butanol, (accessed 9 May 2017).
25 R. Höfer and J. Bigorra, *Green Chem.*, 2007, **9**, 203–212.
26 H. Guo, S. C. Lee, L. Y. Chan and W. M. Li, *Environ. Res.*, 2004, **94**, 57–66.
27 T. Welton, *Chem. Rev.*, 1999, **99**, 2071–2084.
28 I. U. of P. and A. Chemistry, IUPAC Gold Book - dynamic viscosity, η, https://goldbook.iupac.org/html/D/D01877.html, (accessed 11 May 2017).
29 I. U. of P. and A. Chemistry, IUPAC Gold Book - density, ρ, https://goldbook.iupac.org/html/D/D01590.html, (accessed 11 May 2017).
30 C.-C. Chen, H.-J. Liaw, C.-M. Shu and Y.-C. Hsieh, *J. Chem. Eng. Data*, 2010, **55**, 5059–5064.
31 I. U. of P. and A. Chemistry, IUPAC Gold Book - explosivity limits (explosion limits), https://goldbook.iupac.org/html/E/E02274.html, (accessed 11 May 2017).
32 I. Smallwood, *Handbook of Organic Solvent Properties*, Butterworth-Heinemann, 2012.
33 I. U. of P. and A. Chemistry, IUPAC Gold Book - flash point, https://goldbook.iupac.org/html/F/F02419.html, (accessed 11 May 2017).
34 J. H. Hildebrand and R. L. Scott, *Regular solutions*, Prentice-Hall, 1962.
35 C. M. Hansen, *Hansen Solubility Parameters: A User's Handbook, Second Edition*, CRC Press, 2012.
36 F. London, *Trans. Faraday Soc.*, 1937, **33**, 8b–26.
37 V. A. Vaclavik and E. W. Christian, in *Essentials of Food Science*, Springer, New York, NY, 2008, pp. 21–31.
38 R. F. Blanks and J. M. Prausnitz, *Ind. Eng. Chem. Fundam.*, 1964, **3**, 1–8.
39 E. Stefanis and C. Panayiotou, *Int. J. Thermophys.*, 2008, **29**, 568–585.
40 C. M. Hansen and S. Abbott, *Hansen Solubility Parameters in Practice*, Hansen-Solubility, 2008.
41 R. Gani, C. Jiménez-González and D. J. C. Constable, *Comput. Chem. Eng.*, 2005, **29**, 1661–1676.
42 R. Gani, P. A. Gómez, M. Folić, C. Jiménez-González and D. J. C. Constable, *Comput. Chem. Eng.*, 2008, **32**, 2420–2444.
43 S. Yousefinejad and B. Hemmateenejad, *Chemom. Intell. Lab. Syst.*, 2015, **149**, **Part B**, 177–204.
44 J. Marrero and R. Gani, *Fluid Phase Equilibria*, 2001, **183–184**, 183–208.
45 R. W. Taft and M. J. Kamlet, *J. Am. Chem. Soc.*, 1976, **98**, 2886–2894.
46 M. J. Kamlet and R. W. Taft, *J. Am. Chem. Soc.*, 1976, **98**, 377–383.
47 M. J. Kamlet, J. L. Abboud and R. W. Taft, *J. Am. Chem. Soc.*, 1977, **99**, 6027–6038.
48 C. Reichardt, *Chem. Rev.*, 1994, **94**, 2319–2358.
49 A. Botrel, A. le Beuze, P. Jacques and H. Strub, *J. Chem. Soc. Faraday Trans. 2 Mol. Chem. Phys.*, 1984, **80**, 1235–1252.
50 R. W. Taft, J.-L. M. Abboud, M. J. Kamlet and M. H. Abraham, *J. Solut. Chem.*, 1985, **14**, 153–186.
51 C. Reichardt and T. Welton, *Solvents and Solvent Effects in Organic Chemistry*, John Wiley & Sons, 2011.
52 Y. Marcus, *Chem. Soc. Rev.*, 1993, **22**, 409–416.
53 J. Sherwood, PhD Thesis, University of York, 2013.
54 P. Nicolet and C. Laurence, *J. Chem. Soc., Perkin Trans. 2*, 1986, 1071–1079.
55 Y. Marcus, *J. Solut. Chem.*, 1991, **20**, 929–944.
56 C. Reichardt, *Org. Process Res. Dev.*, 2007, **11**, 105–113.
57 P. G. Jessop, *Green Chem.*, 2011, **13**, 1391–1398.
58 C. Reichardt, *Angew. Chem. Int. Ed. Engl.*, 1979, **18**, 98–110.
59 M. H. Abraham, A. Ibrahim and A. M. Zissimos, *J. Chromatogr. A*, 2004, **1037**, 29–47.
60 J. H. Clark, D. J. Macquarrie and J. Sherwood, *Green Chem.*, 2012, **14**, 90–93.
61 R. D. Cramer, *J. Am. Chem. Soc.*, 1980, **102**, 1837–1849.

62 R. D. Cramer, *J. Am. Chem. Soc.*, 1980, **102**, 1849–1859.
63 M. H. Abraham and J. Liszi, *J. Chem. Soc., Faraday Trans. 1*, 1978, **74**, 1604–1614.
64 R. A. Pierotti, *Chem. Rev.*, 1976, **76**, 717–726.
65 C. F. Poole, S. N. Atapattu, S. K. Poole and A. K. Bell, *Anal. Chim. Acta*, 2009, **652**, 32–53.
66 M. H. Abraham, *Chem. Soc. Rev.*, 1993, **22**, 73–83.
67 M. H. Abraham, P. L. Grellier, D. V. Prior, P. P. Duce, J. J. Morris and P. J. Taylor, *J. Chem. Soc., Perkin Trans. 2*, 1989, 699–711.
68 M. H. Abraham, P. L. Grellier, D. V. Prior, J. J. Morris and P. J. Taylor, *J. Chem. Soc., Perkin Trans. 2*, 1990, 521–529.
69 M. H. Abraham and G. S. Whiting, *J. Chromatogr. A*, 1992, **594**, 229–241.
70 B. K. Callihan and D. S. Ballantine, *J. Chromatogr. A*, 2000, **893**, 339–346.
71 A. M. Zissimos, M. H. Abraham, M. C. Barker, K. J. Box and K. Y. Tam, *J. Chem. Soc., Perkin Trans. 2*, 2002, 470–477.
72 US EPA, Toxicity Estimation Software Tool (TEST), https://www.epa.gov/chemical-research/toxicity-estimation-software-tool-test, (accessed 2 March 2017).
73 What about animal testing? - ECHA, https://echa.europa.eu/chemicals-in-our-life/animal-testing-under-reach, (accessed 2 March 2017).
74 B. N. Ames, F. D. Lee and W. E. Durston, *Proc. Natl. Acad. Sci.*, 1973, **70**, 782–786.
75 US EPA, User's Guide for T.E.S.T. (version 4.2) (Toxicity Estimation Software Tool) A Program to Estimate Toxicity from Molecular Structure, https://www.epa.gov/chemical-research/users-guide-test-version-42-toxicity-estimation-software-tool-program-estimate, (accessed 6 June 2017).
76 A. J. F. Griffiths, J. H. Miller, D. T. Suzuki, R. C. Lewontin and W. M. Gelbart, *Introduction to Genetic Analysis*, W. H. Freeman, New York, Seventh Edition edition., 2000.
77 J. McCann, E. Choi, E. Yamasaki and B. N. Ames, *Proc. Natl. Acad. Sci.*, 1975, **72**, 5135–5139.
78 J. McCann, L. Swirsky Gold, L. Horn, R. McGill, T. E. Graedel and J. Kaldor, *Mutat. Res. Toxicol.*, 1988, **205**, 183–195.
79 B. N. Ames, W. E. Durston, E. Yamasaki and F. D. Lee, *Proc. Natl. Acad. Sci.*, 1973, **70**, 2281–2285.
80 D. Mackay and A. Fraser, *Environ. Pollut.*, 2000, **110**, 375–391.
81 W. B. Neely, D. R. Branson and G. E. Blau, *Environ. Sci. Technol.*, 1974, **8**, 1113–1115.
82 D. Mackay, *Environ. Sci. Technol.*, 1982, **16**, 274–278.
83 P. T. Anastas and J. C. Warner, *Green Chemistry: Theory and Practice*, Oxford University Press, 1998.
84 G. W. V. Cave, C. L. Raston and J. L. Scott, *Chem. Commun.*, 2001, 2159–2169.
85 J. H. Clark, F. E. I. Deswarte and T. J. Farmer, *Biofuels Bioprod. Biorefining-Biofpr*, 2009, **3**, 72–90.
86 I. U. of P. and A. Chemistry, IUPAC Gold Book - catalyst, https://goldbook.iupac.org/html/C/C00876.html, (accessed 20 May 2017).
87 R. A. Sheldon, I. Arends and U. Hanefeld, *Green Chemistry and Catalysis*, John Wiley & Sons, 2007.
88 P. T. Anastas, M. M. Kirchhoff and T. C. Williamson, *Appl. Catal. Gen.*, 2001, **221**, 3–13.
89 J. H. Clark and C. N. Rhodes, *Clean Synthesis Using Porous Inorganic Solid Catalysts and Supported Reagents*, 2000.
90 G. J. Sunley and D. J. Watson, *Catal. Today*, 2000, **58**, 293–307.
91 J. W. Comerford, J. H. Clark, D. J. Macquarrie and S. W. Breeden, *Chem. Commun.*, 2009, 2562–2564.
92 K. Köhler, R. G. Heidenreich, J. G. E. Krauter and J. Pietsch, *Chem. – Eur. J.*, 2002, **8**, 622–631.
93 K. Wilson, D. J. Adams, G. Rothenberg and J. H. Clark, *J. Mol. Catal. Chem.*, 2000, **159**, 309–314.
94 H. Robson, *Verified Synthesis of Zeolitic Materials: Second Edition*, Gulf Professional Publishing, 2001.
95 M. E. Davis and R. F. Lobo, *Chem. Mater.*, 1992, **4**, 756–768.

96 D. C. Sherrington, A. P. Kybett and M. Guisnet, in *Supported Catalysts and Their Applications*, 2001, pp. 55–67.
97 Database of Zeolite Structures, http://www.iza-structure.org/databases/, (accessed 27 May 2017).
98 FAU: Framework Type, http://europe.iza-structure.org/IZA-SC/framework.php?STC=FAU, (accessed 24 May 2017).
99 *BEA: Framework Type, http://europe.iza-structure.org/IZA-SC/framework.php?STC=BEA, (accessed 24 May 2017).
100 MOR: Framework Type, http://europe.iza-structure.org/IZA-SC/framework.php?STC=MOR, (accessed 27 May 2017).
101 MFI: Framework Type, http://europe.iza-structure.org/IZA-SC/framework.php?STC=MFI, (accessed 24 May 2017).
102 S. Dasgupta and B. Török, *Org. Prep. Proced. Int.*, 2008, **40**, 1–65.
103 G. B. Bidita Varadwaj, K. Parida and V. O. Nyamori, *Inorg. Chem. Front.*, 2016, **3**, 1100–1111.
104 U. Flessner, D. J. Jones, J. Rozière, J. Zajac, L. Storaro, M. Lenarda, M. Pavan, A. Jiménez-López, E. Rodríguez-Castellón, M. Trombetta and G. Busca, *J. Mol. Catal. Chem.*, 2001, **168**, 247–256.
105 M. Mittelbach, A. Silberholz and M. Koncar, 1995, vol. 3, pp. 497–499.
106 US3282875 A, 1966.
107 K. A. Mauritz and R. B. Moore, *Chem. Rev.*, 2004, **104**, 4535–4586.
108 G. A. Olah, P. S. Iyer and G. K. S. Prakash, *Synthesis*, 1986, **1986**, 513–531.
109 R. Kunin, E. Meitzner, J. Oline, S. Fisher and N. Frisch, *Ind. Eng. Chem. Prod. Res. Dev.*, 1962, **1**, 140–144.
110 F. R. Chen, G. Coudurier, J. F. Joly and J. C. Vedrine, *J. Catal.*, 1993, **143**, 616–626.
111 M. A. Ecormier, K. Wilson and A. F. Lee, *J. Catal.*, 2003, **215**, 57–65.
112 J. H. Clark, G. L. Monks, D. J. Nightingale, P. M. Price and J. F. White, *J. Catal.*, 2000, **193**, 348–350.
113 B. Trost, *Science*, 1991, **254**, 1471–1477.
114 R. A. Sheldon, *Green Chem.*, 2007, **9**, 1273–1283.
115 A. D. Curzons, D. J. C. Constable, D. N. Mortimer and V. L. Cunningham, *Green Chem.*, 2001, **3**, 1–6.
116 D. J. C. Constable, A. D. Curzons, L. M. F. dos Santos, G. R. Geen, R. E. Hannah, J. D. Hayler, J. Kitteringham, M. A. McGuire, J. E. Richardson, P. Smith, R. Lee Webb and M. Yu, *Green Chem.*, 2001, **3**, 7–9.
117 C. Jimenez-Gonzalez, C. S. Ponder, Q. B. Broxterman and J. B. Manley, *Org. Process Res. Dev.*, 2011, **15**, 912–917.
118 T. Werpy, G. Petersen, A. Aden, J. Bozell, J. Holladay, J. White, A. Manheim, D. Eliot, L. Lasure and S. Jones, *Top Value Added Chemicals From Biomass. Volume 1 - Results of Screening for Potential Candidates From Sugars and Synthesis Gas*, 2004.
119 T. J. Farmer and M. Mascal, in *Introduction to Chemicals from Biomass*, eds. J. Clark and F. Deswarte, John Wiley & Sons, Ltd, 2015, pp. 89–155.
120 J. J. Bozell and G. R. Petersen, *Green Chem.*, 2010, **12**, 539–554.
121 D. J. Hayes, S. Fitzpatrick, M. H. B. Hayes and J. R. H. Ross, in *Biorefineries-Industrial Processes and Products*, eds. B. Kamm, P. R. Gruber and M. Kamm, Wiley-VCH Verlag GmbH, 2005, pp. 139–164.
122 http, http://biofinetechnology.com/, (accessed 26 April 2017).
123 P. Losch, A.-S. Felten and P. Pale, *Adv. Synth. Catal.*, 2015, **357**, 2931–2938.
124 T. Morimoto and K. Kakiuchi, *Angew. Chem. Int. Ed.*, 2004, **43**, 5580–5588.
125 K. Tedsree, T. Li, S. Jones, C. W. A. Chan, K. M. K. Yu, P. A. J. Bagot, E. A. Marquis, G. D. W. Smith and S. C. E. Tsang, *Nat. Nanotechnol.*, 2011, **6**, 302–307.
126 P. Lv, Z. Yuan, C. Wu, L. Ma, Y. Chen and N. Tsubaki, *Energy Convers. Manag.*, 2007, **48**, 1132–1139.
127 M. H. Waldner and F. Vogel, *Ind. Eng. Chem. Res.*, 2005, **44**, 4543–4551.

128 S. Heidenreich and P. U. Foscolo, *Prog. Energy Combust. Sci.*, 2015, **46**, 72–95.
129 M. Asadullah, *Renew. Sustain. Energy Rev.*, 2014, **29**, 201–215.
130 R. Chandra, H. Takeuchi and T. Hasegawa, *Renew. Sustain. Energy Rev.*, 2012, **16**, 1462–1476.
131 J.-C. Frigon and S. R. Guiot, *Biofuels Bioprod. Biorefining*, 2010, **4**, 447–458.
132 Å. Davidsson, C. Gruvberger, T. H. Christensen, T. L. Hansen and J. la C. Jansen, *Waste Manag.*, 2007, **27**, 406–414.
133 M. Görling, M. Larsson and P. Alvfors, *Appl. Energy*, 2013, **112**, 440–447.
134 H. Schobert, *Chem. Rev.*, 2014, **114**, 1743–1760.
135 US20120022308 A1, 2012.
136 C. Bellido, M. Loureiro Pinto, M. Coca, G. González-Benito and M. T. García-Cubero, *Bioresour. Technol.*, 2014, **167**, 198–205.
137 H. Amiri, K. Karimi and H. Zilouei, *Bioresour. Technol.*, 2014, **152**, 450–456.
138 M. Kumar and K. Gayen, *Appl. Energy*, 2011, **88**, 1999–2012.
139 E. M. Green, *Curr. Opin. Biotechnol.*, 2011, **22**, 337–343.
140 B. Hahn-Hägerdal, M. Galbe, M. F. Gorwa-Grauslund, G. Lidén and G. Zacchi, *Trends Biotechnol.*, 2006, **24**, 549–556.
141 A. Gupta and J. P. Verma, *Renew. Sustain. Energy Rev.*, 2015, **41**, 550–567.
142 Our Business, http://www.gevo.com/about/our-business-leading-the-way-with-isobutanol/, (accessed 24 April 2017).
143 D. de Guzman, Butamax prepares for bio-isobutanol commercialization, https://greenchemicalsblog.com/2017/04/12/butamax-prepares-for-bio-isobutanol-commercialization/, (accessed 24 April 2017).
144 U. R. Fritsche, R. E. H. Sims and A. Monti, *Biofuels Bioprod. Biorefining*, 2010, **4**, 692–704.
145 Global Bioenergies, *Glob. Bioenergies*, 2015.
146 Isobutene - Pubchem, https://pubchem.ncbi.nlm.nih.gov/compound/8255, (accessed 7 August 2017).
147 B. N. M. van Leeuwen, A. M. van der Wulp, I. Duijnstee, A. J. A. van Maris and A. J. J. Straathof, *Appl. Microbiol. Biotechnol.*, 2012, **93**, 1377–1387.
148 Hu, Du, Z. Tang and Min, *Ind. Eng. Chem. Res.*, 2004, **43**, 7928–7931.
149 Y. Gu and F. Jérôme, *Green Chem.*, 2010, **12**, 1127–1138.
150 A. E. Díaz-Álvarez, J. Francos, B. Lastra-Barreira, P. Crochet and V. Cadierno, *Chem. Commun.*, 2011, **47**, 6208–6227.
151 L. Yu, J. Yuan, Q. Zhang, Y.-M. Liu, H.-Y. He, K.-N. Fan and Y. Cao, *ChemSusChem*, 2014, **7**, 743–747.
152 Metathesis for maximum propylene, http://www.digitalrefining.com/article/1000178,Metathesis_for_maximum_propylene.html#.Wbru9ciGNPY, (accessed 14 September 2017).
153 US5026936 A, 1991.
154 N. Popoff, E. Mazoyer, J. Pelletier, R. M. Gauvin and M. Taoufik, *Chem. Soc. Rev.*, 2013, **42**, 9035–9054.
155 A. Morschbacker, *Polym. Rev.*, 2009, **49**, 79–84.
156 How it is produced - Braskem, http://www.braskem.com/site.aspx/How-it-is-produced, (accessed 14 September 2017).
157 G. P. Belov, *Catal. Ind.*, 2014, **6**, 266–272.
158 Bio-based solvents - Requirements and test methods, https://standards.cen.eu/dyn/www/f?p=204:110:0::::FSP_PROJECT:40174&cs=161BAFBE2B2659903E8B55F9326BA295B, (accessed 13 February 2017).
159 J. Sherwood, J. H. Clark, T. J. Farmer, L. Herrero-Davila and L. Moity, *Molecules*, 2016, **22**, 48.
160 CEN / TC411 Bio-based products, http://www.biobasedeconomy.eu/standardisation/cen-tc411/, (accessed 7 March 2017).
161 BioPreferred|Catalog, https://biopreferred.gov/BioPreferred/faces/catalog/Catalog.xhtml, (accessed 10 May 2017).

162 J. I. García, H. García-Marín and E. Pires, *Green Chem.*, 2014, **16**, 1007–1033.
163 C. S. K. Lin, L. A. Pfaltzgraff, L. Herrero-Davila, E. B. Mubofu, S. Abderrahim, J. H. Clark, A. A. Koutinas, N. Kopsahelis, K. Stamatelatou, F. Dickson, S. Thankappan, Z. Mohamed, R. Brocklesby and R. Luque, *Energy Environ. Sci.*, 2013, **6**, 426–464.
164 H. Kobayashi and A. Fukuoka, *Green Chem.*, 2013, **15**, 1740–1763.
165 M. He, Y. Sun and B. Han, *Angew. Chem. Int. Ed.*, 2013, **52**, 9620–9633.
166 C. Capello, U. Fischer and K. Hungerbühler, *Green Chem.*, 2007, **9**, 927.
167 P. Anastas and N. Eghbali, *Chem. Soc. Rev.*, 2009, **39**, 301–312.
168 Y. Gu and F. Jérôme, *Chem. Soc. Rev.*, 2013, **42**, 9550–9570.
169 J. H. Clark, T. J. Farmer, A. J. Hunt and J. Sherwood, *Int. J. Mol. Sci.*, 2015, **16**, 17101–17159.
170 C. S. M. Pereira, V. M. T. M. Silva and A. E. Rodrigues, *Green Chem.*, 2011, **13**, 2658–2671.
171 B. Schäffner, F. Schäffner, S. P. Verevkin and A. Börner, *Chem. Rev.*, 2010, **110**, 4554–4581.
172 D. F. Aycock, *Org. Process Res. Dev.*, 2006, **11**, 156–159.
173 P. Delgado, M. T. Sanz, S. Beltrán and L. A. Núñez, *Chem. Eng. J.*, 2010, **165**, 693–700.
174 J. Sherwood, M. D. Bruyn, A. Constantinou, L. Moity, C. R. McElroy, T. J. Farmer, T. Duncan, W. Raverty, A. J. Hunt and J. H. Clark, *Chem. Commun.*, 2014, **50**, 9650–9652.
175 Ethyl acetate - SEKAB, http://www.sekab.com/chemistry/ethyl-acetate/, (accessed 12 March 2017).
176 US6809217 B1, 2004.
177 T. Coskun, C. M. Conifer, L. C. Stevenson and G. J. P. Britovsek, *Chem. – Eur. J.*, 2013, **19**, 6840–6844.
178 B. J. Nikolau, M. A. D. N. Perera, L. Brachova and B. Shanks, *Plant J.*, 2008, **54**, 536–545.
179 R. Ciriminna, M. Lomeli-Rodriguez, P. D. Carà, J. A. Lopez-Sanchez and M. Pagliaro, *Chem. Commun.*, 2014, **50**, 15288–15296.
180 Galactic > Products, https://www.lactic.com/en-us/products.aspx, (accessed 12 March 2017).
181 J. Yang, J.-N. Tan and Y. Gu, *Green Chem.*, 2012, **14**, 3304–3317.
182 D. M. L. Cabrera, F. M. Líbero, D. Alves, G. Perin, E. J. Lenardão and R. G. Jacob, *Green Chem. Lett. Rev.*, 2012, **5**, 329–336.
183 S. Salehpour and M. A. Dubé, *Green Chem.*, 2008, **10**, 321–326.
184 WO/2010/022263, 2010.
185 C. Gonzalez-Arellano, L. Parra-Rodriguez and R. Luque, *Catal. Sci. Technol.*, 2014, **4**, 2287–2292.
186 C. J. A. Mota, C. X. A. da Silva, N. Rosenbach, J. Costa and F. da Silva, *Energy Fuels*, 2010, **24**, 2733–2736.
187 D. Buhl, D. M. Roberge and W. F. Hölderich, *Appl. Catal. Gen.*, 1999, **188**, 287–299.
188 M. A. Martin-Luengo, M. Yates, E. S. Rojo, D. Huerta Arribas, D. Aguilar and E. Ruiz Hitzky, *Appl. Catal. Gen.*, 2010, **387**, 141–146.
189 H. L. Parker, J. Sherwood, A. J. Hunt and J. H. Clark, *ACS Sustain. Chem. Eng.*, 2014, **2**, 1739–1742.
190 S. B. Lawrenson, R. Arav and M. North, *Green Chem.*, 2017, **19**, 1685–1691.
191 D. Fegyverneki, L. Orha, G. Láng and I. T. Horváth, *Tetrahedron*, 2010, **66**, 1078–1081.
192 E. I. Gürbüz, J. M. R. Gallo, D. M. Alonso, S. G. Wettstein, W. Y. Lim and J. A. Dumesic, *Angew. Chem. Int. Ed.*, 2013, **52**, 1270–1274.
193 W. Yang and A. Sen, *ChemSusChem*, 2010, **3**, 597–603.
194 8168807, 2012.
195 US20100099895 A1, 2010.
196 A. Alves Costa Pacheco, J. Sherwood, A. Zhenova, C. R. McElroy, A. J. Hunt, H. L. Parker, T. J. Farmer, A. Constantinou, M. De bruyn, A. C. Whitwood, W. Raverty and J. H. Clark, *ChemSusChem*, 2016, **9**, 3503–3512.
197 M. Asadullah, S. Ito, K. Kunimori, M. Yamada and K. Tomishige, *J. Catal.*, 2002, **208**, 255–259.
198 S. Consonni, R. E. Katofsky and E. D. Larson, *Chem. Eng. Res. Des.*, 2009, **87**, 1293–1317.

199 A. Zhang and S.-T. Yang, *Biotechnol. Bioeng.*, 2009, **104**, 766–773.
200 US8455239 B2, 2013.
201 D. Prat, A. Wells, J. Hayler, H. Sneddon, C. R. McElroy, S. Abou-Shehada and P. J. Dunn, *Green Chem.*, 2015, **18**, 288–296.
202 P. N. R. Vennestrøm, C. M. Osmundsen, C. H. Christensen and E. Taarning, *Angew. Chem. Int. Ed.*, 2011, **50**, 10502–10509.
203 D. J. C. Constable, C. Jimenez-Gonzalez and R. K. Henderson, *Org. Process Res. Dev.*, 2007, **11**, 133–137.
204 Benzene - Substance Information - ECHA, https://echa.europa.eu/substance-information/-/substanceinfo/100.000.685, (accessed 4 April 2017).
205 IARC Monographs- Classifications, http://monographs.iarc.fr/ENG/Classification/index.php, (accessed 4 April 2017).
206 F. M. Kerton and R. Marriott, *Alternative Solvents for Green Chemistry*, Royal Society of Chemistry, 2013.
207 R. K. Henderson, C. Jiménez-González, D. J. C. Constable, S. R. Alston, G. G. A. Inglis, G. Fisher, J. Sherwood, S. P. Binks and A. D. Curzons, *Green Chem.*, 2011, **13**, 854–862.
208 D. Prat, O. Pardigon, H.-W. Flemming, S. Letestu, V. Ducandas, P. Isnard, E. Guntrum, T. Senac, S. Ruisseau, P. Cruciani and P. Hosek, *Org. Process Res. Dev.*, 2013, **17**, 1517–1525.
209 ACS-GCI roundtable, The ACS GCI pharmaceutical roundtable solvent selection guide., https://www.acs.org:80/content/acs/en/greenchemistry/research-innovation/research-topics/solvents.html, (accessed 4 April 2017).
210 D. Prat, J. Hayler and A. Wells, *Green Chem.*, 2014, **16**, 4546–4551.
211 F. P. Byrne, S. Jin, G. Paggiola, T. H. M. Petchey, J. H. Clark, T. J. Farmer, A. J. Hunt, C. Robert McElroy and J. Sherwood, *Sustain. Chem. Process.*, 2016, **4**, 7.
212 L. Moity, V. Molinier, A. Benazzouz, R. Barone, P. Marion and J.-M. Aubry, *Green Chem.*, 2014, **16**, 146–160.
213 S. Jin, F. Byrne, C. R. McElroy, J. Sherwood, J. H. Clark and A. J. Hunt, *Faraday Discuss.*, , DOI:10.1039/c7fd00049a.
214 K. Alfonsi, J. Colberg, P. J. Dunn, T. Fevig, S. Jennings, T. A. Johnson, H. P. Kleine, C. Knight, M. A. Nagy, D. A. Perry and M. Stefaniak, *Green Chem.*, 2008, **10**, 31–36.
215 C. M. Alder, J. D. Hayler, R. K. Henderson, A. M. Redman, L. Shukla, L. E. Shuster and H. F. Sneddon, *Green Chem*, 2016, **18**, 3879–3890.
216 C. R. McElroy, A. Constantinou, L. C. Jones, L. Summerton and J. H. Clark, *Green Chem.*, 2015, **17**, 3111–3121.
217 L. Constantinou and R. Gani, *AIChE J.*, 1994, **40**, 1697–1710.
218 P. M. Harper and R. Gani, *Comput. Chem. Eng.*, 2000, **24**, 677–683.
219 ChemSpider | Search and share chemistry, http://www.chemspider.com/, (accessed 11 May 2017).
220 The PubChem Project, https://pubchem.ncbi.nlm.nih.gov/, (accessed 11 May 2017).
221 L. Moity, V. Molinier, A. Benazzouz, B. Joossen, V. Gerbaud and J.-M. Aubry, *Green Chem.*, 2016, **18**, 3239–3249.
222 J. Sherwood, H. L. Parker, K. Moonen, T. J. Farmer and A. J. Hunt, *Green Chem.*, 2016, **18**, 3990–3996.
223 C. Benoît, G. A. Norris, S. Valdivia, A. Ciroth, A. Moberg, U. Bos, S. Prakash, C. Ugaya and T. Beck, *Int. J. Life Cycle Assess.*, 2010, **15**, 156–163.
224 A. Jørgensen, A. L. Bocq, L. Nazarkina and M. Hauschild, *Int. J. Life Cycle Assess.*, 2008, **13**, 96.
225 R. K. Henderson, C. Jiménez-González, D. J. C. Constable, S. R. Alston, G. G. A. Inglis, G. Fisher, J. Sherwood, S. P. Binks and A. D. Curzons, *Green Chem.*, 2011, **13**, 854–862.
226 A. D. Curzons, D. C. Constable and V. L. Cunningham, *Clean Prod. Process.*, 1999, **1**, 82–90.
227 F. R. Mayo, *J. Am. Chem. Soc.*, 1943, **65**, 2324–2329.
228 M. J. Molina and F. S. Rowland, *Nature*, 1974, **249**, 810–812.
229 J. W. Nicholson, in *The Chemistry of Polymers*, 2006, pp. 66–79.

230 K. W. Suh and D. H. Clarke, *J. Polym. Sci. [A1]*, 1967, **5**, 1671–1681.
231 T. Korenaga, H. Tsukube, S. Shinoda and I. Nakamura, *Hazardous Waste Control in Research and Education*, CRC Press, 1994.
232 D. E. Clark, *Chem. Health Saf.*, 2001, **8**, 12–22.
233 J. Sangster, *J. Phys. Chem. Ref. Data*, 1989, **18**, 1111–1229.
234 D. W. Connell, *Aust. J. Chem.*, 1964, **17**, 130–140.
235 S. D. Tommaso, P. Rotureau, O. Crescenzi and C. Adamo, *Phys. Chem. Chem. Phys.*, 2011, **13**, 14636–14645.
236 H. Matsubara, S. Suzuki and S. Hirano, *Org. Biomol. Chem.*, 2015, **13**, 4686–4692.
237 ECHA, Guidance on Information Requirements and Chemical Safety Assessment - Chapter R.11: PBT/vPvB assessment, https://echa.europa.eu/documents/10162/13632/information_requirements_r11_en.pdf/a8cce23f-a65a-46d2-ac68-92fee1f9e54f, (accessed 16 May 2017).
238 F. Solano-Serena, R. Marchal, S. Heiss and J.-P. Vandecasteele, *J. Appl. Microbiol.*, 2004, **97**, 629–639.
239 R. J. Kelly, *Chem. Health Saf.*, 1996, **3**, 28–36.
240 ACROS Organics, Tetrahydrofuran, 99+%, extra pure, stabilized with BHT - Organic Building Blocks Chemicals, https://www.fishersci.se/shop/products/tetrahydrofuran-99-extra-pure-stabilized-bht-acros-organics-5/p-3213221, (accessed 13 June 2017).
241 S. Fujisawa, Y. Kadoma and I. Yokoe, *Chem. Phys. Lipids*, 2004, **130**, 189–195.
242 J. L. E. Erickson and W. H. Ashton, *J. Am. Chem. Soc.*, 1941, **63**, 1769–1769.
243 E. J. Smutny and A. Bondi, *J. Phys. Chem.*, 1961, **65**, 546–550.
244 D. H. R. Barton, G. Page and D. A. Widdowson, *J. Chem. Soc. D*, 1970, 1466a–1466a.
245 G. A. Olah, Y. Halpern and H. C. Lin, *Synthesis*, 1975, **1975**, 315–316.
246 H. Masada and T. Sakajiri, *Bull. Chem. Soc. Jpn.*, 1978, **51**, 866–868.
247 T. Mill and G. Montorsi, *Int. J. Chem. Kinet.*, 1973, **5**, 119–136.
248 J. M. Simmie and W. K. Metcalfe, *J. Phys. Chem. A*, 2011, **115**, 8877–8888.
249 K. M. Vogelhuber, S. W. Wren, L. Sheps and W. C. Lineberger, *J. Chem. Phys.*, 2011, **134**, 064302.
250 A. J. Ragauskas, C. K. Williams, B. H. Davison, G. Britovsek, J. Cairney, C. A. Eckert, W. J. Frederick, J. P. Hallett, D. J. Leak, C. L. Liotta, J. R. Mielenz, R. Murphy, R. Templer and T. Tschaplinski, *Science*, 2006, **311**, 484–489.
251 D. W. Rackemann and W. O. Doherty, *Biofuels Bioprod. Biorefining*, 2011, **5**, 198–214.
252 Y. Román-Leshkov, C. J. Barrett, Z. Y. Liu and J. A. Dumesic, *Nature*, 2007, **447**, 982–985.
253 S. Nishimura, N. Ikeda and K. Ebitani, *Catal. Today*, 2014, **232**, 89–98.
254 Furan - Substance Information - ECHA, https://echa.europa.eu/substance-information/-/substanceinfo/100.003.390, (accessed 23 April 2017).
255 ArgusLab, http://www.arguslab.com/arguslab.com/ArgusLab.html, (accessed 13 September 2016).
256 US3769329 A, 1973.
257 US2876241 A, 1959.
258 J. R. Dodson, A. J. Hunt, H. L. Parker, Y. Yang and J. H. Clark, *Chem. Eng. Process.*, 2012, **51**, 69–78.
259 A. J. Hunt, T. J. Farmer and J. H. Clark, in *Element Recovery and Sustainability*, 2013.
260 US5241112 A, 1993.
261 US5227521 A, 1993.
262 T. G. Ostapowicz, M. Schmitz, M. Krystof, J. Klankermayer and W. Leitner, *Angew. Chem. Int. Ed.*, 2013, **52**, 12119–12123.
263 S. C. Stouten, T. Noël, Q. Wang, M. Beller and V. Hessel, *Catal. Sci. Technol.*, 2015, **6**, 4712–4717.
264 US4570021 A, 1986.
265 US20070088181 A1, 2007.
266 L. Wu, Q. Liu, R. Jackstell and M. Beller, *Org. Chem.*, 2015, **2**, 771–774.
267 A. Brennführer, H. Neumann and M. Beller, *ChemCatChem*, 2009, **1**, 28–41.

268 US2448368 A, 1948.
269 Further improving competitiveness - BASF Intermediates, http://www.intermediates.basf.com/chemicals/topstory/acetylene, (accessed 23 February 2017).
270 US6365792 B1, 2002.
271 US6956141 B1, 2005.
272 G. A. Olah, A. P. Fung and R. Malhotra, *Synthesis*, 1981, **1981**, 474–476.
273 Dimethylhexanediol - CAS 110-03-2 - BASF - We create chemistry, http://www.windenergy.basf.com/group/corporate/wind-energy/en/brand/2_5_DIMETHYL_2_5_HEXANEDIOL, (accessed 19 October 2016).
274 2,5-dimethylhexane-2,5-diol - Substance Information - ECHA, https://echa.europa.eu/substance-information/-/substanceinfo/100.003.393, (accessed 1 August 2017).
275 20120271082, 2012.
276 K. Griesbaum, A. A. Oswald and W. Naegele, *J. Org. Chem.*, 1964, **29**, 1887–1892.
277 J. Sherwood, H. L. Parker, K. Moonen, T. J. Farmer and A. J. Hunt, *Green Chem.*, 2016, **18**, 3990–3996.
278 S. D. Gadkary and S. L. Kapur, *Makromol. Chem.*, 1955, **17**, 29–38.
279 S. L. Kapur and R. M. Joshi, *J. Polym. Sci.*, 1954, **14**, 489–496.
280 J. R. L. Smith, E. Nagatomi and D. J. Waddington, *J. Chem. Soc. Perkin Trans. 2*, 2000, 2248–2258.
281 D. B. Sharp, L. W. Patton and S. E. Whitcomb, *J. Am. Chem. Soc.*, 1951, **73**, 5600–5603.
282 J. Clayden, N. Greeves and S. Warren, *Organic Chemistry*, OUP Oxford, 2012.
283 N. Menschutkin, *Z. Für Phys. Chem.*, 1890, **6U**, 41–57.
284 P. Isnard and S. Lambert, *Chemosphere*, 1988, **17**, 21–34.
285 C. Zhang, H. Yang, F. Yang and Y. Ma, *Curr. Microbiol.*, 2009, **59**, 656–663.
286 B. Gillis and P. Beck, *J. Org. Chem.*, 1963, **28**, 1388–1390.
287 D. B. Denney, D. Z. Denney and J. J. Gigantino, *J. Org. Chem.*, 1984, **49**, 2831–2832.
288 D. Kotkar, S. W. Mahajan, A. K. Mandal and P. K. Ghosh, *J. Chem. Soc. [Perkin 1]*, 1988, 1749–1752.
289 P. F. Vlad and N. D. Ungur, *Synthesis*, 1983, **1983**, 216–219.
290 S. Turner, J. R. Sieber, T. W. Vetter, R. Zeisler, A. F. Marlow, M. G. Moreno-Ramirez, M. E. Davis, G. J. Kennedy, W. G. Borghard, S. Yang, A. Navrotsky, B. H. Toby, J. F. Kelly, R. A. Fletcher, E. S. Windsor, J. R. Verkouteren and S. D. Leigh, *Microporous Mesoporous Mater.*, 2008, **107**, 252–267.
291 D. C. Sherrington and A. P. Kybett, in *Supported Catalysts and Their Applications*, 2001, pp. 27–37.
292 K. T. Tan, K. T. Lee and A. R. Mohamed, *J. Supercrit. Fluids*, 2010, **53**, 88–91.
293 Bis(2-methoxyethyl) ether - Substance Information - ECHA, https://echa.europa.eu/substance-information/-/substanceinfo/100.003.568, (accessed 14 October 2017).
294 US4967020 A, 1990.
295 K. Addo, SIUE student injured in science lab explosion, http://www.stltoday.com/news/local/education/siue-student-injured-in-science-lab-explosion/article_9c05a41d-f3d9-548e-a5e4-7a3af9c45831.html, (accessed 19 June 2017).
296 C. E. Frank, *Chem. Rev.*, 1950, **46**, 155–169.
297 C. E. Redemann, *J. Am. Chem. Soc.*, 1942, **64**, 3049–3050.
298 K. Watanabe, N. Yamagiwa and Y. Torisawa, *Org. Process Res. Dev.*, 2007, **11**, 251–258.
299 Zeon Corporation, Specialty Chemicals - Cyclopentyl methyl ether (CPME) - Products, http://www.zeon.co.jp/business_e/enterprise/spechemi/spechemi5-13.html, (accessed 13 September 2016).
300 T. Karunasekara and C. F. Poole, *J. Chromatogr. A*, 2011, **1218**, 809–816.
301 T. Karunasekara and C. F. Poole, *Talanta*, 2011, **83**, 1118–1125.

302 J. Jover, R. Bosque and J. Sales, 2004, **44**, 1098–1106.
303 T. Karunasekara and C. F. Poole, *J. Chromatogr. A*, 2011, **1218**, 4525–4536.
304 T. Karunasekara and C. F. Poole, *Chromatographia*, 2011, **73**, 941–951.
305 H. H. Rowley and W. R. Reed, *J. Am. Chem. Soc.*, 1951, **73**, 2960–2960.
306 G. Perdoncin and G. Scorrano, *J. Am. Chem. Soc.*, 1977, **99**, 6983–6986.
307 Y. Izumi, K. Matsuo and K. Urabe, *J. Mol. Catal.*, 1983, **18**, 299–314.
308 C. Lacaze-Dufaure and Z. Mouloungui, *Appl. Catal. Gen.*, 2000, **204**, 223–227.
309 H. Nawaz, R. Casarano and O. A. E. Seoud, *Cellulose*, 2012, **19**, 199–207.
310 K. Arnold, B. Davies, R. L. Giles, C. Grosjean, G. E. Smith and A. Whiting, *Adv. Synth. Catal.*, 2006, **348**, 813–820.
311 V. Grignard, *Ann Chim*, 1901, **24**, 433–490.
312 D. Seyferth, *Organometallics*, 2009, **28**, 1598–1605.
313 E. C. Ashby, *Q. Rev. Chem. Soc.*, 1967, **21**, 259–285.
314 F. W. Walker and E. Ashby, *J. Am. Chem. Soc.*, 1969, **91**, 3845–3850.
315 W. Schlenk and W. Schlenk, *Eur. J. Inorg. Chem.*, 1929, **62**, 920–924.
316 E. C. Ashby, J. Laemmle and H. M. Neumann, *Acc. Chem. Res.*, 1974, **7**, 272–280.
317 J. Toney and G. Stucky, *Chem. Commun.*, 1967, 1168–1169.
318 J. Toney and G. D. Stucky, *J. Organomet. Chem.*, 1971, **28**, 5–20.
319 L. J. Guggenberger and R. Rundle, *J. Am. Chem. Soc.*, 1964, **86**, 5344–5345.
320 U. Tilstam and H. Weinmann, *Org. Process Res. Dev.*, 2002, **6**, 906–910.
321 G. Osztrovszky, T. Holm and R. Madsen, *Org. Biomol. Chem.*, 2010, **8**, 3402–3404.
322 H. M. Walborsky, *Acc. Chem. Res.*, 1990, **23**, 286–293.
323 C. L. Hill, J. B. Vander Sande and G. M. Whitesides, *J. Org. Chem.*, 1980, **45**, 1020–1028.
324 A. Kadam, M. Nguyen, M. Kopach, P. Richardson, F. Gallou, Z.-K. Wan and W. Zhang, *Green Chem.*, 2013, **15**, 1880–1888.
325 US3652589 A, 1972.
326 US4144397 A, 1979.
327 US5047431 A, 1991.
328 R. A. Sheldon, *J. Chem. Technol. Biotechnol.*, 1997, **68**, 381–388.
329 Toluene - Pubchem, https://pubchem.ncbi.nlm.nih.gov/compound/toluene, (accessed 10 February 2017).
330 1,8-Cineol - Pubchem, https://pubchem.ncbi.nlm.nih.gov/compound/2758, (accessed 1 August 2017).
331 Guidance on CLP - ECHA, https://echa.europa.eu/guidance-documents/guidance-on-clp, (accessed 1 August 2017).
332 OECD, *Test No. 414: Prenatal Development Toxicity Study*, Organisation for Economic Co-operation and Development, Paris, 2001.
333 GHS (Rev.5) (2013) - Transport - UNECE, http://www.unece.org/trans/danger/publi/ghs/ghs_rev05/05files_e.html, (accessed 11 July 2017).
334 Q. H. Pickering and C. Henderson, *J. Water Pollut. Control Fed.*, 1966, **38**, 1419–1429.
335 J. L. Hamelink, , DOI:10.1520/STP32397S.
336 S. K. Khare, A. Pandey and C. Larroche, *Biochem. Eng. J.*, 2015, **102**, 38–44.
337 Acetone - Pubchem, https://pubchem.ncbi.nlm.nih.gov/compound/180, (accessed 1 August 2017).
338 Ethyne - Pubchem, https://pubchem.ncbi.nlm.nih.gov/compound/6326, (accessed 1 August 2017).
339 Hydrogen - Pubchem, https://pubchem.ncbi.nlm.nih.gov/compound/783, (accessed 1 August 2017).
340 Acetone - Substance Information - ECHA, https://echa.europa.eu/substance-information/-/substanceinfo/100.000.602, (accessed 1 August 2017).
341 US8742187 B2, 2014.

342 J. D. Taylor, M. M. Jenni and M. W. Peters, *Top. Catal.*, 2010, **53**, 1224–1230.
343 2,5-Dimethyl-2,4-hexadiene - Pubchem, https://pubchem.ncbi.nlm.nih.gov/compound/12992, (accessed 2 August 2017).
344 A. V. Ivanov, E. Zausa, Y. B. Taârit and N. Essayem, *Appl. Catal. Gen.*, 2003, **256**, 225–242.
345 P. T. Anastas and M. M. Kirchhoff, *Acc. Chem. Res.*, 2002, **35**, 686–694.
346 M. Dwidar, J.-Y. Park, R. J. Mitchell and B.-I. Sang, *Sci. World J.*, , DOI:10.1100/2012/471417.
347 J. A. Moulijn, M. Makkee and A. E. van Diepen, *Chemical Process Technology*, Wiley, 2013.
348 Carbon monoxide - Pubchem, https://pubchem.ncbi.nlm.nih.gov/compound/281, (accessed 2 August 2017).
349 Hydriodic acid - Pubchem, https://pubchem.ncbi.nlm.nih.gov/compound/24841, (accessed 2 August 2017).
350 Methanol - Pubchem, https://pubchem.ncbi.nlm.nih.gov/compound/887, (accessed 2 August 2017).
351 H. Koch and W. Haaf, *Angew. Chem.*, 1958, **70**, 311–311.
352 M. Kilner and N. J. Winter, *J. Mol. Catal. Chem.*, 1996, **112**, 327–345.
353 H. Alper, J. B. Woell, B. Despeyroux and D. J. H. Smith, *J. Chem. Soc. Chem. Commun.*, 1983, 1270–1271.
354 F. Bertoux, Y. Castanet, E. Civade, E. Monflier and A. Mortreux, *Catal. Lett.*, 1998, **54**, 199–205.
355 M. Beller, J. Seayad, A. Tillack and H. Jiao, *Angew. Chem. Int. Ed.*, 2004, **43**, 3368–3398.
356 US2831877 A, 1958.
357 US2419131 A, 1947.
358 T. N. Pham, T. Sooknoi, S. P. Crossley and D. E. Resasco, *ACS Catal.*, 2013, **3**, 2456–2473.
359 Isobutane - Pubchem, https://pubchem.ncbi.nlm.nih.gov/compound/6360, (accessed 2 August 2017).
360 Boron trifluoride - Pubchem, https://pubchem.ncbi.nlm.nih.gov/compound/6356, (accessed 26 July 2017).